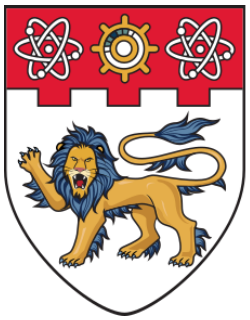

NANYANG TECHNOLOGICAL UNIVERSITY
SINGAPORE

3D JET AND CULVERT SCOUR

TAN SHEAU MAAN
SCHOOL OF CIVIL AND ENVIRONMENTAL ENGINEERING
2018

3D JET AND CULVERT SCOUR

TAN SHEAU MAAN

School of Civil and Environmental Engineering

A thesis submitted to the Nanyang Technological University
in partial fulfilment of the requirement for the degree of
Doctor of Philosophy

2018

Acknowledgement

I would like to express deep gratitude to my supervisor, A/P Lim Siow Yong, for giving me the opportunity to study the simple yet complicated and interesting phenomena of 3D jet and culvert scour. His understanding on my limitation in conducting experiments and his assistance provided by assigning FYP students are invaluable. Thanks for his continuous support and patience throughout these years.

I would like to thank A/P Cheng Nian Sheng for his valuable input on data analysis and the constructive discussions.

The experiments could not have been successfully conducted without the help from Hydraulics lab staff. My thanks go to Mr Daniel Lim Kok Hin, Mr Foo Shiang Kim, Mr. Syed Alwi Bin Sheikh Bin Hussien Alkaff, and Ms Tin Zar Lwin. I am grateful for the assistance from my FYP students: Ms Nuraminah Suyin binte Zaihan, Mr Alkhaff Akhtar, Mr Podianko Surya, Ms Ananya Das, Ms Miao Wan, Mr Pee John, Mr Muhammad Rizal bin A Salam, Ms Sun Qian, and Mr Lam Choon Kit, and also Mr Tay Yee Seng from Ngee Ann Polytechnic. The days with you guys in the lab are very memorable.

Special thanks go to Mr Ong Chee Yung and Mr Tan Han Khiang from Environmental Laboratory I for unquestioning support on some critical tools required for the experiment data collection. I also need to thank the staff from Construction Laboratory on some experimental setup preparation and the staff from EST lab for assistance in software usage.

I need to thank Prof Chiew Yee Meng and his research group: Dr Wei Mao Xing, Dr Prakash Agarwal, Dr Adel Emadzadeh, and Dr Guan Dawei, for their assistance and support, both directly and in-directly, throughout my studies.

I also need to thank A/P Zhao Zhiye and Ms Ho-Woo Siew Cheun for their kind understanding and the subsequent arrangement on research student duty.

I am very grateful to Dr Carmel Heah for telling me that the reason I was unable to find a suitable thesis for reference is that certain aspects of my thesis structure are more similar to those in language studies rather than those typical ones in engineering research.

Many thanks to my undergraduate friends, Dr Chiew Jun Xuan and Ms Wong Tze Ying. Our entirely different research areas enabled us to motivate each other for years. The constant support from my own FYP lab mates, Ms Nurul Huda, Ms Ang Xue Li, Ms Chong Wan Ying, and Ms Lim Siyu are often timely and helpful.

Thanks to my friend Ms Kermaine Sia for the encouragement. Thanks to my teacher Ms Fujita Yoko and Ms Ito Akiko for reminding me of the wonderful world of Japanese language. And I am thrilled to know that I am on Ms Chong Tau Siew's and Mr Gregory Denis Hiller's mind despite the geographical distance.

Many thanks to Dr Calvin Tan from NTU Medical Center for his valuable time, advices, sharing, and offering a listening ear.

Last but not least, many thanks for my parents, Mr Tan Hwa Keong and Ms Pang Kim Peng, for their kind words, encouragement, companion, and always listening ears. Thanks to my brother Mr Tan Sheau Yuan for his kind understanding on why his sister spend so many years in a university.

Table of content

Acknowledgement ii
Table of content iv
Summary vi
List of figures vii
List of tables x
List of symbols xi
Chapter 1 Introduction 1
1.1 Background 1
1.2 Research Scope 2
1.3 Organization of thesis 2
Chapter 2 Literature review 4
2.1 Jet and local scour 4
2.2 2D jet scour 7
2.3 3D jet scour 10
2.3.1 Simple 3D jet scour studies 12
2.3.2 Other 3D jet scour studies 17
2.4 Factors affecting scour 20
2.4.1 Effect of Relative Tailwater Depth 21
2.4.2 Shape effect 23
2.4.3 Scale effect 24
2.4.4 Understanding jet scour and shifting in interest 25
2.5 Summary of other 3D jet studies (NTU studies) 28
2.6 Jet scour prediction equations 28
2.7 Conclusions 33
Chapter 3 Jet and culvert scour experiments in current study 34
3.1 Introduction 34
3.2 General experimental procedure 35
3.3 Small scale jet scour experiments 36
3.4 Deeply submerged jet scour experiments with different jet sizes 39
3.5 Jet scour experiments at unsubmerged and shallowly submerged outlet conditions 42
3.6 Trapezoidal culvert scour experiments with preliminary studies using rectangular culvert 47
3.7 Rectangular culvert scour experiments 53
3.8 Discussions on experimental observation 63
3.9 Conclusions 66

3.10 Acknowledgement 66
Chapter 4 Scour below non-full flowing culvert outlets 67
4.1 Introduction 67
4.2 NTU culvert scour database 68
4.3 Dimensional analysis 70
4.4 Analysis of culvert scour data 71
4.5 Proposed prediction equations 77
4.6 Comparison with other prediction equations 79
4.7 Comparison with Abida's (1988) data 82
4.8 Conclusions 84
Chapter 5 Analysis of 3D Jet and Culvert Scour 85
5.1 Introduction 85
5.2 Length scale for jet size and outlet 85
5.3 Length scale for sediment size 87
5.4 Dimensional analysis and formulation 88
5.5 Maximum Scour Depth 90
5.6 Maximum Scour Width, Length, and Volume 95
5.7 Effect of H/R_h and d_{50}/R_h 102
5.8 Conclusions 103
5.9 Acknowledgements 104
Chapter 6 Conclusions and Recommendations 105
References 107
Appendix I

Summary

3D full flowing horizontal jet scour has been traditionally used to simulate culvert scour in laboratory condition, while non-full flowing culvert scour has received less attention in the past. Current study focused on generalizing both horizontal 3D jet and culvert scour. Several experimental series were conducted and compilation of a database consisting of 738 jet and culvert scour datasets was carried out.

A thorough literature review was carried out and several research gaps in 3D horizontal jet scour phenomena were identified. The effect of relative tailwater depth, effect of relative sediment size, and effect of culvert shape remain areas worth exploring. Several series of experimental studies targeted at each research gap were conducted. Different sediment sizes and circular pipes of different diameter were used to study the relative sediment size effect. Different outlet submergence conditions revealed much about the detailed effect of relative tailwater depth. Observation of scour holes produced by different culvert shapes showed visual differences that were unable to be captured by the measurement of the maximum dimension of the scour hole or the conventional contour and centerline profile plots. The similarity and difference between different kinds of scour produced by full flowing circular jet and non-full flowing culvert under different hydraulic conditions are presented. Both the full flowing jet and the non-full flowing culvert scour were affected by the tailwater depth similarly. Culvert shape affected the jet flow pattern as the jet exiting from the culvert barrel, and this is the most obvious at very shallow tailwater depth condition.

A database consisting of 738 jet and culvert scour experiments was compiled and analyzed. The hydraulic radius (R_h) was found to be a suitable characteristic length scale across different culvert shapes for non-full flowing culvert scour. Analysis using the full database showed that R_h is the suitable characteristic length for both the full flowing jet and the non-full flowing culvert scour. The analysis included determination of a suitable representative sediment size for the 3D jet scour phenomena. For the maximum scour hole depth, the d_{84} is the representative sediment size, and the maximum scour hole width, length, and volume also have sediment size larger than d_{50} as representative sediment sizes. By using $d_{84} = d_{50}\sigma_g$ to formulate a modified densimetric Froude number, $F_{o,d84}$, the non-dimensionalized maximum scour depth can be expressed as $d_{se}/R_h = 1.22F_{o,d84}$.

List of figures

Figure 2.1 Examples of different jet scour. 5
Figure 3.1 Sketch of the longitudinal section and plan view of the culvert or pipe and the sediment bed (a) at the beginning and (b) at the end of an experiment. 35
Figure 3.2 Bed contours at datum level of the small scale jet scour experiments. 38
Figure 3.3 Centerline profiles of the scour holes from the small scale jet scour experiments. 38
Figure 3.4 Normalized contour of the small scale jet scout experiments. 38
Figure 3.5 Normalized centerline of the small scale jet scour experiments. 39
Figure 3.6 The discontinuity on the slope at the upstream face of the ridge during the experiment (a) and after the experiment (b). Photos taken during Run 213. 39
Figure 3.7 Contour at datum level of scour holes produced using different jet sizes. 40
Figure 3.8 Centerline profiles of the scour holes produced using different jet sizes. 41
Figure 3.9 Normalized contour of the scour holes from the jet size experiments. 41
Figure 3.10 Normalized centerline profiles of the scour holes from the jet size experiments. 41
Figure 3.11 Bed contours at datum level at different outlet submergence grouped by jet velocity. .. 43
Figure 3.12 Centerline profiles at different outlet submergence conditions grouped by jet velocity. 44
Figure 3.13 Normalized bed contours of the scour holes at different outlet submergence and grouped by velocity. 45
Figure 3.14 Normalized centerline profiles at different outlet submergence grouped by jet velocity. 46
Figure 3.15 Typical photos of the scour hole under different outlet submergence under similar jet . 47
Figure 3.16 Bed contours at datum level for trapezoidal culvert (a – d) and rectangular culvert (e) scour experiments, grouped by tailwater depth. 49
Figure 3.17 Centerline profiles for trapezoidal culvert (a – d) and rectangular culvert (e) scour experiments, grouped by tailwater depth. 50
Figure 3.18 Normalized bed contours at datum level for trapezoidal culvert (a – d) and rectangular culvert (e) scour experiments, grouped by tailwater depth. 51
Figure 3.19 Normalized centerline profiles for trapezoidal culvert (a – d) and rectangular culvert (e) scour experiments, grouped by tailwater depth. 52
Figure 3.20 Contours at datum level for rectangular culvert scour experiments, grouped by tailwater depth. 55
Figure 3.21 Centerline profiles for rectangular culvert scour experiments, grouped by tailwater depth. 56

Figure 3.22 Normalized contours at datum level for rectangular culvert scour experiments, grouped by tailwater depth.....57
Figure 3.23 Normalized centerline profiles for rectangular culvert scour experiments, grouped by tailwater depth. 58
Figure 3.24 Bed contours at datum level for slotted jet scour experiments, grouped by tailwater depth. 59
Figure 3.25 Centerline profiles for slotted jet scour experiments, grouped by tailwater depth 59
Figure 3.26 Normalized contours at datum level for slotted jet scour experiments, grouped by tailwater depth 60
Figure 3.27 Normalized centerline profiles for slotted jet scour experiments, grouped by tailwater depth.....60
Figure 3.28 Photos of typical equilibrium scour holes under (a) minimum tailwater condition, (b) 5 cm tailwater condition, and (c) slotted jet condition. 62
Figure 3.29 Photos from trapezoidal and rectangular culvert experiments showing the differences between the scour holes at similar tailwater depth.....65
Figure 4.1 Schematic sketch of the recirculating flow at shallow tailwater depth and deeper tailwater depth. 68
Figure 4.2 Plot of d_{se}/R_h versus F_o for compiled experiments.....73
Figure 4.3 Plot of W_{se}/R_h versus F_o for compiled experiments. 74
Figure 4.4 Plot of L_{se}/R_h versus F_o for compiled experiments 75
Figure 4.5 Plot of V_{se}/R_h^3 versus F_o for compiled experiments 76
Figure 4.6 Predicted versus measured data for d_{se}/R_h, W_{se}/R_h, L_{se}/R_h, and V_{se}/R_h^3 calculated by Eqs. (4.6) – (4.9), respectively 77
Figure 4.7 Plots of Eqs. (4.10) to (4.12).....78
Figure 4.8 Comparisons of calculated versus measured d_{se}/R_h using equations proposed by various researchers (see Table 4.2). The dash lines and dotted lines are perfect agreement and +/- 30% error lines respectively.....81
Figure 4.9 Comparisons of calculated versus measured W_{se}/R_h using equations proposed by various researchers (see Table 4.2). The dash lines and dotted lines are perfect agreement and +/- 30% error lines respectively.....82
Figure 4.10 Comparisons of calculated versus measured L_{se}/R_h using equations proposed by various researchers (see Table 4.2). The dash lines and dotted lines are perfect agreement and +/- 30% error lines respectively.....82

Figure 4.11 Comparison of predicted maximum scour depth, d_{se}/R_h using Eq. 4.6 with non-full flowing rectangular culvert scour data from Abida (1988).....83
Figure 5.1 Figures from (a) Breusers and Raudkivi (1991) illustrating maximum scour depth for submerged plane and circular horizontal jets, and from (b) Schiereck (2003) illustrating scour depth for plane jet, circular jet, and culvert. 87
Figure 5.2 d_{se}/R_h vs $F_{o,d50}$ for compiled jet and culvert scour data.....94
Figure 5.3 d_{se}/R_h versus $F_{o,d84}$ for compiled jet and culvert scour data. The solid line in the figure is Eq. (5.6), and the dashed lines are the $\pm 30\%$ error lines.....95
Figure 5.4 (a) W_{se}/R_h, (b) L_{se}/R_h, and (c)V_{se}/R_h^3 versus d_{50}-based F_o respectively. 96
Figure 5.5 (a) W_{se}/R_h plotted against $F_{o,d70}$, and (b) L_{se}/R_h plotted against $F_{o,d75}$. The solid lines in (a) and (b) are Eqs. (5.7) and (5.8), respectively, and the dashed lines are the +/- 30% error lines. 99
Figure 5.6 (a) V_{se}/R_h^3 plotted against $F_{o,d50}^3/\sigma_g$ and (b) V_{se}/R_h^3 plotted against $F_{o,d84}$ The solid lines in (a) and (b) are Eqs. (5.9) and (5.10), respectively, and the dashed lines are the +/- 30% error lines.100
Figure 5.7 Relationship between d_{se}/R_h with (a) W_{se}/R_h,(b) L_{se}/R_h, and (c) V_{se}/R_h^3 respectively, together with best fit Eqs. (5.11), (5.12) and (5.13), respectively, and the dashed lines are the +/- 30% error lines. 101
Figure 5.8 d_{se}/R_h versus $F_{o,d84}$ plot with normalized log10 values of (a) H/R_h, and (b) d_{50}/R_h as colour of markers, respectively. 102
Figure 5.9 d_{se}/R_h plotted against (a) H/R_h and (b) d_{50}/R_h, both with value of log10 of Fo,d84 as marker color. 104

List of tables

Table 2.1 Non-full flowing culvert scour experiments from NTU 28
Table 2.2 Full flowing circular jet scour experiments from NTU 28
Table 2.3 Equation proposed by various researchers for 3D horizonal jet scour at equilibrium phase 31
Table 3.1 Experimental plan for small scale jet scour experiment. 37
Table 3.2 Experimental plan for scale series experiment. 40
Table 3.3 Experimental plan for relative tailwater depth experiments 42
Table 3.4 Experimental plan for the trapezoidal culvert series. 48
Table 3.5 Experimental plan for the rectangular culvert scour experiments. 54
Table 4.1 Detailed hydraulic properties of NTU database and selected Abida's (1988) data. 69
Table 5.1 Details of compiled culvert and jet scour data 92
Table 5.2 Dimensionless numbers and normalized scour hole dimensions of the database 93
Table 5.3 Regression analysis results using different representative sediment sizes for maximum scour depth (738 data points) 94
Table 5.4 Regression analysis results for maximum scour width (551 data points). 97
Table 5.5 Regression analysis results for maximum scour length (609 data points) 97
Table 5.6 Regression analysis results for scour hole volume (466 data points). 97

List of symbols

A = flow area at the brink section

B = downstream channel width

F_o = densimetric Froude number

$F_{o,dx}$ = d_x-based densimetric Froude number

H = tailwater depth

L_{se} = maximum scour hole length at equilibrium stage

P_{wet} = wetted perimeter at brink section

Q = flow rate

R_h = hydraulic radius

S_o = slope of the culvert

U_o = outlet velocity

V_{se} = scour hole volume at equilibrium stage

W_{se} = maximum scour width at equilibrium stage

b = culvert width

d_{50} = median sediment diameter

d_o = outlet diameter for full flowing circular culvert

d_{se} = maximum scour hole depth at equilibrium stage

d_x = x-th percentile of the sediment size distribution

g = gravitational acceleration

h_o = brink depth at culvert outlet

μ = dynamic viscosity

ρ = water density

ρ_s = sediment density

σ_g = sediment gradation

Chapter 1 Introduction

Scour in the vicinity of hydraulic structure is often undesirable that appropriate protection is usually required to ensure safety of users and stability of the hydraulic structure. Scour at culvert outlet caused by water jet exiting the solid culvert barrel into the erodible natural waterway has been investigated in lab scale setting to provide prediction for the extent of necessary protection (Abt et al. 1984). On the other hand, erosion by controlled water jet has many engineering applications, such as excavation (Mih and Kabir 1983; Ortega-Casanova et al. 2011), or jet scour can be part of engineering operation (Yeh et al. 2009). The phenomenon of erosion by jet itself has also attracted attention for theoretical (Iwagaki et al. 1958; Laursen 1953; Rouse 1939) and numerical simulation (Adduce and Sciortino 2006) studies.

1.1 Background

Rouse (1939) studied jet scour theoretically by using two-dimensional (2D) jet. For three dimensional (3D) jet scour, various studies has been conducted for vertical (Kobus et al. 1979), horizontal (Rajaratnam and Berry 1977), or angled (Blaisdell and Anderson 1988) jet scour. The current study focuses on 3D jet scour, covering both “non-full flowing culvert scour” and “full flowing jet scour”. The former has outlet flow depth smaller than the pipe size and is open channel flow at the outlet, while the latter is pressurized pipe flow at the outlet. Opie (1967) was one of the earliest researcher who studied culvert scour. Abt and co-workers (1984) has carried out large amount of experiments for formulation of engineering guideline (Thompson and Kilgore 2006). Ade and Rajaratnam (1998) summarized the various aspects of horizontal turbulent circular jet scour. Liriano et al. (2002) looked into the turbulent flow structure of culvert scour.

Even though the overall understanding of 3D jet and culvert scour is sufficient for engineering applications, as outlined in the engineering manuals (May et al. 2002; Thompson and Kilgore 2006), there are several areas remain debatable. Firstly, the details of scour caused by different culvert shapes have not been well researched in the past. Next, the effect of tailwater depth above the sediment bed downstream of the outlet on the extent of scour has vague or contradicting observations by different researchers, especially at small tailwater depth (Abida and Townsend 1991; Sarathi et al. 2008). Besides, the ratio of sediment size to jet size has not been strictly controlled in laboratory setting due to the cohesive nature of very fine sediment. Thus, the effect of this ratio has remained open for discussion. Lastly, improvement can still be made for the prediction equation and

the chosen characteristic length scale to unite both culvert and jet scour. This is because current practice assumed full flowing culvert barrel even when the flow depth at outlet is less than the outlet height.

1.2 Research Scope

The current study involved laboratory scale studies of selected areas in culvert and jet scour, as well as an extensive data compilation from available literature. The scope of study is limited to near horizontal jet with no jet offset distance. The sediment is non-cohesive and only a single outlet is considered. There is no density difference between the incoming jet flow and the receiving tailwater body.

Several experiment series were carried out to investigate the earlier identified gaps:

1. The effect of culvert shape was investigated by using a trapezoidal model culvert and a rectangular model culvert while using the same sediment for both model culverts.

2. The effect of tailwater depth was investigated by carrying out experiments with tailwater depth ranging from smaller than jet size to several times of the jet size.

3. The effect of sediment size relative to jet size was tested by separately varying the sediment sizes and pipe sizes.

The data collected from the experiments as well as from available literature were analyzed. Suitable length scales applicable for both culvert and jet scour were proposed, which were then used to formulate prediction equations.

1.3 Organization of thesis

This thesis consists of 6 chapters. Chapter 2 presents the literature review, highlighting the research gaps and discussed about their current state. Chapter 3 outlines the general experimental methodology and presents the experimental results. Chapter 4 focuses on the effect of culvert shape and the available past experimental data is compared and analyzed together with the experimental data from current study. Chapter 5 presents the analysis of compiled data and the selection of suitable

length scales for prediction equations. Chapter 6 concludes this thesis followed by outlining some future work.

Chapter 2 Literature review

This chapter reviews previous works in 3D horizontal jet and culvert scour. Selected important works in related fields such as 2D plane jet scour and various type of 3D jet scour are also included to appreciate different kinds of jet scour and their similarity in nature. The influence of relative tailwater depth, jet outlet shape, and scale effect are discussed in detail. Advances in jet scour research are briefly presented. The literature review then emphasizes on the formulation of generalized empirical equations for scour hole dimension prediction. The different justification and formulation by different researchers are highlighted.

The review covers investigation using non-cohesive sediments, focusing on 3D horizontal jet scour studies with no jet offset. The current work is limited to scour below horizontal or near horizontal culvert outlet, and for non-full flowing condition a culvert on mild slope with outlet control is assumed. The headwall at the outlet is assumed not affecting the scour action significantly. The focus of current work is the maximum scour hole dimensions at the equilibrium stage, and thus the time evolution of scour is not within the scope of current study.

For consistency of discussion, several common terminologies are used in this review. The ratio of tailwater depth (H) to jet outlet height (d_o) is expressed as "relative tailwater depth". When the tailwater depth is shallower than the jet outlet height ($H/d_o < 1$), it is termed as unsubmerged outlet. When the relative tailwater depth is more than d_o ($H/d_o > 1$), it is referred as shallowly submerged outlet, and when it is larger than $10d_o$ ($H/d_o >> 1$), it is referred as deeply submerged outlet. When the discussion emphasizes on different type of outlet conditions, the term "relative submergence" is used. Similarly, the ratio of mean sediment size (d_{50}) to jet outlet size is referred as "relative sediment size" (d_{50}/d_o). The ratio of jet outlet size to downstream channel width (B) is referred as "relative downstream channel width" (B/d_o). As for the flow condition within the model culvert barrel, "full flowing' means pressurized flow before the outlet, and "non-full flowing" means open channel flow with a free water surface before the outlet.

2.1 Jet and local scour

A wall jet is defined as a jet discharging from an outlet parallel to a wall (Breusers and Raudkivi 1991). When a wall jet is issued next to an erodible wall, scour will occur. For jet scour study, water and, occasionally, air have been used as the fluid medium. When the jet outlet is at some distance away

from the erodible boundary and still remains submerged within the same fluid, it is called an offset jet. However, when a water jet is discharged into air before plunging into the water body below and scour the erodible boundary within, it is called a plunging jet. A plunging jet can have curved trajectory due to gravity (Blaisdell and Anderson 1988) or an almost straight trajectory at high speed (Pagliara et al. 2008). Beside horizontal jet and vertical jet, jet can also be applied at an angle towards the erodible bed, termed as angled jet. The jet angle is usually downwards (Pagliara et al. 2008) or it can be upward (Mehraein et al. 2011) relative to the erodible bed. When the jet is tilted at small angle, it is referred as slope effect (Abt et al. 1985). Figure 2.1 shows some examples of different jet scour. Even though jet has been studied extensively, a wall jet that is issued adjacent to an erodible surface exhibits different characteristic compared to an ordinary free jet.

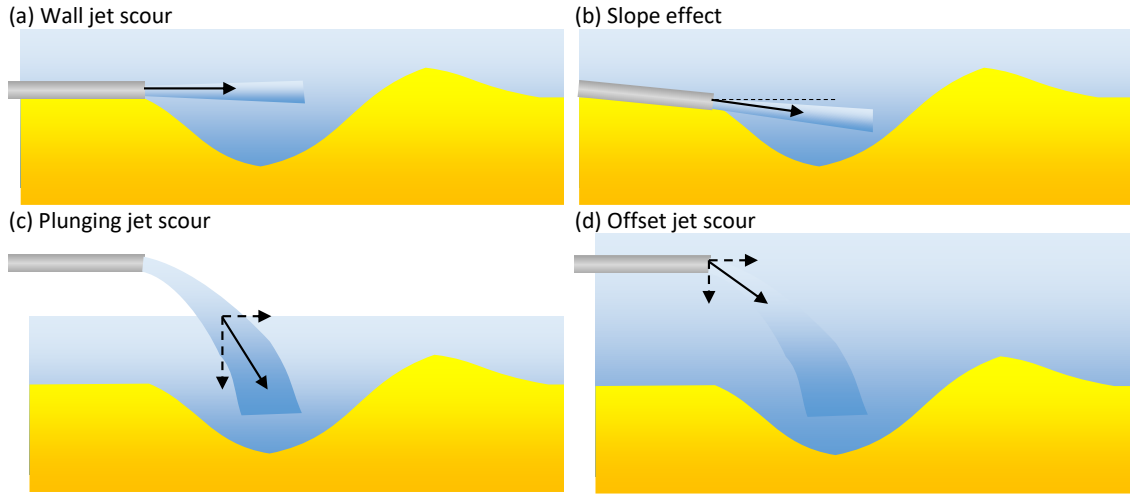

Figure 2.1 Examples of different jet scour.

Scour is defined as the enlargement of flow section due to removal of the boundary materials by the fluid in motion (Laursen 1953). For rivers and natural channels, scour refers to the removal of materials from bed and banks by the flowing water (May et al. 2002). Scour happens both naturally and as the results of manmade alteration to the natural channel.

General scour or natural scour occurs throughout the natural channel such as channel bend scour, natural channel degradation, or channel migration. Constriction scour or contraction scour happens when the natural flow area is reduced, usually by man-made obstruction, increasing the flow scouring capacity. Local scour happens in the immediate vicinity of a man-made hydraulic structure due to change in the water flow velocity and/or direction in the presence of the hydraulic structure, such as bridge abutment, pier, and spur dike. Total scour is the summation of these different kinds of scour (Breusers and Raudkivi 1991; May et al. 2002). Scour can also be divided into clear water scour and

live bed scour. In the former, there is no upstream supply of bed materials into the region of interest, while in the latter, upstream flow continuously transports bed materials into the region of interest.

According to the intensity and progress of the scouring action, scour process can be divided into four phases: initiation, development, stabilization, and equilibrium phase (Hoffmans and Verheij 1997). During the initiation phase, scour is rigorously forming the scour hole. During the development phase, the upstream section of a growing scour hole stabilizes. During the stabilization phase, the scour hole grows slower. The scour hole remains virtually unchanged when the equilibrium phase, also known as asymptotic stage, is reached (May et al. 2002). The equilibrium phase can be defined by the almost absent sediment movement at the location of maximum scour (Chatterjee et al. 1994), or a small difference in the bed level measured over a fixed duration (Day et al. 2001), or simply when the scour hole remains virtually unchanged (Faruque et al. 2006).

This review focuses on 3D horizontal jet and culvert scour. Culvert scour is usually modeled in laboratory as a jet scour with low tailwater depth, with the jet outlet unsubmerged or shallowly submerged. On the other hand, deeply submerged jet scour experiments are mainly for more theoretical understanding of the jet scour phenomena. Both 2D and 3D jet have been used to study scour depth, which is regarded as the most important scour hole dimensions for engineering purpose. While 2D scour has been used in early research as simplification of real life scenario, 3D jet scour is required for certain scenarios such as culvert scour. 3D jet scour is different from 2D jet scour by having recirculating flow at both sides of the jet flow or within the scour hole, and the 3D jet swinging from side to side have been observed (Ali and Lim 1986; Bohan 1970; Liriano 1999). On the other hand, 2D jet has hydraulic jump, jet flipping, but no lateral jet expansion or recirculation flow in the plane of the jet.

From the field study by Scheer (1968), 21 out of 55 of the surveyed culverts that were larger than 2.1 m had scour hole at the outlet, and half of these were less than 0.6 m in depth. He noted that the later requirement of cutoff wall installation and riprap protection effectively reduced the scour hazard, and the scour hole itself acts as energy dissipater. While all observed gully scour were related to alteration of the channel, only 4 of the 7 sites had scour hole deeper than 0.76 m. Scheer (1968) suggested using a threshold Froude number to predict the presence of scour. Alternatively, the highest permissible velocity below scour threshold should be calculated taking into account the normal flow depth and soil type. The recommended cut off wall depth is the addition of both the basic depth by requirement and the maximum predicted scour depth.

2.2 2D jet scour

Early study on jet scour focused on theoretical understanding of the scour process. Scaling and similitude properties of sediment transport were explored (Rouse 1939) and different scour processes were discussed generally focusing on the incoming flow and the limiting velocity for scour to occur (Laursen 1953).

Rouse (1939) discussed the criteria of similarity in sediment transport. He used 2D vertical jet scour as an example to apply dimensional analysis to a scour phenomenon. The jet was observed to have two flow patterns, either deflected vertically upwards or flowed along the sediment ridge, resulting in different scour hole time evolution profiles. Analysis using non-dimensionalized scour hole size, time and velocity, the experimental observations collapsed into 2 curves, each corresponding to one jet flow pattern. The scour depth was shown as a function of inlet velocity, scour duration, sediment settling velocity, sediment gradation, and a characteristic length of boundary geometry. The resulting dimensionless number is very complex and its exponent contains the ratio of jet velocity to sediment settling velocity, which is interestingly similar to the “incomplete similarity” concept in dimensional analysis (Barenblatt 1996)

Laursen (1953) deduced the nature of scour from theoretical understanding of scour process based on conservation of mass. As scour progresses, the rate of scour will reduce over time due to increase in cross section and decrease in flow velocity. Thus, there should be a limit of scour which would be approached asymptotically. The discussion assumed that the fluid movement at the boundary will be reduced to zero as the boundary expands to infinity and scour has already ceased to happen before the fluid ceases to move. A series of 2D horizontal submerged jet scour experiment was presented. The scour rate was found to be a linear function to logarithmic of time, and similarity of scour hole profiles was established. A limiting scour velocity was defined as the velocity that is able to move the sediment particle but unable to transport it beyond the ridge for several minutes. When this velocity is reached, the scour has reached its limiting dimension. The concept was again illustrated by defining a capacity function for live bed scour experiment using the continuity equation (Laursen 1953).

O’Loughlin et al. (1970) studied the effect of Reynolds number using 2D jet scour experiments. Shallower scour was observed when the smaller diameter glass beads was used. Placing a screen near the jet outlet, believed to be reducing the eddy size, resulted in smaller scour hole by one order of magnitude, suggesting the strong influence by the jet turbulence. The authors recommended particle Reynolds number should be greater than 2500 to avoid viscous effect.

In laboratory condition, the 2D jet usually simulates dam spillage flow (Mason and Arumugam 1985), ski jump flow, weir flow, or flow over grade control structure. Horizontal jet can be issued from under a sluice gate (Chatterjee et al. 1994), or produced from a horizontal nozzle (Hill and Younkin 2006). Angled jet can be produced by weir flow, from ski-jump, or issued from suspended outlet for better control of the jet entrance angle (Pagliara et al. 2006). Submerged 2D jet scour could contain hydraulic jump and, for some special circumstances, jet flipping might occur (Xie and Lim 2014) or the jet impinging location was oscillating (Bey et al. 2007). Common scour protection such as rigid apron downstream of sluice gate (Chatterjee et al. 1994) or larger sediments has been studied

Chartterjee et al. (1994) conducted sluice gate jet scour experiment with rigid protection up to equilibrium stage (at most about 5 hours) and focused on sediment transport equation. By repeating the same experiments, measurement of scour profile development, equilibrium stage velocity distribution, and continuous measurement of dynamic pressure at the location of maximum scour were done. They found that the time required to reach equilibrium stage, characterized by no sediment movement at the maximum scour depth location, depends on the jet velocity and sediment size. Time dependent volume of scour per unit width, location of maximum scour depth, and location of ridge peak were related to the jet velocity, jet thickness, and sediment size. However, the proposed equations are not dimensionally homogeneous. Similarity of scour profiles were verified with relationship proposed by earlier researchers. By studying other earlier equations, the authors found that inclusion of sediment fall velocity and apron length is necessary to obtain time dependent equations for maximum scour depth for each sediment type and scour stage. The authors established the equilibrium maximum scour depth as a function of Froude number, regardless of the sediment size. The author further worked out the volumetric sediment transport rate and correlated it with the fluid power of jet.

Hogg et al. (1997) studied scour by 2D horizontal turbulent jet scour from theoretical point of view. They highlighted that a wall jet is different from a free jet and a fully developed turbulent boundary layer. A fully developed turbulent boundary layer has an almost constant shear stress near the boundary, which is absent for a turbulent wall jet. The wall jet characteristic was found to be dependent on the surface roughness. New scaling law was proposed accordingly by calibrating with available experimental data and invoking several assumptions. Next, the authors extended analysis of incipient motion of particle on a horizontal surface to an inclined surface, and considered specific conditions during scouring. A Gaussian-like model for boundary shear stress distribution was assumed. The authors theoretically predicted steady state of scour hole profiles, taking into account of the

realistic angle of repose at the upstream of the ridge, and the prediction agreed with the experimental data by Rajaratnam (1981) up to end of scour hole as the model did not account for flow separation over the ridge. The temporal evolution of scour hole was calculated by adopting a bedload transport model in a sediment conservation equation.

Hopfinger et al. (2004) studied the turbulent instability on curved surface, known as Görtler vortices, and their contribution in plane jet scour. Additional contribution of the vortices increased the effective shear stress in scour action. They evaluated the time evolution of scour hole depth and identified two regimes. At the end of the first regime, a quasi-steady state of scour hole was reached, and in the second regime towards the asymptotic scour depth, the Görtler vortices contributed in the slow growing of scour hole.

Dey and Sarkar (2006) investigated the velocity and turbulence aspects of plane jet scour, focusing on the transition of the jet from smooth apron surface to flowing over rough sediment bed. They then looked at plane jet scour downstream of an apron in detail (Dey and Sarkar 2006) and also the effect of seepage (Sarkar and Dey 2007). Dey and Sarkar (2006) observed faster jet decay with a faster growing boundary layer on rough beds. Smooth transition of flow velocity, turbulence, and stresses in changing bed roughness were observed and the flow was self-preserving. The equilibrium scour hole profile and the time evolution of maximum scour depth were calculated from threshold condition of sediment particle. Comparison of the calculated profiles with experimental measurement was satisfactory. Dey and Sarkar (2006) studied comprehensively by using different combinations of experimental conditions to study the effect of apron length, sluice gate opening, tailwater depth, and jet velocity using sediments of different sizes and gradations. Similarity of non-dimensional scour hole profiles and its representation by polynomials were presented. The non-dimensional time scale and effect of different parameters on scour depth were presented graphically. The existence of launching apron made by large stones further reduced scour hole size. The maximum scour depth can be predicted by a multiplicative function consisting of densimetric Froude number, relative apron length, relative tailwater depth, and relative sediment size. Sarkar and Dey (2007) found that upward seepage velocity was able to deflect the jet flow, resulting in smaller scour hole. Increased seepage velocity accelerated the decay of the plane jet and reduced the bed shear stress of the scour affected area.

Balachandar and co-workers (Bey et al. 2007; Bey et al. 2008; Deshpande et al. 2007; Karki et al. 2007) studied 2D jet scour in great extent. The experiments were always carried out using selected velocities to enable direct comparison across different experimental setting within the same investigation, or

even across different publications. The experiments within a single publication may not be large in number, but they were well designed to test various parameters and to obtain detailed measurement. Bey et al. (2007) studied the role of fluid structure for plane jet scour. The authors presented detailed observation of the scour process before the equilibrium state. Detailed velocity measurements were carried out after equilibrium state was attained. The plane jet bends downward upon exiting from the nozzle and there was a recirculating zone along the longitudinal direction in the upper part of tailwater body above the scour hole. Triple correlations and quadrant analysis indicated presence of sweep and ejection events. Karki et al. (2007) studied offset plane jet and square jet. Scour hole shape was affected by the offset distance and jet flipping was similarly observed at low relative tailwater depth for plane jet scour. Deshpande et al. (2007) look at startup conditions and relative tailwater depth. The way of adjustment to get the desired flow velocity did not affect long duration scouring, and relative tailwater depth of 8 represents a separation point which jet flipping was observed at lower submergence and moving jet impingement location at higher submergence. Bey et al. (2008) varied relative tailwater depth at the beginning of scouring experiment (within 1 hour for an 24-hour experiment) and also looked at the effect of downstream channel width on plane jet scour. The authors proposed to differentiate whether a (plane) jet is deeply submerged by noting the occurrence of the jet flipping phenomena. They suggested that the distinction is related to jet velocity, and whether the tailwater depth had been increasing or decreasing. Channel width was thought to be affecting velocity characteristics and was related to whether the scour is two-dimensional with scour hole profile remained consistent across the flume width.

Melville and Lim (2014) summarized the effect of various parameter on 2D horizontal jet scour. The effect of each parameter were expressed as a ratio to the baseline condition, and each ratio was assumed to have multiplication relationship with the main function representing the jet intensity. The factors considered include effect of tailwater depth, sediment size, sediment gradation, and apron length. 309 available laboratory data were collected and selectively analyzed for each parameter. The authors also evaluated different 2D horizontal jet scour equations proposed by other researchers. The proposed equation was compared to earlier equations and the proposed equation has the best prediction accuracy.

2.3 3D jet scour

While 2D jet scour is convenient for theoretical investigation and has been used as simplification for engineering purpose, 3D jet scour retains the complex nature of actual jet scour which, for some instances, cannot be ignored. An example is the culvert scour, where the erosion on the channel banks

could be so severe that engineering protection must be applied on both sides of the culvert outlet. Even though similar in nature, certain measurement or quantification fundamental in 2D jet scour, such as scour profile time development and sediment transport rate, is unable to be conveniently obtained in 3D jet scour. Phenomenon unique in 3D jet scour has been attracting interest as the understanding of 2D jet scour has been maturing. In this section, 3D jet scour is reviewed and the progress in understanding this phenomenon is highlighted.

Generally, there are two approaches in 3D jet scour experiments, depending on the parameters of interest, understanding in the scour phenomena, and the availability of technology. Early researchers conducted short duration experiments from less than an hour (Bohan 1970) to several hours (Ruff et al. 1982) to gain initial understanding and investigate large number of factors. Bohan (1970) roughly grouped tailwater depth as high or low and concluded that "low" tailwater depth caused more severe scour. Abt and co-workers (for example Ruff et al. (1982)) then investigated various parameters under this tailwater condition. Abida and Townsend (1991) studied various parameters of unsubmerged non-full flowing box culvert scour using 2-hour experiments. As time progresses, other researchers ran long duration experiments until the scour has reached equilibrium condition to obtain the maximum scour hole dimensions (for example Rajaratnam and Berry (1977)). The first approach allows collection of large amount of information within a short time, while the second approach provides conservative estimation and allows detailed observations. Some researchers were able to conduct long duration experiments investigating different parameters systematically (Blaisdell and Anderson 1988; Blaisdell and Anderson 1988; Sarathi et al. 2008). Some exceptions are researchers investigating a large number of additional parameters. Pagliara et al. (2010) conducted experiments with duration for about 1 hour or less to investigate the effect of different scour protection screen and its location in addition to the common angled jet parameters.

Breussers and Raudkivi (1991) discussed about the nature of jet scour. The authors proposed relationship between scour depth, jet size, jet velocity and sediment threshold shear velocity based on data from Clarke (1962) and Rajaratnam and Berry (1977). On the other hand, data from Bohan (1970) and Abt et al. (1984) were used to illustrate about culvert scour. The normalized scour hole dimensions were plotted against Froude number (Fr) or ratio of outlet velocity to the sediment threshold shear velocity. The effect of tailwater was found to be important that Fr or the velocity ratio alone is unable to capture the effect of free surface.

Hoffmans attempted the jet scour problem by deriving semi-empirical equation from Newton's second law and calibrating using corresponding experimental data (Hoffmans 1998; Hoffmans and Verheij 1997; Hoffmans 2009). He started from 2D plunging jet and horizontal jet, where the difference is the jet impact angle, before discussing about 3D horizontal jet scour (Hoffmans 1998). Data from Clarke (1962) and Rajaratnam and Berry (1977) were used to calibrate a coefficient related to sediment size, and data from Ruff et al. (1982), Doehring and Abt (1994), and Blaisdell and Anderson (1989) were used for verification. Even though the two groups of data have different relative tailwater depths, the proposed equation performed the best compared to some equations proposed by other researchers. Furthermore, Hoffmans (2009) refined his earlier work on plunging jets by introducing a critical friction factor and also taking into account of air entrainment.

2.3.1 Simple 3D jet scour studies

Simple horizontal 3D jet scour studies with no offset jet distance are presented in this section.

Clarke (1962) has done experiments on deeply submerged scour experiments and used two of the smallest outlet pipe sizes of 2.38 mm and 4.78 mm. His experiment data has high densimetric Froude number (F_o) among the compiled experimental data used by the present author.

On the other hand, Opie (1967) used very large model culverts with diameters up to 91.4 cm, which remains as one of the largest lab scale study. He also investigated the effect on scour when different transitions were installed at the outlet. Valid data of full flowing outlet with no special transition or jet offset distance was selected for analysis in the present work.

Bohan's (1970) work has been used as a reference for researches and guidelines. Scale series experiments using pipe diameter from 0.038 m to 0.305 m were conducted, although data from the smallest pipe size were discarded because their Reynolds numbers were not in the turbulent region. Two types of tailwater depth, based on observed similar flow pattern, were tested. The "minimum tailwater" experiments with relative tailwater depth lesser than 0.5 were conducted for 20 mins, and the "maximum tailwater" experiments with relative tailwater depth larger than 0.5 were conducted for 30 mins, respectively. Time evolution test up to 24 hours were conducted for 3 selected conditions, and the scour was observed to be still progressing at the end of the test. A comparison of scour using culverts of circular, arch, rectangular, and box shapes with the same cross-sectional area to a 0.102 m diameter circular culvert showed that culvert shape has insignificant effect on scour hole geometry. Bohan's data had been extended to 5 hours (Breusers and Raudkivi 1991) or 72 hours (Ade and

Rajaratnam 1998) for analysis. However, due to the 20-30 mins short experiment duration and the dimensionless time scale is a function of the densimetric Froude number (Rajaratnam and Berry 1977), these data are not included in current author's data analysis.

Abt and co-workers (Abt et al. 1984; Abt et al. 1985; Abt et al. 1987; Doehring and Abt 1994; Mendoza et al. 1983; Ruff et al. 1982) followed up using relative tailwater depth equals or less than 0.5, where the scour was more severe. They have done systematic experimentation on effect of sediment size and uniformity, jet size, relative tailwater depth, presence of headwall, outlet slope effect, outlet shape effect, and drop height. They found that the effect of sediment gradation in reducing scour hole size was more profound for smaller sediment. The effect of relative tailwater depth was insignificant in the range investigated. By using hydraulic radius (R_h) as the characteristic length, scour holes produced from culverts of different shapes were compared to that of circular culvert, which is always the smallest in comparison. The presence of headwall did not affect much on scour hole, and a headwall deeper than the maximum anticipated scour depth was recommended. A sloped culvert generally produced larger scour hole than that produced by a horizontal culvert. For culvert with drop height, larger scour holes were observed as the drop height increased. Abt et al. (1984) summarized selected data from Ruff et al. (1982) focusing on sediment type and culvert diameter and conducted regression analysis on the data using Discharge Intensity (DI), relative sediment size, and sediment gradation as the main parameter. The equation was later amended with multiplicative factors to account for outlet slope and shape (Thompson and Kilgore 2006).

On the other hand, Abt et al. (1983) studied the scour hole ridge. When DI $\leqslant$ 1, the jet dispersed radially outwards from the scour hole along a fan shaped ridge. When DI was larger, the jet scoured a long cavity and produced an elliptical ridge. Ridge height was influenced by tailwater depth. The authors defined a rectangular region of influence, which its length includes both the scour hole and the ridge, and its width the ridge width, to indicate a region at the culvert outlet that is under influence of scouring.

Rajaratnam and Berry (1977) investigated erosion by circular wall jets. They conducted experiments using air jets on polystyrene beds and sand beds, and water jets on sand beds. The time evolution of characteristics of scour hole were observed. The air and water jet experiments had similar scour hole geometry regardless of the density of the bed particle, but the difference is the absence of a high ridge in the former compared to the water jet experiments. The water jet experiments also required a longer duration to reach the asymptotic state. By using the jet diameter as characteristic length, similarities

among the scour hole profiles and half cross sections were presented. Various scour hole dimensions were shown to be a function of the densimetric Froude number (F_o) and the relative sediment size. The ridge height showed two different curves because of the difference in the fluid density, evidenced of the different sediment transportation mode caused by the air and water jet. The velocity profiles along center plane at asymptotic state was recorded for air jet experiment. It shows that the jet first expanded like a free jet, after the location of maximum depth, the jet was like a wall jet.

Rajaratnam and Diebel (1981) were interested in the effect of relative tailwater depth and relative downstream channel width, and found that these factors affected the location of maximum scour depth. The similarity of scour hole profiles was established when the scoured profiles were viewed separately using the location of maximum scour depth as point of separation. When the relative tailwater depth was in the order of 1 and relative downstream channel was 1 to 3.5, the maximum scour depth was nearer to the outlet compared to deeply submerged experiments (Rajaratnam and Berry 1977). This is probably resulting from the limited lateral jet expansion and the restriction by tailwater depth. The ridge shape was also different from that of deeply submerged water jet and the flattened ridge was of similar magnitude to that of air jet scour.

Rajaratnam and Humphries (1983) found that relative tailwater depth heavily influenced the lateral expansion of bluff wall jet. The authors conducted scour experiments with tailwater depth same as the jet height. The similarity of scour hole centerline profile was verified and correlation of normalized scour hole dimensions with densimetric Froude number (F_o) were done. Scour hole formed in an erodible bottom enhanced the non-linear jet transverse expansion compared to a rigid bottom.

Ali and Lim (1986) studied 2D and 3D horizontal jet scour by using a square pipe (3D jet) and wider rectangular pipes of the same height up to the width of the flume (2D jet). Other 2D jet scour were done with flow under a sluice gate. Flow patterns within the scour hole were measured after securing the scour hole with an aluminum foil coated with the same sediment. The hydraulic radius was used to normalize the scour hole volume, and this ratio was then related neatly with the normalized scour depth for both 2D and 3D jets respectively. This suggests the scour hole volume is as representative as the scour hole depth to quantify the extent of scouring action. Sediment fall velocity, sediment median diameter, and densimetric Froude number are used as important functions to predict asymptotic scour depth. Depending on the jet type, different characteristic length scales were used for the correlation equation. A critical tailwater depth was found to be producing shallowest scour hole for 2D jet scour. The centerline velocity distribution pattern differentiates 2D and 3D jet scour.

The former has a decreasing velocity in the scour hole and increased velocity downstream of the scour hole, and recirculation at the upstream slope of the scour hole was present at asymptotic state. Whereas for 3D unsubmerged jet scour, reverse flow was present at the beginning of experiments, and for 3D just submerged jet scour, it was present at the asymptotic state. For both 3D cases, the flow velocity always decreases towards downstream.

Abida and Townsend (1991) was one of the few who studied unsubmerged non-full flowing culvert scour. They used different non-cohesive sediments and varied the box culvert width for 2-hour duration scour tests. The authors claimed that they were studying 2D scour, different from 3D circular jet scour, even though the relative downstream channel width suggests that their study is a 3D one with high possibility that flume wall limiting scour hole growth (Lim 1995; Rajaratnam and Diebel 1981). The relative downstream channel width, relative tailwater depth, relative sediment size (based on an effective sediment size calculated from every 10^{th} percentile of sediment size distribution), and a flow parameter were identified as important dimensionless numbers. The authors chose culvert height and effective particle diameter as characteristic length for data analysis. The effect of relative tailwater depth could be sorted into three regions. Increasing from zero tailwater depth, the scour depth first increased until $H/d_o < 0.2$ (where H is tailwater depth and d_o is jet diameter), then the scour depth decreases with increasing tailwater depth until $H/d_o > 1$, after which tailwater depth has no effect on scour depth. A smaller relative channel width resulted in smaller scour depth and longer scour length. Larger and more non-uniform sediment produced smaller scour hole. An equation based on a 2D jet scour study was modified to predict scour depth when the relative tailwater depth is between 0.3 to 0.7 and tailwater depth is equal to culvert flow depth (Abida 1988; Abida and Townsend 1991).

Lim and Chin (1992) focused on the effect of sediment gradation (σ_g) by varying the sediment gradation while holding the median diameter constant. They found that scour hole size reduction of about 50% was achieved by increasing the σ_g to 2.5.

Lim (1995) varied the ratio of downstream channel to pipe diameter to study the extend of influence of relative downstream channel width. From their unsubmerged jet scour experiments, it was found that the scour hole was distorted when the lateral jet diffusion was limited for the narrowest downstream channel studied, while for other cases the scour hole maximum dimensions were affected while the shape was still maintained. An enveloping equation for maximum scour depth based on a compilation of 150 data was proposed and compared to equations proposed by Abt et al. (1984), Breusers and Raudkivi (1991), and Abt et al. (1987) after converting them into similar form

using densimetric Froude number (F_o) as the main dimensionless number. From the analysis, F_o is the most important dimensionless number, while relative downstream channel width and relative sediment size are of lesser importance.

Chiew and Lim (1996) studied deeply submerged horizontal circular air jet and water jets over sand bed. For the same F_o, air jet formed larger scour hole compared to water jet, especially for large F_o. The air jet data was analyzed together with data of air jet from Rajaratnam and berry (1977). Water jet produced higher ridge than air jet and ridge height was dependent on fluid density. An experiment with continuous ridge removal was carried out and the final scour hole size was similar to one produced by air jet. Thus, the different sediment transportation mode due to the density difference between the fluid and sediment particle is the main reason for the difference between air and water jet ridge.

Ade and Rajaratnam (1998) conducted an extensive review on scour by circular horizontal turbulent jets. Beside the commonly investigated variables such as the jet velocities, jet diameter, sediment size, sediment gradation, and relative submergence, other less commonly researched variables including downstream channel width, relative density difference and jet offset distance were reviewed. The authors suggested that different parameters might have different weightage under different hydraulic conditions. For example, when $F_o>10$, jet submergence must be considered. Over 350 scour experiments were compiled and analyzed together with the authors' experiments using water jets for sand and gravel beds, and air jets for canola seeds. The authors observed migrating dunes when sediment $d_{50} = 0.24$ *mm* was used, and the scour hole was still growing after 186 hours. For non-full flowing outlet, an equivalent diameter of $\sqrt{(4A/\pi)}$ was defined and the brink depth was used to calculate submergence ratio. The equations by Rajaratnam and Diebel (1981), Abt et al. (1984), Breusers and Raudkivi (1991) and Lim (1995) were reviewed. The authors proposed equations for maximum scour depth according to the value of F_o and the relative submergence. By using the pipe diameter (d_o) as characteristic length scale, the author discussed various important length scales of the scour hole, such as the distance to location of maximum scour depth, the maximum scour length, the maximum half width, the distance to maximum ridge height, the maximum ridge height, and the volume of scour. The density difference of the fluid-sediment system was discussed together with the air jet experiments (Ade and Rajaratnam 1998).

Liriano et al. (2002) observed the velocities, turbulent intensities, and Reynolds stresses within scour hole caused by circular wall jet at different extent of scour, which was decided from earlier

observations (Liriano 1999). Bursting analysis showed that different bursting event including sweep, ejection, outward interactions, and inward interactions appeared at different location at respective stages of scour. The jet flow was found to be only responsible for part of the scour action, and turbulent structure contributed the rest.

Balachandar and co-workers (Faruque et al. 2006; Sarathi et al. 2008; Sui et al. 2008). have done investigations on the various aspect influencing 3D jet scour, including the influence of tailwater depth, sediment size and densimetric Froude number. Faruque et al. (2006) used 2 different square nozzles and conduct scour experiments at relative tailwater depth from 2 to 6. The same Froude numbers were used for both outlets such that direct comparison across different relative water depth could be done. The authors speculated that different parameters have important influence at different hydraulic conditions. They proposed a scaling parameter to improve scaling the time variation of the scour hole. Next, Sarathi et al. (2008) used 2 different sediments, wider range of F_o, and relative tailwater depth. They focused on influence of various parameters on scaling of scour hole time development. Sediment sorting was reported even though both sediments were supposed to be uniform. They proposed detailed prediction equation for the scour hole dimensions. For example, the function of scour hole depth is a function of relative tailwater depth at low tailwater depth. Scour hole width and length were determined as linear function of F_o. A power law form was selected for scour hole volume. The coefficient and exponent of the equation were either constant or a function of the relative tailwater depth. The proposed equation performed the best compared to published equation. Sui et al. (2008) used 2 different square nozzles and 2 different uniform sediments, and focused on the resulting 4 different relative sediment sizes. The authors also focused on the relative downstream channel width, even though they were in range usually deemed large enough to be ignored. Different characteristic lengths and dimensionless numbers were used when comparing data by different researchers and when proposing prediction equations.

2.3.2 Other 3D jet scour studies

Other 3D jet scour, including vertical jet, offset jet and plunging jet studies, as well as some with specific study objectives or configurations, such as the presence of cross flow or suction, are presented in this section.

Chiew and Lim (1996) included offset jet in their study and found that the maximum scour depth was both the function of offset distance and F_o. Ade and Rajaratnam (1998) modified F_o to include the acceleration due to drop height for offset jet scour.

Blaisdell and Anderson (1988; 1988) studied scour at cantilevered pipe outlet by carrying out a carefully planned experiment series. Their experiments simulated natural plunge pool, so the experiment configuration of sediment bed was different from other scour experiments. The original sediment bed level was half a pipe diameter higher than the tailwater depth. A channel was made within the sediment bed, from the position of the pipe outlet towards downstream, and the scoured sediments were removed from it throughout the experiments. Dimensionless discharges, pipe offset distance, sediment size, sediment gradation, and pipe slope were among the investigated parameters. For some experiments, the suspended materials within the scour hole were removed at the end of the 7-days experiment, and the accrual scour hole was measured. The authors observed "beaching", which is an extensive scouring of the banks due to strong recirculating currents at both sides of the jet. They have found a "beaching limit" which is a function of relative sediment size and the dimensionless discharge. The analysis of scour hole size was done by using projection of scour hole slope to the original bed level, eliminating the effect of "beaching".

Mih and Kabir (1983) investigated clearing of fine sediments in gravel bed with 10 minutes of submerged jet tests. Different jet diameter, jet angle and nozzle height were tested using a half jet at the side wall of the experimental flume, enabling visualization of the scour hole cross section. The authors observed that fine sediments were cleaned at a depth deeper than the scour depth, which means the flow penetrated deeper into the course sediment and scoured away the finer sediments. From this observation, measurement of jet velocity with a fixated scour hole should be noted that a non-porous fixed boundary has been used instead.

Kobus et al. (1979) used steady vertical jets and pulsating jets in their study. They measured the flow field of vertical air jet impinging on rough solid bed and then conducted water jet experiments using erodible sand bed. The jet Reynolds number, relative nozzle distance, relative equivalent sand roughness sediment Reynolds number, relative jet velocity, Strouhal number, and pulsation amplitude influenced the flow field and the scouring process. Four zones were observed within the impinging jet flow field. They are the potential core region, the free jet, the impinging region, and the deflected wall jet.

They categorized the scour hole into two groups based on a combination function of stagnation pressure, flow rate and grain fall velocity. Visually, the two types differ by having a weakly or strongly deflected jet. In one group, the jet remained attached to the eroded bed, while in another group, the jet separated from the bed and scour deeper into the center of the scour hole. By moving the nozzle

from far towards the bed, the jet first caused erosion of the first kind with attached deflected jet, which was also the maximum scour capacity. Moving further in, the scour process changed into a transitional state before changing into scour of the second kind. When the nozzle was too near to the bed, the jet became an injection into the bed and no scour occur. On the other hand, if the nozzle distance was fixed, increasing the jet velocity will have similar sequence of effect, firstly causing erosion of the first kind, following by that of second kind and finally jet injection. The pulsating jet scoured more effectively and was supported by the better correlation of the fluctuating component in the radial direction. The pulsation amplified the lifting and transportation of sediment by reducing the central jet axis velocity, subsequently widening the pressure field and reducing the seepage velocity into the bed. (Kobus et al. 1979).

Steven (1986), as quoted in Abida (1988), used hydrograph sequence consisting repeated flow rate below design flow rate. The resulting maximum scour depth and width were larger than if a single flow rate was used. This suggests changing flow conditions may cause more severe scour.

Rajaratnam and co-workers also investigated vertical jet and angled jet scour. Aderibigbe and Rajaratnam (1996) worked on submerged circular impinging vertical turbulent jet, focusing on impinging distance, jet diameter, and sediment size. The two distinct scour modes were further investigated and the applicability of the conventional Shields' diagram for strongly deflected jet scour mode was highlighted. Rajaratnam and Mazurek (2002) conducted angled air jet on polystyrene bed scour experiments. By comparing with earlier investigation using vertical jets and horizontal jets, they concluded that the angle of impingement and the erosion parameter, which is the function of F_o and dimensionless impingement distance are important parameters. Rajaratnam and Mazurek (2003) experimented with unsubmerged vertical circular impinging jets with shallow tailwater generated by overflowing jet flow. The maximum scour depth and scour hole radius were found to be a function of F_o', which was calculated from the velocity and jet diameter on original sand bed level, U_o' and d_o', respectively.

Pagliara and co-workers studied hydraulics of 2D and 3D plunge pool scour, both with and without protection (Pagliara et al. 2008; Pagliara et al. 2006; Pagliara and Palermo 2008; Pagliara et al. 2010). Pagliara et al. (2008) extended their 2D plunge pool studies (Pagliara et al. 2006) into 3D plunge pool. The circular jet size, jet angle, tailwater depth, and downstream channel width were systematically varied. The scoured surface was sorted according to jet angle and relative tailwater depth. Secondary flow was observed and depended on jet angle and relative tailwater depth and even the ridge. For the

same jet angle, the scour hole was deeper at deeper tailwater depth, while for the same tailwater depth, a smaller jet impact angle produced a deeper scour hole. Since the scour hole might have width limited by the flume wall, the author devised a "width parameter" to determine whether the scour hole is 2D or 3D. It is the ratio of scour width, extrapolated if necessary, to the flume width. If the width parameter is smaller than 1.5, the scour is 3D, and if it is larger than 3, the scour would be decided as 2D. The authors augmented their 2D plunge pool scour equation by adding the "width parameter", and additional multiplicative factors for effect of tailwater and jet angle. The authors observed increasing difference between dynamic and static scour hole as jet angle increased or the tailwater depth decreased. This issue has been noted earlier for better understanding of prototype scour (Pagliara et al. 2004). Note that the authors used d_{90} when calculating the densimetric Froude number. The authors also amended the same existing multiplicative factor, possibly suggesting the different experimental conditions interacting with existing parameters.

Karki et al. (2007) conducted square offset jet experiments. The shape of scour hole varied according to offset distance, and the maximum scour depth, measured with respect to the outlet invert level, remained almost unchanged. Sui et al. (2009) studied square jet scour under model ice cover. Ice cover changes the water velocity vertical profile. The scour hole remained similar at a given F_o and relative tailwater depth. However, going from low to high relative tailwater depth, existence of ice cover affected the trend of changes for maximum scour depth and width, which some trend opposite to that of without ice cover.

Other 3D jets studies including upward inclined circular wall jet scour by Mehraein et al. (2011), and impinging swirling jets scour by Ortega-Casanova et al. (2011).

2.4 Factors affecting scour

Factors besides the jet velocity, sediment median diameter, sediment density and fluid density, which all have been included in formulation of F_o, are discussed in this section. The selected factors are relative tailwater depth, scale effect, and shape factor. These factors have been receiving less attention than those used on F_o formulation, but their influence on scour are nonetheless worthy of attention.

2.4.1 Effect of Relative Tailwater Depth

The relative tailwater depth is roughly categorized into deeply submerged jet ($H/d_o \gg 1$), shallowly submerged jet ($H/d_o \geqslant 1$), and unsubmerged jet ($H/d_o < 1$) for the discussion, where H is the tailwater depth and d_o is the jet diameter.

A deeply submerged outlet ($H/d_o >> 1$) allows almost unbounded jet expansion vertically and horizontally. The recirculating flow cells will appear at both sides and on top of the outlet, but their strength has minimal influence on the scour action. The ridge formation is not restricted by the tailwater depth, and the ridge itself is capable to disperse and divert the jet flow. The ridge height depends on the density of fluid and corresponding mode of sediment transportation. Comparing to scour hole depth, air jet produces low ridge (Rajaratnam and Berry 1977) while water jet produces high ridge. Due to negligible influence from the surrounding water, the scour holes always have similar shape and centerline profiles. All available literature on air jet scour is obviously considered as deeply submerged.

As scour progresses, the jet transports the lifted particles over the migrating and growing ridge. When the jet is unable to transport the lifted particles over the ridge, the scour has reaches equilibrium stage. However, in fact, turbulence always causes some movement of sediment particles which means scour seldom stop completely. So, some researcher defined slightly different criteria for equilibrium scour stage. In cases when the obstruction of jet by dune is the main cause of scour reaching equilibrium stage, the upstream side of ridge constantly has sediment clouds, which was sediment lifted or pushed by centerline jet velocity and fell once encountering the weakened deflected jet outside of jet centerline (observation in experiments of current study). The ridge removal experiments (Chiew and Lim 1996) illustrated the obstruction by ridge could be significant that at equilibrium stage, the jet still penetrates into the ridge without contributing to scour. For sediment diameter smaller than 0.5 mm, the scour limit might not exist as the transportation over the ridge was observed to be continuous and increasing the scour hole size (Ade and Rajaratnam 1998), possibly because of different scour action when ripples formed for sediment diameter smaller than 0.6 mm (Chien and Wan 1999).

For shallowly submerged jets ($H/d_o \geqslant 1$), the upward jet expansion is limited. The water surface might reflect and absorb some of the energy, and the recirculating flow cells are smaller but stronger compared to a deeply submerged case. The recirculating flow causes the different shape in scour hole, especially region before the location of maximum scour depth, that the scour hole no longer has the

same shape as the deeply submerged condition. For strong jet, the ridge height may be limited by tailwater depth. Due to continuity of flow that the water must flow downstream, or flow as part of a recirculating flow cell, the ridge could be "shaved" that a sharp peak is missing (observation in experiments of current study).

For unsubmerged jets ($H/d_o < 1$), the jet is visibly plunging downwards due to gravity. The jet then dispersed mainly within the scour hole and flowed over the flat ridge. The ridge is limited by the tailwater depth, jet outlet velocity, and outlet shape. Rectangular jet was observed to have straight forward jet flow that no ridge was formed (observations in experiments of current study), while trapezoidal or circular outlet produces more easily dispersed jets and the ridge formed downstream of scour hole. The plunging of the jet caused deep scour hole just below the outlet, possibly shifting the location of maximum depth, resulting in a scour hole centerline profile that is different from previous cases. The strong recirculating flow at both sides of scour hole, which is also influenced by the downstream channel width, might cause additional scour beside the outlet resulting in a wide scour hole at the outlet. Very narrow downstream channel width have resulted in distorted scour hole (Lim 1995).

The discussion above expresses that even though various jet scour problems have been viewed as a single problem, the relative tailwater depth alone could have heavy influence, both on the jet expansion directly and on recirculating flow indirectly, on the formation of scour hole and ridge. The recirculating flow at both sides and on top of outlet is related to the jet strength and tailwater depth. Chiew & Lim (1996) observed deeper scour depth when the ridge was continuously removed for deeply submerged jet scour experiment. This observation stressed the importance of "ridge resistance", yet this is difficult to be quantified and at low tailwater the ridge may be shaved by the main jet flow or may not form. Thus, it is challenging to deal 3D horizontal jet scour problem as a simple problem.

Understanding on the importance of relative tailwater depth progresses with time. Bohan (1970) simply classified tailwater depth as "low" and "high", from which the 'low" condition received subsequent attention (Ruff et al. 1982), though no significant effect for this range of relative tailwater depth was observed for the scour and ridge formation (Abt et al. 1983). Findings from Rajaratnam and Diebel (1981) suggests that effect of relative tailwater depth and relative downstream channel are significant for strong jet having strong recirculating and entrained flow. Rajaratnam and Humphries (1983) found that lateral expansion of the bluff wall jet is a function of tailwater depth. Ali and Lim

(1986) found that relative tailwater depth of about 2 produced minimum scour depth and the effect of tailwater depth could be neglected for relative tailwater depth over 16 for 2D horizontal jet scour. On the other hand, Abida and Townsend (1991) observed maximum scour depth at relative tailwater depth of 0.2 and once the outlet was submerged the tailwater depth have no effect on scour depth for rectangular culvert scour. In the review by Ade and Rajaratnam (1998), the value of $F_o = 10$ was used to decide whether the relative tailwater depth parameter is important. Garde and Raju (2000) noted that early researchers were aware of tailwater depth which produces maximum and minimum depth, though the exact type of jet scour investigated is not known. Thus, the weightage of relative tailwater depth should be included as part of the scour hole dimension prediction equation. Generally, the effect of relative tailwater is greatest at unsubmerged outlet, and gradually reduces as tailwater depth increases.

Tailwater depth is usually expressed as ratio between jet size and tailwater depth (H). For circular jet scour, the pipe diameter (d_o) is the jet size. For non-full flowing culvert, the brink depth (h_o) is used as jet size. This relative tailwater depth tells the submergence of the jet outlet. Simplest classification of outlet condition suggests the dimensionless number H/d_o has different meaning when it is smaller than 1, larger than 1, or above the range in which tailwater depth is influencing the scour action. Its value will be maximum at 1 for non-full flowing culvert outlet. This means that H/d_o might have different function at different ranges, in which its strength is different. In addition, the brink depth for non-full flowing culvert is a function of tailwater depth, flow rate, and channel shape.

2.4.2 Shape effect

Bohan (1970) checked whether different shapes such as circular, arch, rectangular, and box culverts affect the scour formation, and observed generally that the scour hole shapes were rather similar. Ruff et al. (1982) used circular and square culverts and found that circular culvert produced larger scour hole. Abt et al. (1987) investigated shape effect by using circular, square, arch, and rectangular shaped culverts. Their findings were presented as ratio of scour hole size by a particular culvert shape relative to that produce by a circular one, which is generally the smaller in comparison. These ratio are used as the corrective factors on culvert shape effect (Thompson and Kilgore 2006).

The culvert shape is believed to be affecting the scouring action by the flow pattern when the water jet is leaving the solid culvert barrel. For unsubmerged outlet, the way in which the jet plunges into the tailwater body and the subsequence jet dispersion is believed to be affected by the culvert shape, especially the length of flat bottom of the culvert and the side wall slope or curve of culvert

(observation in experiments from current study). The culvert shape is taken into account when calculating the flow area, flow velocity, and hydraulic radius at the outlet.

2.4.3 Scale effect

The criteria for similarity in sediment transport has received attention early (Rouse 1939) as the pi-theorem dimensional analysis inherently assumed only one homogeneous fluid phase. Breusers and Raudkivi (1991) outlined three similarity criteria that need to be maintained between model and prototype, which are geometric similarity, Froude number similarity, and sediment transport similarity.

Heller (2011) reviewed the scale effects for fluid-sediment systems in hydraulics engineering models. The scale effect is caused by the difficulty to maintain a constant force ratio for the model and prototype. The magnitude of scale effect is in proportion with the scale factor. One of the model-prototype similarities is mechanical similarity, which includes geometric, kinematic and dynamic similarities, and each corresponding to similarity in shape, motion, and force ratios. Froude similarity is important for open channel hydraulics which is characterized by negligible friction and turbulence. Reynolds similarity is important when viscous force is important. As is it impossible to obtain exact model similarity, priority must be put on the most important force ratio to minimize scale effects from other sources. Scale series is recommended to study similitude and should be done together with inspectional analysis using a set of governing equations, dimensional analysis, and calibrate with prototype data. The three ways to handle scale effect are avoidance, compensation and correction. For example, scale effect can be avoided by changing the fluid or sediment used. Distorting geometric similarity related to model roughness and sediment diameter could compensate scale effect. Correction can be done to model results after sufficient data are obtained.

Scale effect has been mentioned in pier scour research (Ettema et al. 1998; Lança et al. 2013; Lee and Sturm 2009; Sheppard et al. 2004; Sheppard et al. 2000). Ettema et al. (1998) discussed about the Froude number similarity which is naturally unachievable. The sediments in rivers ranged from 0.1 to 10 mm in diameter. However, as sediment finer than 0.6 mm is ripple-forming and sediments finer than 0.06 mm is considered cohesive, exact scaling of particle mobility is impossible. Lab scale experiments use sediment with size similar to those present in prototype. The scour depth does not scale linearly with pier width; however, such a conservative prediction suits engineering design purpose. Sheppard et al. (2000) proposed a scour scale factor to replace the geometric scale ratio, and improved prediction for bridge pier scour. Sheppard et al. (2004) conducted experiments up to the lower limit of prototype range, supporting their earlier findings about the presence of functional

dependence of normalized scour depth on relative sediment diameter. The maximum value of scour depth was when the relative sediment size is about 50.

Lee and Sturm (2009) analyzed bridge scour data from laboratory and field studies and found the scour depth was maximum when relative sediment size is 25. Observing different scouring pattern for different sediments, the authors proposed that scour occurs in two phases, the sediment particle is first lifted by the fluctuating vertical velocity component, and then swept out of the scour hole by the phase-averaged streamwise periodic velocity component. Two corresponding time scales were proposed. The ratio of these two time scales tells whether the scour process is transport limited or suspension limited. When they are at the same magnitude, meaning the scour action is at optimum, the scour depth is maximum. Lança et al. (2013) also found that the maximum scour depth decreases with relative sediment size larger than 100.

On the other hand, jet scour researchers Day et al. (2001) and Hager (2007) treated "scale effect" differently. Day et al. (2001) reasoned that the scale effect was due to the low flow Reynolds number. Hager (2007) based his tests on Froude similarity with restrictions that include the tailwater depth should be at least 5cm, the flow Reynolds number and particle Reynolds number should be in the turbulent range, and the median sand diameter used should be in the order of 1 mm to avoid the viscous effect. Bohan (1970) has similarly discarded the data from the smallest pipe experiments as the Reynolds number was too small.

For investigations on other kind of jet scour concerning scale effect, Yeh et al. (2009) carried out large scale moving vertical jet scour to simulate the scour resulting from moving ships discharging ballast water in shallow water depth. Hunter et al. (2013) were aware of the effect of system scale in their impinging jet scour experiment as the normalized data from different setups did not collapse. Carr et al. (2015) used Lie group scaling for one-dimensional unsteady suspended sediment transport and identified conditions for unscaled sediment diameter.

2.4.4 Understanding jet scour and shifting in interest

As time progress, interest in jet scour research has changed from understanding on jet scour phenomena and obtaining engineering design requirement as more detailed and frequent measurement techniques becomes more widely available.

For measurement, the early measurement of one directional point velocity has been satisfactory to produce evidence of main jet flow to support the observed scour phenomena, for example Rajaratnam and Berry (1977) and Ali and Lim (1986). Others observed flow pattern in the downstream channel, for example Stevens (1969) and Blaisdell and Anderson (1988). Similar measurement and observations are easier for 2D jet scour problem due to the simplified flow nature. For example, 2D jet flipping phenomena can be visualized by dye injection and the captured by video recording (Xie and Lim 2014). Hill and Youkin (2006) measured 2D horizontal plane jet scour velocity profile by using particle velocimetry (PIV) technique with fabricated solid "scour hole",

3D jet scour is characterized by complex 3D flow pattern. Location of the scour hole and its continued growth makes real time measurement of velocity field very challenging. Even real time measurement of scour hole development can be challenging due to the rapid changing scour hole surface. Real time scour hole development for 2D weir scour could be obtained by using a multiple transducer array and proper filtering of data (Guan et al. 2015). Liriano et al. (2002) used acoustic Doppler velocimeter to measure the velocity components at various section plane above a fixated 3D jet scour hole at different scour stage. Bey et al (2007) measured 2D jet scour velocity at equilibrium state using laser Doppler anemometer.

Predicting the scour hole development has been attempted by various researchers using different methods. Most of the researchers used empirical equations to predict scour hole size. This method generally predicts scour depth with earlier equations being dimensional inconsistent on both sides of the equations and more recent equations are dimensionally homogeneous by utilizing common dimensionless number. Hogg et al. (1997) attempted 2D scour hole prediction from calculating bed shear stress and the corresponding sediment motion criteria. Adduce and Sciortino (2006) have carried out a similar attempt of numerical simulation of scour downstream of a sill. Some "black box" prediction methods are receiving attention even though the engineering practicality and physical meaning is regarded as less important. For example, Liriano and Day (2001) used artificial neural network to predict scour by 2D and 3D horizontal jets, Najafzadeh and Lim (2015) used neuro-fuzzy group method of data handling with particle swarm optimization (NF-GMDH-PSO) network to predict scour downstream of sluice gate with protection apron, and Laucelli and Giustolisi (2011) obtained complex equations for scour depth downstream of grade control structure by using evolutionary polynomial regression.

Researchers have long been aware of the "interaction" between different parameters in scouring action, and usually represented by including different parameters in an empirical equation. The contributions of various parameters were usually assumed additive and were represented by multiplying terms. Examples including the multiplicative K-factors for 2D jet scour (Melville and Lim 2014) and multiplicative functions for plunge pool scour (Pagliara et al. 2008; Pagliara et al. 2006; Pagliara and Palermo 2008; Pagliara et al. 2010). Other researchers applied the "incomplete similarity" (Barenblatt 1996) concept, which is usually shown as the exponent of dimensionless number contains variable values. This method contrasts the traditional way of dimensional analysis and signifies the complex interaction of various factors to the scouring action. The resulting equation, however, can be vague in physical meaning. Incomplete similarity has been used by Cheng (2011) to formulate equation for bed load discharge prediction, by D'Agostino & Ferro (2004) to predict scour below grade control structure, by Pagliara et al. (2014) on scour below W-weirs, by Scurlock et al. (2012) for scour below 3D grade control structure,

To understand the interaction between various parameters, recent experiments were usually designed such that multiple direct comparison, and perhaps estimation of existence of interaction, can be done. Balacandar and co-workers varied the parameters such that the same F_o were used at different tailwater depth or outlet size, for example Sarathi et al. (2008). Both the relative tailwater depth and relative downstream channel could have different degree of influence on scour depending on F_o value.

Turbulence has been observed to be affecting jet scour. Different configuration before the jet nozzle produced different scour hole (Opie 1967). "Turbulent bursting" has been described as intermittent uplifting and transportation of sediment (Chien and Wan 1999). Liriano (1999) has shown that the turbulence of circular jet has comparable magnitude in all x-, y-, and z-direction components and even suggested that the scour hole is partly formed by the turbulent fluctuation components (Liriano et al. 2002).

Thus, given the complex nature of 3D turbulent jet scour, both the model experiments and numerical investigation together with good observation method and understanding of the phenomena are required to obtain more detailed understanding and prediction of the extent of scour.

2.5 Summary of other 3D jet studies (NTU studies)

This section provides a summary of other jet scour studies compiled for data analysis in Chapters 4 and 5. These experiments were conducted in Nanyang Technological University. Both full-flowing and non-full flowing jet scour experiments were carried out. For the current study, Akhtar (2014), Surya (2014), Miao (2015), Das (2015) and the author focused on non-full flowing jet scour, while Zaihan (2014), Pee (2016), and Salam (2016) have done experiments on circular full-flowing jet scour on scale effect and tailwater effect. Tables 2.1 and 2.2 list the studies on non-full flowing and full flowing jet scour experiment respectively. The experimental variables of each series, except jet velocity and narrow range relative tailwater depth, or specific experimental setting, are highlighted.

Table 2.1 Non-full flowing culvert scour experiments from NTU

Researcher	Experiment variable	Model culvert shape
Leow (2006)	sediment size and uniformity	Rectangular
Peh (2007)	wide model culvert	Rectangular
Tan (2009)	large sediment size	Trapezoidal
Ma (2010)	large sediment size	Trapezoidal
Theodosius (2012)	triangular culvert	Triangular
Tan (2013)	-	Rectangular
Akhtar (2014)	non-uniform sediments	Rectangular
Surya (2014)	non-uniform sediments	Trapezoidal
Miao (2015)	non-uniform variable	Trapezoidal
Das (2015)	shape effect (compare with current study)	Trapezoidal, Rectangular
Current study	shape effect (compare with Das (2016)), slotted jet	Rectangular

Table 2.2 Full flowing circular jet scour experiments from NTU

Researcher	Experiment variable
Lim (unpublished)	various variables
Tay (1996)	shallowly submerged to deeply submerged tailwater depth
Seah (1997)	unsubmerged to deeply submerged tailwater depth
Lau (1998)	small difference in sediment non-uniformity
Chia (2000)	jet diameter
Tan (2003)	-
Zaihan (2014)	small scale jet scour
Salam (2016)	unsubmerged and shallowly submerged scour
Pee (2016)	jet diameter

2.6 Jet scour prediction equations

This section discusses 3D jet scour prediction equations. As for 2D jet scour, early 2D free falling jet scour equations for scour depth has been analyzed by Mason and Arumugam (1985), and Melville and

Lim (2014) have summarized equations for 2D horizontal jets. Mason and Arumugam (1985) noted that the formulae suitable for model scale prediction did not perform as well for prototype scale, and vice versa.

Various equations have been proposed by different researchers to predict maximum scour dimensions caused by 3D horizontal jet scour. Most of the equations focused only on scour depth as undermining of culvert foundation is undesirable. While most of the equations are empirical equations, Iwagaki et al. (1958) studied 3D jet scour problem analytically while Hoffmans (1998) proposed semi-empirical equations. Other researchers have their own preferred form of equation or method of formulating equation. Some equations were adapted into engineering manuals.

The available engineering manuals use equation obtained from systematic study done by Abt and co-workers. The manual published by the Construction Industry Research and Information Association (CIRIA) (May et al. 2002) suggested formulae by Ruff et al. (1982) for circular and square culvert scour maximum scour depth prediction. The maximum scour length and maximum scour width are 7 times and 5 times the maximum scour depth, respectively. The manual recommended installation of headwall, and directed the reader to works by Breusers and Raudkivi (1991) and Hoffmans and Verheij (1997) for more details. The Hydraulic Engineering Circular 14, also known as HEC-14 3rd edition (Thompson and Kilgore 2006) presented culvert flow classification for outlet velocity calculation. Adaptation of works by Bohan (1970) and Abt and co-workers were presented as scour hole dimensions prediction equations. The equations and their respective tables of coefficients has included the duration (peak flow duration or at least 30 minutes), velocity, hydraulic radius (assumed full flowing outlet), sediment gradation, drop height, and culvert slope.

Iwagaki et al (1958) derived analytical equation for 3D circular jet scour depth from continuity equation by using polar coordinate system, by which 3D jet can be treated as 2D. The derivation started from ideal fluid and flat solid bottom, then extended to include boundary layer theory, jet diffusion, unsubmerged jet outlet, and sediment transport theory. The authors worked on vertical circular jets and inclined circular jet. Experiment verification for both vertical and inclined unsubmerged jets was carried out. Interestingly, a dimensionless number same as F_o was found to be able to describe sediment characteristics.

Proposing equation from data can be done by visually curve fitting or regression analysis. The former is used by most early researchers for engineering practicality and the latter is more recent and usually

includes more parameters. Curve fitting can be done for best fit or enveloping equation (Ade and Rajaratnam 1998; Lim 1995). Some researchers favor simple equations, for example Chiew and Lim (1996) and Rajaratnam (Ade and Rajaratnam 1998) almost always used F_o only in their equations.

Different approaches have been used to improve prediction accuracy or to include more parameters of the equations. One of the underlying assumption is that the different variables affecting scour hole dimension can be super positioned by multiplying the respective variables. Examples are equation proposed by Pagliara and co-workers using different multiplicative functions for each variables of a plunging jet (Pagliara et al. 2010) and K-factors used by Melville and co-workers (Melville and Lim 2014). Piecewise equation is proposed by some researchers for example Lim (1995). Sorting data into groups and proposing equations for each group has been done by Ade and Rajaratnam (1998). Hoffmans (1998) proposed semi empirical equations. Some recent equations have specific function for certain parameter depending on the range of another parameter, for example Sarathi et al. (2008), whose equations contained grouping, piecewise, and extra functions for coefficients. In summary, one of the clear trends is the increasing use of densimetric Froude number to replace Froude number. Densimetric Froude number has been used as early as 1970 (O'Loughlin et al. 1970).

For 3D horizontal jet scour, systematic regression analysis has been carried out by Secadiningrat (2012), Shue (2013), and Surya (2014). Shue (2013) analysis of full flowing jet scour using linear regression. Secadiningrat (2012) analyzed non-full flowing data using multiple linear regression. His work was then expanded by Surya (2014) to include incomplete similarity analysis concept. However, due to the relatively small number of dataset, the marginal improvement of incomplete similarity was offset by the large number of coefficients.

Table 2.3 lists the equations for equilibrium scour hole dimensions formed by simple horizontal 3D jet. The equations are presented in chronological order. Even for such a limited pool of equations in jet scour research, some trends can be seen in the development of the equations. Firstly, different velocity ratios were used in earlier days, and almost only F_o is used in recent studies. Next, the format of the equations started as complex form and moved towards simpler form, and recent studies tried to incorporate effect of different parameters. From this evolution, it shows that the researchers were aware of effect of different parameters on scour action, thus the earlier complex form. However, the relative smaller effect of other parameters makes F_o as the most important dimensionless number for engineering purpose. Additional of other parameters, or even other prediction method (see section 2.4.4) are new efforts to obtain generalized scour prediction equations.

Table 2.3 Equation proposed by various researchers for 3D horizonal jet scour at equilibrium phase

Researcher	Proposed equation(s)
Rajaratnam and Berry (1977)	$\frac{d_{se}}{d_o} = F_o - 2$ as in Hoffmans (1997)
Rajaratnam and Diebel (1981)	$\frac{d_{se}}{d_o} = 0.41\ F_o - 0.067$
Abt et al. (1984)	$\frac{d_{sm}}{d_o(\sigma_g)^{0.4}} = \frac{3.65}{\sigma_g^{0.4}}\left[\left(\frac{Q}{g^{0.5}d_o^{2.5}}\right)\left(\frac{d_{50}}{d_o}\right)^{0.2}\right]^{0.57}$ $\frac{d_{se}}{R_h} = 14.68\ F_o^{0.57}\left(\frac{d_{50}}{4R_h}\right)^{0.4}(\sigma_g)^{-0.4}$ as in Lim (1995) $\frac{W_{sm}}{d_o(\sigma_g)^{0.4}} = \frac{19.25}{\sigma_g^{0.4}}\left[\left(\frac{Q}{g^{0.5}d_o^{2.5}}\right)\left(\frac{d_{50}}{d_o}\right)^{0.2}\right]^{0.64}$ $\frac{L_{sm}}{d_o(\sigma_g)^{0.4}} = \frac{35.22}{\sigma_g^{0.4}}\left[\left(\frac{Q}{g^{0.5}d_o^{2.5}}\right)\left(\frac{d_{50}}{d_o}\right)^{0.2}\right]^{0.51}$ $\frac{V_{sm}}{d_o^3(\sigma_g)^{0.4}} = \frac{550}{\sigma_g^{0.4}}\left[\left(\frac{Q}{g^{0.5}d_o^{2.5}}\right)\left(\frac{d_{50}}{d_o}\right)^{0.2}\right]^{1.71}$
Ali and Lim (1986)	$\frac{d_{se}}{R_h} = 2.3\left(\frac{U_o}{w}\right)^{\frac{1}{2}}\left(\frac{d_{50}}{R_h}\right)^{\frac{3}{8}}F_o^{\frac{3}{4}} - 1.19$ low tailwater depth (*H/do* ≅ 1)
Abida the Townsend (1991)	$\frac{d_s}{d_o} = \left(\exp\frac{F_r-2}{2.03} - 0.373\right)\left(\frac{d_m}{H}\right)^{-0.275}$ 0.3 < *H/d*$_o$ < 0.7, and tailwater depth is equal to culvert flow depth.
Breussers and Raudkivi (1991)	Jet scour $\frac{d_s}{d_o} = 0.08\ \frac{U_o}{u_{*c}}$ Culvert scour $\frac{d_s}{d_o} = 0.65\ \left(\frac{U_o}{u_{*c}}\right)^{1/3}$ $\frac{d_{se}}{R_h} = 4.4\ F_o^{0.33}$ as in Lim (1995)
Lim (1995)	Best fit $\frac{d_{se}}{R_h} = 1.28\ F_o$ Enveloping $\frac{d_{se}}{R_h} = 1.8\ F_o \quad for\ 1 < F_o < 10$ $\frac{d_{se}}{R_h} = 18 \quad for\ F_o > 10$
Chiew and Lim (1996)	$\frac{d_{se}}{R_h} = 0.84\ F_o$ $\frac{W_{se}}{R_h} = 7.60\ F_o^{0.75}$ $\frac{L_{se}}{R_h} = 17.64\ F_o^{0.75}$
Hoffmans (1998)	Maximum scour depth $y_{m,e} = c_{3H}\left[\frac{Q(U_1-U_2)}{g}\right]^{\frac{1}{3}}$, $c_{3H} = \frac{7}{(D_{90*})^{1/3}}$ for *d*$_{90}$ < 0.0125m, $D_{90*} = d_{90}\left(\frac{\Delta g}{\nu^2}\right)^{1/3}$ *U*$_1$ = mean jet velocity, *U*$_2$ = mean downstream velocity

Ade and Rajaratnam (1998)	d_{se} Best fit $\frac{d_{se}}{R_h} = 1.8\,F_o - 1.24$ d_{se} Enveloping $\frac{d_{se}}{R_h} = 2(\,F_o + 1)$ d_{se} Enveloping (unsubmerged, 0.6 < F_o <10) $\frac{d_{se}}{R_h} = 2\,F_o$ d_{se} Enveloping (unsubmerged, 10 < F_o <100) $\frac{d_{se}}{R_h} = 19 + 0.1\,F_o$ W_{se} Best fit $\frac{W_{se}}{R_h} = 7.2(\,F_o - 0.2)$ W_{se} Enveloping $\frac{W_{se}}{R_h} = 7.2(\,F_o + 2)$ L_{se} Best fit $\frac{L_{se}}{R_h} = 12(\,F_o - 0.27)$ L_{se} Enveloping $\frac{L_{se}}{R_h} = 13.2\,(F_o + 2)$
Liriano (1999)	$\frac{d_{se}}{d_o} = a\ln(F_o) + b$ where $a = 0.87\left(\frac{H}{d_o}\right)^{-0.37}$, $b = 0.20\ln\left(\frac{H}{d_o}\right) - 0.24$
Sarathi et al. (2008)	Depth $\frac{d_{se}}{d_o} = A\ln(F_o - B)$ for 0.5 ≤ H/d_o ≤ 3, $A = 0.66\ln\left(\frac{H}{d_o}\right) + 2.34$ $B = 1.31\ln\left(\frac{H}{d_o}\right) + 1.73$ for H/d_o ≥ 4, $\frac{d_{se}}{d_o} = 2.55\ln(F_o) - 2.44$ Width for H/d_o = 1, $\frac{W_{se}}{d_o} = 2.1F_o - 0.95$ for H/d_o ≥ 2, $\frac{W_{se}}{d_o} = 2.1F_o - 1.2$ Length $\frac{L_{se}}{d_o} = 2.86F_o + 3.24$ Volume $\frac{V_{se}}{d_o^3} = MF_o^N$ for H/d_o = 1, $M = 1.14;\ N = 2.76$ for 2 ≤ H/d_o ≤ 4, $M = 0.12\left(\frac{H}{d_o}\right) - 0.12;\ N = 4.20 - 0.27\left(\frac{H}{d_o}\right)$ for 6 ≤ H/d_o ≤ 18, $M = 0.3;\ N = 3.19$
Sui et al. (2008)	$\frac{d_{se}}{H} = 3\times10^{-5}\left(\frac{F_o\left(\frac{B}{d_o}\right)^{0.1}}{\frac{H}{d_o}}\right)^3 - 3.3\times10^{-3}\left(\frac{F_o\left(\frac{B}{d_o}\right)^{0.1}}{\frac{H}{d_o}}\right)^2 + 28.5\times10^{-2}\left(\frac{F_o\left(\frac{B}{d_o}\right)^{0.1}}{\frac{H}{d_o}}\right)$

2.7 Conclusions

This chapter has presented a literature review of past researches in jet scour, focusing on 3D jet and culvert scour which is the scope of current study. The most important dimensionless number has been agreed to be the densimetric Froude number given its wide use by recent researchers, appreciating the importance of both the properties of the incoming jet flow and the sediment. Current understanding on 3D horizontal jet scour is sufficient for engineering protection purpose at the culvert outlet. Other factors such as relative tailwater depth, culvert shape, and relative sediment size, even though known to be influencing the scouring process, remained debatable or have contradicting observations. These areas that are worthy for further investigation are highlighted in the review.

The effect of culvert shape has only been investigated on the extent of its influences on scour hole size, but the detailed observation is absent in available literature. The effect of relative tailwater depth has mostly been investigated in narrow range covering only unsubmerged outlet or wide range covering only submerged outlet. The transition of the value of this dimensionless number from smaller than unity to larger than that remains unknown. Especially when this dimensionless number is used in scour prediction equation, it is believed to have different meaning depending on its value. As for the relative sediment size, constraint on sediment size has led to negligence of this dimensionless parameter. However, given the similar research carried out in pier scour, a database compiled of experiments with different experimental conditions provided an opportunity to look further into this aspect. The corresponding experiments have been carried out and will be presented in Chapter 3. in Chapter 4, the effect of culvert shape is discussed in detail by presenting both the current study experimental results and the evidence from a compiled database.

The reviewed equations are mostly for jet scour and assumed full flowing outlet. Thus, the analysis of data presented in Chapter 5 will merge this gap by analyzing both the data of jet and culvert scour together. Following the trend, F_o will be used as the main parameter in the scour hole size prediction equation. The influences of relative tailwater depth and relative sediment size are also discussed.

Chapter 3 Jet and culvert scour experiments in current study

3.1 Introduction

This chapter presents the experiments performed during current study. The experiments investigated the research gaps in 3D jet and culvert scour research highlighted in Chapter 2. The general experimental procedure for both 3D jet and culvert scour experiments is outlined first. Next, five series of experiments are presented in Sections 3.3 – 3.7. The presentation in this chapter focuses on visual observations of the experiments. The measurement of scour hole contours at the datum level and the centerline profiles are presented and discussed. Dimensional analysis and data analysis of the current data together with the compiled database from previous studies is presented in Chapters 4 and 5.

The 5 series of experiments are:

1. Small scale circular jet scour experiments (Section 3.3) investigating the effect of relative sediment size and relative tailwater depth.

2. Scale series circular jet scour experiments (Section 3.4) investigating the effect of relative sediment size.

3. Jet scour experiments at unsubmerged and shallowly submerged outlet conditions (Section 3.5) investigating the effect of relative tailwater depth.

4. Trapezoidal culvert scour experiments (Section 3.6) investigating culvert shape effect.

5. Rectangular culvert scour experiments with slotted jet experiments (Section 3.7) investigating culvert shape effect.

Each series of experiments are first presented individually, and the discussion across different series is presented in subsequent section. The presentation focuses on the general experimental plan and the observation on scour hole contours at the datum level and the centerline profiles. Comparison between different experimental runs is done by normalizing the contours and centerline profiles using the maximum dimensions along the respective axes respectively. Subsequent section discusses the experimental findings collectively.

3.2 General experimental procedure

The general experimental procedure and setup are the same for both culvert scour and jet scour experiments. The experimental flume consists of an upstream section, where the model culvert is installed. The middle section is the sand bed with sufficient depth. The end of the flume is a sand trap followed by an adjustable tailgate. Figure 3.1 shows the sketch of the longitudinal section and plan view of the culvert or pipe and the sediment bed at the beginning and at the end of an experiment.

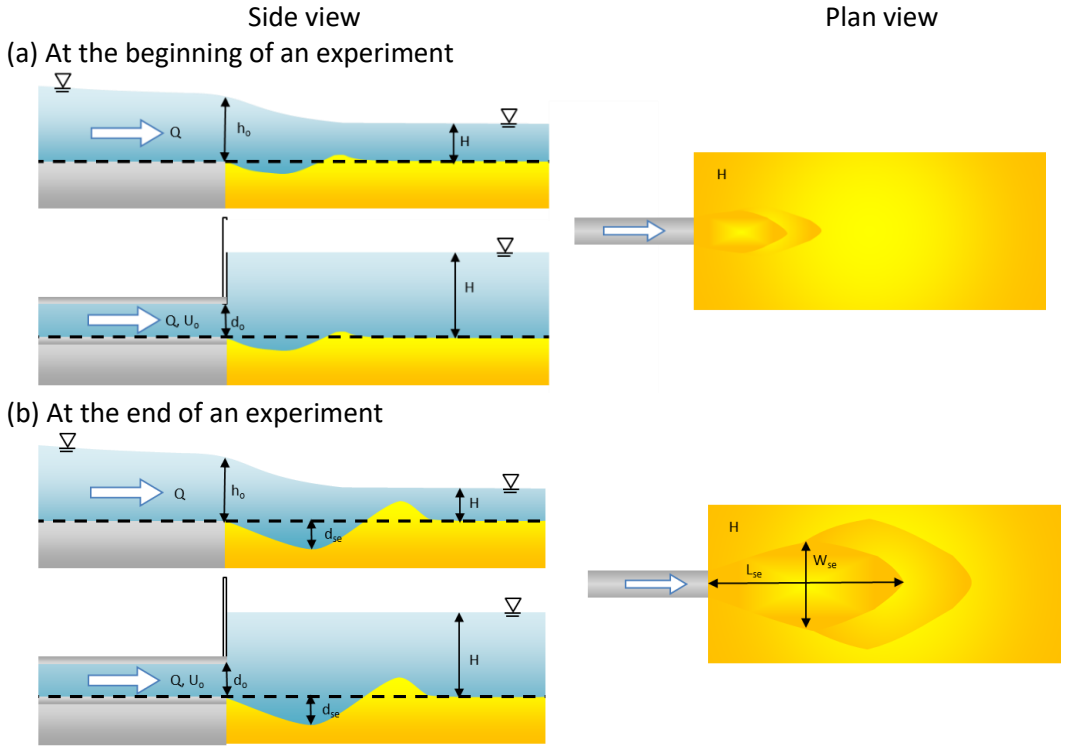

Figure 3.1 Sketch of the longitudinal section and plan view of the culvert or pipe and the sediment bed (a) at the beginning and (b) at the end of an experiment.

The sediment bed was first leveled and checked to be at the same height as the culvert or pipe invert. This level is denoted as the "datum level" and all flow properties and scour measurements are measured with reference to this level. If the sediment is non-uniform, it must be mixed thoroughly before leveling. Next, water was filled slowly into the sediment bed and caution should be taken to avoid any scouring prior to the start of the experiment. At the same time, the tailgate was adjusted to the desired tailwater level. After water started overflowing from the tailgate, the main jet flow was started and adjusted to the desired flowrate. Adjustment at the tailgate might be required. The experiment was started when the main jet flow was adjusted to the desired flow rate and the desired tailwater depth was achieved.

After the experiment had started (Figure 3.1a), the flowrate and tailwater depth were recorded. For culvert scour experiments, the flow depths within and along the culvert barrel and the brink depth were also recorded. The experiments were run for about at least 2 days. When beginning a new series of experiments, visual observation and checking of experimental condition were done frequently to ensure stability of the experiment, and to ensure the equilibrium scour state was reached at the end of the experiment. 2 days of experimental duration is sufficient to ensure the scour hole has reached equilibrium condition.

Before ending the experiment (Figure 3.1b), the flowrate, tailwater depth, brink depth and flow depth along the culvert barrel were again recorded. After recording the test duration and stopping the main jet flow, water was drained slowly to ensure the scoured area was not disturbed. The maximum scour length (L_{se}) and width (W_{se}) were measured when the water level was at the datum level. A white thread was used to mark out the zero-level contour of the scour hole when applicable. The water was then further drained, and threaded contours were taken at appropriate levels whenever applicable. When the water was drained to below the scour hole maximum depth, the maximum scour depth (d_{se}) of the scour hole was located and recorded. Next, the centerline profile, or the thalweg for asymmetrical hole, of the scour hole was recorded from the outlet to the end of sediment ridge. The volume of the scour hole (V_{se}) was measured by laying a piece of plastic sheet larger than the scour hole and filling in water of known volume until water level reached the datum level.

Experimental Series 1 and 2 were carried out in a flume 8 m long, 0.3 m wide, and 0.6 m deep. The circular pipes used were at least 1 m long and aligned horizontally along the centerline of the flume on a solid surface before the sand bed section. The sand bed was 15 cm deep and 1.5 m long. Experimental Series 3, 4, and 5 were conducted in a flume 3.7 m long, 1 m wide, and 0.6 m deep. The upstream section was 2 m long, where the 1.7 m long model culvert was installed along the centerline of the flume. The sediment bed was 1.5 m long and 0.3 m deep.

3.3 Small scale jet scour experiments

A series of small scale experiments using a 4 mm diameter circular jet was conducted. The experiments used 2 different sediments and varied tailwater depths, even though the tailwater depths tested were almost entirely in the range having minimal effect as reported in the literature. Table 3.1 lists the experimental plan. Detailed experimental parameters and results are listed in the Appendix. Figures

3.2 – 3.5 show the contours at datum level, centerline profiles, normalized contours, and normalized centerline profiles of the scour hole respectively.

Table 3.1 Experimental plan for small scale jet scour experiment.

Jet velocity, U_o (m/s), and Run no.		Sediment properties			
		d_{50} = 1.55 mm, σ_g = 1.2		d_{50} = 0.77 mm, σ_g = 1.15	
H/d_o	7.5	U_o = 2.110 Run 111	U_o = 1.504 Run 121	U_o = 2.150 Run 211	U_o = 1.519 Run 221
	15	U_o = 2.124 Run 112	U_o = 1.501 Run 122	U_o = 2.150 Run 212	U_o = 1.505 Run 222
	22.5	U_o = 2.110 Run 113	U_o = 1.504 Run 123	U_o = 2.128 Run 213	U_o = 1.518 Run 223
	30	-	U_o = 1.757 Run 124	-	-

Note: H = tailwater depth, U_o = mean jet velocity, d_o = jet diameter, d_{50} = median sediment diameter, σ_g = sediment gradation

From Figure 3.2, the contours can be categorized into 3 groups. They are the largest 3 contours, the smallest 3 contours, and the rest in between these 2 groups. In ascending order, the 3 groups correspond to those produced by the larger sand with lower velocity, those produced by the finer sand with lower velocity and those by larger sand with higher velocity, and those produced by finer sand with higher velocity. The corresponding densimetric Froude number (F_o) falls into 3 distinct groups (F_o = 9.47 – 9.49, 13.31 – 13.61, and 19.06 – 19.26, refer to Appendix). This verified that F_o is suitable to correlate the scour hole dimensions across different sediment sizes. The effects of sediment size and tailwater depth are minimal, and possibly related to the value of other parameters including F_o.

From Figure 3.3, slight distortion at the peak of the ridge can be seen for the runs tested using the smallest relative tailwater depth of 7.5. The distortion is more obvious for the runs using finer sand with high velocity. The upstream side of the ridge has two slopes, caused by the water jet unable to lift the scoured sediment over the high ridge during the experiments. This suggested that if a ridge removal test was done under the same condition, the scour hole might be larger. Figure 3.6 shows some relevant photographs on the different slopes during and after the experiment.

Besides, near to the jet outlet, the entrained flow at both sides of the jet resulted in slight depressed area of sand is sometimes show up in contour plot (Figure 3.2). From Figures 3.4 and 3.5, the non-dimensionalized scour hole contours and centerline profiles show that the scour holes are all similar despite the different experimental conditions.

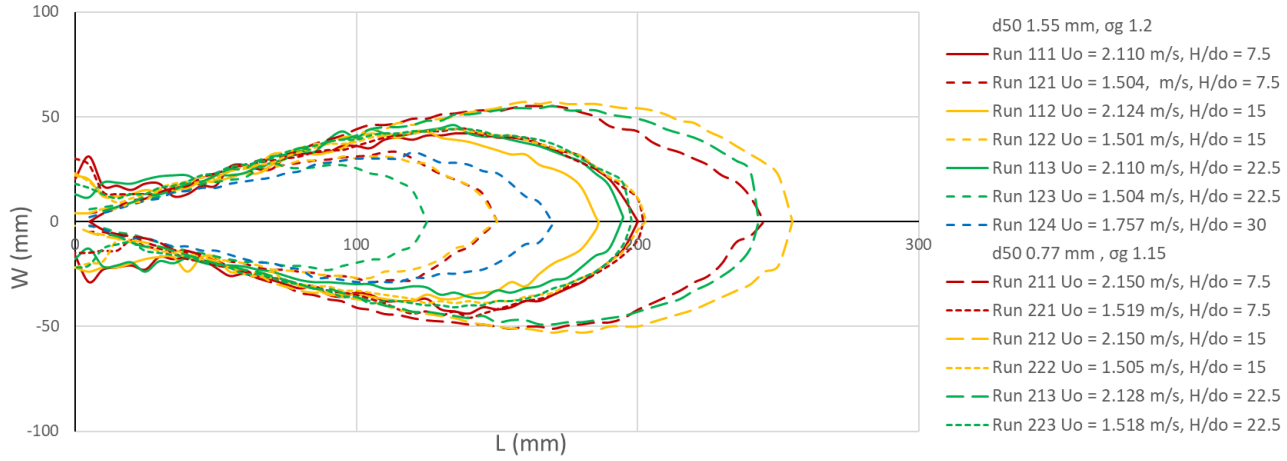

Figure 3.2 Bed contours at datum level of the small scale jet scour experiments.

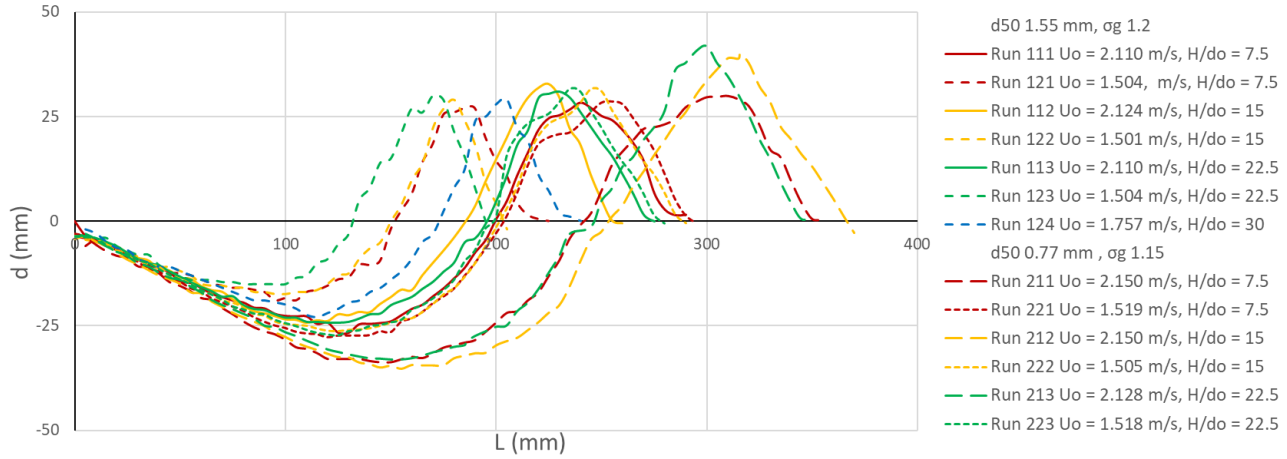

Figure 3.3 Centerline profiles of the scour holes from the small scale jet scour experiments.

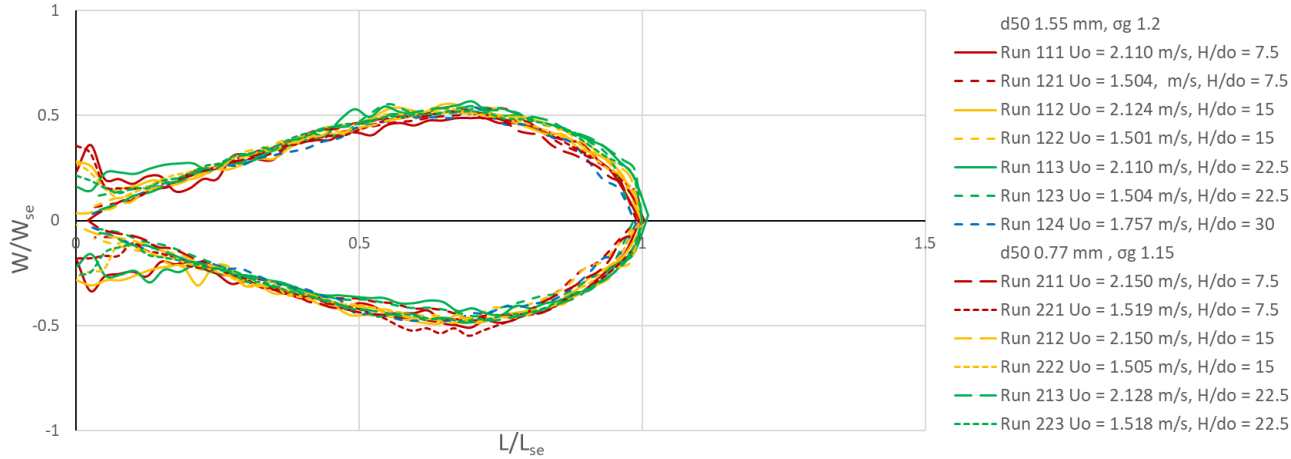

Figure 3.4 Normalized contour of the small scale jet scout experiments.

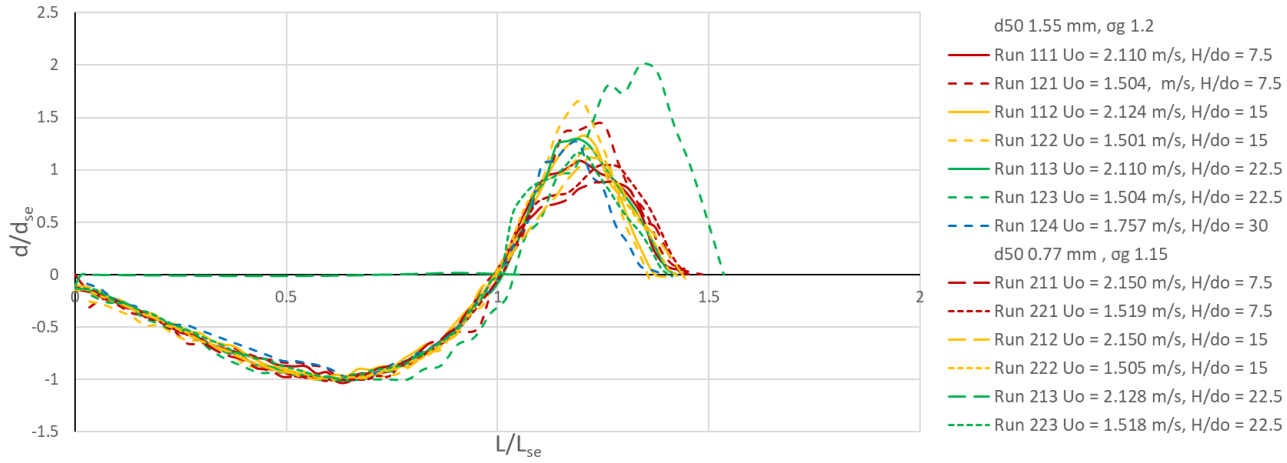

Figure 3.5 Normalized centerline of the small scale jet scour experiments.

(a) (b)

Figure 3.6 The discontinuity on the slope at the upstream face of the ridge during the experiment (a) and after the experiment (b). Photos taken during Run 213.

3.4 Deeply submerged jet scour experiments with different jet sizes

This series of experiments used the same sediment (d_{50} = 0.77 mm, σ_g = 1.17) and jet diameter of 8 mm, 12 mm, 16 mm, and 20 mm. The tailwater depth was maintained at H/d_o = 15 to minimize its influence. The jet velocities were controlled such that the widest possible range was covered for a particular jet size, and also to ensure common F_o were used across different jet sizes, such that direct comparison could be done. Table 3.2 lists the experimental plan. The detailed record can be found in the Appendix.

Table 3.2 Experimental plan for scale series experiment.

Run no.		Jet velocity, U_o (m/s)							
		U_o = 0.5	U_o = 0.6	U_o = 0.8	U_o = 1	U_o = 1.1	U_o = 1.2	U_o = 1.5	U_o = 2.1
Jet size, d_o (mm)	8	-	-	-	Run 19	-	Run 18	Run 17	Run 16
	12	-	Run 10,15	Run 11,14	Run 12	-	Run 13	-	-
	16	-	Run 1, 3	Run 2	Run 4	Run 5	-	-	-
	20	Run 9	Run 6	Run 7	Run 8	-	-	-	-

Figures 3.7 – 3.10 show the bed contours, centerline profiles, normalized bed contours, and normalized centerline profiles of the experiments respectively. The scour holes were all different sizes due to the jet size despite the same velocity was used. Figures 3.9 and 3.10 show that all the scour holes collapsed into the same normalized contours and profiles. This shows that the jet size does not affect scour hole similarity as long as the tailwater depth is maintained at the same deeply submerged condition. The normalized contours show some of the distortion caused by recirculating flows near the jet outlet. The normalized centerline profiles show some scour hole have high normalized ridge peak, and those runs are not those with the highest jet velocity. This suggests that the scour hole ridge is affected by both the velocity and sediment properties.

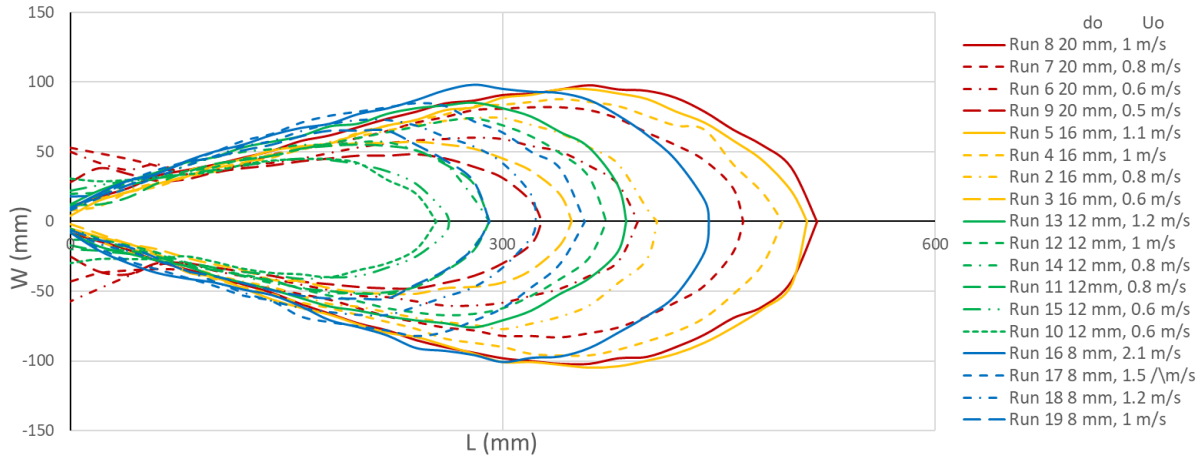

Figure 3.7 Contour at datum level of scour holes produced using different jet sizes.

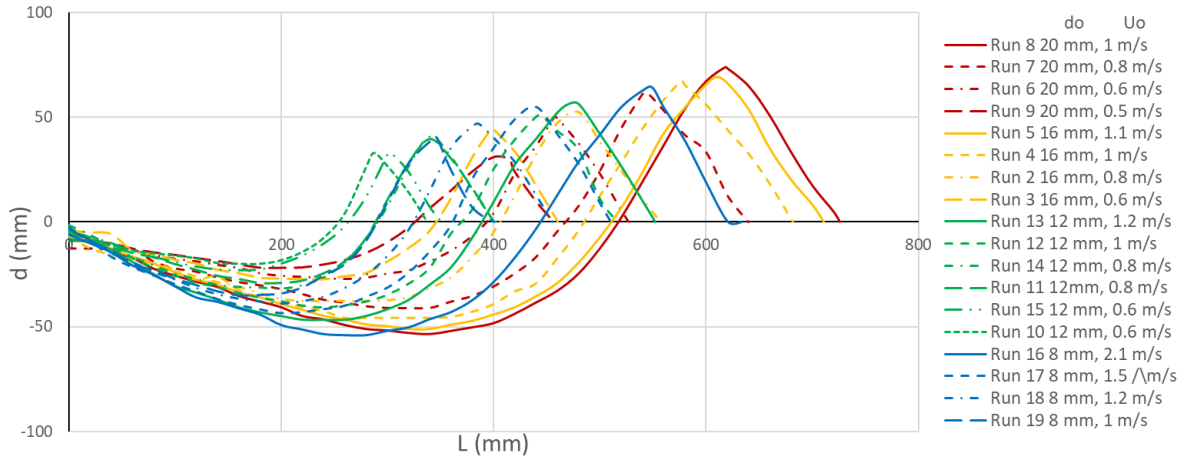

Figure 3.8 Centerline profiles of the scour holes produced using different jet sizes.

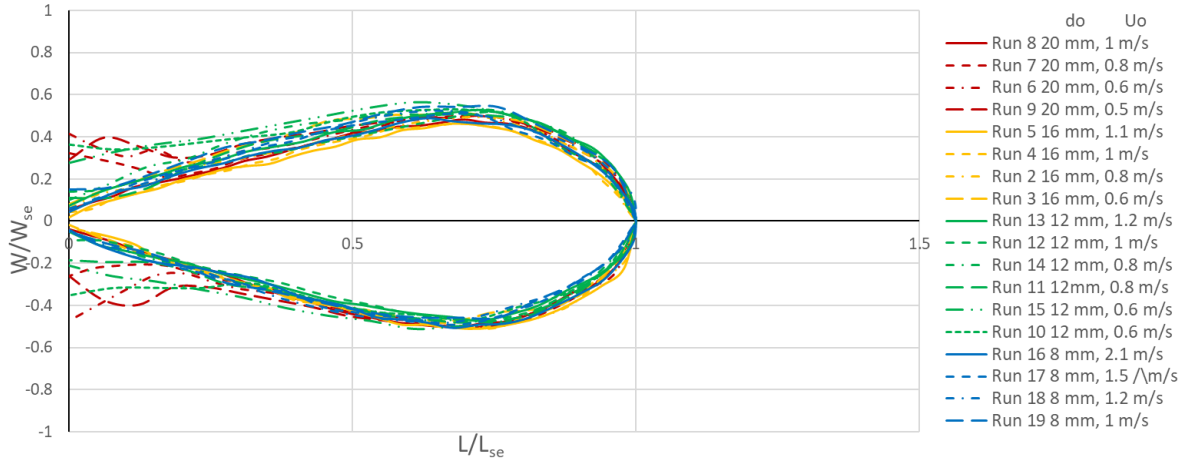

Figure 3.9 Normalized contour of the scour holes from the jet size experiments.

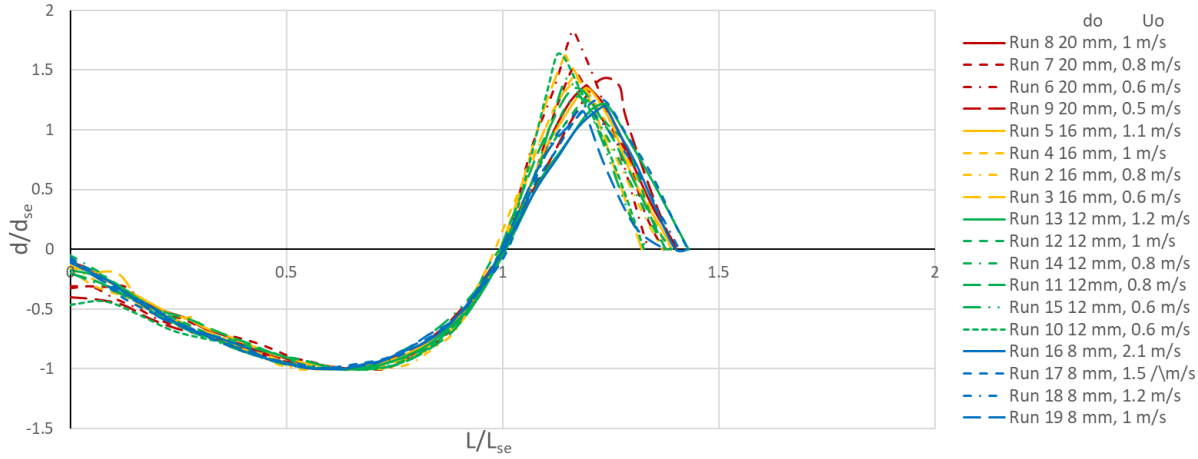

Figure 3.10 Normalized centerline profiles of the scour holes from the jet size experiments.

3.5 Jet scour experiments at unsubmerged and shallowly submerged outlet conditions

A series of experiments was conducted at H/d_o = 0.5, 1, 2, and 4 using a 27.5 mm diameter circular pipe. The objective of this series is to investigate in more details about the effect of tailwater depth and to explore the influence of H/d_o when its value is smaller or slightly larger than unity. Table 3.3 lists the experimental plan. Similarity, the jet flow rate was planned to ensure the same velocity was used at different relative tailwater depth to enable direct comparison.

Table 3.3 Experimental plan for relative tailwater depth experiments

Run no.		Jet velocity, U_o (m/s)				
H/d_o	0.5	U_o = 0.730 Run 12	U_o = 0.800 Run 5	U_o = 0.992 Run 16	U_o = 1.041 Run 8	
	1	U_o = 0.746 Run 11	U_o = 0.826 Run 4	U_o = 0.993 Run 15	U_o = 1.160 Run 7	
	2		U_o = 0.834 Run 3	U_o = 1.027 Run 13	U_o = 1.169 Run 6	U_o = 1.258 Run 10
	4		U_o = 0.823 Run 1	U_o = 0.991 Run 14	U_o = 1.143 Run 2	U_o = 1.258 Run 9

Figures 3.11 – 3.14 show the bed contours, centerline profiles, normalized contours, and normalized centerline profiles of the scour holes. The presentation splits the experiments according to the jet velocity. From the figures, the difference due to the relative tailwater depth is consistent. Generally, under the same velocity range, the lower tailwater depth resulted in wider and more irregular scour hole. For the highest velocity used (Figure 3.11e and 3.12e), the scour holes produced at H/d_o = 2 have similar appearance as those produced under unsubmerged outlet condition. This suggests that occurrence of wide or irregular scour hole depends on both the relative tailwater depth and the jet velocity. The tailwater depth affects most heavily on the scour hole ridge (Figure 3.12). The recirculating flows at both sides of the outlet contribute to the irregular scour hole width especially at the location before the maximum scour depth. Some of the recirculating flow and plunging effect due to the unsubmerged outlet can be seen from the centerline profiles having deep and flatter section before the location of maximum scour depth.

From the normalized bed contour plot (Figure 3.13), the sides affected by the recirculating flows can be seen being wider than the width of the main scour hole. Thus, in practice, caution need to be taken if a culvert outlet is expected to have unsubmerged or shallowly submerged outlet condition as the strength of the recirculating flows must not be overlooked. On the other hand, the normalized centerline profiles (Figure 3.14) show that the upstream section affected by the plunging flow

generally does not exceed the maximum scour depth of the main scour hole. The difference in ridge height is more obvious in the normalized plot.

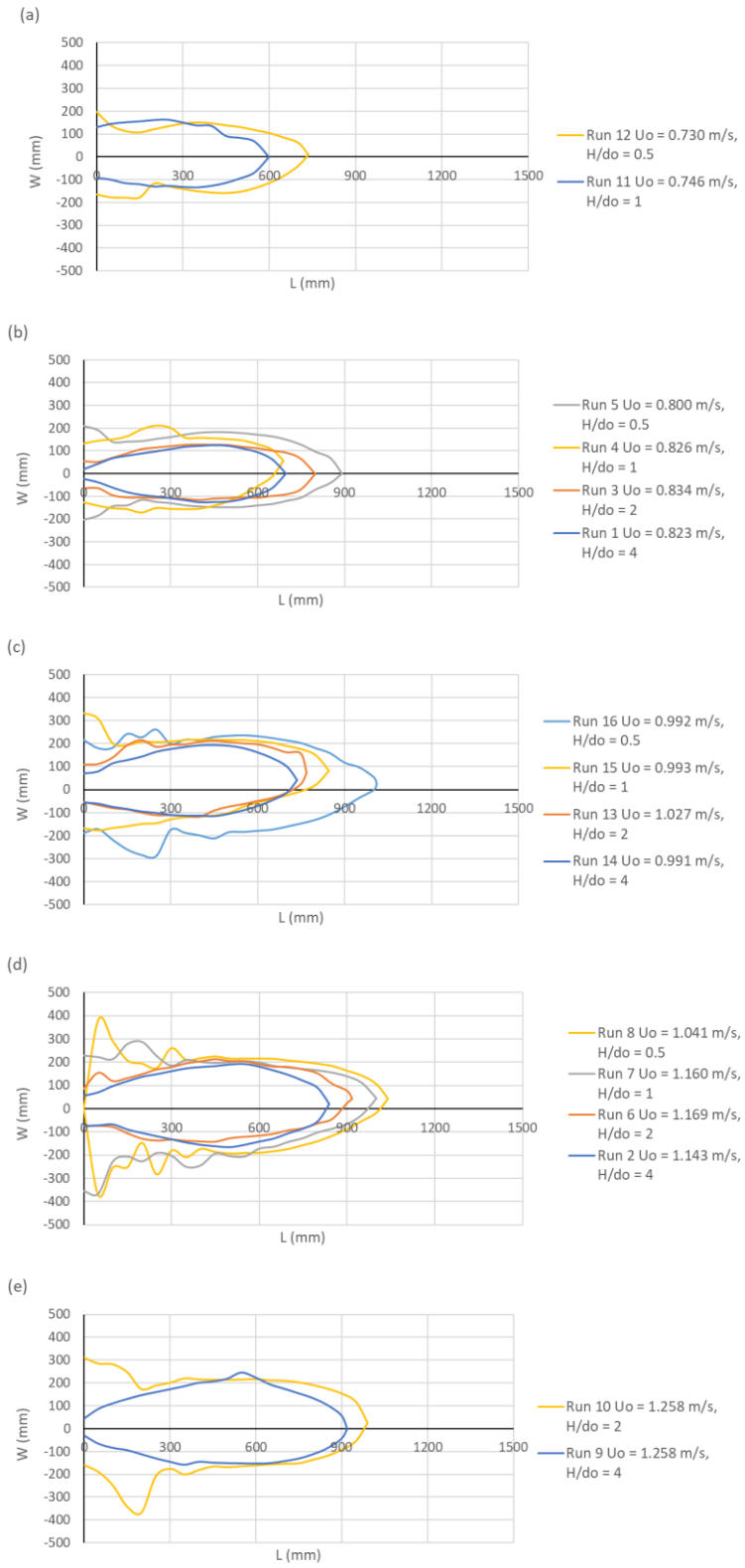

Figure 3.11 Bed contours at datum level at different outlet submergence grouped by jet velocity.

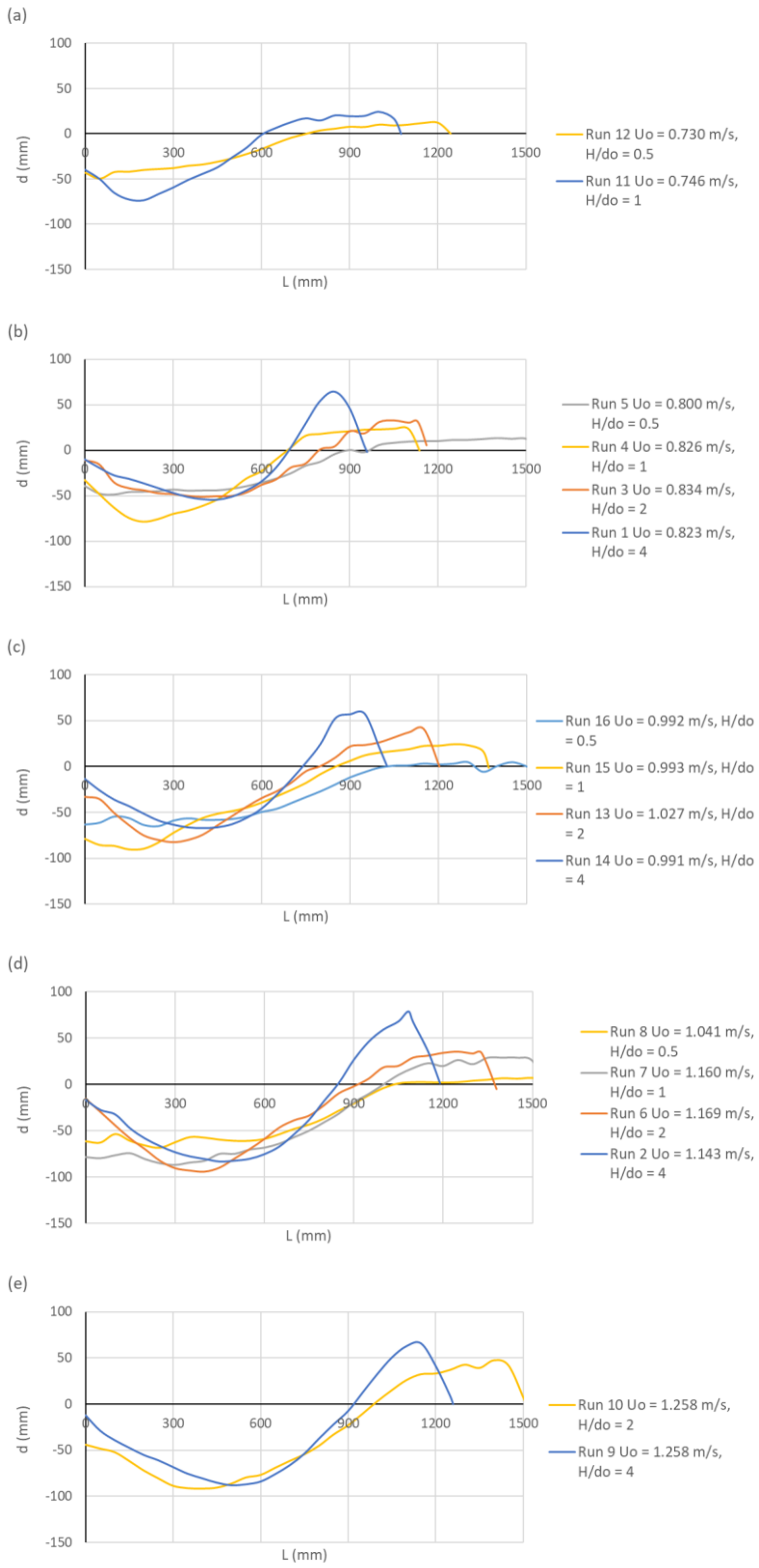

Figure 3.12 Centerline profiles at different outlet submergence conditions grouped by jet velocity.

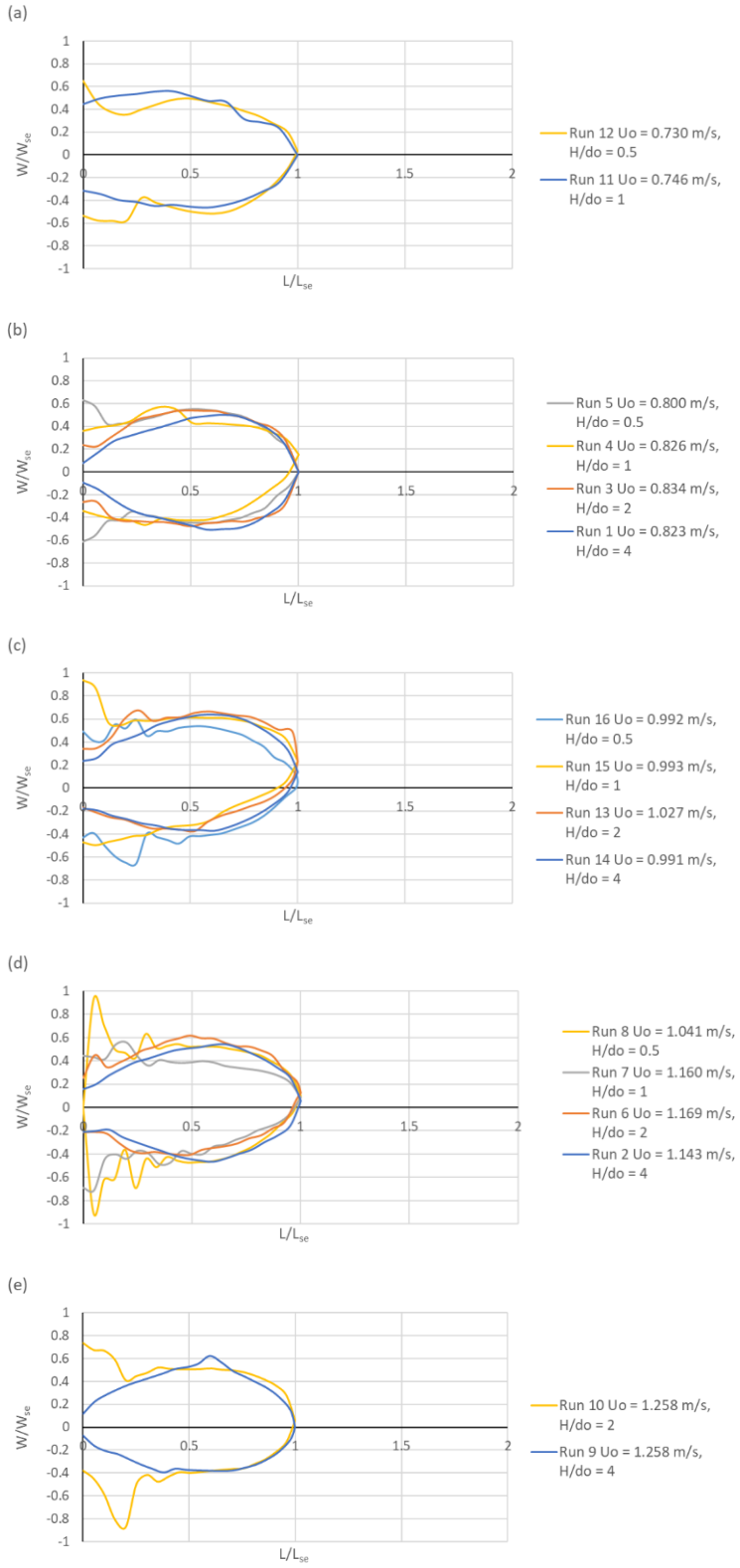

Figure 3.13 Normalized bed contours of the scour holes at different outlet submergence and grouped by velocity.

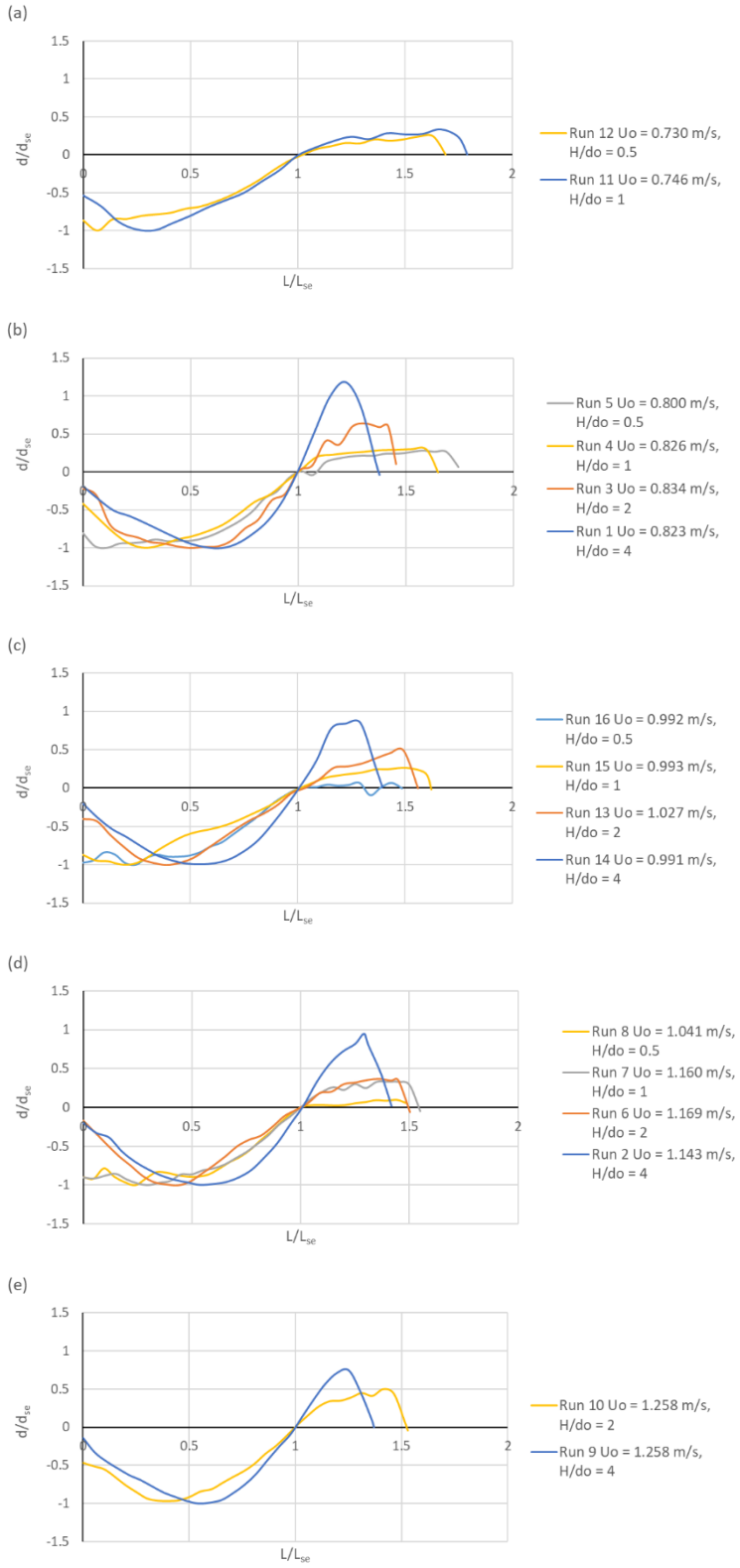

Figure 3.14 Normalized centerline profiles at different outlet submergence grouped by jet velocity.

Typical photos of the scour holes are shown in Figure 3.15. The photos clearly show the difference between each scour hole as affected by the jet outlet submergence. The tailwater depth is the availability of space for the jet energy to diffuse, and the lack of it resulting in strong recirculating flow

and plunging flows at unsubmerged outlet condition. The total area affected by the jet scour including the ridge area is larger when the outlet submergence is low. This is usually not documented as jet scour research focuses on the scouring action rather than the sediment depositing action downstream of the scour hole.

(a) Run 16 H/d_o = 0.5

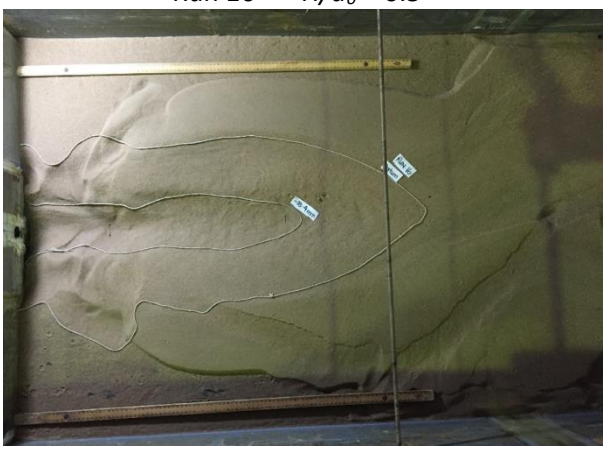

Thread contour at datum level and -33 mm.

(b) Run 15 H/d_o = 1

Thread contour at datum level and -34 mm.

(c) Run 13 H/d_o = 2

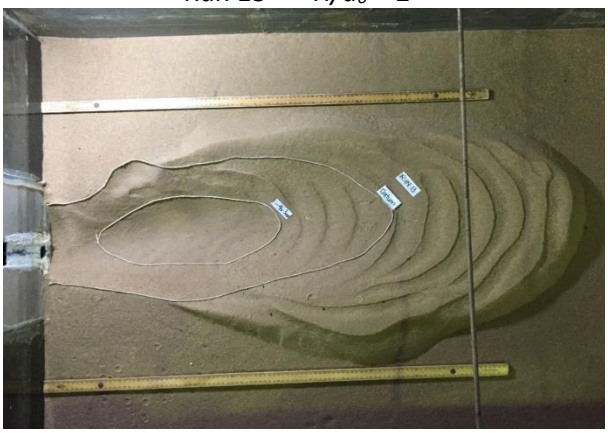

Thread contour at datum level and -43 mm.

(d) Run 14 H/d_o = 4

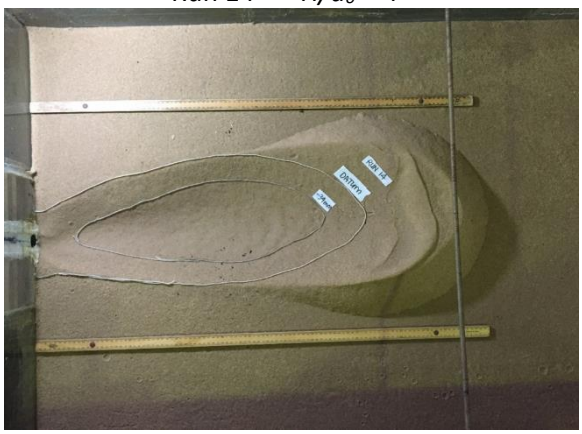

Thread contour at datum level and -34 mm.

Figure 3.15 Typical photos of the scour hole under different outlet submergence under similar jet velocity of 1 m/s.

3.6 Trapezoidal culvert scour experiments with preliminary studies using rectangular culvert

Trapezoidal model culvert with 50 mm base and slope H:V = 1:1 (H = horizontal, V = vertical) was used in this series of experiments. The sediment has d_{50} = 0.49 mm and σ_g = 1.47. The experiments were carried out at pre-planned tailwater depth range. The outlet velocity was varied by varying the pump

flow rate, but since it is affected by the tailwater depth, precise control is impossible. Even though the resulting outlet velocity is in a rather narrow range, the experimental results shows that culvert scour is very sensitive to the jet velocity. Table 3.4 lists the experimental plan for the trapezoidal culvert experiment series. A few runs were carried out as preliminary studies using a 50 mm wide rectangular culvert.

Table 3.4 Experimental plan for the trapezoidal culvert series.

Trapezoidal culvert		Flow velocity at culvert outlet, U_o (m/s)				
H (mm)	minimum	U_o = 0.498 Run 3	U_o = 0.634 Run 14	U_o = 0.671 Run 15	U_o = 0.694 Run 10	
	20	U_o = 0.444 Run 8	U_o = 0.510 Run 9	U_o = 0.588 Run 16		
	40	U_o = 0.308 Run 17	U_o = 0.325 Run 5	U_o = 0.337 Run 7	U_o = 0.356 Run 6	U_o = 0.361 Run 4
	50	U_o = 0.301 Run 18	U_o = 0.349 Run 13	U_o = 0.371 Run 12	U_o = 0.440 Run 11	
Rectangular culvert						
H (mm)	40	U_o = 0.373 Run 19	U_o = 0.337 Run 20	U_o = 0.344 Run 21	U_o = 0.455 Run 22	

Note: *H* = minimum means the tailwater is very shallow

Figures 3.16 - 3.19 show the bed contours at datum, centerline profiles, normalized bed contours, and normalized centerline profiles of the experiments, grouped by tailwater depth. For the minimum tailwater depth experiments (Figures 3.16a and 3.17a), the scour holes were widened by strong plunging flows and subsequent recirculating flows. As the tailwater depth increased, the scour holes shape become more regular, but the ridge was still flattened due to the tailwater depth. The normalized plots (Figures 3.18 and 3.19) show the gradual changes of the scour hole as tailwater depth increases. Similarly, in practice, if shallow tailwater depth is expected at the culvert outlet, the width of the scoured area needs to be considered when applying scour protective measures.

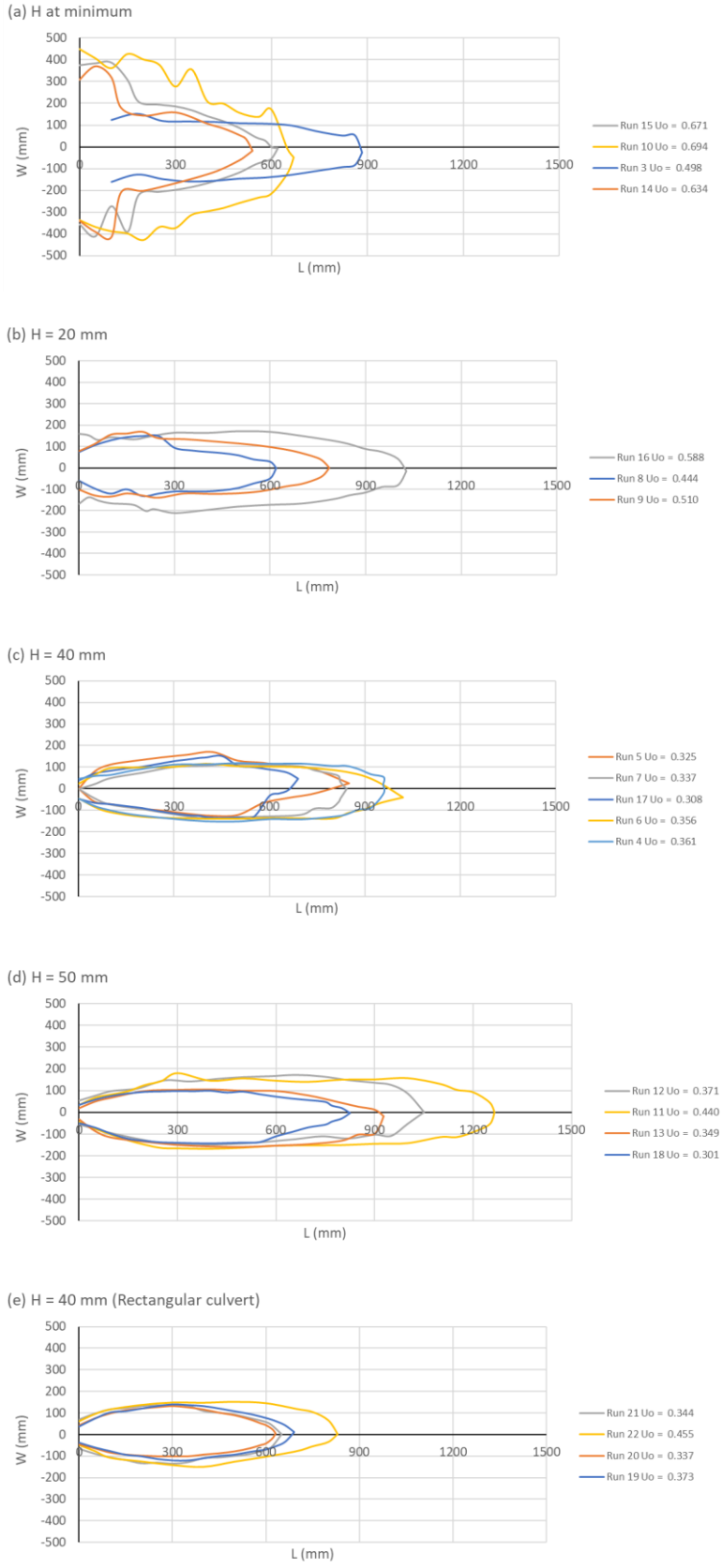

Figure 3.16 Bed contours at datum level for trapezoidal culvert (a – d) and rectangular culvert (e) scour experiments, grouped by tailwater depth.

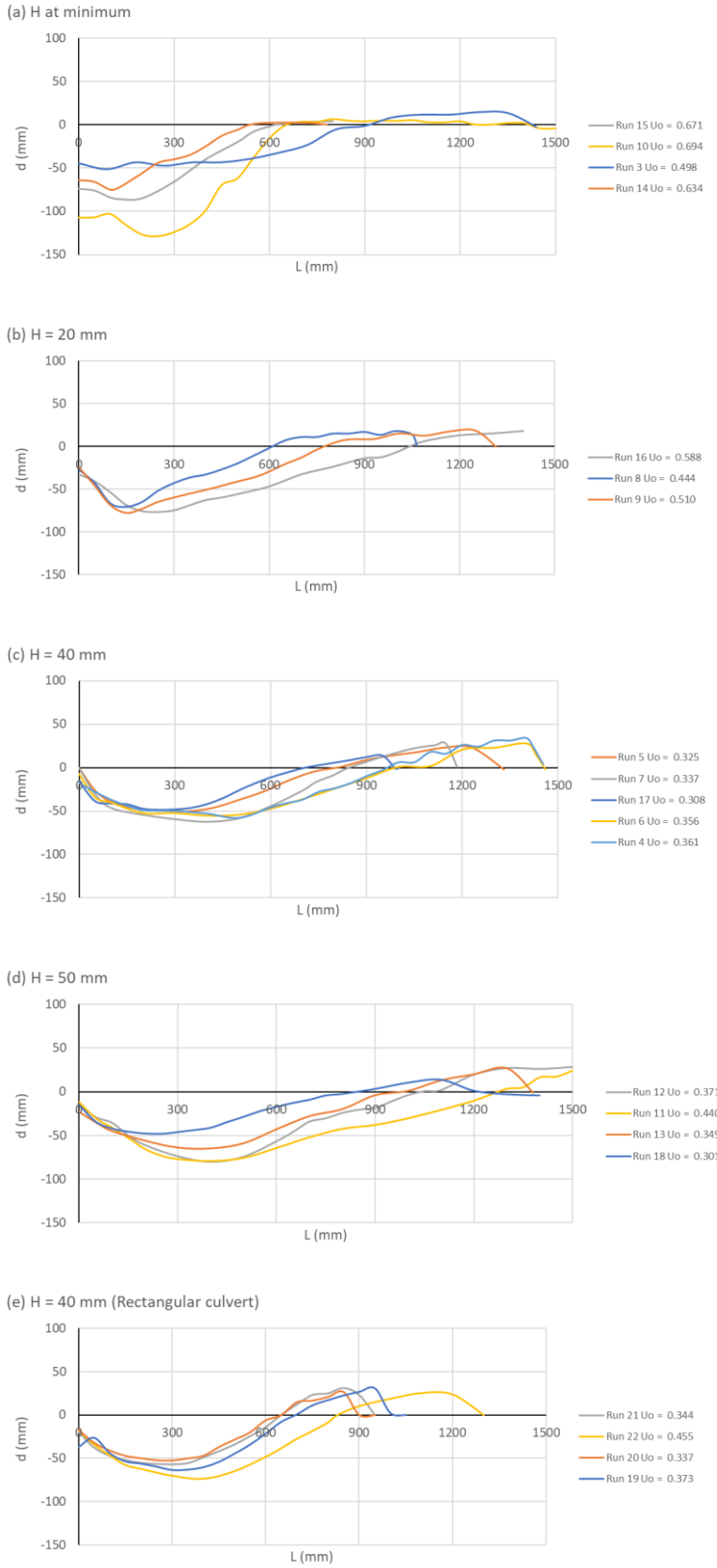

Figure 3.17 Centerline profiles for trapezoidal culvert (a – d) and rectangular culvert (e) scour experiments, grouped by tailwater depth.

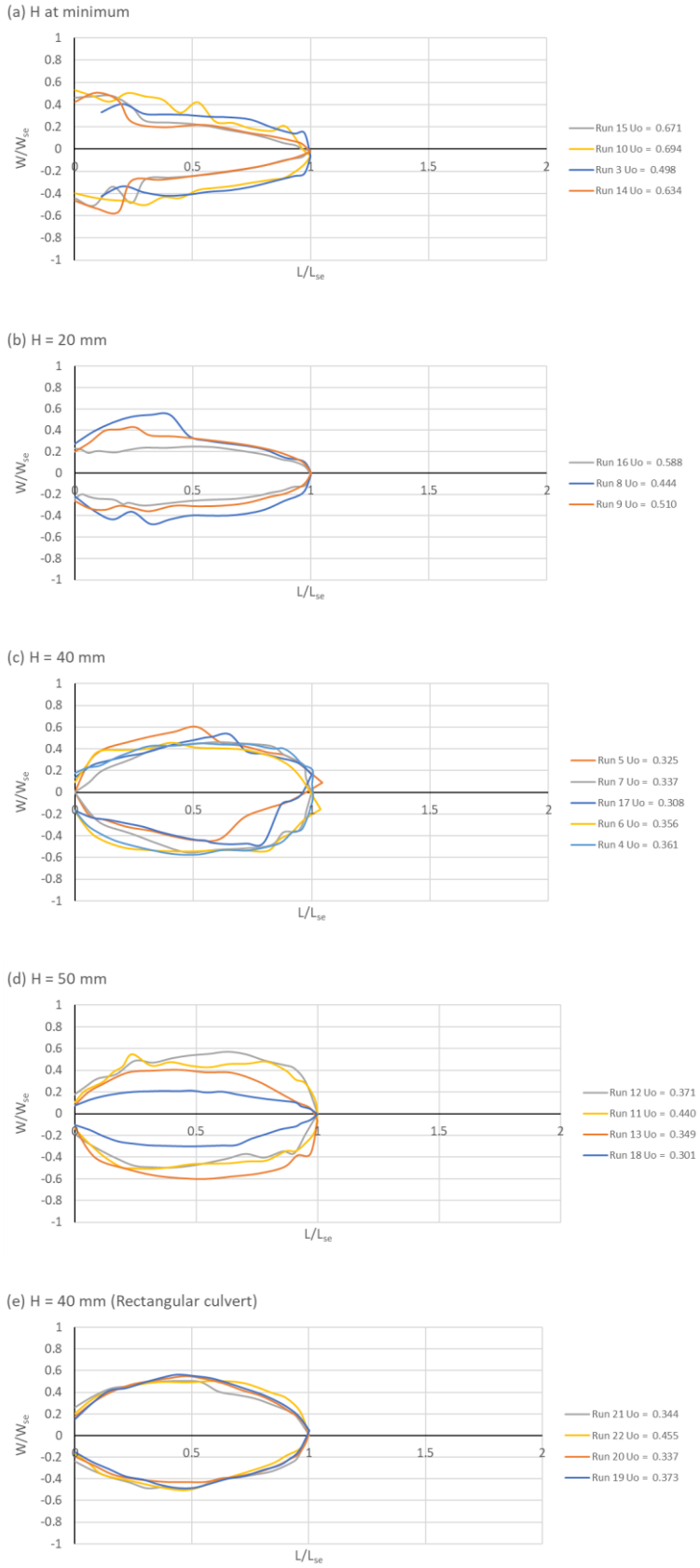

Figure 3.18 Normalized bed contours at datum level for trapezoidal culvert (a – d) and rectangular culvert (e) scour experiments, grouped by tailwater depth.

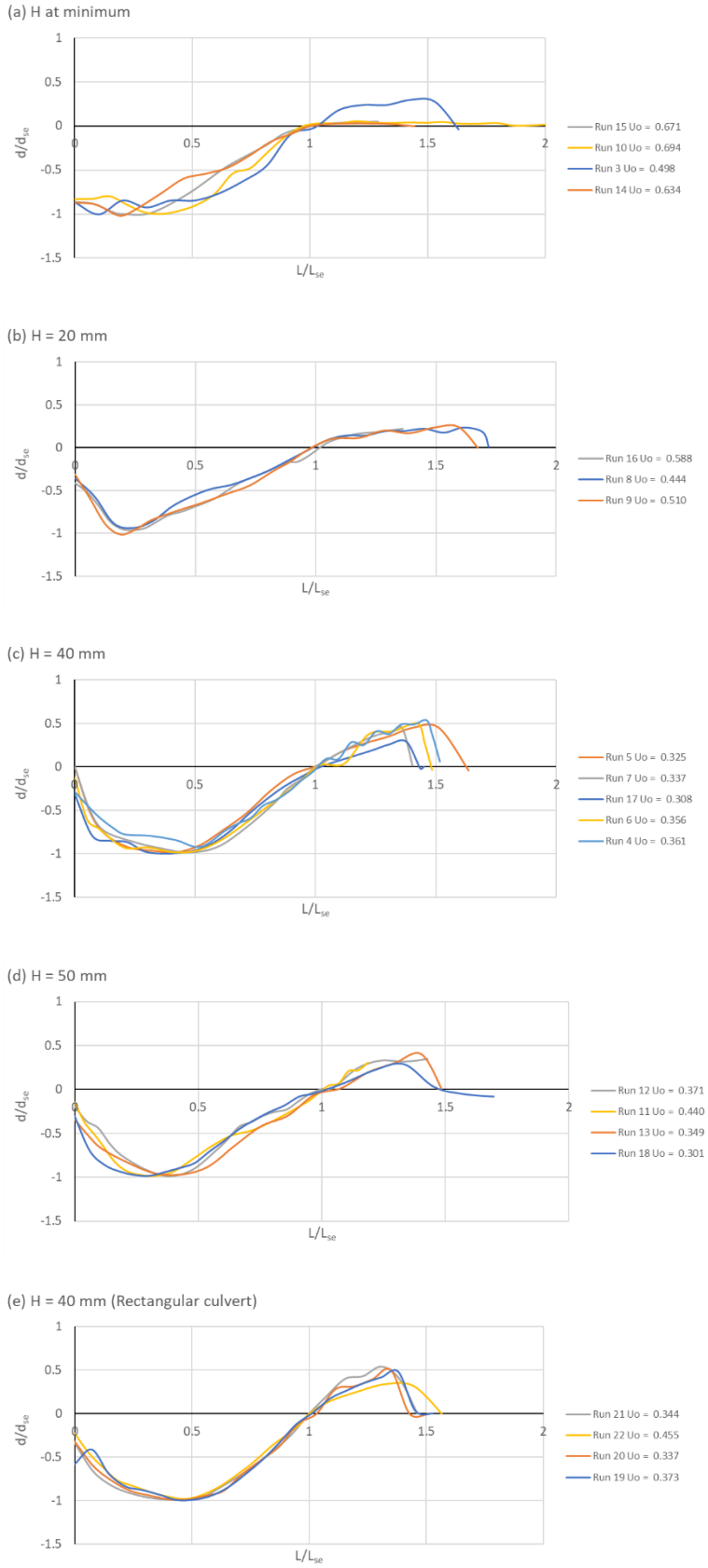

Figure 3.19 Normalized centerline profiles for trapezoidal culvert (a – d) and rectangular culvert (e) scour experiments, grouped by tailwater depth.

3.7 Rectangular culvert scour experiments

To investigate the effect of culvert shape, another series of experiments using rectangular culvert with 50 mm base width was carried out. The experiments used the same sediment with d_{50} = 0.5 mm and σ_g = 1.45. The same tailwater levels were planned to compare the results with those from the trapezoidal culvert. Table 3.5 lists the experimental conditions.

Two special series of experiments with tailwater level much higher than culvert base width were conducted. These culvert outlet jet flow has a low aspect ratio (b/h_o, b = base width, h_o = brink depth), and will be referred as the "slotted jet" runs. The aim of these experiments is two folds. Firstly, these runs allow investigation on the difference between a typical "low tailwater" and a "high tailwater" culvert scour, similar to the investigations on tailwater level effect in full flowing jet scour. Secondly, the experiments also aim to investigate the difference in scouring action between an open channel slotted jet (very small aspect ratio) and full flowing a wall jet (large aspect ratio) with outlet submerged under tailwater. At the outlet or brink location, the former is expected to have a vertical velocity profile in accordance to that of an open channel flow and the latter would have a typical turbulent jet flow velocity profile.

A special experimental run (Run A) was conducted in accordance with the hydraulic condition of Run AW46 from Abida's (1988) experiments. This is to obtain the time multiplicative factor for extrapolating selected Abida's 2-hour scour experiments up to the equilibrium state such that data comparison with the equation proposed in current study can be done (see Section 4.7).

Figures 3.20 – 3.23 show bed the contours at datum, centerline profiles, normalized bed contours, and normalized centerline profiles of the rectangular culvert scour experiments. The profiles are grouped by tailwater depth. Figures 3.20 and 3.21 from (a) to (e) show the gradual changes of the scour hole appearance when the tailwater depth decreases. The scour hole shapes became more irregular and widened near the culvert outlet, and the location of the maximum scour depth was enlarged and shifted upstream. The low tailwater depth caused excessive scour due to the recirculating flow on both sides of the culvert outlet This is similar to the "beaching" phenomenon reported by Blaisdell and Anderson (1988) in their offset plunging jet experiments. This is also a possible factor in Bohan's (1970) investigation where he found more scour under minimum tailwater condition. The plunging of the jet at the outlet is stronger at low tailwater, causing the shift and flattened area of the location of the maximum scour depth. In Figure 3.20e, when the tailwater depth was at minimum level, which means the water depth was adjusted to flow with very shallow depth

over the sediment bed and directly into the sand trap, the bed scouring happened along the entire sand bed that the scour hole length was unable to be recorded. Besides, in Figure 3.21, the ridge formation was heavily influenced by the tailwater depth, and all of them were flat without a sharp peak.

Table 3.5 Experimental plan for the rectangular culvert scour experiments.

		Flow velocity at culvert outlet, U_o (m/s)					
H (mm)	minimum	U_o = 0.668 Run 20	U_o = 0.705 Run 17	U_o = 0.723 Run 19			
	20	U_o = 0.490 Run 13	U_o = 0.512 Run 14	U_o = 0.586 Run 10	U_o = 0.595 Run 15	U_o = 0.625 Run 16	U_o = 0.679 Run 25
	30	U_o = 0.380 Run 8	U_o = 0.450 Run 9	U_o = 0.507 Run 7	U_o = 0.610 Run 6		
	40	U_o = 0.335 Run 23	U_o = 0.375 Run 24	U_o = 0.487 Run 5	U_o = 0.562 Run 22		
	50	U_o = 0.301 Run 26	U_o = 0.324 Run 18	U_o = 0.352 Run 21	U_o = 0.402 Run 11	U_o = 0.483 Run 12	U_o = 0.527 Run 27
Slotted jet runs							
H (mm)	80	U_o = 0.312 Run H5	U_o = 0.347 Run H6	U_o = 0.411 Run H7	U_o = 0.451 Run H8		
	100	U_o = 0.291 Run H1	U_o = 0.331 Run H4	U_o = 0.394 Run H3	U_o = 0.486 Run H2		
Special run							
H (mm)	53	U_o = 0.475 Run A	*to obtain multiplicative factor to compare with Abida's (1999) data				
Run 1 – 4 are the Runs 19 – 22 in rectangular culvert data from Das (2015) (Section 3.6)							

In Figure 3.22, despite the different experimental conditions, the normalized bed contours generally have similar oval shape. In Figure 3.23, the normalized centerline profiles are similar except for the ridge section, which is strongly affected by the tailwater depth. The ridge is the results of deposition of sediment scoured from the upstream and its height can be limited by the flow area available for the water to flow downstream, especially at low tailwater depth. This is also the reason the maximum scour length for minimum tailwater experiments was not available as there is no ridge formed and the centerline of the scour hole were all below the datum level. Figure 3.21e shows that the centerline profiles are slightly different from the rest.

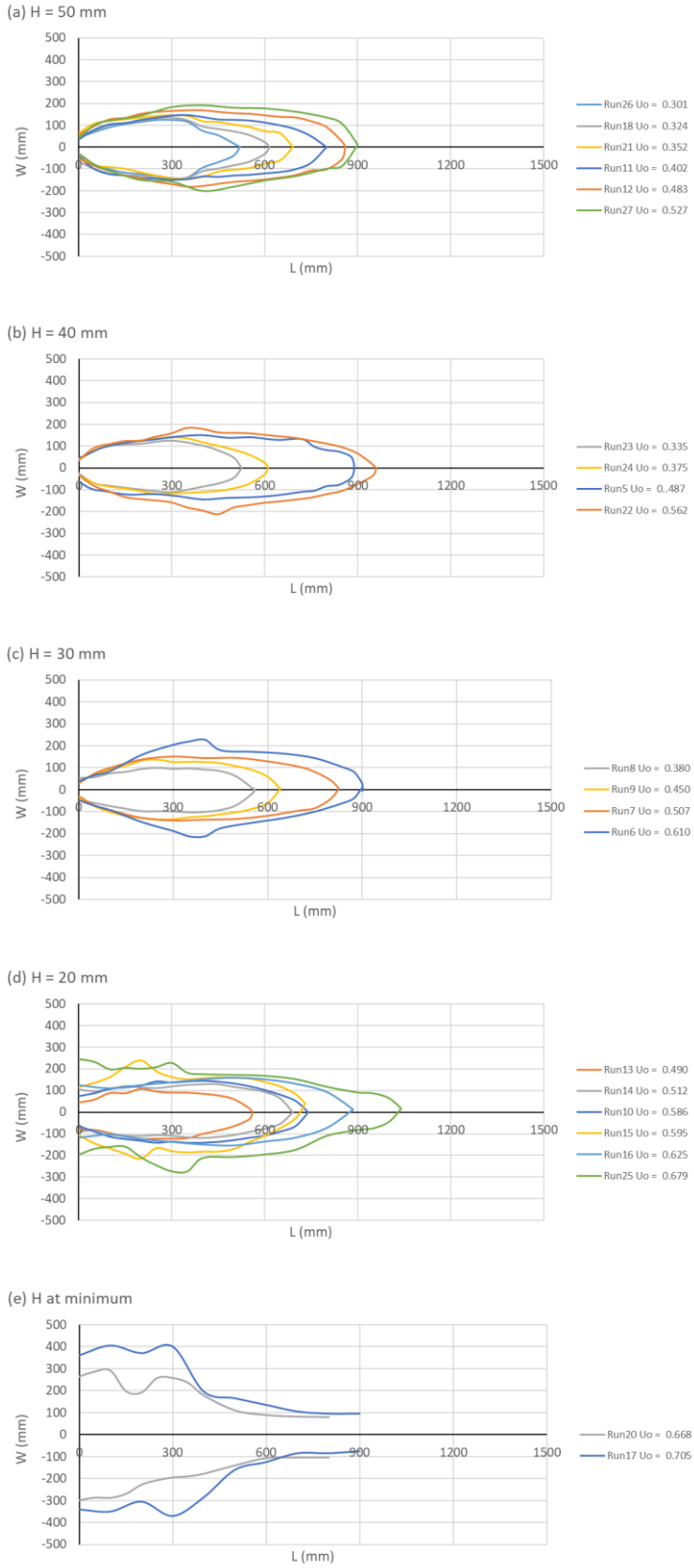

Figure 3.20 Contours at datum level for rectangular culvert scour experiments, grouped by tailwater depth.

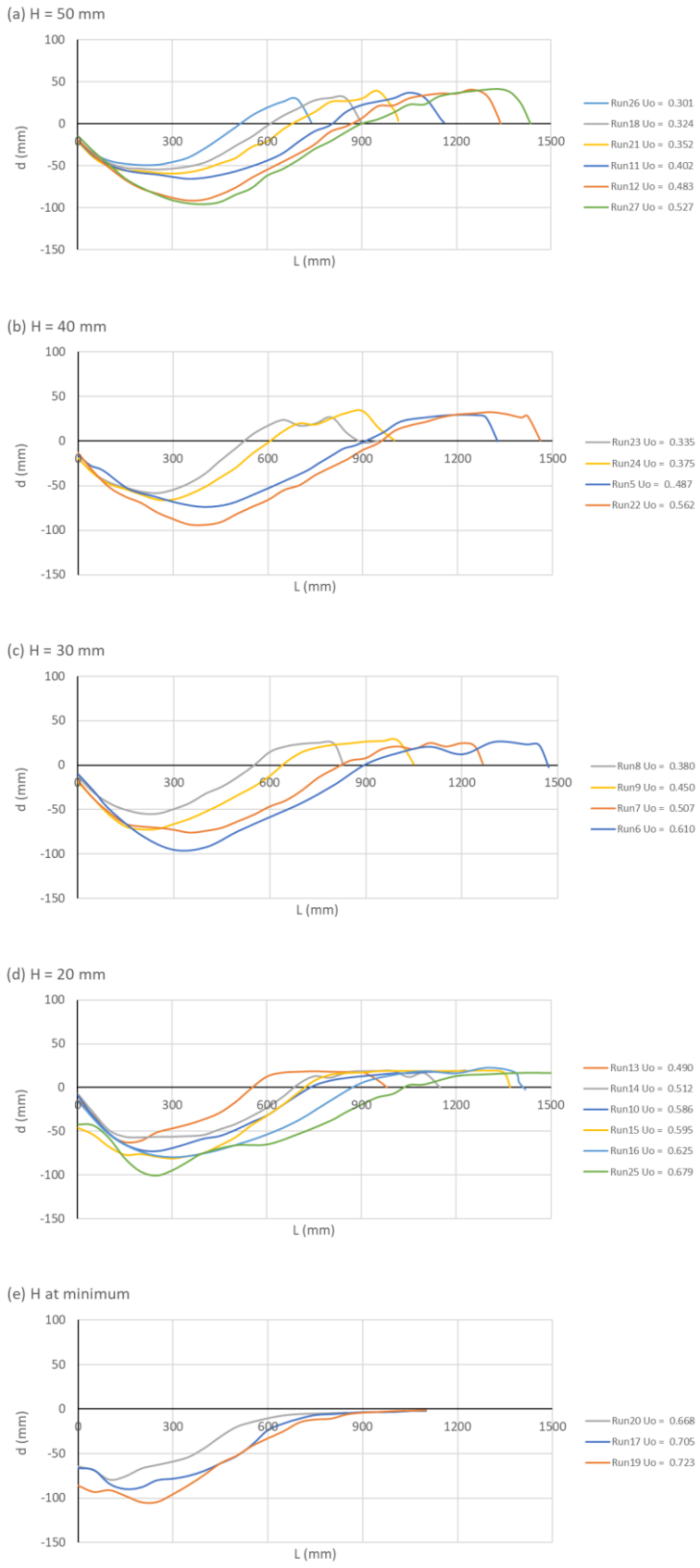

Figure 3.21 Centerline profiles for rectangular culvert scour experiments, grouped by tailwater depth.

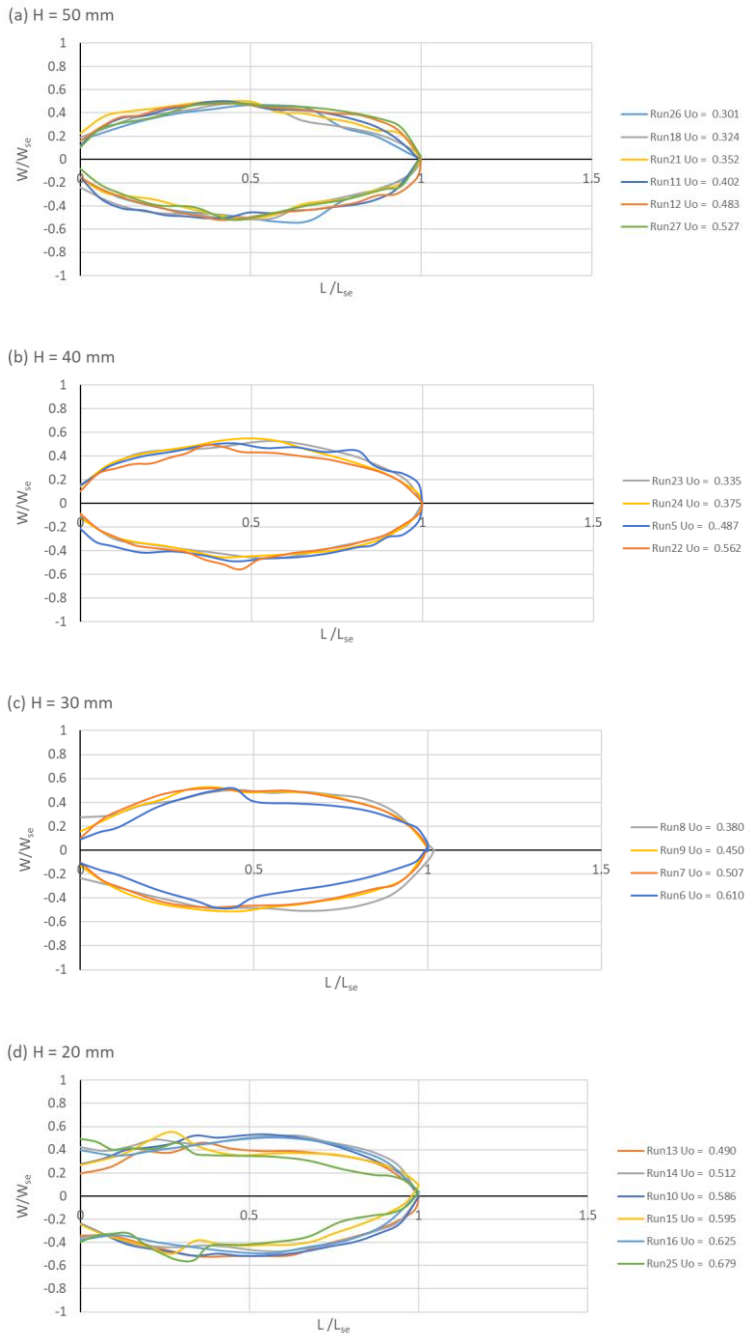

Figure 3.22 Normalized contours at datum level for rectangular culvert scour experiments, grouped by tailwater depth.

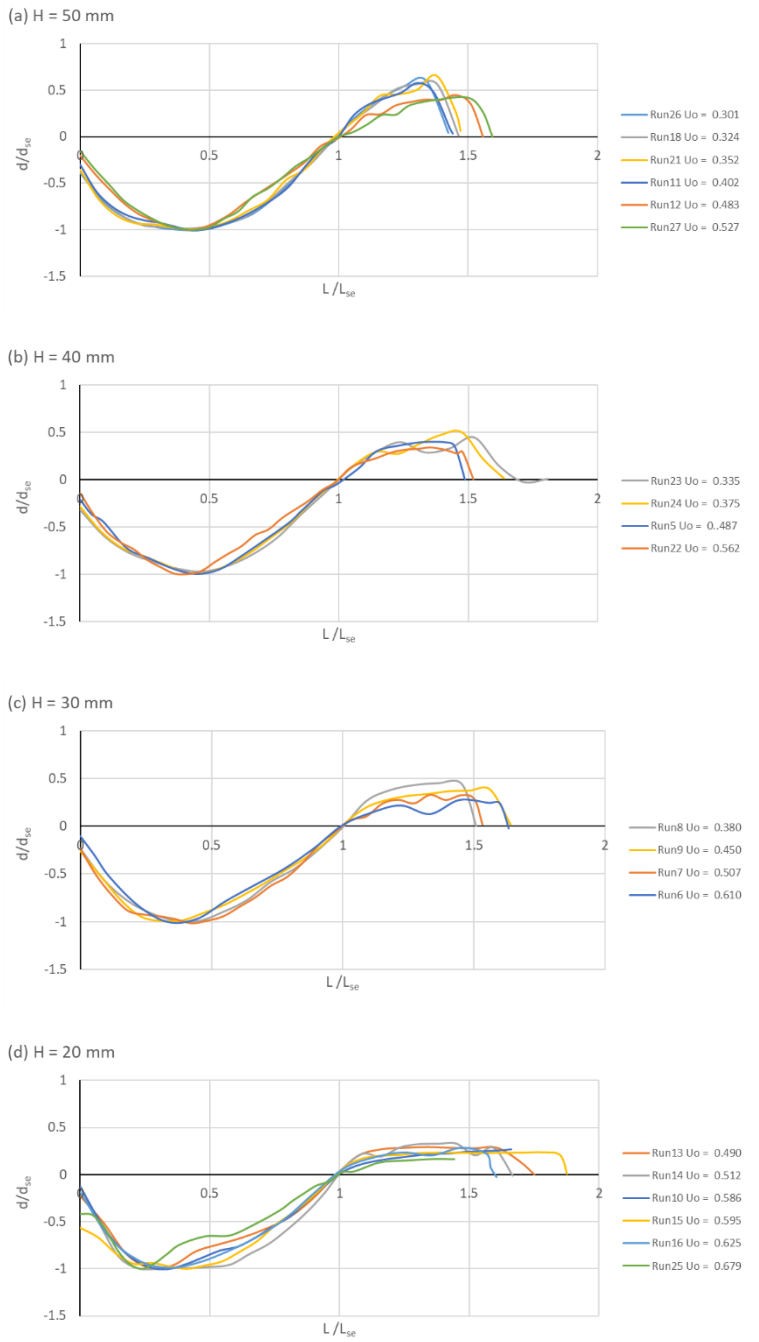

Figure 3.23 Normalized centerline profiles for rectangular culvert scour experiments, grouped by tailwater depth.

The slotted jet runs bed contours, centerline profiles, normalized bed contours, and normalized centerline profiles are shown in Figures 3.24 – 3.27 respectively. The slotted jet runs are different from the rest by having sharp ridges downstream of the scour hole (Figure 3.25) and the scour holes were asymmetrical (Figure 3.24). These features are also shown in the normalized bed contour and thalweg plots (Figure 3.26 and 3.27). Thus, the slotted jet experiments demonstrated that given sufficient

tailwater depth, scour by a non-full flowing culvert can be visually similar to those observed in deeply submerged full flowing jet scour experiments.

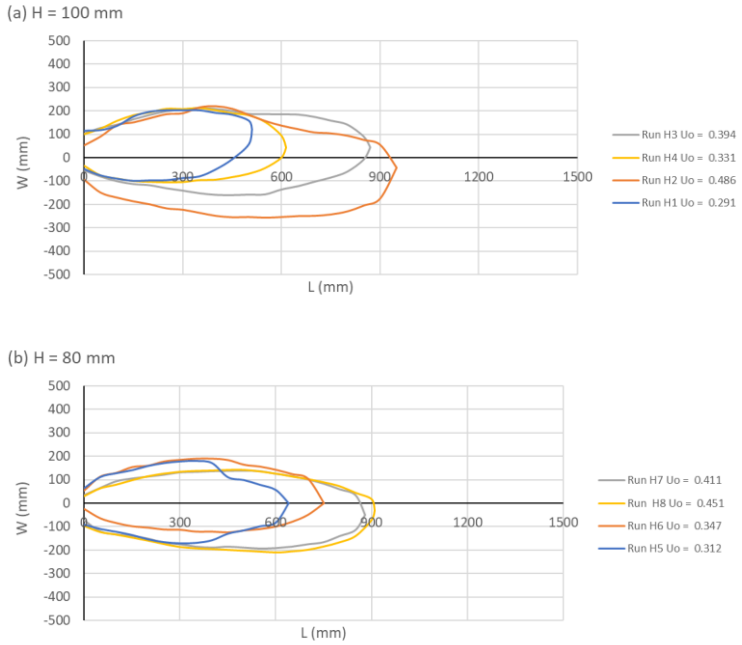

Figure 3.24 Bed contours at datum level for slotted jet scour experiments, grouped by tailwater depth.

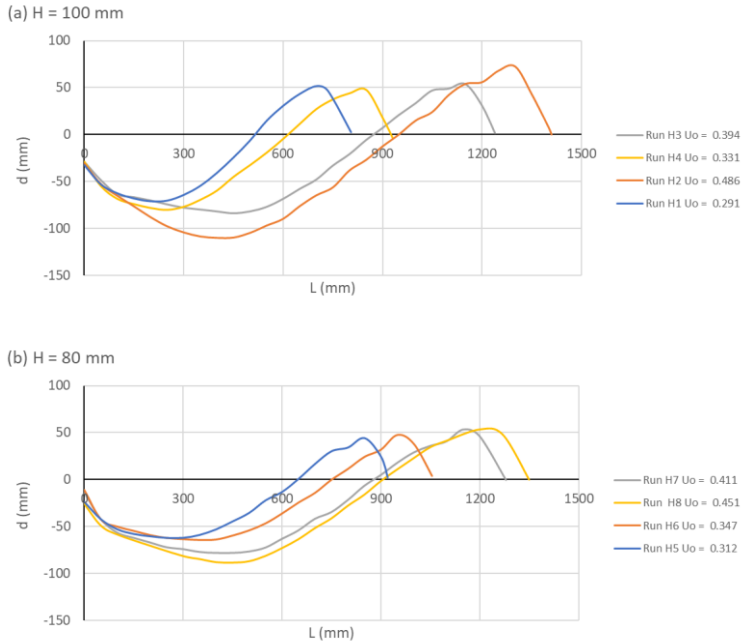

Figure 3.25 Centerline profiles for slotted jet scour experiments, grouped by tailwater depth

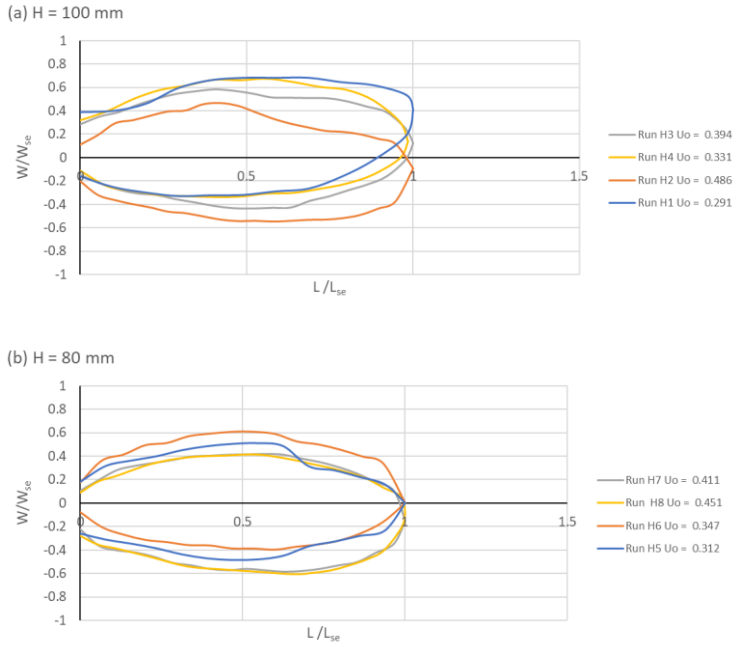

Figure 3.26 Normalized contours at datum level for slotted jet scour experiments, grouped by tailwater depth

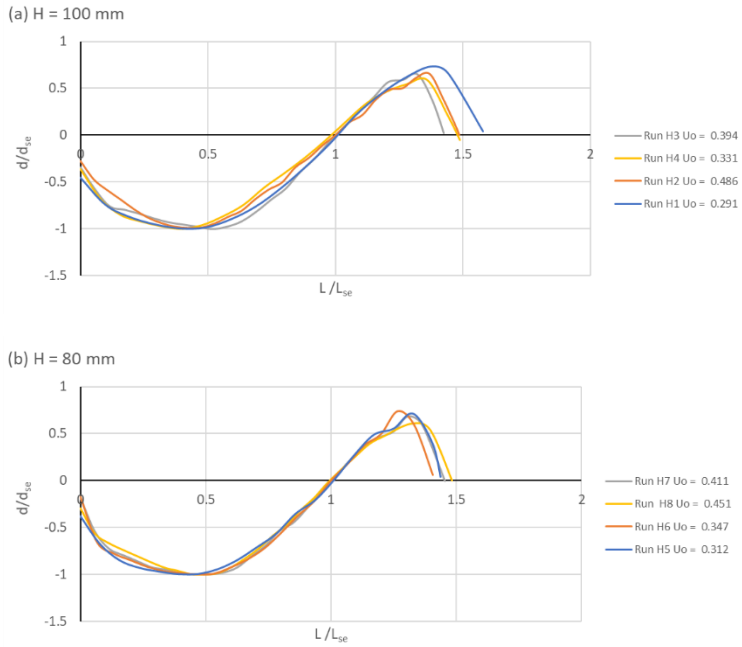

Figure 3.27 Normalized centerline profiles for slotted jet scour experiments, grouped by tailwater depth

Figure 3.28 shows photos of typical equilibrium scour holes formed under different tailwater conditions. The tailwater conditions are minimum tailwater (Figure 3.28a), normal tailwater (Figure 3.28b), and slotted jet condition (Figure 3.28c). At low tailwater depth with strong plunging outflow, the scouring action is mainly contributed by the recirculating flow upwards and outwards of the scour

hole. Irregular scour hole shape having large width at datum level could be formed by excessive recirculating flow. At higher tailwater depth with weaker plunging flow, the entrainment flow from the surrounding deeper pool of water contributes to the scouring action. At even higher tailwater level, the jet expansion contributes to scouring.

Observations of the normal rectangular culvert scour and the slotted jet scour suggest that the scour phenomena may generally be one same problem, a point as considered by the earlier researchers such as Rouse (1939) and Laursen (1953). However, the specific features or process of different kinds of jet scour (eg. 2D or 3D, horizontal or vertical jet) has led to various more detailed studies. The current work attempts in a data analysis to generalize both culvert and jet scour, and this will be presented in Chapter 5.

(a)
Run 17
H = 6 mm
(minimum)

Thread
contours at
datum,
-10 mm,
-40 mm,
-70 mm

(b)
Run 12
H = 50 mm

Thread
contours at
datum,
-40 mm,
-80 mm

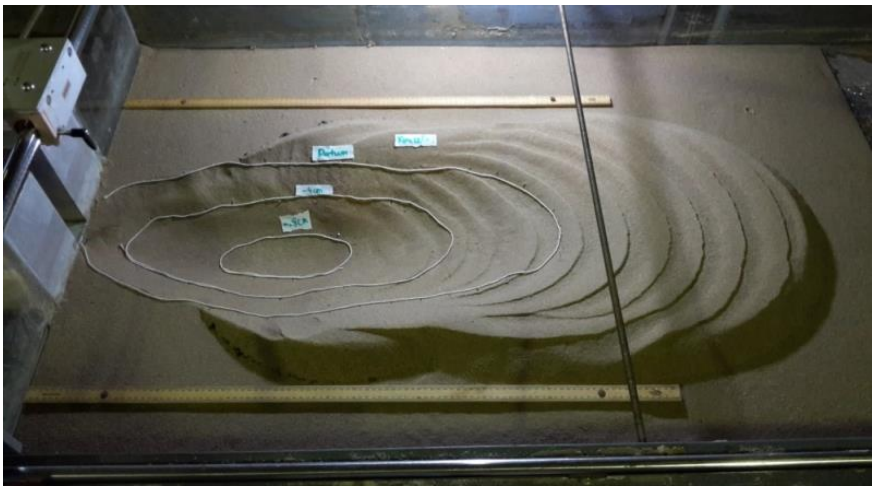

(c)
Run H2
H = 100 mm
(slotted jet)

Thread
contours at
datum,
-50 mm,
-80 mm,
-105 mm

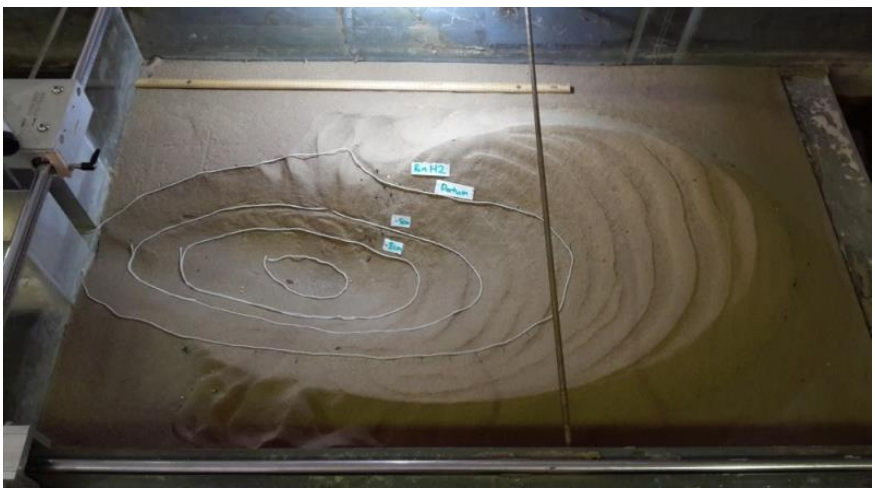

Figure 3.28 Photos of typical equilibrium scour holes under (a) minimum tailwater condition, (b) 5 cm tailwater condition, and (c) slotted jet condition.

3.8 Discussions on experimental observation

This section presents discussions among the presented experimental series. By comparing the observations from each experimental series, the similarity and difference from different kind of horizontal culvert and jet scour can be observed.

For full flowing jet scour, the experiments on unsubmerged and shallowly submerged outlet conditions (Section 3.5) shows that the scour hole is different from those under deeper submergence (Section 3.3 and 3.4). Especially the width of the scour affected area needs to be considered when low tailwater depth is expected in practice.

For the culvert shape effect on scour, photos of the trapezoidal and rectangular culverts scour experiments are shown in Figure 3.29. The photos are selected for similar tailwater depth and F_o conditions for comparison on both rectangular and trapezoidal culverts. The scour hole surface topology shapes are visually different despite having similar contour and centerline profiles. Generally, the scour hole produced by trapezoidal outlet has larger plan view scour area compared to the rectangular outlet. For the same tailwater depth, the trapezoidal culvert has larger flow area at the brink compared to a rectangular outlet. This difference in flow area is more for high tailwater level compared to low tailwater level. The hydraulic radius (R_h) for trapezoidal culvert is larger at higher tailwater depth, and getting closer to that of rectangular culvert at lower tailwater depth. Hence, by using R_h to non-dimensionalize the scour hole maximum dimensions, the resulting dimensionless numbers have similar order of magnitude and enables comparison.

A closer look at Figure 3.29d shows the difference of scour action at the minimum tailwater depth between trapezoidal and rectangular culverts. The minimum tailwater depth (typically H = 6 – 7 mm for rectangular culvert and H = 10 – 13 mm for trapezoidal channel) were achieved by lowering the tailgate until the water simply overflows into the sand trap. The water jet out of a rectangular channel flowed straight and eroded the sediment bed along centerline until no maximum length could be recorded. On the other hand, the water from a trapezoidal channel dispersed laterally and resulted in a relatively short scour hole. The possible reason for this expansion is that when water flowing out from a side slope of a trapezoidal (or triangular) channel, the flow is “affected” by the height difference of the angled side slope. Even though the out flow appeared as one single jet, the flow from the side slope tends to be going outwards away from the main jet upon entering the tailwater. On the other hand, the flow out of a rectangular channel has a vertical side wall and

experienced no “height difference” when leaving the solid channel, and continues flowing forward with the usual pattern of jet expansion.

The experiments using full flowing jet scour (Sections 3.3 – 3.5) and non-full flowing culvert scour (Sections 3.6 and 3.7) have scour holes that looks rather similar from the contours and centerline profile plots. Both kinds of scour are affected by the tailwater depth especially at shallow tailwater depth, even though the definition of relative tailwater depth is slightly different for both full flowing jet scour and non-full flowing culvert scour. The jet size for full flowing jet outlet is used to compare with the tailwater depth, and it is independent of the tailwater depth. On the other hand, the brink depth of the non-full flowing culvert scour is used to compare with tailwater depth, and it is a function of the tailwater depth, flowrate and culvert shape.

This discussion highlighted the similarity and difference of non-full flowing culvert scour and full-flowing jet scour. Both jet and culvert scour are similarly affected by the tailwater depth, and the jet flow is affected by the culvert shape. The feature of the scour hole may not able to be fully captured by using only the maximum scour hole dimensions. Even both the contour and centerline profile plots might not be sufficient to capture the entire scour affected area at low tailwater depth. Besides, the photos show different ridge formation under different scour and hydraulic conditions. Despite the deposited sediment downstream of a scour hole is generally not an engineering concern, its possible effect on the surrounding should still be considered in practice.

Trapezoidal culvert	Rectangular culvert
(a) H = 50 mm	
	
Run18AD F_o = 3.38 h_o/H = 1.00	Run26 F_o = 3.34 h_o/H = 1.00
(b) H = 40 mm	
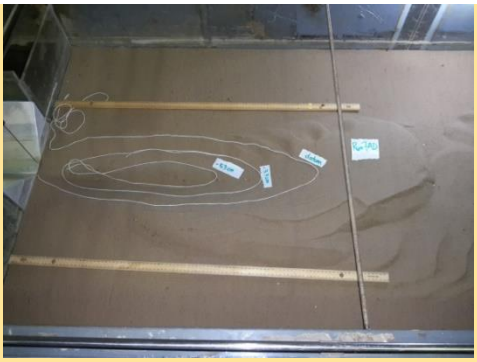	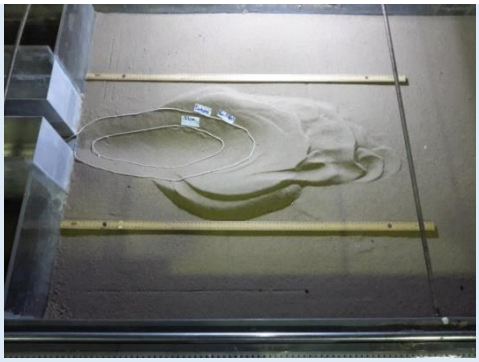
Run7AD F_o = 3.79 h_o/H = 1.03	Run23 F_o = 3.73 h_o/H = 1.00
(c) H = 20 mm	
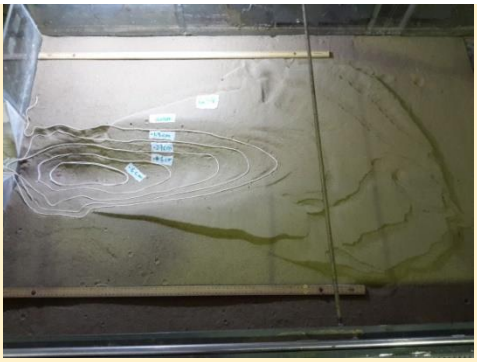	
Run9AD F_o = 5.72 h_o/H = 1.00	Run14 F_o = 5.69 h_o/H = 0.99
(d) minimum H	
	
Run15AD F_o = 7.53 h_o/H = 1.71 H = 10.5 mm	Run20 F_o = 7.43 h_o/H = 2.36 H = 6.7 mm

Figure 3.29 Photos from trapezoidal and rectangular culvert experiments showing the differences between the scour holes at similar tailwater depth.

3.9 Conclusions

A total of 5 series of experiments were conducted to study the identified research gaps highlighted earlier in detail. The research gaps are the effect of relative tailwater depth, relative sediment size, and culvert shape on 3D jet and culvert scour. Each experimental series was designed to target at one of the research gaps. Overall, the experiments used circular pipes with diameters of 4 – 27.5 mm, trapezoidal culvert with 5 mm base width and H:V = 1:1 side slope, and rectangular culvert with 50 mm base width. The sediment properties covered d_{50} of 0.49 – 1.55 mm and σ_g of 1.15 – 1.47. Outlet submergence for full flowing outlet conditions covered H/d_o = 0.5 – 30. As for non-full flowing culvert scour, minimum tailwater depth and slotted jet experiments have been carried out.

Both jet and culvert scour are affected by the relative tailwater depth. Excessive scouring at both sides of the outlet should be expected when the tailwater depth is shallow. Given sufficient tailwater depth, the culvert scour can produce scour hole that is very similar to one produced by jet scour under deep submergence outlet condition. The culvert shape affects how the water jet spreads and subsequently scours the sediment bed. The photos of the experiments show that the maximum scour hole dimensions and the contour plot and centerline profiles are not sufficient to quantify the detail of the scouring action.

The effect of relative sediment size will be presented in Chapter 4 with the analysis of a compiled database of culvert scour data.

3.10 Acknowledgement

The experiments presented in Sections 3.3 – 3.6 are carried out by Zaihan (2014), Pee (2016), Salam (2016), and Das (2015), respectively.

Chapter 4 Scour below non-full flowing culvert outlets

4.1 Introduction

Culverts are usually designed with a fully flowing barrel and the outlet scour hole size prediction equations are formulated from full flowing jet scour experiments (Chapter 2). However, the culvert barrel can be flowing partially full with an unsubmerged outlet. This outlet condition is referred as "non-full flowing" condition and the resulting scouring phenomenon is different (Section 3.8). This chapter investigates the culvert shape effect on scour below non-full flowing rectangular, trapezoidal, and triangular model culverts. A total of 171 experiments have been compiled and analyzed.

Culvert is considered hydraulically long if it is designed with full flowing capacity (Chow 1959), with the critical flow depth within the culvert barrel or the exit tailwater level higher than the culvert crown. In this case, the culvert outlet is submerged. However, a culvert may not be flowing full and the downstream tailwater depth can be lower than the culvert crown height. This unsubmerged exit condition means the culvert is considered as hydraulically short (Chow 1959).

Even though deeply submerged jet scour has been researched more thoroughly, this tailwater depth condition is unrealistic or impossible for an actual culvert installation. Bohan (1970) and Ruff et al. (1982) conducted experiments with tailwater depth (H) less than half of the circular culvert diameter (d_o), which is the condition known to be producing more severe scour hole. Breusers and Raudkivi (1991) pointed out that for scour at culvert outlet, the tailwater depth cannot be ignored. Ade and Rajaratnam (1998) categorized the scour conditions into 2 groups by the densimetric Froude number (F_o) and the relative tailwater depth (H/d_o), confirming the importance of relative tailwater depth and F_o in culvert scour.

Culvert scour, especially with shallow tailwater condition, is observed to have complex secondary flow pattern which heavily influences the scouring action (Figure 4.1). These flow patterns are unable to be captured in the (usual) two-dimensional theoretical analysis (assuming a plane jet scour), or even the analysis of the maximum scour hole dimensions data. The long exposure photos captured by Blaisdell and Anderson (1988) and the velocity measurements by Liriano (1999) at culvert scour holes are snippets of the complex flow in a culvert scour with shallow tailwater depth. Secondary flows that directly contributed to scour hole development were also observed in present study.

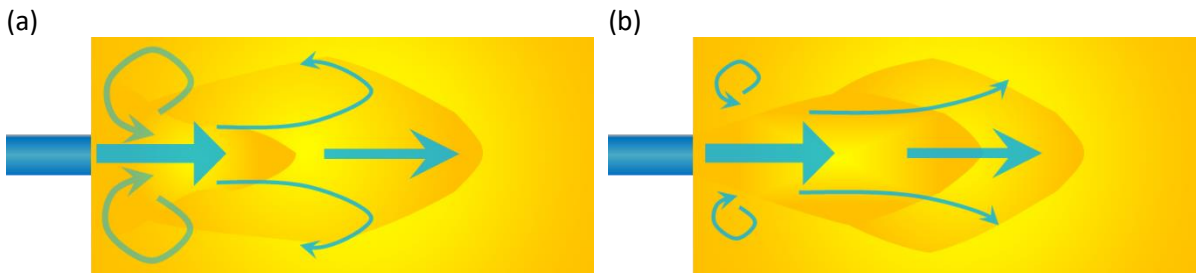

Figure 4.1 Schematic sketch of the recirculating flow at shallow tailwater depth and deeper tailwater depth.

On the other hand, Abida and Townsend (1991) have investigated scour under partially flowing and unsubmerged rectangular culvert outlet. They found that there is a tailwater condition which corresponds to maximum scour depth.

The following sections present the analysis of 171 non-full flowing culvert scour data compiled from the present and past studies in Nanyang Technological University (NTU). Subsequently, equations are proposed and compared with existing equations for full flowing jet scour. The proposed equation is then verified using selected data from Abida (1988).

4.2 NTU culvert scour database

A total of 171 experiments conducted in Hydraulics Laboratory at NTU were compiled. These included the current study (Section 3.7) and previous works from Akhtar (2014), Das (2015), Leow (2006), Ma (2010), Miao (2015), Peh (2007), Surya (2014), Tan (2013), Tan (2009), and Theodosius (2012). Table 4.1 lists the hydraulic conditions of the culverts and sediments used in these experiments.

Table 4.1 Detailed hydraulic properties of NTU database and selected Abida's (1988) data.

Shape	Base width, b (mm)	Side slope (H:V)	d_{50} (mm)	σ_g	Q (L/s)	h_o (mm)	H (mm)	U_o (m/s)	F_o	h_o/H	h_o/R_h	Duration (hr)	No. of runs	Reference	Notation in Fig. 4.1 – 4.4
Rectangular	78	-	1.76	1.13	0.641 - 1.521	17 - 29	12 - 17	0.456 - 0.715	2.704 - 4.236	1.059 - 2.083	1.436 - 1.744	44 - 48.6	14	Leow (2006)	A
Rectangular	78	-	3.8	3.28	0.899 - 1.393	19 - 25	12 - 12	0.607 - 0.714	2.446 - 2.880	1.583 - 2.083	1.487 - 1.641	44 - 48	7	Leow (2006)	B
Rectangular	160	-	3.1	3.56	3.873 - 5.419	28 - 37	23 - 38	0.824 - 1.007	3.680 - 4.497	0.947 - 1.360	1.350 - 1.463	28 - 29.3	14	Peh (2007)	C
Trapezoidal	120	1:1.732	4.9	1.27	4 - 5.9	36 - 48	23 - 39	0.677 - 1.013	2.404 - 3.597	1.000 - 1.696	1.443 - 1.563	41.8 - 95	13	Tan (2009)	D
Trapezoidal	120	1:1.732	5.2	1.26	4.2 - 5.6	33 - 44	32 - 38	0.815 - 0.915	2.809 - 3.155	1.031 - 1.257	1.411 - 1.524	24 - 26	4	Ma (2010)	D
Triangular	-	1:1	1.63	1.19	0.620 - 3.089	33 - 63	18.8 - 55.8	0.544 - 0.778	3.351 - 4.791	1.066 - 2.364	2.828[a]	48 - 50	21	Theodosius (2012)	E
Rectangular	50	-	1.63	1.19	0.645 - 2.041	20 - 50	10 - 37	0.430 - 1.116	2.648 - 6.871	1.351 - 2.000	1.800 - 3.000	48	13	Tan (2013)	F
Rectangular	50	-	1.8	2.67	0.685 - 1.856	18 - 40	6.5 - 34.5	0.680 - 1.003	3.982 - 5.874	1.130 - 3.538	1.720 - 2.600	43 -- 93	14	Akhtar (2014)	G
Trapezoidal	100	2:5	1.62	3.71	1.77 - 4.705	26.6 - 54	20.8 - 45.9	0.508 - 0.734	3.133 - 4.528	1.025 - 1.431	1.422 - 1.778	44 - 71	8	Surya (2014)	H
Trapezoidal	100	2:5	1.69	3.83	1.66 - 3.86	25 - 81.5	17.5 - 81.4	0.320 - 0.731	1.938 - 4.422	1.001 - 1.469	1.399 - 2.078	45.6 - 72	8	Miao (2015)	H
Trapezoidal	100	2:5	1.69	3.83	2.26 - 2.49	36 - 36.9	36.1 - 36.3	0.537 - 0.588	3.250 - 3.559	0.997 - 1.021	1.552 - 1.564	46 - 48	3	N/A[b]	H
Trapezoidal	50	1:1	0.49	1.47	0.609 - 2.332	17 - 52	10.3 - 50.3	0.301 - 0.694	3.379 - 7.789	0.988 - 1.714	1.464 - 1.932	19[c], 43 – 72	16	Das (2015)	I
Rectangular	50	-	0.49	1.47	0.668 - 0.909	39.6 - 41.2	39.6 - 40.9	0.337 - 0.455	3.786 - 5.105	0.999 - 1.010	2.584 - 2.648	39.8 - 47.8	4	Das (2015)	J
Rectangular	50	-	0.5	1.45	0.5 - 2.473	15.7 - 101.7	5.9 - 101.5	0.291 - 0.723	3.240 - 8.037	0.987 - 3.000	1.628 - 5.068	41 - 120	32	Current study	J
Rectangular	5.1 - 25.4	-	0.47, 1.35	1.22, 1.64	1.25 - 3.87	1.3 - 5.8	0.9 - 5.8	0.264 - 1.121	1.783 - 12.857	0.927 - 2.778	1.128 - 3.118	2	27	Abida (1988)	-

[a]Triangular culvert has the same h_o/R_h values

[b]Experiments carried out by the author after Miao (2015) has finished her project

[c]Short duration run as the scour hole was too large.

4.3 Dimensional analysis

Dimensional analysis is used to obtain a generalized functional relationship for the scour hole dimension. The equilibrium state scour hole dimensions, i.e. the maximum depth (d_{se}), width (W_{se}), length (L_{se}), and volume (V_{se}), are the dependent variables. They are a function of the experimental hydraulics conditions, including the mean outlet flow velocity ($U_o = Q/A$, where Q = discharge, A = flow area at the brink section), tailwater depth (H), culvert shape, median sediment diameter (d_{50}), sediment gradation (σ_g), and sediment density (ρ_s). Depending on the culvert shape, the U_o is calculated by using the brink depth (h_o) at the culvert outlet. The culvert shape is represented by the hydraulic radius (R_h), defined as the flow area (A) at the brink section divided by its wetted perimeter (P_{wet}). For a rectangular culvert:

$$R_h = \frac{A}{P_{wet}} = \frac{bh_o}{b+2h_o} \tag{4.1}$$

For a full flowing circular jet scour experiments, R_h is equal to $d_o/4$, where d_o is the outlet diameter (Abt et al. 1985; Ade and Rajaratnam 1998). Thus, R_h and d_o can be related by using a multiplying coefficient.

Other parameters include the downstream channel width (B), slope of the culvert (S_o), gravitational acceleration (g), water density (ρ) and its dynamic viscosity (μ). Thus, the scour hole dimensions can be related to the experimental hydraulics conditions by the following equation:

$$d_{se}, W_{se}, L_{se}, V_{se} = f(U_o, \rho, \mu, b, h_o, R_h, H, d_{50}, \sigma_g, \rho_s, g, B, S_o) \tag{4.2}$$

Considering the experimental conditions, the R_h, ρ, and U_o were chosen as the repeating variables for dimensional analysis of Eq. (4.2), yielding:

$$\left[\frac{d_{se}}{R_h}, \frac{W_{se}}{R_h}, \frac{L_{se}}{R_h}, \frac{V_{se}}{R_h^3}\right] = f\left(F_o, \frac{h_o}{H}, \frac{h_o}{R_h}, \frac{d_{50}}{R_h}\ \sigma_g, \frac{\rho_s}{\rho}, \frac{B}{R_h}, S_o, \frac{\rho U_o R_h}{\mu}\right) \tag{4.3}$$

Eq. (4.3) can be simplified by considering the factors that are held constant in the experiments. The Reynolds number can be ignored because the culvert flow was always turbulent and fluid viscosity is not important. Non-cohesive sediment was used and the culvert was horizontal ($S_o = 0$). The culvert invert and the original sand bed level were set at the same level and this is used as the datum reference. The flumes used are wide so that the experiments were conducted with a large downstream channel width to avoid side wall effect on the scour formation. The important dimensionless parameters that remains are:

$$\left[\frac{d_{se}}{R_h}, \frac{W_{se}}{R_h}, \frac{L_{se}}{R_h}, \frac{V_{se}}{R_h^3}\right] = f\left(F_o, \frac{h_o}{H}, \frac{h_o}{R_h}, \frac{d_{50}}{R_h}\ \sigma_g\right) \tag{4.4}$$

where F_o = densimetric Froude number, defined as

$$F_o = \frac{U_o}{\sqrt{\left(\frac{\rho_S - \rho}{\rho}\right) g d_{50}}} \tag{4.5}$$

The F_o captures both the strength of the jet and sediment properties, and it is different from the flow Froude number. It represents the ratio of tractive force of water on sediment particle to the weight of sediment particle (Lim 1995). The ratio of brink depth to tailwater depth (h_o/H) represents the resistance or cushioning by the tailwater pool against the force of the jet. A large ratio ($h_o/H > 1$) means the jet is plunging into the tailwater at the outlet. A small ratio ($h_o/H \sim 1$) means a relatively high tailwater for the particular flowrate. In this case, the tailwater acts as an energy dissipator and reduces the scouring ability by enhancing the diffusion of the jet in the pool of water below the outlet. The ratio of brink depth to brink hydraulic radius (h_o/R_h) indirectly measures the aspect ratio of the brink flow area for rectangular culverts. The term d_{50}/R_h is related to the ratio of the size of the sediment to the size of the culvert outlet, similar to the function of d_{50}/d_o for full flowing scour. The term σ_g indicates the non-uniformity of the sediment.

4.4 Analysis of culvert scour data

A database of 171 experiments from current study and previous works done by final year project students at NTU is analyzed to formulate predictive formulae. The hydraulic conditions of the experiments are listed in Table 4.1. The data consists of 3 culvert shapes, different d_{50} of uniform and non-uniform sediments, and varying tailwater conditions.

Figure 4.2 shows the non-dimensionalized maximum scour depth (d_{se}/R_h) versus F_o. The data are presented in terms of the culvert shapes and types of sediments used. Generally, the data of different experimental conditions scattered but nonetheless followed an increasing trend as F_o increases. The following discussion is done by comparing the data from specific groups that have similar hydraulic conditions.

The effect of sediment size and gradation can be observed by comparing dataset with the same model culvert. The influence of sediment uniformity can be assessed by a closer look at Series F and Series G. Both used the same rectangular culvert and d_{50}, but Series G used sediment with larger non-uniformity (see Table 4.1). For similar F_o values, non-uniform sediment produced smaller scour hole consistently. Thus, σ_g is an important factor to be included in correlation. The effect of sediment size can be seen by observing Series F and Series J. It might seem that larger sediments produced larger scour hole for the same F_o values compared to smaller sediment. This is a false impression because F_o is reduced by the d_{50} in the denominator while holding other variables constant. Thus, F_o alone may not be sufficient to capture the effect of sediment size as the influence of d_{50} is magnified. The overall relative weightage of d_{50} in the correlation might need to be reduced.

The simplest form of culvert shape effect can be seen by comparing two rectangular culverts with different base width, such as Series B and Series C. The plot shows that a smaller base width produced a larger scour hole at the same F_o. This is contradicting to the idea that R_h should able to scale the scour hole accordingly such that non-dimensionalizing a larger scour hole from a larger culvert should result in similar value as non-dimensionalizing a smaller scour hole produced from a smaller culvert. The different data trend suggests that the culvert outlet size should be considered as scale-related factor and its relative weightage still require further investigation. Similar comparison can be made between data from Series A and Series F. The size difference between the data series is smaller. Their data mostly clustered together despite having slightly different slope.

For different culvert shape, Series E and Series F have similar R_h range and the data points clustered together, suggesting that R_h is useful across different shape especially when the culvert sizes are of similar range. The comparison between Series I and series J supports R_h as a characteristic length scale across culverts of different shapes.

In conclusion, for maximum scour depth, F_o is able to capture the flow intensity and most of the effect of sediment size, while σ_g is important to relate the uniformity of sediment. R_h is an appropriate characteristic length scale to use over similar outlet flow area size. Other factor such as h_o/H should also be considered in formulation of a scour depth predicting formula.

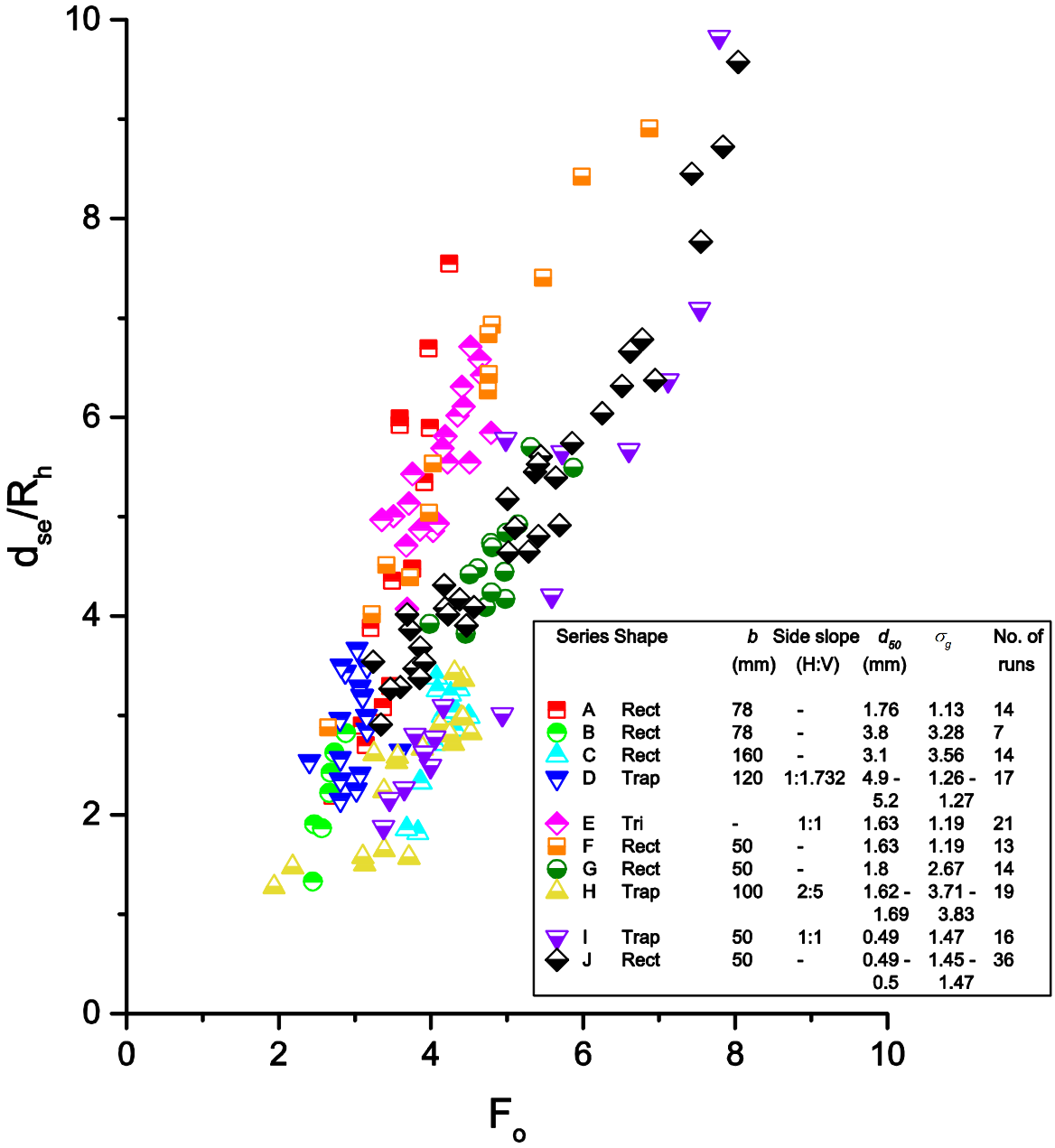

Figure 4.2 Plot of d_{se}/R_h versus F_o for compiled experiments.

The other scour dimensions, i.e. maximum scour width (W_{se}/R_h), length (L_{se}/R_h), and volume (V_{se}/R_h^3) against F_o are shown in Figures 4.3 – 4.5, respectively. They show similar trend as Figure 4.2. In Figure 4.3, the W_{se}/R_h plot appeared more dispersed compared to the d_{se}/R_h versus F_o plot, suggesting the scour hole width is more sensitive to various experimental conditions, especially combined effect of the tailwater ratio h_o/H, σ_g, and the culvert shape. In Figure 4.4, the L_{se}/R_h versus F_o plot shows most data clustered together. The data trend supports the usefulness of both R_h and F_o as characteristic parameters for culvert shapes and sediment size generally. Figure 4.5 shows V_{se}/R_h^3 versus F_o. Log-log scale is used to better present the data as values of V_{se}/R_h spans several orders of magnitude. Theoretically, for a known shape, the volume can be calculated from the length dimensions. Indeed,

if all the scour holes have similar shape such as the case of deeply submerged circular jet scour, the scour hole volume can be estimated with certain confident. Thus, V_{se}/R_h^3 is considered to have an overall representation of the scour hole.

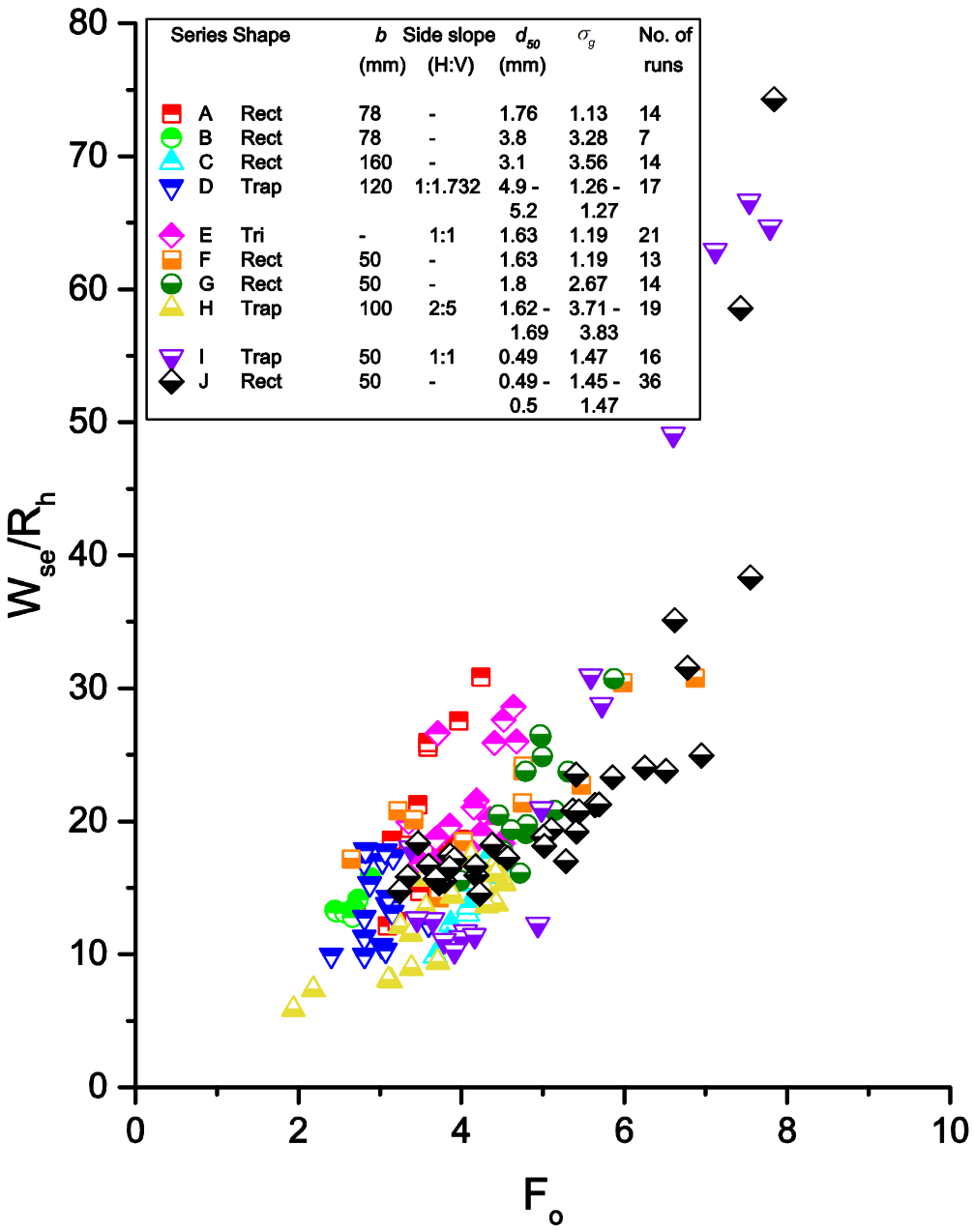

Figure 4.3 Plot of W_{se}/R_h versus F_o for compiled experiments.

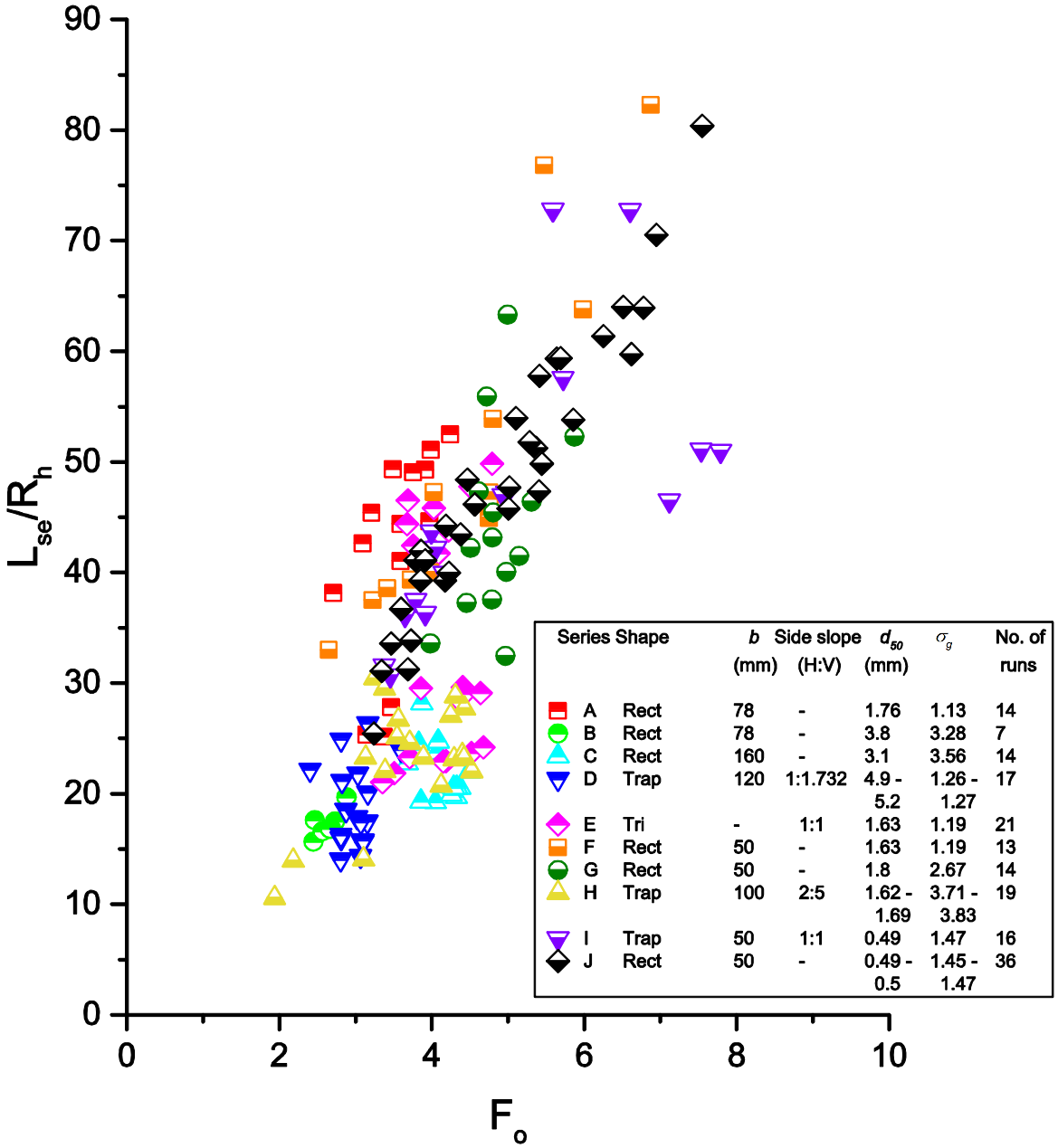

Figure 4.4 Plot of L_{se}/R_h versus F_o for compiled experiments

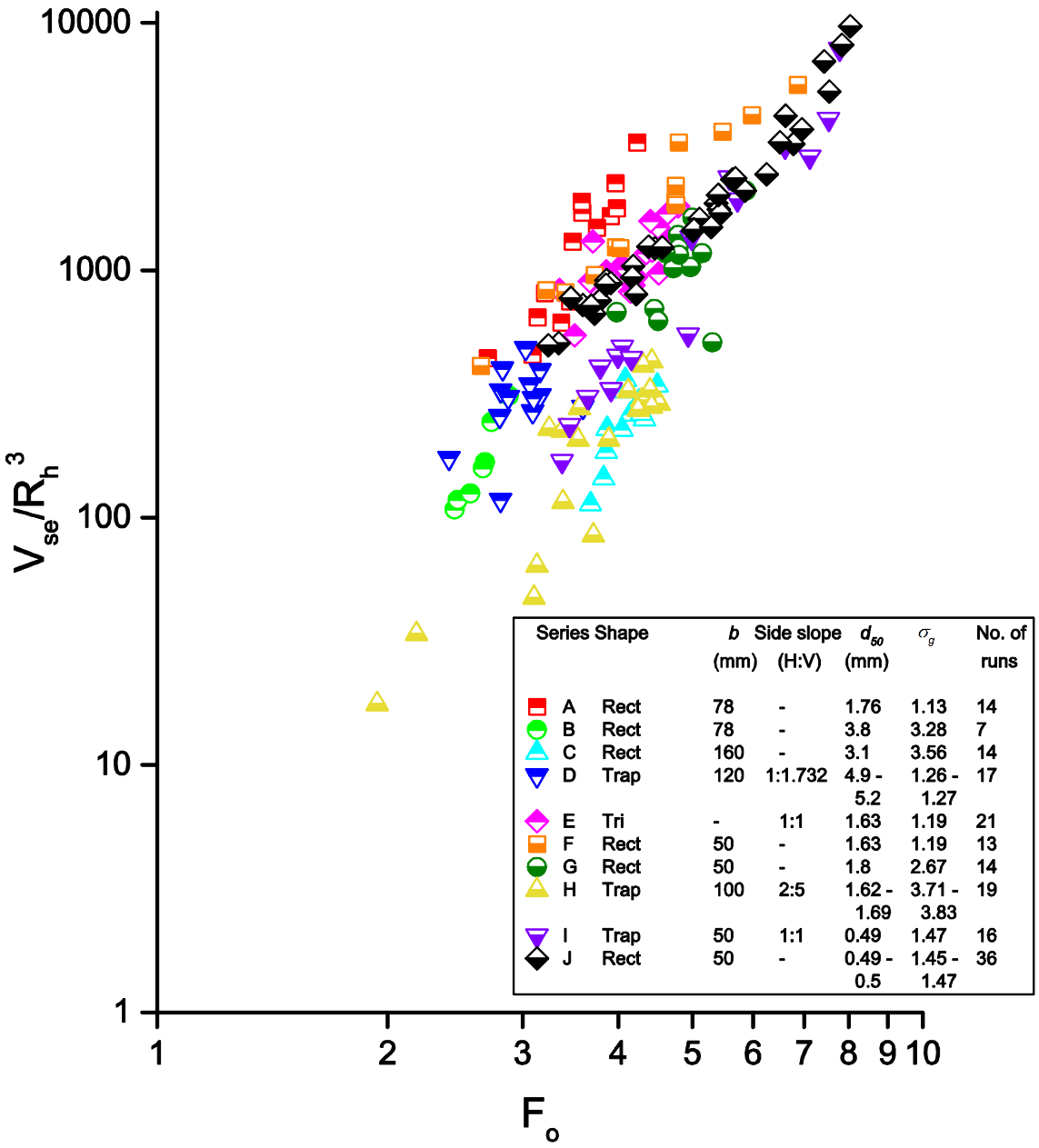

Figure 4.5 Plot of V_{se}/R_h^3 versus F_o for compiled experiments

In conclusion, beside the commonly used d_{se}/R_h, V_{se}/R_h can be more representative than W_{se}/R_h and L_{se}/R_h because it involves the overall results of scouring action. From the analysis, it is clear that W_{se}/R_h is heavily influenced by plunging flow recirculating pattern and surrounding entrainment flow pattern, while L_{se}/R_h could be influenced by flow expansion due to culvert shape. Depending on the scour hole dimension in consideration, sometimes the plots show that F_o is unable to solely capture the effect of different sediment size, and the influence of d_{50} in F_o for d_{se}/R_h should be reduced while F_o seems to be just appropriate for L_{se}/R_h. For all cases, σ_g proved to be an important parameter.

4.5 Proposed prediction equations

Regression analysis was carried out to determine the best prediction equations for d_{se}/R_h, W_{se}/R_h, L_{se}/R_h, and V_{se}/R_h^3. The following equations are proposed to predict the maximum scour hole dimensions, with the prediction results shown in Figure 4.6.

$$\frac{d_{se}}{R_h} = 0.96F_o^{1.08}\left(\frac{h_o}{H}\right)^{0.40}\left(\frac{1}{\sigma_g}\right)^{0.43} \qquad R^2 = 0.846 \qquad (4.6)$$

$$\frac{W_{se}}{R_h} = 3.91F_o^{1.06}\left(\frac{h_o}{H}\right)^{0.55}\left(\frac{1}{\sigma_g}\right)^{0.21} \qquad R^2 = 0.792 \qquad (4.7)$$

$$\frac{L_{se}}{R_h} = 7.77F_o^{1.21}\left(\frac{h_o}{H}\right)^{-0.18}\left(\frac{1}{\sigma_g}\right)^{0.34} \qquad R^2 = 0.678 \qquad (4.8)$$

$$\frac{V_{se}}{R_h^3} = 17.82F_o^{2.95}\left(\frac{h_o}{H}\right)^{0.66}\left(\frac{1}{\sigma_g}\right)^{1.17} \qquad R^2 = 0.895 \qquad (4.9)$$

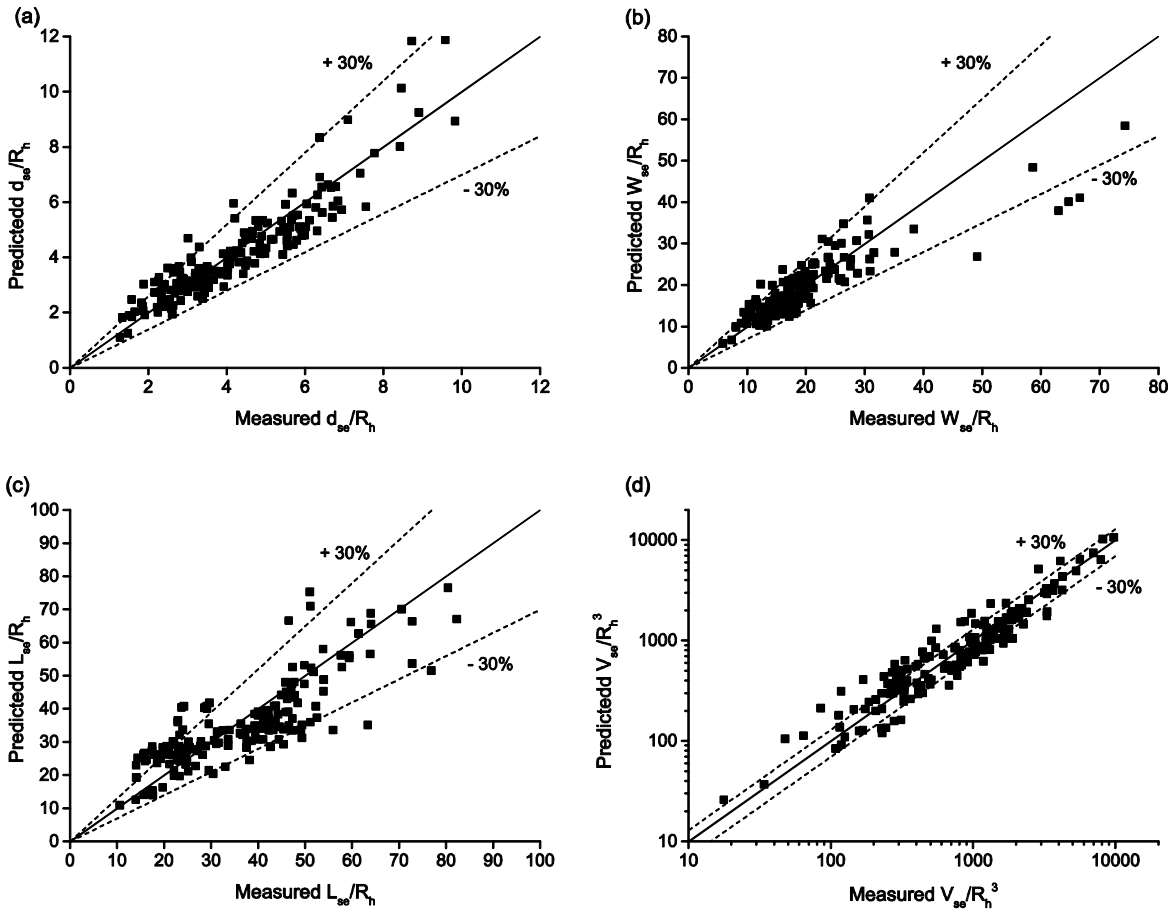

Figure 4.6 Predicted versus measured data for d_{se}/R_h, W_{se}/R_h, L_{se}/R_h, and V_{se}/R_h^3 calculated by Eqs. (4.6) – (4.9), respectively

The exponents of h_o/H in Eqs. (4.8) and (4.9) are comparatively lower than the exponent of other dimensionless numbers in the equations. This shows that h_o/H is not as important for L_{se}/R_h and V_{se}/R_h^3 as compared to its weightage for d_{se}/R_h and W_{se}/R_h in Eqs. (4.6) and (4.7).

Usually the maximum scour depth is the only scour dimension available in predictive scour formulas. Hence, when judgment is required on the size of area or volume for scour protection, the inter-relatonships of W_{se}, L_{se}, and V_{se} as a function of d_{se}, as given in Eqs. (4.10) – (4.12), would be useful:

$$\frac{W_{se}}{R_h} = 7.14\,(\frac{d_{se}}{R_h})^{0.66} \qquad R^2 = 0.723 \qquad (4.10)$$

$$\frac{L_{se}}{R_h} = 7.67\,\left(\frac{d_{se}}{R_h}\right) + 6.40 \qquad R^2 = 0.649 \qquad (4.11)$$

$$\frac{V_{se}}{R_h^3} = 26.63\,(\frac{d_{se}}{R_h})^{2.41} \qquad R^2 = 0.880 \qquad (4.12)$$

Figure 4.7 shows the plots of Eqs. (4.10) – (4.12). Equation (4.10) was derived without considering the 6 large W_{se}/R_h data points. Thus, caution is needed if plunging flow and very low tailwater depth is expected. Equation (4.11) used all available data and it is noted that some triangular culvert data (Fig. 4.6b) have relatively shorter L_{se} for the same d_{se}, as compared to other culvert shapes.

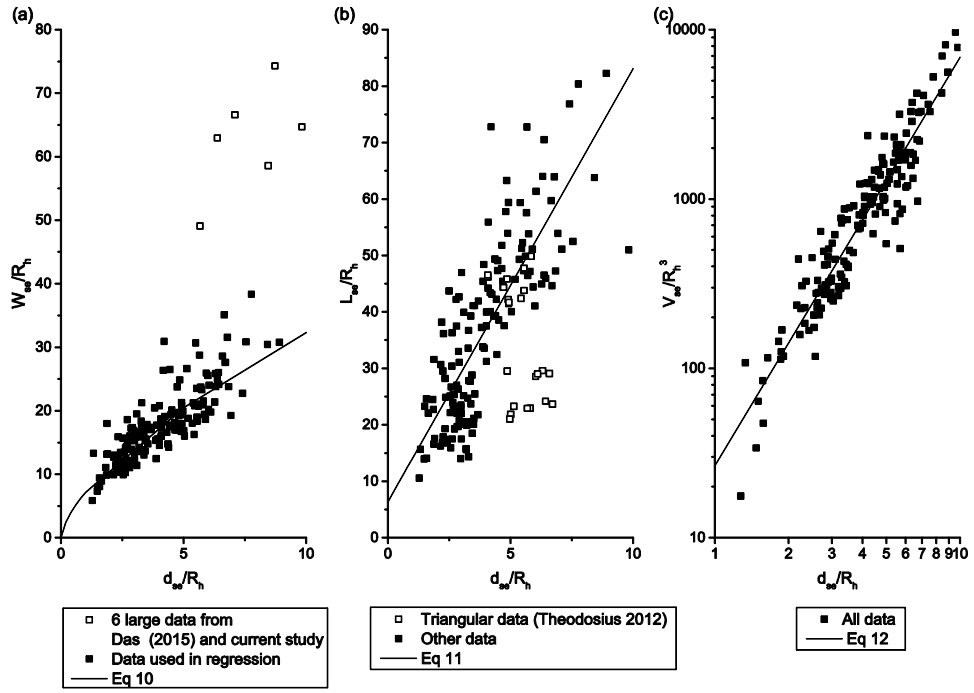

Figure 4.7 Plots of Eqs. (4.10) to (4.12).

4.6 Comparison with other prediction equations

To the best of the author's knowledge, there is no published equation for 3D non-full flowing culvert scour. For comparison, existing full flowing jet scour prediction equations are used for comparison purpose. These equations are listed in Table 4.2. The d_o in these equations for circular jet experiments were replaced by $4R_h$ to be consistent with R_h as the characteristic length scale used in this study.

Ali and Lim (1986) proposed equation for d_{se}/R_h based on outlet velocity, sediment settling velocity, sediment size, hydraulic radius, and densimetric Froude number. Lim (1995) proposed best fit and enveloping curves based on unsubmerged full flowing horizontal circular jet scour experiments. The equations proposed by Breusers and Raudkivi (1991) and Abt et al. (1984) were converted into the form used in Table 4.2. Chiew and Lim (1996) proposed equations for equilibrium scour hole dimensions produced for deeply submerged circular jets. Ade and Rajaratnam (1998) proposed equations based on a compiled database from many past studies. Their equations corresponding to deeply submerged experiments and unsubmerged experiments for $F_o < 10$ were used.

Figures 4.8 – 4.10 show comparisons of the calculated non-dimensionalized scour dimensions d_{se}/R_h, W_{se}/R_h, and L_{se}/R_h using the equations listed in Table 4.2. These figures show that the calculated values are mostly over-predict and non-full flowing outlet conditions generally produced smaller scour hole than the full flowing conditions. Thus, there is fundamental difference between the scour mechanism between a pressurized full flowing jet scour and an open channel flow type of scour under a non-full flowing culvert outlet. While enveloping curves equations were proposed for safety purpose, a suitable set of equations specifically for non-full flowing culvert scour are important, so as not to over provide for the scour protection requirement. The proposed Eqs. (4.6) – (4.9) performed better (Figure 4.6) and are recommended for prediction of scour hole dimensions below a non-full flowing culvert outlet.

Table 4.2 Existing equations proposed by other researchers

Researcher	Equation type	
Lim (1995)	d_{se} Best fit	$\frac{d_{se}}{R_h} = 1.28\ F_o$
	d_{se} Enveloping	$\frac{d_{se}}{R_h} = 1.8\ F_o$
Breusers and Raudkivi (1991) [a]	d_{se}	$\frac{d_{se}}{R_h} = 4.4\ F_o^{0.33}$
Abt et al (1984) [a]	d_{se}	$\frac{d_{se}}{R_h} = 14.68\ F_o^{0.57} \left(\frac{d_{50}}{4R_h}\right)^{0.4} (\sigma_g)^{-0.4}$
Chiew and Lim (1996)	d_{se}	$\frac{d_{se}}{R_h} = 0.84\ F_o$
	W_{se}	$\frac{W_{se}}{R_h} = 7.60\ F_o^{0.75}$
	L_{se}	$\frac{L_{se}}{R_h} = 17.64\ F_o^{0.75}$
Ade and Rajaratnam (1998)	d_{se} Best fit	$\frac{d_{se}}{R_h} = 1.8\ F_o - 1.24$
	d_{se} Enveloping	$\frac{d_{se}}{R_h} = 2(\ F_o + 1)$
	d_{se} Enveloping (unsubmerged, F_o <10)	$\frac{d_{se}}{R_h} = 2\ F_o$
	W_{se} Best fit	$\frac{d_{se}}{R_h} = 7.2(\ F_o - 0.2)$
	W_{se} Enveloping	$\frac{d_{se}}{R_h} = 7.2(\ F_o + 2)$
	L_{se} Best fit	$\frac{d_{se}}{R_h} = 12(\ F_o - 0.27)$
	L_{se} Enveloping	$\frac{d_{se}}{R_h} = 13.2\ (F_o + 2)$
Ali and Lim (1986) [b]	d_{se}	$\frac{d_{se}}{R_h} = 2.3 \left(\frac{U_o}{w}\right)^{\frac{1}{2}} \left(\frac{d_{50}}{R_h}\right)^{\frac{3}{8}} F_o^{\frac{3}{4}} - 1.19$

[a] as expressed in Lim (1995)

[b] w was calculated according to equation proposed by Cheng (1997).

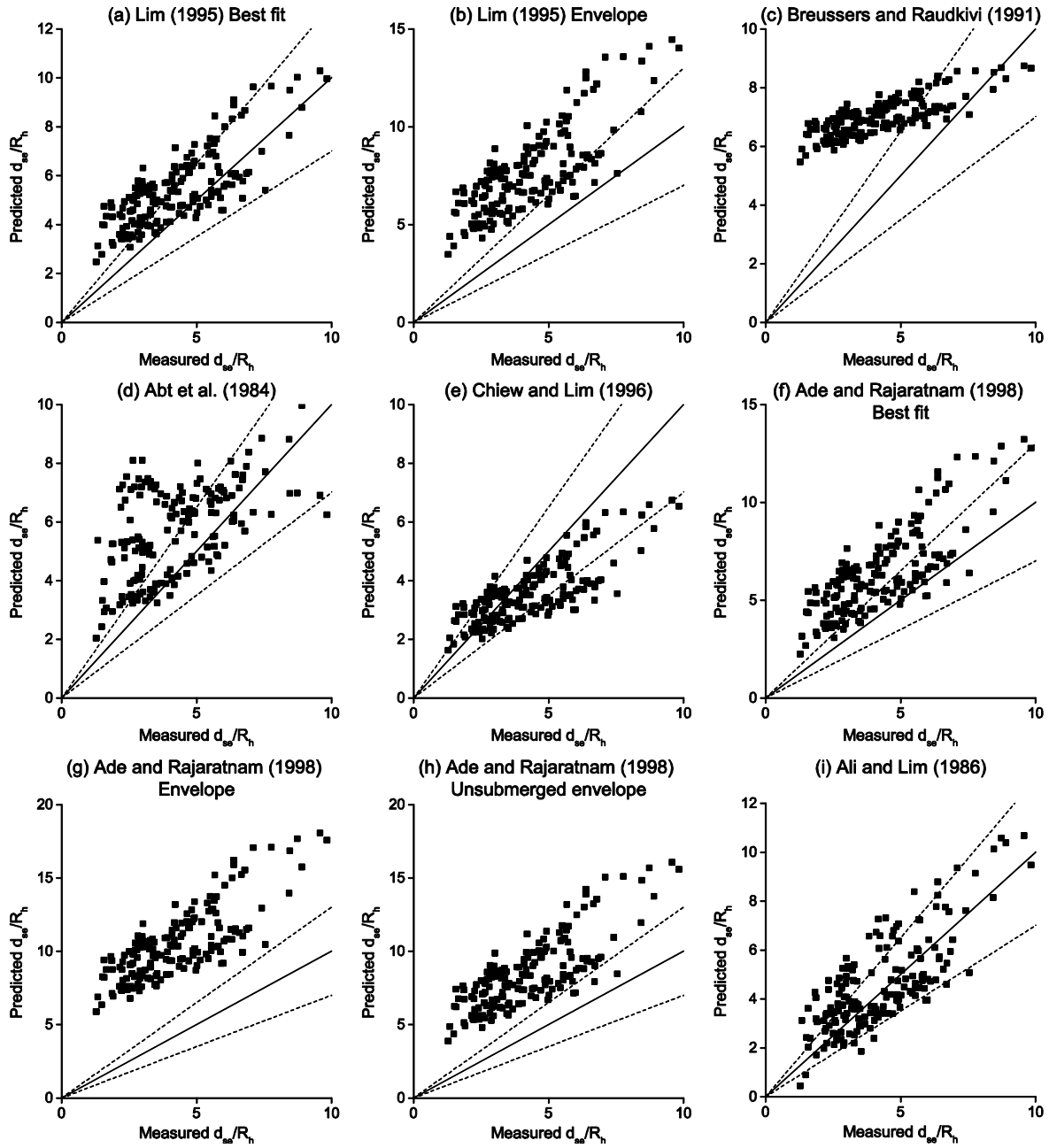

Figure 4.8 Comparisons of calculated versus measured d_{se}/R_h using equations proposed by various researchers (see Table 4.2). The dash lines and dotted lines are perfect agreement and +/- 30% error lines respectively.

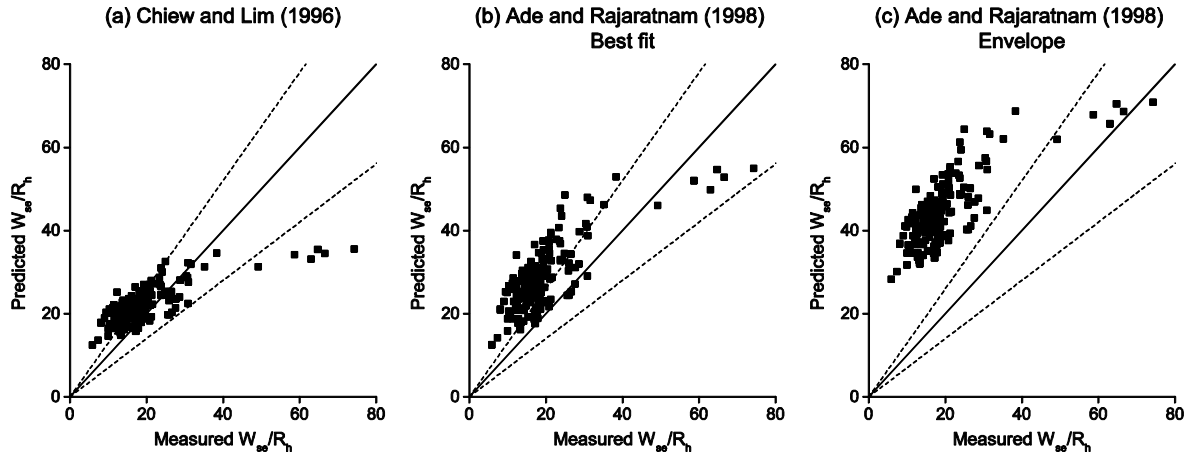

Figure 4.9 Comparisons of calculated versus measured W_{se}/R_h using equations proposed by various researchers (see Table 4.2). The dash lines and dotted lines are perfect agreement and +/- 30% error lines respectively.

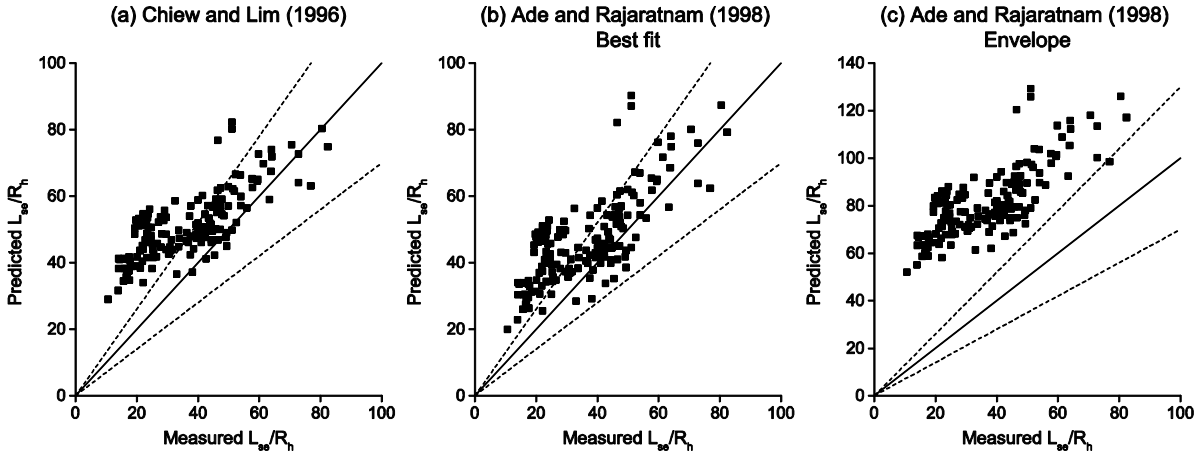

Figure 4.10 Comparisons of calculated versus measured L_{se}/R_h using equations proposed by various researchers (see Table 4.2). The dash lines and dotted lines are perfect agreement and +/- 30% error lines respectively.

4.7 Comparison with Abida's (1988) data

Abida (1988) conducted experiments with rectangular culvert. He investigated various parameters including sediment size (d_{50}), sediment gradation (σ_g), culvert width (b), and downstream channel width (W). The scour experiments were conducted for 2 hours. The ratio of downstream channel width to culvert width is about 2 to 10. It is possible that the side wall effect of the narrow downstream channel might have affected the scouring action (Lim 1995; Rajaratnam and Berry 1977).

Abida used the model culvert height and width as the characteristic lengths to non-dimensionalize scour hole dimensions and flow rate. This choice of characteristic length scale could not reflect the

actual outlet flow velocity as the flow velocity is calculated using the brink depth. Thus, in the current study, R_h was used as the characteristic length scale to re-analyze Abida's data.

Of all of Abida's (1988) 75 experiments, 27 experiments were found to be appropriate and were selected for comparison with the current proposed equation. An additional experiment (Run A in Table 3.5) was carried out to determine a time scale factor to extend Abida's 2-hour run to the equilibrium scour stage. A series of Abida's experiment used a rectangular culvert of 5.1 cm wide with sediment of d_{50} = 0.47 mm and σ_g = 1.64. Run A used similar flow velocity and tailwater depth with Abida's Run AW46. A single time extension factor was determined even though he has conducted experiments under a variety of hydraulic conditions. Only the scour hole depth was used for comparison as scour hole width development might have been influenced by the narrow flume width. In addition, the time development for scour width and length were observed to be different from that of scour depth, contrasting to observation in deeply submerged jet scour.

Figure 4.11 shows the predicted d_{se}/R_h versus measured d_{se}/R_h of the selected data using Eq. 4.6. The originally reported d_{se} has been multiplied by a factor of 1.36, based on the measured scour depth of Run A on comparing the 2 hours scour depth (58 mm) with the equilibrium scour depth (79 mm). Figure 4.11 shows that the predicted and measured values agree well and within acceptable range of +/- 30% error lines.

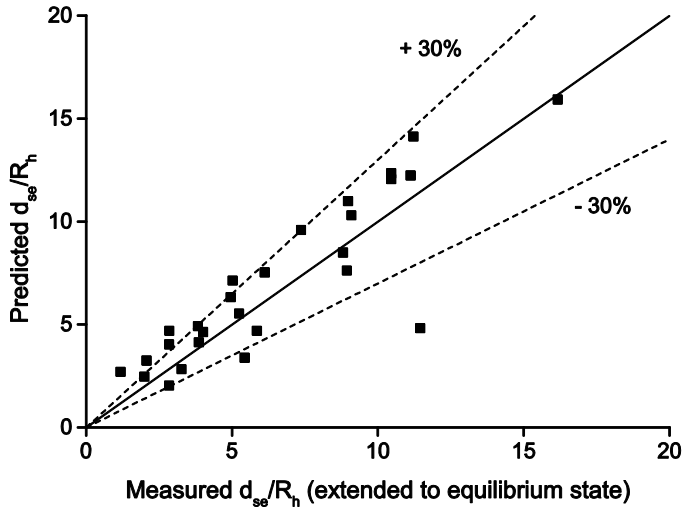

Figure 4.11 Comparison of predicted maximum scour depth, d_{se}/R_h using Eq. 4.6 with non-full flowing rectangular culvert scour data from Abida (1988).

4.8 Conclusions

This chapter presents the analysis of a compiled culvert scour database from current and previous NTU studies. A database of 171 non-full flowing culvert scour experiments were analyzed and F_o is found to be the dominant parameter to capture the effect of sediment size. The ratio h_o/H is more important for scour hole depth d_{se}/R_h and width W_{se}/R_h, but less important for length L_{se}/R_h and volume V_{se}/R_h. In all cases, σ_g is found to be heavily influencing scour hole sizes. The hydraulic radius (R_h) at the brink of the culvert outlet was found to be able to unify data across different culvert shapes.

Equations for prediction of the maximum scour depth, width, length, and volume have been proposed. By using the database, a comparison with existing full flowing jet scour equations was done. Extensive over-prediction of the compiled data suggesting the different scour mechanism between a pressurized full flowing jet and an open channel non-full flowing culvert flow. Some relevant data from Abida (1988) were used to compare with the proposed equation and the agreement was reasonable.

Chapter 5 Analysis of 3D Jet and Culvert Scour

5.1 Introduction

This chapter presents analysis of the compiled 3D jet and culvert scour data together. These 2 kinds of scour have been treated as the same engineering problem despite the difference between them. While culvert usually has water flowing partially full within its barrel and has an unsubmerged outlet condition, majority of the research were done using full flowing model culvert. Some jet scour studies used deeply submerged outlet condition which is unlikely to be found at a real culvert outlet. Circular jet has been used to simulate culvert scour for formulation of scour hole size prediction equations (Ruff et al. 1982). Almost all the proposed 3D horizontal jet scour prediction equations are based on full flowing jet scour data, and then assumed the outlet is flowing full when it is not (Thompson and Kilgore 2006).

This chapter focuses on the length scale suitable for analyzing both 3D jet and culvert scour data. For local scour in general, typical important length scales are those representing the hydraulic structure, surrounding flow properties, and sediment properties. For 3D jet and culvert scour, these important length scales are the jet outlet size and the sediment size. In Chapter 4, the hydraulic radius (R_h) has been shown to be a suitable characteristic length scale for culvert scour regardless of culvert shape.

In this chapter, firstly, the length scales used to represent outlet size and sediment size for both 3D jet and culvert scour are reviewed. The current practice is presented, and its shortcoming or limitation is highlighted. Next, improvement in data analysis is done by using a common length scale for both jet and culvert scour. 738 datasets of jet and culvert scour data were compiled for the analysis. Besides, the analysis will search for the most suitable representative sediment size.

5.2 Length scale for jet size and outlet

Traditionally, pipe diameter (d_o) has been used as characteristic length scale for circular outlet in (full flowing) jet scour research. It can represent both the property of the hydraulic structure and the incoming flow, as long as the water is flowing fully at the outlet. However, for non-full flowing condition and unsubmerged outlet condition, or non-circular outlet, “diameter” is not a suitable length scale. Researchers have used hydraulic radius (Abt et al. 1987; Ali and Lim 1986) or equivalent diameter (Ade and Rajaratnam 1998) in place of d_o. For non-full flowing circular outlet, Ade and

Rajaratnam (1998) defined a length scale as an equivalent pipe diameter (=,$\sqrt{4A/\pi}$) based on the area of flow at outlet (*A*). After experimenting with model culvert of different shapes, including circular, square, arch, and two rectangular of different aspect ratio, Abt et al. (1987) modified the Discharge Intensity ($DI = Q/g^{0.5}d_o^{2.5}$) (Abt et al. 1984) to include the hydraulic radius ($DI^* = Q/(A\sqrt{gR_h}$) (where *Q* is the incoming flow rate and *g* is the gravity acceleration). Normalization of the scour hole dimensions were done using R_h. However, in the adaptation of this into engineering manual (Thompson and Kilgore 2006), a form of Froude number $Q/\sqrt{gR_h^5}$ is used, and R_h is calculated assuming the outlet is flowing full. Abida and Townsend (1991) simply implemented the culvert width and height in the definition of Froude number, defined as $Q/(b\sqrt{gh^3})$ (where *b* is the culvert width and *h* is the culvert height) in their study of rectangular culvert scour.

On the other hand, some researchers consider various 2D and 3D jet scour problems together, believing the scour process have similar nature regardless of the outlet type and condition (Ali and Lim 1986; Breusers and Raudkivi 1991; Schiereck 2004). Ali and Lim (1986) proposed an equation for maximum scour depth for different outlet condition and different characteristic length scales were used for different cases. Among the types of scour covered by the equation are deeply submerged 2D jet from a well-rounded nozzle, deeply submerged 2D jet from a sharp sluice gate, and 2D and 3D jet with low tailwater depth. They used the hydraulic radius as the characteristic length for 3D jet scour. Breusers and Raudkivi (1991) presented the maximum scour depth of both submerged 2D horizontal plane jet and 3D horizontal circular jet in the same log-log plot (Figure 6.7 in Breusers and Raudkivi (1991), reproduced in Figure 5.1a). The clustered data trend for both 2D and 3D jets only differ in the slope. Schiereck (2004) outlined a similar plot (Figure 4-4 in Schiereck (2004), reproduced in Figure 5.1b), adding culvert scour data, which again only differs from other data clusters in the slope. Thus, it is possible to generalize different kinds of jet scour, and the mentioned plots suggest the differences between each kind of scour may be only a factor relating to the slope of the data cluster.

Based on the findings of the above review, the following analysis will be done using R_h which is equal to $d_o/4$ for a circular outlet and hence different from the traditional d_o by a factor of 4.

(a)

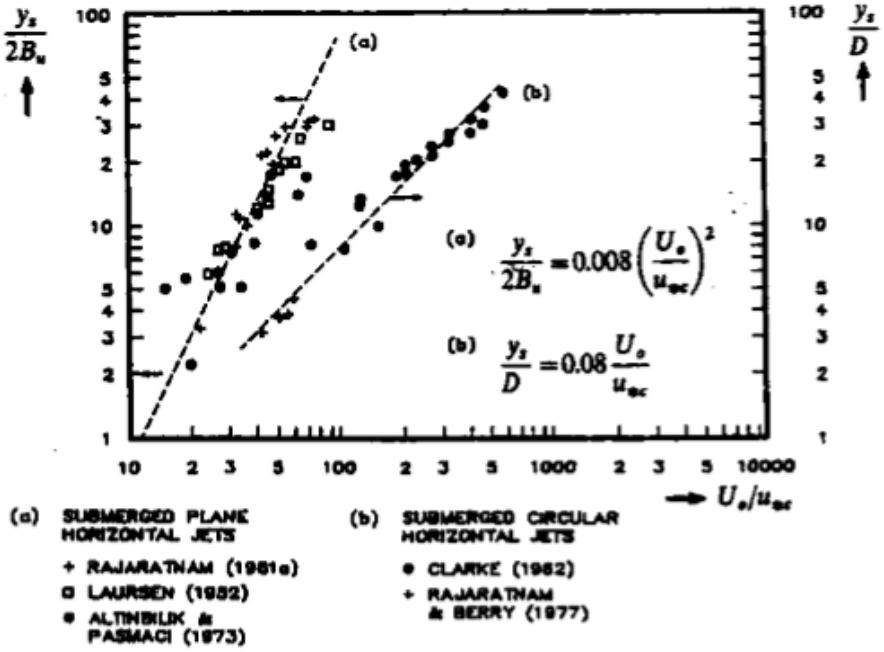

(b)

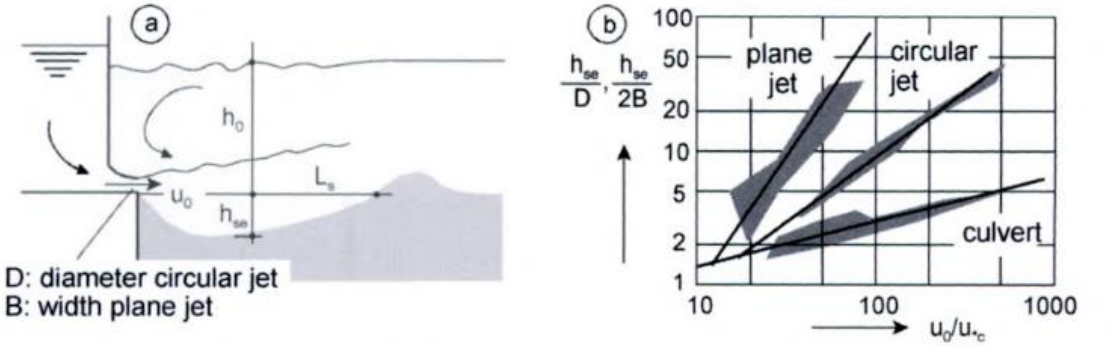

Figure 5.1 Figures from (a) Breusers and Raudkivi (1991) illustrating maximum scour depth for submerged plane and circular horizontal jets, and from (b) Schiereck (2003) illustrating scour depth for plane jet, circular jet, and culvert.

5.3 Length scale for sediment size

Another important length scale in scour is related to the sediment property, which is usually included in scour prediction equation as an independent length scale ratio or as part of a dimensionless number. In jet scour research, the densimetric Froude number (F_o) is usually formulated by using the median sediment diameter (d_{50}) (Ade and Rajaratnam 1998). F_o represents the ratio of average flow velocity to the settling velocity of a representative sediment grain. The sediment settling velocity has also been used to scale the jet velocity (Ali and Lim 1986; Breusers and Raudkivi 1991). In either way, a single sediment size is used in F_o or settling velocity calculation to represent the property of the sediment.

However, natural sediment can be highly non-uniform, with value of the geometric standard deviation $\left(\sigma_g = \sqrt{\frac{d_{84}}{d_{16}}}\right)$ about 4 (Breusers and Raudkivi 1991). Typical values of σ_g are 2.10 for gravel and 1.87 for sand (May et al. 2002). The non-uniformity of sediment is being considered when a sediment size other than d_{50} or σ_g is used. Abt et al. (1984) used both the relative sediment size (d_{50}/d_o) and σ_g in their equations. Hoffmans (1998) used the 90th percentile of sediment size (d_{90}) because sediment size larger than d_{50} should have dominant effect in the scour process. Ali and Lim (1986) used both F_o and the ratio of flow velocity to particle fall velocity in their scour depth prediction. Pagliara et al. (2008) used d_{90} for F_o and still included σ_g separately for 2D and 3D plunge pool scour prediction equations. Hager (2007) mentioned that σ_g is not important if d_{50} is used in F_o calculation. Abida and Townsend (1991) used an effective grain size which is calculated from every 10th percentile of sediment size.

The chosen sediment sizes in various jet scour prediction equations are either for convenience, as the median is a commonly used statistical property, or by reasoning that coarser sediments has more influence in the scour process. The different sediment size used indicates the need to determine a suitable representative sediment size, which includes both the central tendency and the variability of the sediment size distribution.

On the other hand, in hydraulic engineering, researchers have come up with a representative sediment size to express the surface roughness. The surface roughness of a channel bed is a function of bed sediment size distribution, which directly influences the channel resistance, vertical profile of flow velocity, and the channel flow capacity. Even though local scour is very different from the condition where the roughness height was originally used, the concept of a representative sediment size is very similar.

For scouring processes, the inertia of sediment bed could be better represented using a single grain size. Such an attempt has been made by Cheng (2016), which discussed the equivalent roughness height of a sediment bed by assuming that the grain size follows the lognormal distribution. A similar approach will be employed in the following data analysis.

5.4 Dimensional analysis and formulation

Dimensional analysis is carried out using common parameters for both full flowing jet scour and non-full flowing culvert scour. The main different between these 2 kinds of scour is the presence of free surface for the incoming flow at the outlet for the latter. Thus, the hydraulic radius (R_h) at the outlet

brink is used to measure the dimension of the incoming flow. For full flowing outlet, R_h calculated by dividing the flow area by the outlet perimeter. For non-full flowing outlet, it is calculated by dividing the flow area (A_o) by the wetted perimeter at the brink (P_{wet}). This method allows the actual flow area to be used in calculation of R_h, reflecting the actual condition of outlet as opposed to assuming full flowing outlet (Thompson and Kilgore 2006). For a circular full flowing outlet, R_h is equal to $d_o/4$, which means the non-dimensionalized scour hole length scale is only differs by a factor of 4 compared to when d_o is used traditionally for circular jet scour research. For similar outlet condition, a larger culvert or jet outlet would have a larger R_h. Thus, R_h is similar to d_o as a scaling factor and has similar function as d_o in dimensionless numbers.

The other important parameters include the incoming flow velocity (U_o), tailwater depth (H), sediment median diameter (d_{50}) and geometric standard deviation of sediments (σ_g). The density of the sediment particles (ρ_s) and the fluid (ρ) are usually expressed as relative density difference ($\frac{\rho_s-\rho}{\rho}$). This usually has the value around 1.65 for water-sand system, but it can be up to 3 order of magnitude larger for air-sediment system (Chiew and Lim 1996). The downstream channel width (B) is usually assumed less important, as it affects final scour hole dimensions only under certain circumstances. This study is limited to near horizontal incoming flow with no jet offset, thus both the culvert channel slope (S_o) and offset distance are ignored. As this current study focuses on equilibrium stage data, the experimental duration is not considered

With the above considerations, the maximum scour depth (d_{se}), width (W_{se}), length (L_{se}), and volume (V_{se}) can be expressed as

$$\mathrm{d}_{se}, W_{se}, L_{se}, V_{se} = f(R_h, U_o, H, d_{50}, \sigma_g, \rho, \rho_s, B) \quad (5.1)$$

By performing dimensional analysis, the above function can be reformulated as

$$\frac{\mathrm{d}_{se}}{R_h}, \frac{\mathrm{W}_{se}}{R_h}, \frac{\mathrm{L}_{se}}{R_h}, \frac{\mathrm{V}_{se}}{R_h^3} = f(F_o, \sigma_g, \frac{H}{R_h}, \frac{d_{50}}{R_h}, \frac{B}{R_h}) \quad (5.2)$$

In Eq. (5.2), R_h is selected as the characteristic length and used to scale all length parameters. $F_o (= \frac{U_o}{\sqrt{\frac{\rho_s-\rho}{\rho} g d_{50}}})$ is defined based on d_{50}, and σ_g is used to represent the non-uniformity of sediment.

The densimetric Froude number is given by a ratio of average flow intensity to the settling velocity of sediment grain. If d_{50} is included, the settling velocity is only associated with the median sediment size. For scouring processes, the scour depth provides a measure of dynamic equilibrium between the bed inertia (or resistance) and the flow intensity. For non-uniform sediment, the bed resistance can be

better described using the equivalent roughness height rather than the median grain diameter. If the sediment size is log-normally distributed, the equivalent roughness height can be expressed as

$$k_s = d_{50}\sigma_g^n \quad (5.3)$$

where n is an exponent. For example, if n = 1, $k_s = d_{84}$, and if n =2.33, $k_s = d_{99}$. Generally, the exponent can be associated with a particular diameter according to the following formula (Cheng 2016)

$$\mathrm{d_x} = d_{50}\sigma_g^{\sqrt{2}\left[\mathrm{erf}^{-1}\left(\frac{x-50}{50}\right)\right]} \quad (5.4)$$

where d_x is a particular sediment size. With this consideration, it is proposed here that F_o is redefined as

$$F_{o,dx} = \frac{U_o}{\sqrt{\frac{\rho_S-\rho}{\rho}gd_x}} \quad (5.5)$$

In Eq. (5.2), H/R_h is the relative tailwater depth. It implies the available water body for energy diffusion in full flowing outlet condition, while it indirectly implies the plunging tendency of incoming jet into the tailwater body in non-full flowing outlet condition. The commonly used H/d_o in full flowing circular outlet is scaled by a factor of 4 as $R_h = d_o/4$. For non-full flowing outlet, R_h replaces the brink depth h_o in the relative tailwater depth ratio H/h_o, which is equal or smaller than 1. Since R_h is function of h_o, H/R_h has similar meaning as H/h_o.

The term d_{50}/R_h is the relative sediment size. Similarly, it is usually expressed as d_{50}/d_o for circular full flowing outlet. The term B/R_h compares the width of the downstream channel to the jet size, also quantifies as the space for jet energy diffusion. Similarly, for full flowing circular outlet, $B/R_h = 4B/d_o$ in circular jet scour studies. d_{se}/R_h, W_{se}/R_h, L_{se}/R_h, and V_{se}/R_h^3 are the normalized maximum scour depth, width, length, and volume, respectively.

In the subsequent data analysis, Eq. (5.4) is used to calculate various sediment percentiles ranging from d_{50} to d_{99}. The corresponding densimetric Froude number $F_{o,dx}$ is calculated. Next, regression analysis is performed to find the most suitable representative sediment size d_x.

5.5 Maximum Scour Depth

738 datasets of jet and culvert scour data were compiled from available literature and experiments conducted in NTU, Singapore. The details of the database are listed in Tables 5.1 and 5.2. About half of the data were collected from NTU using different culvert and sediment combinations. The other data largely concerned circular jet only. Faruque et al. (2006) and Sarathi et al. (2008) investigated

square jet scour. Full flowing 3D jet experiments data from Ali and Lim (1986) are included for analysis. Abt et al. (1987) investigated outlet of different non-circular shapes. Air jet data were also included in the analysis for verification purpose.

In this analysis, R_h has been found to be suitable for both culvert and jet scour of various outlet shapes. In Figure 5.2, by plotting d_{se}/R_h against F_o, the data trend shows a single cluster consisting of both culvert and jet scour data. The data cluster together despite the various outlet conditions, outlet shapes, sediment properties and tailwater conditions. This also means other parameters such as H/R_h, d_{50}/R_h and B/R_h are of less importance. The effect of relative tailwater depth and relative sediment size is weak, and the effect of relative downstream channel width can be ignored under most experimental conditions.

Table 5.3 lists the R^2 values of the $F_{o,dx}$ regression analysis using sediment size of from d_{50} *to* d_{99} , together with their equations using Eq. (5.4). From the analysis, R^2 improves as d_x increases up to the best R^2 for $d_x = d_{80}$, then R^2 decreases for $d_x > d_{80}$. Considering both the statistical output and the practicality of the equation, the 84th percentile $d_{84} = d_{50}\sigma_g$ is decided to be the most suitable as the representative sediment diameter. A modified densimetric Froude number, $F_{o,d84}$, using d_{84} as the characteristic sediment size, with $d_{84} = d_{50}\sigma_g$ is proposed. A corresponding equation is proposed for d_{se}/R_h:

$$\frac{d_{se}}{R_h} = 1.22F_{o,d84} \quad (5.6)$$

Eq (5.6) shows that an estimation of the maximum scour hole depth can be based on $F_{o,d84}$ alone. This has also eliminated the need to include σ_g separately. On a side note, it is interesting to note that the same representative sediment size of d_{84} is found to be suitable for both 3D jet scour and in other hydraulics engineering applications (Cheng 2016).

The normalized scour depth data is plotted against $F_{o,d84}$ in Figure 5.3, and the improvement of the closer data clustering is obvious. This analysis shows that R_h and $F_{o,d84}$ are able to unify the data compiled across different experimental conditions and it means other dimensionless numbers commonly used in 3D jet scour studies are of lesser importance.

Table 5.1 Details of compiled culvert and jet scour data

Source	Type	Shape	d_o (mm)	b (mm)	side slope	d_{50} (mm)	σ_g	H (mm)	U_o (m/s)	no of runs
NTU data (full flowing)	F	Circular	4 -- 40	-	-	0.25 - 8.7	1.11 - 4.09	6 - 500	0.503 - 12.83	207
Lim and Chin (1992)	F	Circular	15	-	-	1.65	1.25 - 2.5	200	0.79 - 4.55	17
Lim (1995)	F	Circular	15 - 26	-	-	1.65	1.25	7.05 - 12.22	0.312 - 4.02	20
Chiew and Lim (1996)	AIR	Circular	4	-	-	0.94	1.29	-	36.63 - 151.65	8
	F	Circular	12.7 - 25.4	-	-	0.25-1.65	1.25 - 1.44	200 - 550	0.53 - 5.78	33
Clarke (1962)	F	Circular	2.38 - 14.3	-	-	0.82 - 2.02	1.22 - 1.38	159 - 279	2.1 - 12	25
Opie (1967)	F	Circular	309 - 914.4	-	-	25.3 - 204.2	0.99-1.18	122 - 488	2.18 - 4.21	12
Rajaratnam and Berry (1977)*	AIR	Circular	6.35 - 23.5	-	-	1.4	1.26 - 1.5	-	10.058 - 54.864	26
	F	Circular	25.4	-	-	1.4	1.5	610	1.28 - 1.81	4
Rajaratnam and Diebel (1981)*	F	Circular	12.7 - 25.4	-	-	1.05	1.5	2.5 - 43	0.41 - 2.32	17
Rajaratnam and Humphries (1983)*	F	Rectangular	31	50	-	0.11	1.5	31	0.089 - 0.404	8
Ade and Rajaratnam (1998)	F	Circular	5 - 25.4	-	-	0.24 - 7.2	1.33 - 1.46	14.25 - 620	2.2 - 5.5	12
	AIR	Circular	12.5	-	-	1.47	1.12	-	20.3 - 80	7
Ruff et al. (1982)	NF, F	Circular	102 - 457	-	-	1.86 - 7.62	1.32 - 4.78	0 - 205.65	1.119 - 5.479	56
		Square	102	-	-					
Abt et al. (1987)	F	Square	100	-	-	1.86	1.33	-	-	19
		Rectangular	100	160	-					
		Rectangular	100	200	-					
		Arch	100	150	-					
Ali and Lim (1986)	F	Square	50.8	-	-	0.82	1.13	50.8	0.112 - 0.947	7
Liriano (1999)	F	Circular	13 - 311	-	-	0.38 – 9	1.4	6.5 - 466.5	-	49
Faruque et al. (2006)	F	Square	-	26.6 - 76	-	2.46	1.24	53.2 - 456	0.78 - 1.31	9
Sarathi et al. (2008)	F	Square	-	26.6	-	0.71 - 2.46	1.14 - 1.24	26.6 - 478.8	0.42 - 2	31
NTU data (non-full flowing)	NF	Rectangular	-	50 - 160	-	0.49 - 5.2	1.13 - 3.83	5.9 - 101.5	0.291 - 1.116	171
		Trapezoidal	-	50 - 120	1 - 2.5					
		Triangular	-	-	1					

* unrecorded σ_g assumed as 1.5

Table 5.2 Dimensionless numbers and normalized scour hole dimensions of the database

Source	F_o	$F_{o,\,d84}$	d_{se}/R_h	W_{se}/R_h	L_{se}/R_h	V_{se}/R_h^3
NTU data (full flowing)	3.586 - 64.502	3.121 - 52.498	2.5 – 56	17.7 - 279.2	38.8 - 561.6	420 - 2032640
Lim and Chin (1992)	4.83 - 27.85	3.62 - 24.901	1.6 - 36.8	16 - 154.667	61.333 - 288	948.148 - 606814.815
Lim (1995)	1.909 - 24.598	1.707 - 22.001	3.231 - 19.467	16.923 - 152	26.154 - 308.267	1092.399 - 237037.037
Chiew and Lim (1996) AIR	7.84 - 32.46	6.903 - 28.579	12 – 57	38 - 205	155 - 510	-
Chiew and Lim (1996)	4.83 - 85.28	4.32 - 71.067	2.667 - 63.937	21.333 - 240.63	77.165 - 457.953	-
Clarke (1962)	14.16 - 104.16	12.82 - 88.667	28.252 - 176.471	113.566 - 648.739	198.881 - 1136.134	-
Opie (1967)	1.69 - 3.41	1.699 - 3.36	1.376 - 4.854	2.76 - 23.676	13.792 - 37.511	6.716 - 1658.664
Rajaratnam and Berry (1977) AIR	2.72 - 13.3	2.221 - 11.849	1.14 - 18.457	-	-	-
Rajaratnam and Berry (1977)	8.57 - 12.14	6.997 - 9.912	12.756 - 18.425	-	-	-
Rajaratnam and Diebel (1981)	3.13 - 17.93	2.556 - 14.64	2.646 - 26.016	-	-	-
Rajaratnam and Humphries (1983)	2.11 - 9.57	1.723 - 7.814	2.2 - 10.12	-	-	-
Ade and Rajaratnam (1998)	6.29 - 88.2	5.454 - 72.995	9.37 - 76.4	32.598 - 296.8	80.63 - 720	-
Ade and Rajaratnam (1998) AIR	5.67 - 22.31	5.358 - 21.081	6.976 - 24.64	21.76 - 97.6	89.6 - 265.6	-
Ruff et al. (1982)	5.711 - 31.577	2.661 - 27.381	2.202 - 13.507	14.238 - 109.25	24.871 - 191.247	316.264 - 60830.024
Abt et al. (1987)	7.2 - 21.81	6.243 - 18.912	9.258 - 13.431	-	-	-
Ali and Lim (1986)	2.795 - 9.672	2.629 - 9.099	1.652 - 7.4	-	-	-
Liriano (1999)	3.4 - 9	2.874 - 7.606	2.2 - 7.6	-	26 - 72	-
Faruque et al. (2006)	3.9 - 6.6	3.502 - 5.927	4.366 - 10.337	18.647 - 37.594	37.368 - 86.466	6123.342 - 6269.135
Sarathi et al. (2008)	3.9 - 10	3.502 - 9.366	4.135 - 16	18.647 - 80.301	43.308 - 127.82	1105.143 - 45463.877
NTU data (non-full flowing)	1.938 - 8.037	0.99 - 6.675	1.275 - 9.827	5.865 - 74.303	10.582 - 82.294	17.655 - 9681.923

Table 5.3 Regression analysis results using different representative sediment sizes for maximum scour depth (738 data points).

d_x	Exponent of σ_g	Equation	R^2	$d_{se}/R_h = 10^b * F_{o,dx}^m$		
				m	b	10^b
50	0.00	$d_{50} = d_{50}$	0.8442	1.017	-0.006	0.986
55	0.13	$d_{55} = d_{50}\sigma_g^{0.13}$	0.8534	1.022	0.000	1.000
60	0.25	$d_{60} = d_{50}\sigma_g^{0.25}$	0.8614	1.026	0.008	1.018
65	0.39	$d_{65} = d_{50}\sigma_g^{0.39}$	0.8681	1.029	0.018	1.042
70	0.52	$d_{70} = d_{50}\sigma_g^{0.52}$	0.8736	1.029	0.030	1.072
75	0.67	$d_{75} = d_{50}\sigma_g^{0.67}$	0.8775	1.027	0.045	1.110
80	0.84	$d_{80} = d_{50}\sigma_g^{0.84}$	0.8796	1.023	0.065	1.160
84	1.00	$d_{84} = d_{50}\sigma_g$	0.8794	1.016	0.085	1.216
85	1.04	$d_{85} = d_{50}\sigma_g^{1.04}$	0.8790	1.014	0.090	1.230
90	1.28	$d_{90} = d_{50}\sigma_g^{1.28}$	0.8739	0.998	0.125	1.333
95	1.64	$d_{95} = d_{50}\sigma_g^{1.64}$	0.8584	0.966	0.183	1.523
99	2.33	$d_{99} = d_{50}\sigma_g^{2.33}$	0.8095	0.887	0.299	1.991

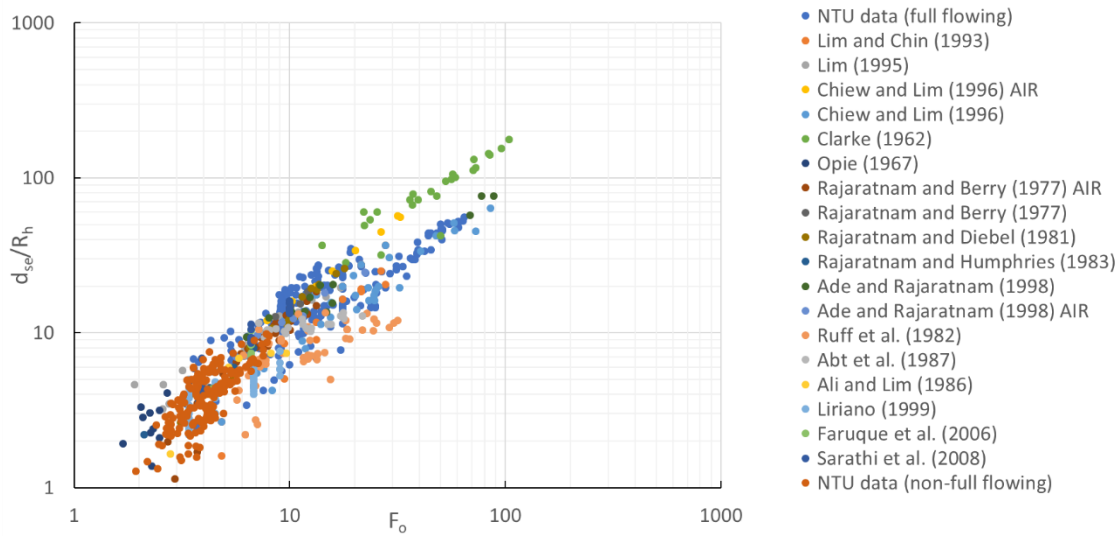

Figure 5.2 d_{se}/R_h vs $F_{o,d50}$ for compiled jet and culvert scour data.

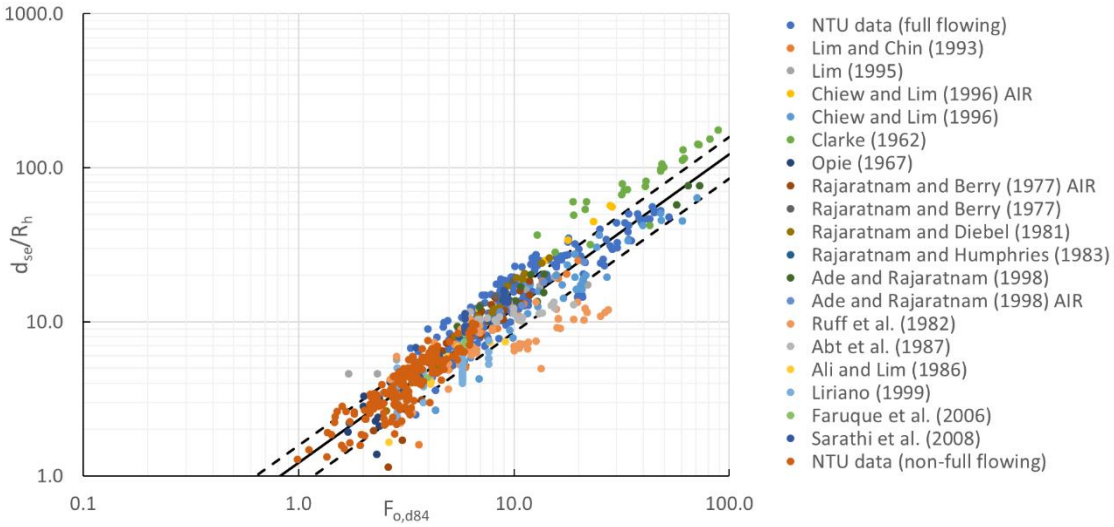

Figure 5.3 d_{se}/R_h versus $F_{o,d84}$ for compiled jet and culvert scour data. The solid line in the figure is Eq. (5.6), and the dashed lines are the $\pm 30\%$ error lines.

5.6 Maximum Scour Width, Length, and Volume

The analysis of maximum scour width (W_{se}), length (L_{se}), and volume (V_{se})are presented in this section. The conventional plots of normalized maximum width (W_{se}/R_h), length (L_{se}/R_h), and volume (V_{se}/R_h^3) versus d_{50}-based F_o are shown in Figure 5.4. The same analysis as those done for the maximum scour depth (d_{se}/R_h) was carried out for W_{se}/R_h, L_{se}/R_h, and V_{se}/R_h^3. The same regression analysis is applied for maximum scour width, length, and volume. Tables 5.4, 5.5, and 5.6 show the regression results. 551, 609, 466 data are available for the regression for W_{se}, L_{se}, and V_{se} respectively.

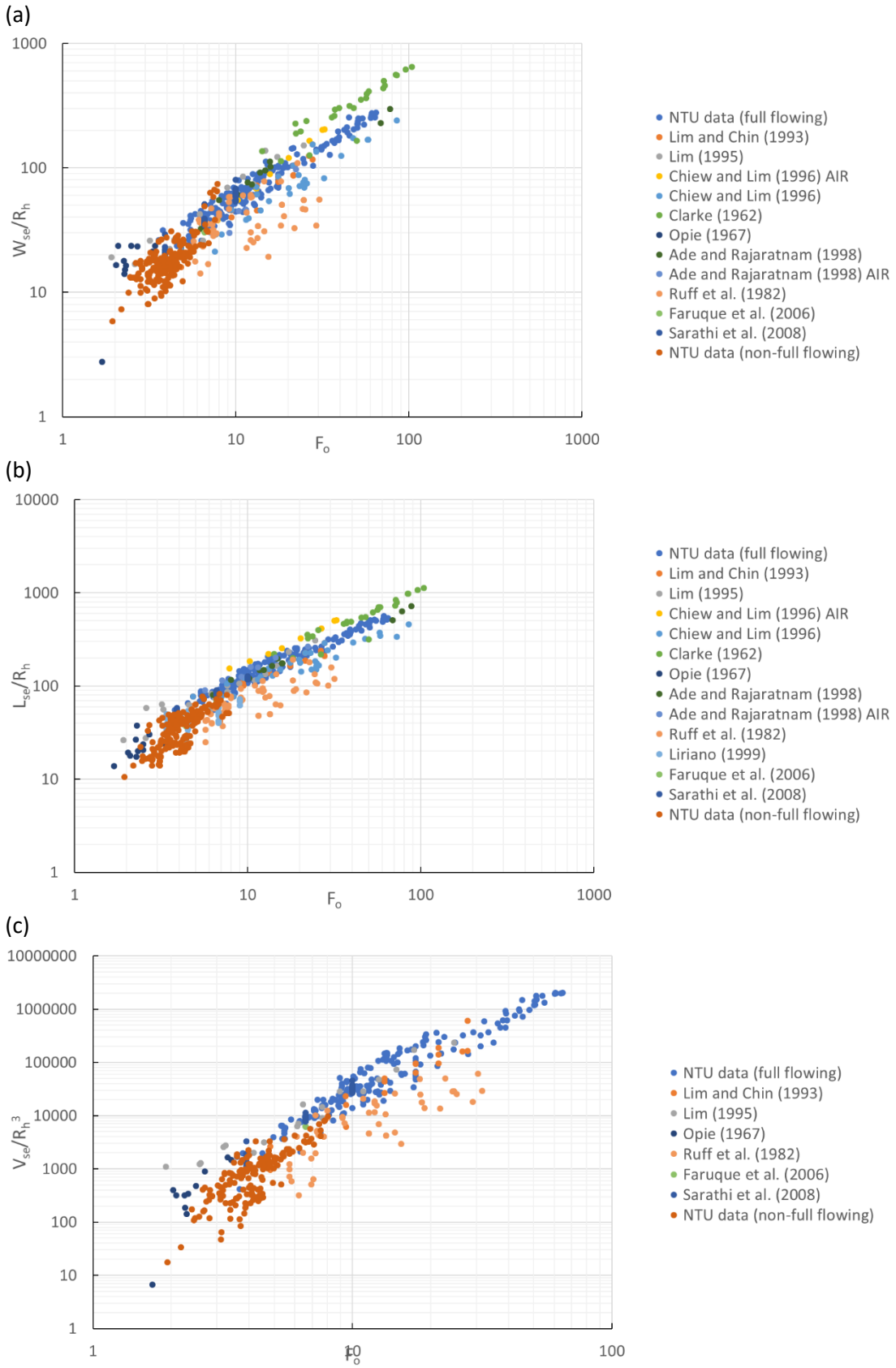

Figure 5.4 (a) W_{se}/R_h, (b) L_{se}/R_h, and (c)V_{se}/R_h^3 versus d_{50}-based F_o respectively.

Table 5.4 Regression analysis results for maximum scour width (551 data points).

d_x	Exponent of σ_g	Equation	R^2	$W_{se}/R_h = 10^b * F_{o,dx}^m$		
				m	b	10^b
50	0.00	$d_{50} = d_{50}$	0.9131	1.019	0.678	4.770
55	0.13	$d_{55} = d_{50}\sigma_g^{0.13}$	0.9192	1.022	0.688	4.872
60	0.25	$d_{60} = d_{50}\sigma_g^{0.25}$	0.9237	1.023	0.699	5.001
65	0.39	$d_{65} = d_{50}\sigma_g^{0.39}$	0.9264	1.022	0.713	5.161
70	0.52	$d_{70} = d_{50}\sigma_g^{0.52}$	0.9271	1.019	0.729	5.361
75	0.67	$d_{75} = d_{50}\sigma_g^{0.67}$	0.9256	1.014	0.749	5.612
80	0.84	$d_{80} = d_{50}\sigma_g^{0.84}$	0.9211	1.004	0.774	5.939
84	1.00	$d_{84} = d_{50}\sigma_g$	0.9142	0.992	0.799	6.296
85	1.04	$d_{85} = d_{50}\sigma_g^{1.04}$	0.9123	0.989	0.805	6.384
90	1.28	$d_{90} = d_{50}\sigma_g^{1.28}$	0.8965	0.966	0.848	7.046
95	1.64	$d_{95} = d_{50}\sigma_g^{1.64}$	0.8647	0.922	0.916	8.240
99	2.33	$d_{99} = d_{50}\sigma_g^{2.33}$	0.7872	0.825	1.047	11.151

Table 5.5 Regression analysis results for maximum scour length (609 data points).

d_x	Exponent of σ_g	Equation	R^2	$L_{se}/R_h = 10^b * F_{o,dx}^m$		
				m	b	10^b
50	0.00	$d_{50} = d_{50}$	0.9023	1.053	0.952	8.944
55	0.13	$d_{55} = d_{50}\sigma_g^{0.13}$	0.9092	1.057	0.960	9.115
60	0.25	$d_{60} = d_{50}\sigma_g^{0.25}$	0.9146	1.060	0.970	9.333
65	0.39	$d_{65} = d_{50}\sigma_g^{0.39}$	0.9185	1.061	0.982	9.604
70	0.52	$d_{70} = d_{50}\sigma_g^{0.52}$	0.9206	1.059	0.998	9.943
75	0.67	$d_{75} = d_{50}\sigma_g^{0.67}$	0.9207	1.055	1.016	10.374
80	0.84	$d_{80} = d_{50}\sigma_g^{0.84}$	0.9182	1.048	1.039	10.935
84	1.00	$d_{84} = d_{50}\sigma_g$	0.9134	1.038	1.063	11.549
85	1.04	$d_{85} = d_{50}\sigma_g^{1.04}$	0.9119	1.035	1.068	11.702
90	1.28	$d_{90} = d_{50}\sigma_g^{1.28}$	0.8994	1.014	1.109	12.847
95	1.64	$d_{95} = d_{50}\sigma_g^{1.64}$	0.8724	0.975	1.174	14.928
99	2.33	$d_{99} = d_{50}\sigma_g^{2.33}$	0.8026	0.881	1.303	20.070

Table 5.6 Regression analysis results for scour hole volume (466 data points).

d_x	Exponent of σ_g	Equation	R^2	$V_{se}/R_h^3 = 10^b * F_{o,dx}^m$		
				m	b	10^b
50	0.00	$d_{50} = d_{50}$	0.9008	3.076	1.140	13.809
55	0.13	$d_{55} = d_{50}\sigma_g^{0.13}$	0.9144	3.107	1.153	14.228
60	0.25	$d_{60} = d_{50}\sigma_g^{0.25}$	0.9258	3.129	1.175	14.951
65	0.39	$d_{65} = d_{50}\sigma_g^{0.39}$	0.9348	3.143	1.206	16.055
70	0.52	$d_{70} = d_{50}\sigma_g^{0.52}$	0.9411	3.146	1.247	17.678
75	0.67	$d_{75} = d_{50}\sigma_g^{0.67}$	0.9443	3.138	1.303	20.068
80	0.84	$d_{80} = d_{50}\sigma_g^{0.84}$	0.9435	3.115	1.375	23.709
84	1.00	$d_{84} = d_{50}\sigma_g$	0.9387	3.079	1.453	28.376
85	1.04	$d_{85} = d_{50}\sigma_g^{1.04}$	0.9370	3.070	1.472	29.651
90	1.28	$d_{90} = d_{50}\sigma_g^{1.28}$	0.9212	2.989	1.610	40.709
95	1.64	$d_{95} = d_{50}\sigma_g^{1.64}$	0.8847	2.831	1.834	68.225
99	2.33	$d_{99} = d_{50}\sigma_g^{2.33}$	0.7904	2.464	2.267	185.134

The regression analysis results show that the representative sediment size that is most suitable for W_{se}/R_h, L_{se}/R_h, and V_{se}/R_h^3 are d_{70}, d_{75}, and d_{75} respectively, different from the results for d_{se}/R_h. This can be attributed to the heavy influence or various factors towards these scour hole dimensions. Even so, the analysis results collectively show that a sediment diameter larger than the median diameter should be used.

As opposed to the maximum scour depth, where the force of gravity has the strongest influences, the scour hole width and length has been shown to be influenced by the recirculating flows, relative downstream channel size, and relative tailwater depth. The scour hole width could be widened near the original bed level by strong recirculating flows (see Figures 3.28 and 3.29) when the tailwater depth is low. The scour hole was distorted at small relative downstream channel width (Lim 1995).

On the other hand, the scour hole length represents an equilibrium between the jet strength, sediment properties, fluid/sediment density difference, the ridge height, downstream channel width, and outlet shape. For example, air jet has been known to produce scour hole with low ridge compared to deeply submerged water jet. The present study also observed that at minimum tailwater depth level, the scour hole length could be unobtainable for rectangular culvert scour while the scour hole is relatively short for trapezoidal culvert scour (see Figure 3.29). The scour hole volume is the collective function of depth, width, and length, and the detailed shape is unable to be represented by only these 3 main dimensions. Thus, it is not surprising that V_{se}/R_h^3 also has d_{75} as the most suitable representative sediment size.

Predictive equations have been proposed for W_{se}/R_h and L_{se}/R_h as shown below. The equations focused on simplicity and physical meaning between the scour hole size and the jet and sediment properties.

$$\frac{W_{se}}{R_h} = 5.36\, F_{o,d70} \tag{5.7}$$

$$\frac{L_{se}}{R_h} = 10.37\, F_{o,d75} \tag{5.8}$$

For V_{se}/R_h^3, the proposed equation is a function of the traditional d_{50}-based F_o after rearrangement of the terms.

$$\frac{V_{se}}{R_h^3} = 20.07\, \frac{F_{o,d50}^3}{\sigma_g} \tag{5.9}$$

Given the strong influence of force of gravity for scour hole volume, as it is for the scour hole depth, and the fact that the scour hole volume is another overall representative parameter, as analyzed by Ali and Lim (1986), an equation using d_{84} for V_{se}/R_h^3 is also proposed.

$$\frac{V_{se}}{R_h^3} = 28.38\, F_{o,d84}^3 \qquad (5.10)$$

Figure 5.5 shows the distribution of W_{se}/R_h and L_{se}/R_h, plotted against respective $F_{o,dx}$ that has the best regression results. The equations and their +/- 30% error lines are shown in the plots. Figure 5.6 shows the distribution of the data points for the 2 equations proposed for V_{se}/R_h^3. The regression analysis was carried out without the sand experiments data with d_o > 102 mm from Ruff et al. (1982). For W_{se}/R_h and V_{se}/R_h^3, a data point from Opie with extreme low value is not used during regression analysis. This data point corresponds to an experiment carried out using a sediment size of nearly 20 cm, and different scour mechanism is likely to have caused such low value. The proposed equations predict higher values for the excluded data points, thus it is deemed sufficient for engineering purpose.

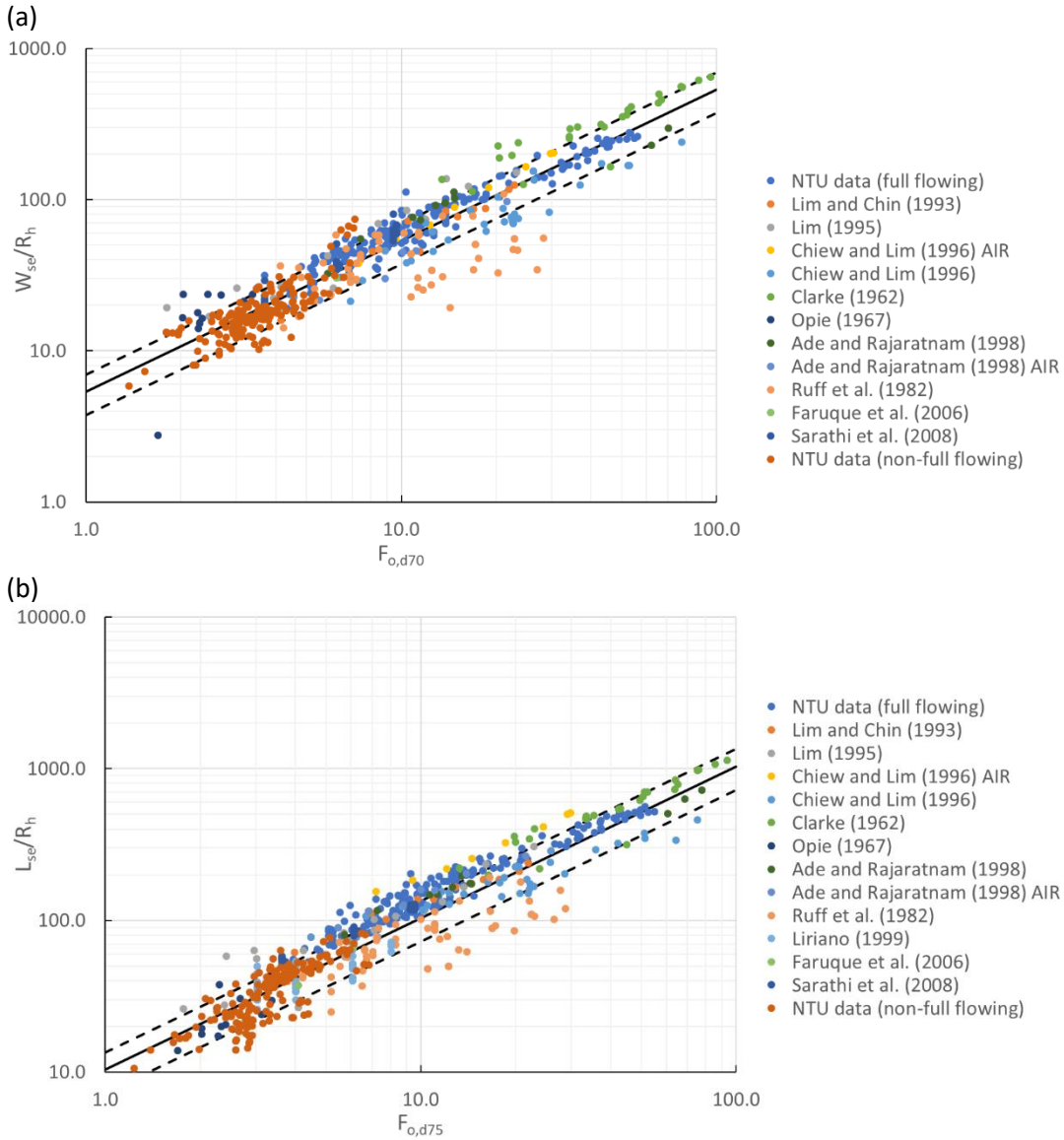

Figure 5.5 (a) W_{se}/R_h plotted against $F_{o,d70}$, and (b) L_{se}/R_h plotted against $F_{o,d75}$. The solid lines in (a) and (b) are Eqs. (5.7) and (5.8), respectively, and the dashed lines are the +/- 30% error lines.

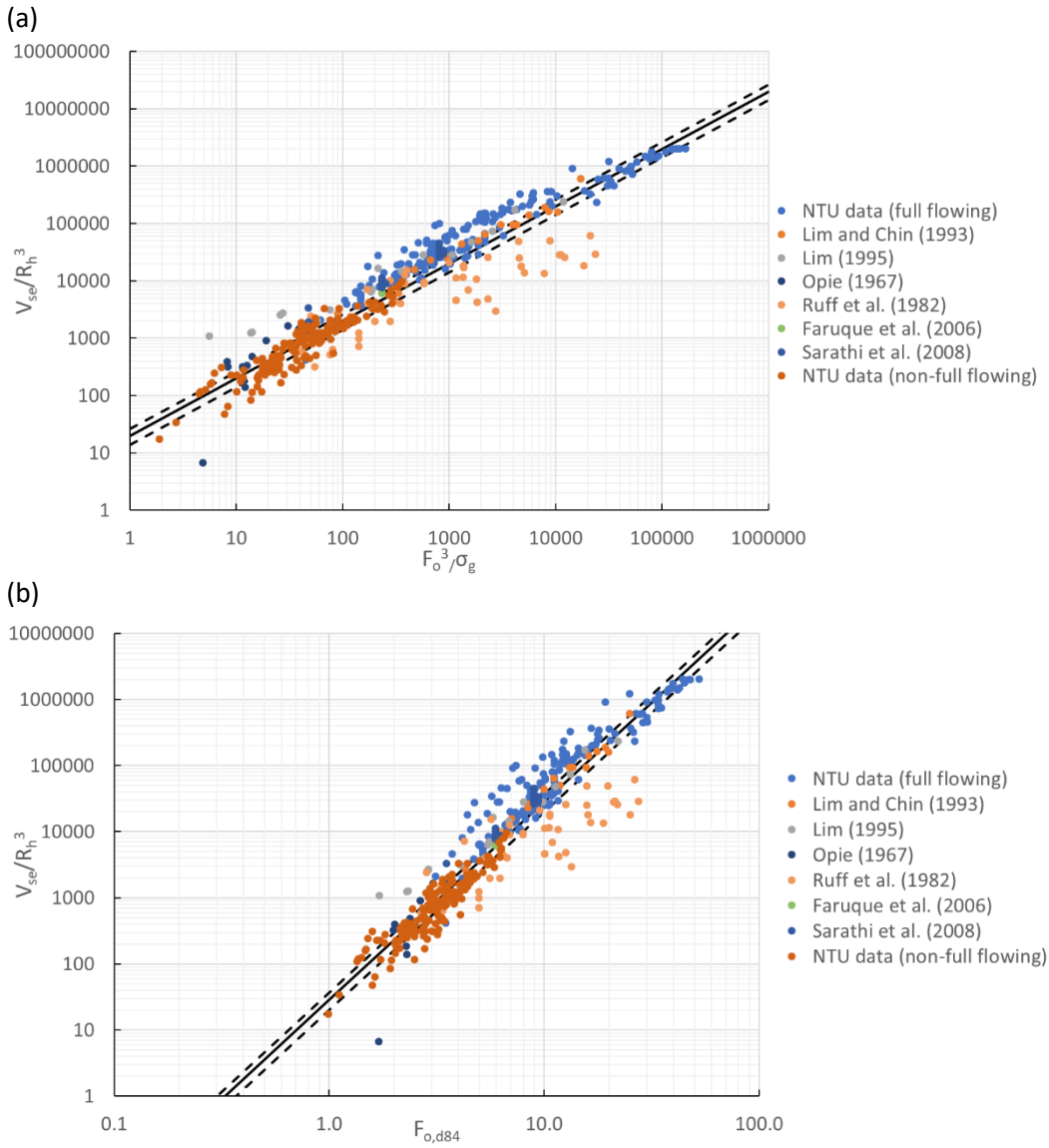

Figure 5.6 (a) V_{se}/R_h^3 plotted against $F_{o,d50}^3/\sigma_g$ and (b) V_{se}/R_h^3 plotted against $F_{o,d84}$ The solid lines in (a) and (b) are Eqs. (5.9) and (5.10), respectively, and the dashed lines are the +/- 30% error lines.

Figure 5.7 shows the relationship between d_{se}/R_h with W_{se}/R_h, L_{se}/R_h, and V_{se}/R_h^3 respectively. Power law regression were carried out and the best fit equations and +/- 30% lines are also plotted together in the figure. The best fit equations are as follows:

$$\frac{W_{se}}{R_h} = 5.56 \frac{d_{se}}{R_h}^{0.92} \quad (5.11)$$

$$\frac{L_{se}}{R_h} = 10.99 \frac{d_{se}}{R_h}^{0.94} \quad (5.12)$$

$$\frac{V_{se}}{R_h^3} = 17.6 \frac{d_{se}}{R_h}^{2.9} \quad (5.13)$$

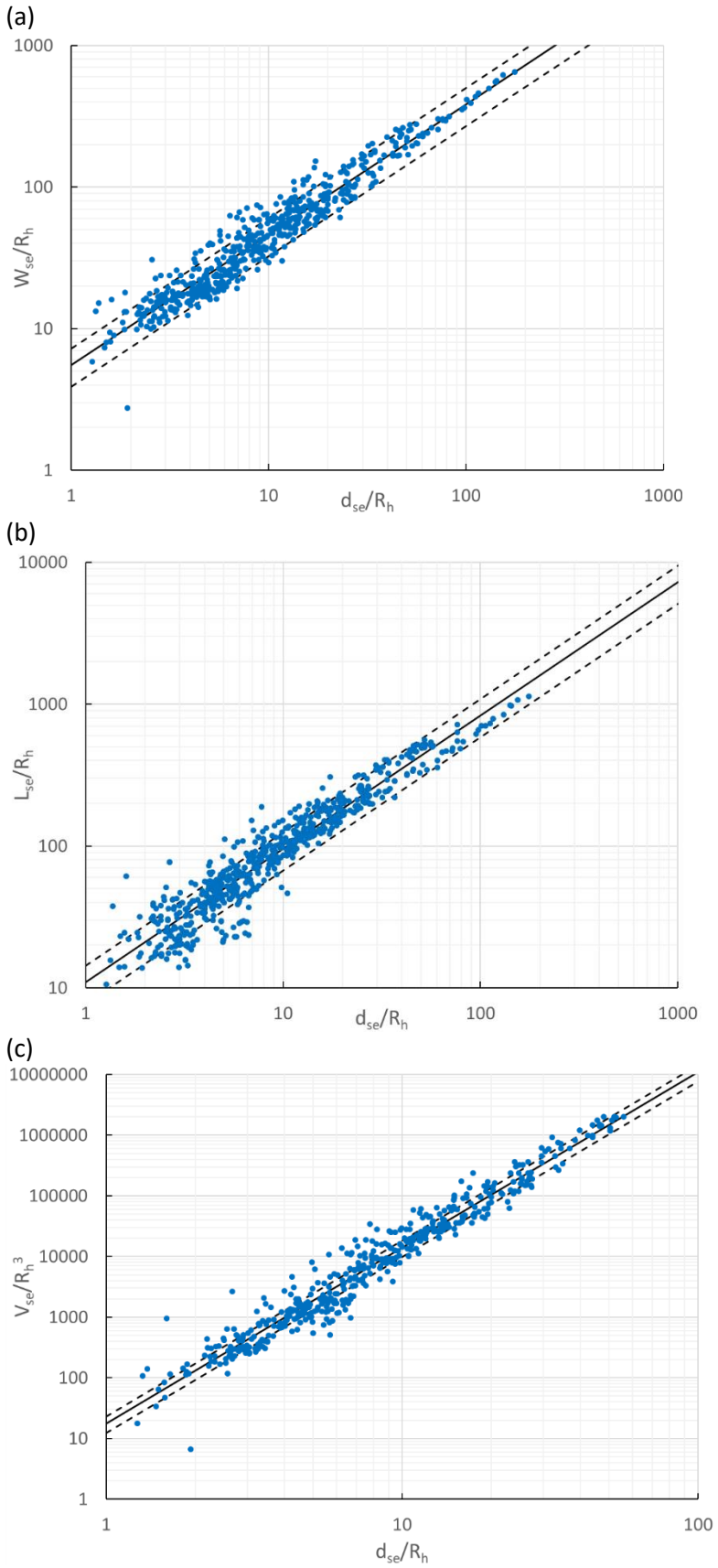

Figure 5.7 Relationship between d_{se}/R_h with (a) W_{se}/R_h,(b) L_{se}/R_h, and (c) V_{se}/R_h^3 respectively, together with best fit Eqs. (5.11), (5.12) and (5.13), respectively, and the dashed lines are the +/- 30% error lines.

For fast approximation, the normalized scour hole size can be simplified from Eqs. (5.11) to (5.13) and calculated as follows:

$$\frac{W_{se}}{R_h} = 6\ \frac{d_{se}}{R_h} \tag{5.14}$$

$$\frac{L_{se}}{R_h} = 11\ \frac{d_{se}}{R_h} \tag{5.15}$$

$$\frac{V_{se}}{R_h^3} = 18\ \frac{{d_{se}}^3}{R_h} \tag{5.16}$$

5.7 Effect of H/R_h and d_{50}/R_h

Continuing from the discussion about relative tailwater depth (H/R_h) and relative sediment size (d_{50}/R_h), Figure 5.8 shows the d_{se}/R_h versus $F_{o,d84}$ plot with values of H/R_h and d_{50}/R_h show as color of the markers respectively. The color of the markers is represented as the normalized log10 values of either H/R_h or d_{50}/R_h.

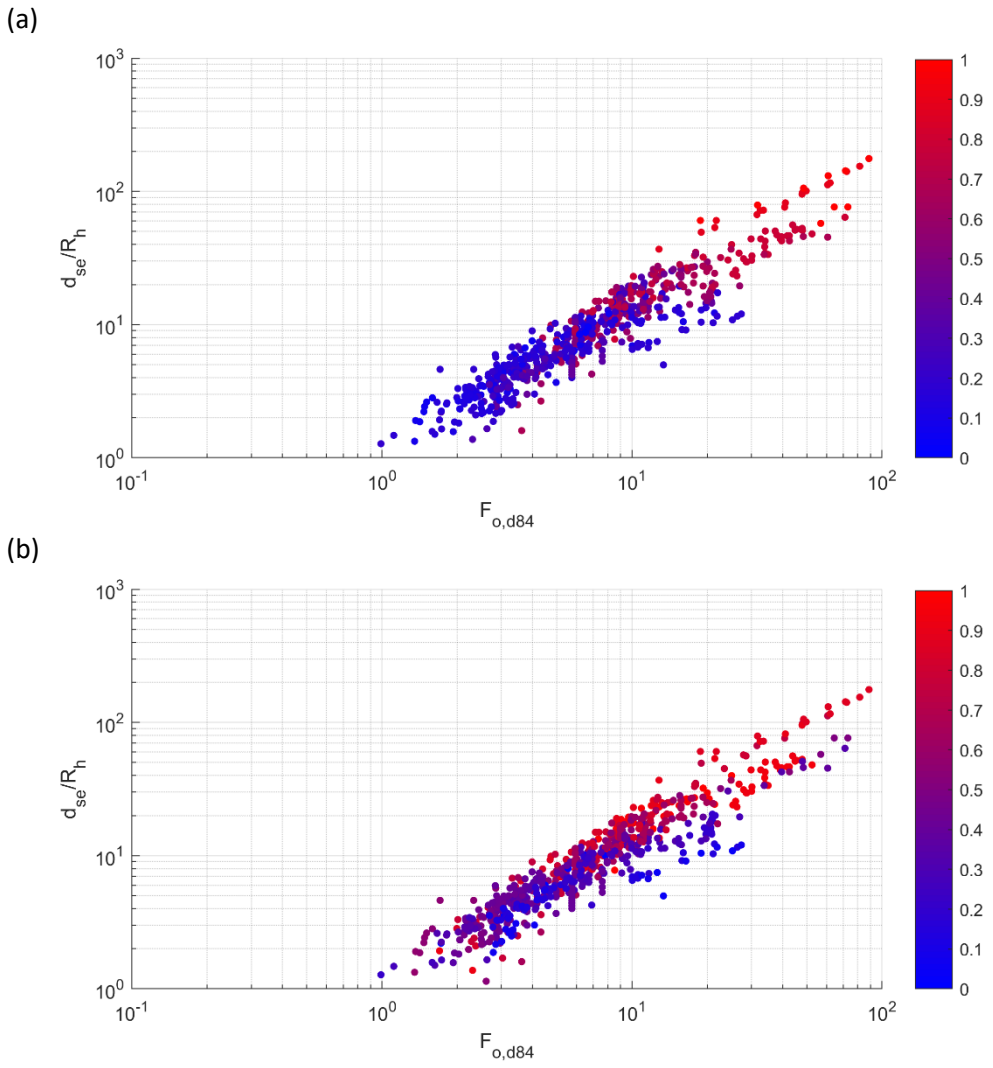

Figure 5.8 d_{se}/R_h versus $F_{o,d84}$ plot with normalized log10 values of (a) H/R_h, and (b) d_{50}/R_h as colour of markers, respectively.

From Figure 5.8, both the influences of relative tailwater depth (Figure 5.8a) and relative sediment size (Figure 5.8b) are weak compared to $F_{o,d84}$ as no clear trend can be seen from the plot. Majority of the data points display a mixed of either H/R_h or d_{50}/R_h. Figure 5.8a shows that for the non-full flowing culvert scour, which has tailwater depth limited by brink depth, the data points occupies mainly in the lower values of $F_{o,d84}$ cluster.

The influence of both H/R_h and d_{50}/R_h can be seen in Figure 5.9 in which the full database is again plotted as d_{se}/R_h against H/R_h and d_{50}/d_o with the log10 value of $F_{o,d84}$ displayed as marker color. Layering according to $F_{o,d84}$ values can be seen from both plots, which is expected as a larger $F_{o,d84}$ should produce a larger (and deeper) scour hole. In both sub plots, going in the x-direction from left to right does not have an obvious peak or dip, suggesting no strong dependency of the d_{se}/R_h values on both H/R_h and d_{50}/d_o. This is unlike the dependency of relative tailwater depth on scour hole depth in 2D jet scour as identified by Ali and Lim (1986).

The regions in Figure 5.9 with missing data show the limitation of the jet and culvert scour experiments. Usually, when a large model culvert is used, the outlet flow velocity is smaller with a smaller relative tailwater depth due to equipment constraint. On the other hand, by using small jet size, both high tailwater depth and jet velocity can be achieved.

5.8 Conclusions

Based on the analysis of a compiled database of 738 experimental data of jet and culvert scour, both R_h and $F_{o,d84}$ have been found to be suitable for predicting the maximum scour depth of both culvert and jet scour of various outlet shapes. By using d_{84} as the representative sediment diameter, a modified densimetric Froude number $F_{o,d84}$ is proposed to capture the non-uniformity of sediments. For maximum scour width, length, and volume, either d_{70} or d_{75} are found to be the most suitable sediment diameter. Equations are proposed for each of the normalized scour hole dimensions. Further analysis shows that the effect of relative tailwater depth and relative sediment size is very weak in 3D jet and culvert scour.

(a)

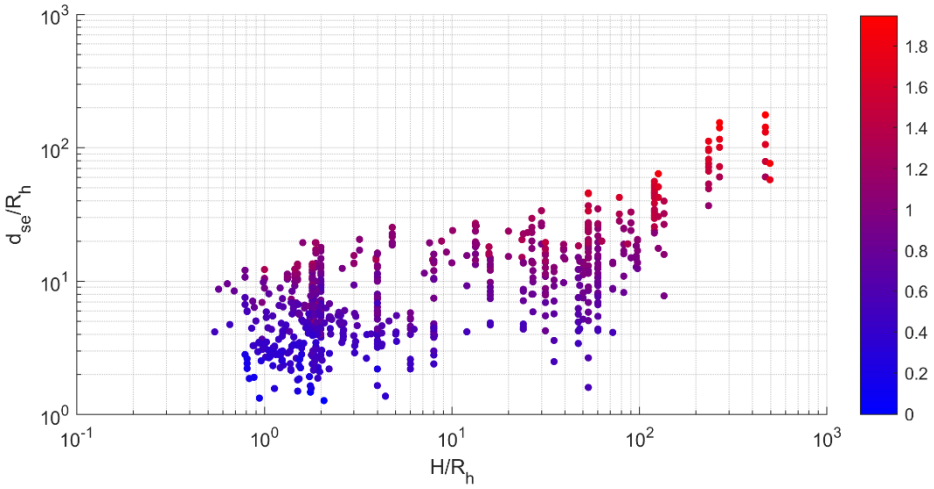

(b)

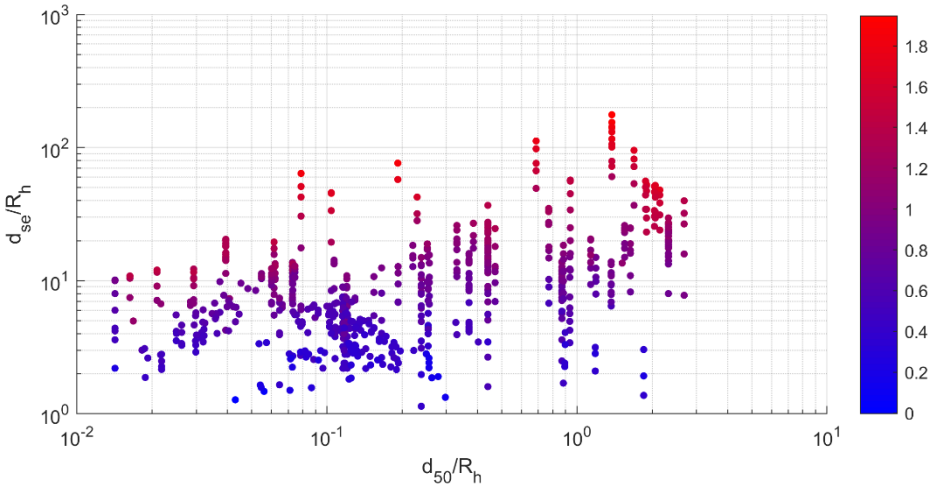

Figure 5.9 d_{se}/R_h plotted against (a) H/R_h and (b) d_{50}/R_h, both with value of log10 of Fo,d84 as marker color.

5.9 Acknowledgements

The authors acknowledge the contribution of the following for the NTU jet and culvert scour data: Akhtar (2014), Chia (2000), Das (2015), Lau (1998), Leow (2006), Ma (2010), Miao (2015), Peh (2007), Seah (1997), Surya (2014), Tan (2013), Tan (2009), Tay (1996), Theodosius (2012), See and Sheng (1993), Pee (2016), Salam (2016), Sally, Edmund, and Andy.

Chapter 6 Conclusions and Recommendations

Current study focused on generalizing both horizontal 3D jet and culvert scour. Full flowing 3D horizontal jet scour has been widely studied and used to simulate culvert scour. However, non-full flowing culvert scour has received lesser attention in the past.

A thorough literature review revealed that despite present understanding of 3D horizontal jet and culvert scour phenomena is sufficient for formulation of engineering guideline, there remains several areas that are worth exploring. The research gaps identified are the effect of relative tailwater depth, effect of relative sediment size, and effect of culvert shape. Several series of experimental studies were carried out accordingly. In each experiment series, different sediments, circular pipes of different diameter, different outlet submergence conditions, and different culvert shapes were used. The visual observations were presented and discussed. This provided strong evidence on the similarity and difference between different kinds of scour produced by full flowing circular jet and non-full flowing culvert under different hydraulic conditions. Non-full flowing culvert scour could produce scour hole similar to those produced by deeply submerged full flowing jet scour under certain hydraulic condition. The limitation on representing scour hole by using only the maximum scour hole dimensions and the conventional contour and centerline profiles plots was highlighted.

A database consists of 738 jet and culvert scour experimental dataset was compiled. Data analysis was first carried out using only the culvert scour data, and R_h was found to be a suitable characteristic length scale for different culvert shapes. Next, data analysis using both the jet and culvert scour data further confirmed the versatility of R_h as a characteristic length scale. Analysis was also done for identifying a suitable characteristic length scale for the sediment size. The sediment sizes are formulated from d_{50} and σ_g. It was found that for the maximum scour hole depth, d_{84} is the representative sediment size. On the other hand, the maximum scour hole width, length, and volume also reveals sediment size larger than d_{50} as the representative sediment size. Modified densimetric Froude number, $F_{o,dx}$, where d_x is the identified representative sediment size, was used to formulate scour dimension prediction equations. The equations are compact as σ_g is already included in $F_{o,dx}$. For the maximum scour hole depth, the effect of relative tailwater depth and relative sediment size are weak compared to the d_{84}-based densimetric Froude number, $F_{o,d84}$.

Current work is limited to simple 3D horizontal scour. Future work can extend the similar analysis to 3D offset jet scour and angled jet scour. Generalizing both 2D and 3D jet scour can be done by

identifying the suitable characteristic length scale. Following the R_h calculation method in current study, for a 2D jet issued from a very wide rectangular outlet, R_h = ½ jet height. This is only different by a factor of one-half from the characteristic length, which usually is the jet height, in 2D jet scour researches. Thus, more work is required to test the suitability of the hydraulic radius to be generalized across different kind of jet scour.

Furthermore, vertical jet scour and 2D jet scour are known to have 2 distinct regions which the scouring action and the resulting scour hole shapes are different. For vertical jet, the difference is due to how the jet is deflected within the scour hole. For 2D jet, the difference is whether the jet flipping phenomena occurs. These are not present in 3D horizontal jet scour. Thus, it will be interesting to identify the region of vertical jet scour and 2D plane jet scour in which the hydraulic radius is the characteristic length.

The representative sediment size identified for maximum scour hole depth in current study is d_{84}, which is the same as the one for surface roughness in hydraulic engineering. It will be interesting to see whether the same sediment size percentile is suitable for other kinds of jet scour.

References

Abida, H. (1988). "A Laboratory Investigation of Local Scour Downstream of Box Culvert Outlets and an Alternative Measure for its Control." Master of Applied Science, University of Ottawa, Ottawa, Ontario, Canada.

Abida, H., and Townsend, R. (1991). "Local Scour Downstream of Box-Culvert Outlets." *Journal of Irrigation and Drainage Engineering*, 117(3), 425-440.

Abt, S., Kloberdanz, R., and Mendoza, C. (1984). "Unified Culvert Scour Determination." *Journal of Hydraulic Engineering*, 110(10), 1475-1479.

Abt, S., Ruff, J., and Doehring, F. (1985). "Culvert Slope Effects on Outlet Scour." *Journal of Hydraulic Engineering*, 111(10), 1363-1367.

Abt, S., Ruff, J., Doehring, F., and Donnell, C. (1987). "Influence of Culvert Shape on Outlet Scour." *Journal of Hydraulic Engineering*, 113(3), 393-400.

Abt, S. R., Ruff, J. F., and Mendoza, C. (1983). "Mound Formation At Culvert Outlet." *JAWRA Journal of the American Water Resources Association*, 19(4), 571-576.

Adduce, C., and Sciortino, G. (2006). "Scour due to a horizontal turbulent jet: Numerical and experimental investigation." *Journal of Hydraulic Research*, 44(5), 663-673.

Ade, F., and Rajaratnam, N. (1998). "Generalized study of erosion by circular horizontal turbulent jets." *Journal of Hydraulic Research*, 36(4), 613-636.

Aderibigbe, O. O., and Rajaratnam, N. (1996). "Erosion of loose beds by submerged circular impinging vertical turbulent jets." *Journal of Hydraulic Research*, 34(1), 19-33.

Akhtar, A. (2014). "Rectangular Culvert Scour with Non-Uniform Sand." *Final Year Project Report*, Nanyang Technological University, Singapore.

Ali, K. H. M., and Lim, S. Y. (1986). "Local Scour Caused by Submerged Wall Jets." *ICE Proceedings*, 607-645.

Barenblatt, G. I. (1996). *Scaling, Self-similarity, and Intermediate Asymptotics: Dimensional Analysis and Intermediate Asymptotics*, Cambridge University Press, Cambridge

Bey, A., Faruque, M. A., and Balachandar, R. (2007). "Two-Dimensional Scour Hole Problem: Role of Fluid Structures." *Journal of Hydraulic Engineering*, 133(4), 414-430.

Bey, A., Faruque, M. A. A., and Balachandar, R. (2008). "Effects of varying submergence and channel width on local scour by plane turbulent wall jets." *Journal of Hydraulic Research*, 46(6), 764-776.

Blaisdell, F. W., and Anderson, C. L. (1988). "A comprehensive generalized study of scour at cantilevered pipe outlets." *Journal of Hydraulic Research*, 26(4), 357-376.

Blaisdell, F. W., and Anderson, C. L. (1988). "A comprehensive generalized study of scour at cantilevered pipe outlets." *Journal of Hydraulic Research*, 26(5), 509-524.

Blaisdell, F. W., and Anderson, C. L. (1989). "Scour at cantilevered outlets: plunge pool energy dissipator design criteria." *ARS-76*, U. S. Department of Agriculture, Agricultural Research Service, Washington, D.C.

Bohan, J. P. (1970). "Erosion and Riprap requirements at Culverts and Storm-drain Outlets." U.S. Army Engineer Waterways Experiment Station, Mississippi.

Breusers, H. N. C., and Raudkivi, A. J. (1991). *Scouring*, A.A. Balkema, Rotterdam.

Carr, K., Ercan, A., and Kavvas, M. (2015). "Scaling and Self-Similarity of One-Dimensional Unsteady Suspended Sediment Transport with Emphasis on Unscaled Sediment Material Properties." *Journal of Hydraulic Engineering*, 141(5), 04015003.

Chatterjee, S., Ghosh, S., and Chatterjee, M. (1994). "Local Scour due to Submerged Horizontal Jet." *Journal of Hydraulic Engineering*, 120(8), 973-992.

Cheng, N.-S. (1997). "Simplified Settling Velocity Formula for Sediment Particle." *Journal of Hydraulic Engineering*, 123(2), 149-152.

Cheng, N.-S. (2011). "Application of Incomplete Self-Similarity Argument for Predicting Bed-Material Load Discharge." *Journal of Hydraulic Engineering*, 137(9), 921-931.

Cheng, N.-S. (2016). "Representative Grain Size and Equivalent Roughness Height of a Sediment Bed." *Journal of Hydraulic Engineering*, 142(1), 06015016.

Chia, H. H. (2000). "Effects of the Characterization of Sediment Mixtures for Culvert Scour."Final Year Project Report, Nanyang Technological University, Singapore.

Chien, N., and Wan, Z. (1999). *Mechanics of Sediment Transport*, ASCE Press, Virginia.

Chiew, Y., and Lim, S. (1996). "Local Scour by a Deeply Submerged Horizontal Circular Jet." *Journal of Hydraulic Engineering*, 122(9), 529-532.

Chow, V. T. (1959). *Open-Channel Hydraulics*, McGraw-Hill, New York.

Clarke, F. R. W. (1962). "The Action of Submerged Jets on Moveable Material." M.S. Thesis, London University, London.

D'Agostino, V., and Ferro, V. (2004). "Scour on Alluvial Bed Downstream of Grade-Control Structures." *Journal of Hydraulic Engineering*, 130(1), 24-37.

Das, A. (2015). "Scour Below A Non-full Flowing Trapezoidal Culvert Outlet." *Final Year Project Report*, Nanyang Technological University, Singapore.

Day, R. A., Liriano, S. L., and White, W. R. (2001). "Effect of tailwater depth and model scale on scour at culvert outlets." *Proceedings of the Institution of Civil Engineers: Water and Maritime Engineering*, 148(3), 189-198.

Deshpande, N., Balachandar, R., and Mazurek, K. A. (2007). "Effects of submergence and test startup conditions on local scour by plane." *Journal of Hydraulic Research*, 45(3), 370-387.

Dey, S., and Sarkar, A. (2006). "Response of velocity and turbulence in submerged wall jets to abrupt changes from smooth to rough beds and its application to scour downstream of an apron." *Journal of Fluid Mechanics*, 556, 387-419.

Dey, S., and Sarkar, A. (2006). "Scour Downstream of an Apron Due to Submerged Horizontal Jets." *Journal of Hydraulic Engineering*, 132(3), 246-257.

Doehring, F., and Abt, S. (1994). "Drop Height Influence on Outlet Scour." *Journal of Hydraulic Engineering*, 120(12), 1470-1476.

Ettema, R., Melville, B., and Barkdoll, B. (1998). "Scale Effect in Pier-Scour Experiments." *Journal of Hydraulic Engineering*, 124(6), 639-642.

Faruque, M., Sarathi, P., and Balachandar, R. (2006). "Clear Water Local Scour by Submerged Three-Dimensional Wall Jets: Effect of Tailwater Depth." *Journal of Hydraulic Engineering*, 132(6), 575-580.

Garde, R. J., and Raju, K. G. R. (2000). *Mechanics of sediment transportation and alluvial stream problems*, New Age International, New Delhi.

Guan, D., Melville Bruce, W., and Friedrich, H. (2015). "Live-Bed Scour at Submerged Weirs." *Journal of Hydraulic Engineering*, 141(2), 04014071.

Hager, W. H. (2007). "Scour in hydraulic engineering." *Proceedings of the ICE - Water Management*, 159-168.

Heller, V. (2011). "Scale effects in physical hydraulic engineering models." *Journal of Hydraulic Research*, 49(3), 293-306.

Hill, D. F., and Younkin, B. D. (2006). "PIV measurements of flow in and around scour holes." *Experiments in Fluids*, 41(2), 295-307.

Hoffmans, G. (1998). "Jet Scour in Equilibrium Phase." *Journal of Hydraulic Engineering*, 124(4), 430-437.

Hoffmans, G. J. C. M., and Verheij, H. J. (1997). *Scour Manual*, A.A. Balkema, Rotterdam.

Hoffmans, I. G. J. C. M. (2009). "Closure problem to jet scour." *Journal of Hydraulic Research*, 47(1), 100-109.

Hogg, A. J., Huppert, H. E., and Dade, W. B. (1997). "Erosion by planar turbulent wall jets." *Journal of Fluid Mechanics*, 338, 317-340.

Hopfinger, E. J., Kurniawan, A., Graf, W. H., and Lemmin, U. (2004). "Sediment erosion by Görtler vortices: the scour-hole problem." *Journal of Fluid Mechanics*, 520, 327-342.

Hunter, T. N., Peakall, J., Unsworth, T. J., Acun, M. H., Keevil, G., Rice, H., and Biggs, S. (2013). "The influence of system scale on impinging jet sediment erosion: Observed using novel and

standard measurement techniques." *Chemical Engineering Research and Design*, 91(4), 722-734.

Iwagaki, Y., Smith, G. L., and Albertson, M. L. (1958). *Analytical Study of the Mechanics of Scour for Three-Dimensional Jet*, Colorado State Univ. Research Foundation, Fort Collins, Colorado.

Karki, R., Faruque, M. A. A., and Balachandar, R. (2007). "Local scour by submerged offset jets." *Proceedings of the Institution of Civil Engineers - Water Management*, 160(3), 169-179.

Kobus, H., Leister, P., and Westrich, B. (1979). "Flow Field And Scouring Effects of Steady and Pulsating Jets Impinging on A Movable Bed." *Journal of Hydraulic Research*, 17(3), 175-192.

Lança, R., Fael, C., Maia, R., Pêgo, J., and Cardoso, A. (2013). "Clear-Water Scour at Comparatively Large Cylindrical Piers." *Journal of Hydraulic Engineering*, 139(11), 1117-1125.

Lau (1998). "Culvert Scour in Graded Material."Final Year Project Report, Nanyang Technological University, Singapore.

Laucelli, D., and Giustolisi, O. (2011). "Scour depth modelling by a multi-objective evolutionary paradigm." *Environmental Modelling & Software*, 26(4), 498-509.

Laursen, M. (1953). "Observations on the Nature of Scour." *Proc., The Fiifth Hydraulics Conference,* Iowa, 179-197.

Lee, S. O., and Sturm, T. W. (2009). "Effect of sediment size scaling on physical modeling of bridge pier scour." *Journal of Hydraulic Engineering*, 135(10), 793-802.

Leow, C. S. (2006). "Erosion below Non-Full Flowing Rectangular Outlet." *Final Year Project Report*, Nanyang Technological University, Singapore.

Lim, S. Y. (1995). "Scour Below Unsubmerged Full-Flowing Culvert Outlets." *Proceedings of the ICE - Water Maritime and Energy*, 136-149.

Lim, S. Y., and Chin, C. O. (1992). "Scour by circular wall Jets with non-uniform sediments." *Advances in hydro-science and engineering*, S. S. Y. Wang, ed., 1989-1994.

Liriano, S. L. (1999). "The influence of near bed turbulent flow structures on scour hole development at pipe culvert outlets." Ph.D Thesis, University of Herfordshire, Hertfordshire, United Kingdom.

Liriano, S. L., and Day, R. A. (2001). "Prediction of scour depth at culvert outlets using neural networks." *Journal of Hydroinformatics*, 3(4), 231.

Liriano, S. L., Day, R. A., and Rodney White, W. (2002). "Scour at culvert outlets as influenced by the turbulent flow structure." *Journal of Hydraulic Research*, 40(3), 367-376.

Ma, Y. (2010). "Bed Protection Below Culvert Outlets." *Final Year Project Report*, Nanyang Technological University, Singapore.

Mason, P., and Arumugam, K. (1985). "Free Jet Scour Below Dams and Flip Buckets." *Journal of Hydraulic Engineering*, 111(2), 220-235.

May, R., Ackers, J., and Kirby, A. (2002). *Manual on scour at bridges and other hydraulic structures* CIRIA, London.

Mehraein, M., Neyshaboury, S. A. A. S., and Ghodsian, M. (2011). "Local scour due to an upwards inclined circular wall jet." *Proceedings of the Institution of Civil Engineers: Water Management*, 164(3), 111-122.

Melville, B. W., and Lim, S.-Y. (2014). "Scour Caused by 2D Horizontal Jets." *Journal of Hydraulic Engineering*, 140(2), 149-155.

Mendoza, C., Abt, S., and Ruff, J. (1983). "Headwall Influence on Scour at Culvert Outlets." *Journal of Hydraulic Engineering*, 109(7), 1056-1060.

Miao, W. (2015). "Scour Below Non-full Flowing Trapezoidal Culvert Outlet." *Final Year project Report*, Nanyang Technological University, Singapore.

Mih, W., and Kabir, J. (1983). "Impingement of Water Jets on Nonuniform Streambed." *Journal of Hydraulic Engineering*, 109(4), 536-548.

Najafzadeh, M., and Lim, S. Y. (2015). "Application of improved neuro-fuzzy GMDH to predict scour depth at sluice gates." *Earth Science Informatics*, 8(1), 187-196.

O'Loughlin, E. M., Mehrotra, S. C., Chang, Y. C., and Kennedy, J. F. (1970). "Scale Effects In Hydraulic Model Tests of Rock Protected Structures." Iowa Institure of Hydraulic Research, University of Iowa, Iowa.

Opie, T. R. (1967). "Scour at Culvert Outlets." M.Sc. thesis, Colorado State University, Fort Collins.

Ortega-Casanova, J., Campos, N., and Fernandez-Feria, R. (2011). "Experimental study on sand bed excavation by impinging swirling jets." *Journal of Hydraulic Research*, 49(5), 601-610.

Pagliara, S., Amidei, M., and Hager, W. (2008). "Hydraulics of 3D Plunge Pool Scour." *Journal of Hydraulic Engineering*, 134(9), 1275-1284.

Pagliara, S., Hager, W., and Minor, H. (2006). "Hydraulics of Plane Plunge Pool Scour." *Journal of Hydraulic Engineering*, 132(5), 450-461.

Pagliara, S., Hager, W. H., and Minor, H.-E. "Plunge pool scour in prototype and laboratory." *Proc., Int. Conf. on Hydraulics of Dams and River Structures*, 165–172.

Pagliara, S., Kurdistani, S., and Cammarata, L. (2014). "Scour of Clear Water Rock W-Weirs in Straight Rivers." *Journal of Hydraulic Engineering*, 140(4), 06014002.

Pagliara, S., and Palermo, M. (2008). "Plane plunge pool scour with protection structures." *Journal of Hydro-environment Research*, 2(3), 182-191.

Pagliara, S., Roy, D., and Palermo, M. (2010). "3D plunge pool scour with protection measures." *Journal of Hydro-environment Research*, 4(3), 225-233.

Pee, J. (2016). "Scale Series Experiments Of Scour On Non-Cohesive Sediment By Deeply Submerged Circular Jet " *Final Year Project Report*, Nanyang Technological University, Singapore.

Peh, F. W. (2007). "Erosion Below Non-Full Flowing Rectangular Culvert Outlets." *Final Year Project Report*, Nanyang Technological University, Singapore.

Rajaratnam, N. (1981). "Erosion By Plane Turbulent Jets." *Journal of Hydraulic Research*, 19(4), 339-358.

Rajaratnam, N., and Berry, B. (1977). "Erosion By Circular Turbulent Wall Jets." *Journal of Hydraulic Research*, 15(3), 277-289.

Rajaratnam, N., and Diebel, M. (1981). "Erosion Below Culvert-like Structures." *Fifth Canadian Hydrotechnical Conference*, CSCE, Fredericton, New Brunswick, 469 - 484.

Rajaratnam, N., and Humphries, J. (1983). "Diffusion of Bluff Wall Jets in Finite Depth Tailwater." *Journal of Hydraulic Engineering*, 109(11), 1471-1485.

Rajaratnam, N., and Mazurek, K. A. (2002). "Erosion of a polystyrene bed by obliquely impinging circular turbulent air jets." *Journal of Hydraulic Research*, 40(6), 709-716.

Rajaratnam, N., and Mazurek, K. A. (2003). "Erosion of Sand by Circular Impinging Water Jets with Small Tailwater." *Journal of Hydraulic Engineering*, 129(3), 225-229.

Rouse, H. (1940). "Criteria for Similarity in the Transportation of Sediment." *Proc., Hydraulics Conference*, University of Iowa Studies in Engineering, Iowa, 33-49.

Ruff, J. F., Abt, S. R., Mendoza, C., Shaikh, A., and Kloberdanz, R. (1982). "Scour at Culvert Outlets in Mixed Bed Materials." FHWA, Washington.

Salam, M. R. A. (2016). "Difference In Effect Of Tailwater Depth On Circular Jet And Culvert Scour." *Final Year Project Report*, Nanyang Technological University, Singapore.

Sarathi, P., Faruque, M. A. A., and Balachandar, R. (2008). "Influence of tailwater depth, sediment size and densimetric Froude number on scour by submerged square wall jets." *Journal of Hydraulic Research*, 46(2), 158-175.

Sarkar, A., and Dey, S. (2007). "Effect of seepage on scour due to submerged jets and resulting flow field." *Journal of Hydraulic Research*, 45(3), 357-364.

Scheer, A. C. (1968). "Large Culvert Studies in Montana." Montana State University, Montana.

Schiereck, G. J. (2004). *Introduction to Bed, Bank and Shore Protection*, Spon Press, London and New York.

Scurlock, S., Thornton, C., and Abt, S. (2012). "Equilibrium Scour Downstream of Three-Dimensional Grade-Control Structures." *Journal of Hydraulic Engineering*, 138(2), 167-176.

Seah, L. H. (1997). "Erosion at Culvert Outlet."Final Year Project Report, Nanyang Technological University, Singapore.

Secadiningrat, J. R. (2012). "Analysis of Culvert Scour." *Final Year Project Report*, Nanyang Technological University, Singapore.

Sheppard, D. M., Odeh, M., and Glasser, T. (2004). "Large scale clear-water local pier scour experiments." *Journal of Hydraulic Engineering*, 130(10), 957-963.

Sheppard, D. M., Pritsivelis, A., and Glasser, T. (2000). "Method for obtaining prototype local scour depths from physical model tests." *Proc., Joint Conference on Water Resource Engineering and Water Resources Planning and Management 2000*, ASCE, Virginia.

Shue, C. L. (2013). "Analysis of 3-D jet scour." *Final Year Project Report*, Nanyang Technological University, Singapore.

Stevens, M. A. (1969). "Scour in riprap at culvert outlets." Doctor of Philosophy, Colorado State University, Fort Collins, Colorado.

Sui, J., Faruque, M. A., and Balachandar, R. (2009). "Local Scour Caused by Submerged Square Jets under Model Ice Cover." *Journal of Hydraulic Engineering*, 135(4), 316-319.

Sui, J., Faruque, M. A. A., and Balachandar, R. (2008). "Influence of channel width and tailwater depth on local scour caused by square jets." *Journal of Hydro-environment Research*, 2(1), 39-45.

Surya, P. (2014). "Correlation of Scour Below A Non-full Flowing Culvert Outlet." *Final Year Project Report*, Nanyang Technological University, Singapore.

Tan, B. E. (2013). "Scour Below a Non-Full Flowing Rectangular Culvert Outlet." *Final Year Project Report*, Nanyang Technological University, Singapore.

Tan, J. J. P. (2009). "Scour Downstream of Unsubmerged Non-full Flowing Trapezoidal Culvert Outlet." *Final Year Project Report*, Nanyang Tecnological University, Singapore.

Tan, Y. P. (2003). "Protection Apron Below A Cluvert Outlet." *Final Year Project Report*, Nanyang Technological University, Singapore.

Tay, S. P. (1996). "Erosion Below a Culvert Outlet."Final Year Project Report, Nanyang Technological University, Singapore.

Theodosius, S. (2012). "Localized Scour Downstream of Unsubmerged Non-full Flowing Triangular Culvert Outlet." *Final Year Project Report*, Nanyang Technological University, Singapore.

Thompson, P. L., and Kilgore, R. T. (2006). "Hydraulic Design of Energy Dissipators for Culverts and Channels." FHWA, Virginia.

Xie, C., and Lim, S. (2014). "Effects of Jet Flipping on Local Scour Downstream of a Sluice Gate." *Journal of Hydraulic Engineering*, 141(4), 04014088.

Yeh, P.-H., Chang, K.-A., Henriksen, J., Edge, B., Chang, P., Silver, A., and Vargas, A. (2009). "Large-scale laboratory experiment on erosion of sand beds by moving circular vertical jets." *Ocean Engineering*, 36(3), 248-255.

Zaihan, N. S. (2014). "Small scale 3D jet scour." *Final Year Project Report*, Nanyang Technological University, Singapore.

Appendix

Tay, S. P. (1996). "Erosion Below a Culvert Outlet." *Final Year Project Report*, Nanyang Technological University, Singapore.

Database #	**Original Run #**	Duration hr	F/NF	W mm	**Shape**	**do mm**	**b mm**	**slope**	**ho mm**	Q L/s	Uo m/s	**H mm**	**d50 mm**	**sigma_g**
Tay_96-01	**M1**	94	F	1000	**Circular**	**15**	-	-	-	-	8.050	**200**	**8.7**	**1.11**
Tay_96-02	**M2**	72.75	F	1000	**Circular**	**15**	-	-	-	-	8.460	**200**	**8.7**	**1.11**
Tay_96-03	**M3**	95	F	1000	**Circular**	**15**	-	-	-	-	6.590	**200**	**8.7**	**1.11**
Tay_96-04	**M4**	73	F	1000	**Circular**	**15**	-	-	-	-	5.410	**200**	**8.7**	**1.11**
Tay_96-05	**M5**	-	F	1000	**Circular**	**15**	-	-	-	-	6.100	**200**	**8.7**	**1.11**
Tay_96-06	**M6**	-	F	1000	**Circular**	**15**	-	-	-	-	5.620	**200**	**8.7**	**1.11**
Tay_96-07	**M7**	49	F	1000	**Circular**	**15**	-	-	-	-	3.420	**200**	**8.7**	**1.11**
Tay_96-08	**N1**	74	F	1000	**Circular**	**15**	-	-	-	-	4.010	**100**	**8.7**	**1.11**
Tay_96-09	**N2**	48.75	F	1000	**Circular**	**15**	-	-	-	-	2.700	**100**	**8.7**	**1.11**
Tay_96-10	**N3**	49.75	F	1000	**Circular**	**15**	-	-	-	-	5.080	**100**	**8.7**	**1.11**
Tay_96-11	**N4**	68.5	F	1000	**Circular**	**15**	-	-	-	-	3.400	**100**	**8.7**	**1.11**
Tay_96-12	**N5**	53	F	1000	**Circular**	**15**	-	-	-	-	5.700	**100**	**8.7**	**1.11**
Tay_96-13	**N6**	51.5	F	1000	**Circular**	**15**	-	-	-	-	4.400	**100**	**8.7**	**1.11**
Tay_96-14	**N7**	48	F	1000	**Circular**	**15**	-	-	-	-	7.910	**100**	**8.7**	**1.11**
Tay_96-15	**P1**	49.5	F	1000	**Circular**	**15**	-	-	-	-	3.780	**50**	**8.7**	**1.11**
Tay_96-16	**P2**	72	F	1000	**Circular**	**15**	-	-	-	-	4.720	**50**	**8.7**	**1.11**
Tay_96-17	**P3**	50	F	1000	**Circular**	**15**	-	-	-	-	5.300	**50**	**8.7**	**1.11**
Tay_96-18	**P4**	66.5	F	1000	**Circular**	**15**	-	-	-	-	6.340	**50**	**8.7**	**1.11**
Tay_96-19	**P5**	48	F	1000	**Circular**	**15**	-	-	-	-	2.900	**50**	**8.7**	**1.11**
Tay_96-20	**P6**	72	F	1000	**Circular**	**15**	-	-	-	-	3.420	**50**	**8.7**	**1.11**
Tay_96-21	**P7**	48	F	1000	**Circular**	**15**	-	-	-	-	7.030	**50**	**8.7**	**1.11**
Tay_96-22	**Q1**	48.5	F	1000	**Circular**	**15**	-	-	-	-	3.580	**18**	**8.7**	**1.11**
Tay_96-23	**Q2**	49.5	F	1000	**Circular**	**15**	-	-	-	-	3.830	**18**	**8.7**	**1.11**
Tay_96-24	**Q3**	49.5	F	1000	**Circular**	**15**	-	-	-	-	4.920	**18**	**8.7**	**1.11**
Tay_96-25	**Q4**	48	F	1000	**Circular**	**15**	-	-	-	-	4.310	**18**	**8.7**	**1.11**
Tay_96-26	**Q7**	48.5	F	1000	**Circular**	**15**	-	-	-	-	5.710	**18**	**8.7**	**1.11**

Tay, S. P. (1996). "Erosion Below a Culvert Outlet." *Final Year Project Report*, Nanyang Technological University, Singapore.

Database #	**dse** **mm**	Wse mm	Lse mm	Vse ml	Rh mm	**Fo**	dse/Rh	Wse/Rh	Lse/Rh	Vse/Rh3
Tay_96-01	**100**	540	935	12650	3.75	**21.452**	26.667	144.000	249.333	239881.481
Tay_96-02	**91**	485	950	16000	3.75	**22.544**	24.267	129.333	253.333	303407.407
Tay_96-03	**95**	390	833	10500	3.75	**17.561**	25.333	104.000	222.133	199111.111
Tay_96-04	**76**	345	750	6575	3.75	**14.417**	20.267	92.000	200.000	124681.481
Tay_96-05	**89**	360	795	8900	3.75	**16.255**	23.733	96.000	212.000	168770.370
Tay_96-06	**76**	345	750	7500	3.75	**14.976**	20.267	92.000	200.000	142222.222
Tay_96-07	**57**	215	495	1900	3.75	**9.114**	15.200	57.333	132.000	36029.630
Tay_96-08	**66**	255	593	3420	3.75	**10.686**	17.600	68.000	158.133	64853.333
Tay_96-09	**30**	170	407	649	3.75	**7.195**	8.000	45.333	108.533	12306.963
Tay_96-10	**87**	339	718	6590	3.75	**13.537**	23.200	90.400	191.467	124965.926
Tay_96-11	**53**	222	497	1730	3.75	**9.060**	14.133	59.200	132.533	32805.926
Tay_96-12	**95**	400	774	9740	3.75	**15.189**	25.333	106.667	206.400	184699.259
Tay_96-13	**75**	307	630	4150	3.75	**11.725**	20.000	81.867	168.000	78696.296
Tay_96-14	**111**	535	863	18860	3.75	**21.079**	29.600	142.667	230.133	357641.481
Tay_96-15	**68**	249	560	2910	3.75	**10.073**	18.133	66.400	149.333	55182.222
Tay_96-16	**89**	336	675	5700	3.75	**12.578**	23.733	89.600	180.000	108088.889
Tay_96-17	**74**	337	640	5630	3.75	**14.123**	19.733	89.867	170.667	106761.481
Tay_96-18	**99**	380	892	9200	3.75	**16.895**	26.400	101.333	237.867	174459.259
Tay_96-19	**50**	160	450	1050	3.75	**7.728**	13.333	42.667	120.000	19911.111
Tay_96-20	**60**	235	515	2095	3.75	**9.114**	16.000	62.667	137.333	39727.407
Tay_96-21	**102**	377	951	12830	3.75	**18.734**	27.200	100.533	253.600	243294.815
Tay_96-22	**70**	235	520	2350	3.75	**9.540**	18.667	62.667	138.667	44562.963
Tay_96-23	**73**	230	555	2650	3.75	**10.206**	19.467	61.333	148.000	50251.852
Tay_96-24	**81**	300	780	5880	3.75	**13.111**	21.600	80.000	208.000	111502.222
Tay_96-25	**85**	260	650	4200	3.75	**11.485**	22.667	69.333	173.333	79644.444
Tay_96-26	**95**	350	805	8150	3.75	**15.216**	25.333	93.333	214.667	154548.148

Seah, L. H. (1997). "Erosion at Culvert Outlet." *Final Year Project Report*, Nanyang Technological University, Singapore.

Database #	**Original Run #**	Duration hr	F/NF	W mm	**Shape**	**do mm**	**b mm**	**slope**	**ho mm**	Q L/s	Uo m/s	**H mm**	**d50 mm**	**sigma_g**
Seah_97-01	**R1**	60 - 90	F	1000	**Circular**	**40**	-	-	-	-	2.050	**270**	**8.7**	**1.11**
Seah_97-02	**R2**	60 - 90	F	1000	**Circular**	**40**	-	-	-	-	2.540	**270**	**8.7**	**1.11**
Seah_97-03	**R3**	60 - 90	F	1000	**Circular**	**40**	-	-	-	-	2.870	**270**	**8.7**	**1.11**
Seah_97-04	**R4**	60 - 90	F	1000	**Circular**	**40**	-	-	-	-	3.220	**270**	**8.7**	**1.11**
Seah_97-05	**R5**	60 - 90	F	1000	**Circular**	**40**	-	-	-	-	3.550	**270**	**8.7**	**1.11**
Seah_97-06	**R6**	60 - 90	F	1000	**Circular**	**40**	-	-	-	-	4.300	**270**	**8.7**	**1.11**
Seah_97-07	**S1**	36 - 60	F	1000	**Circular**	**40**	-	-	-	-	1.380	**350**	**8.7**	**1.11**
Seah_97-08	**S2**	36 - 60	F	1000	**Circular**	**40**	-	-	-	-	1.710	**350**	**8.7**	**1.11**
Seah_97-09	**S3**	36 - 60	F	1000	**Circular**	**40**	-	-	-	-	2.050	**350**	**8.7**	**1.11**
Seah_97-10	**S4**	36 - 60	F	1000	**Circular**	**40**	-	-	-	-	2.350	**350**	**8.7**	**1.11**
Seah_97-11	**S5**	36 - 60	F	1000	**Circular**	**40**	-	-	-	-	2.850	**350**	**8.7**	**1.11**
Seah_97-12	**S6**	36 - 60	F	1000	**Circular**	**40**	-	-	-	-	3.440	**350**	**8.7**	**1.11**
Seah_97-13	**S7**	36 - 60	F	1000	**Circular**	**40**	-	-	-	-	4.000	**350**	**8.7**	**1.11**
Seah_97-14	**S8**	36 - 60	F	1000	**Circular**	**40**	-	-	-	-	4.390	**350**	**8.7**	**1.11**
Seah_97-15	**T1**	36 - 60	F	1000	**Circular**	**40**	-	-	-	-	2.060	**500**	**8.7**	**1.11**
Seah_97-16	**T2**	36 - 60	F	1000	**Circular**	**40**	-	-	-	-	2.470	**500**	**8.7**	**1.11**
Seah_97-17	**T3**	36 - 60	F	1000	**Circular**	**40**	-	-	-	-	2.950	**500**	**8.7**	**1.11**
Seah_97-18	**T4**	36 - 60	F	1000	**Circular**	**40**	-	-	-	-	3.490	**500**	**8.7**	**1.11**
Seah_97-19	**T5**	36 - 60	F	1000	**Circular**	**40**	-	-	-	-	3.940	**500**	**8.7**	**1.11**
Seah_97-20	**T6**	36 - 60	F	1000	**Circular**	**40**	-	-	-	-	4.470	**500**	**8.7**	**1.11**
Seah_97-21	**U1**	36 - 60	F	1000	**Circular**	**40**	-	-	-	-	1.350	**20**	**8.7**	**1.11**
Seah_97-22	**U2**	36 - 60	F	1000	**Circular**	**40**	-	-	-	-	1.990	**20**	**8.7**	**1.11**
Seah_97-23	**U3**	36 - 60	F	1000	**Circular**	**40**	-	-	-	-	2.180	**20**	**8.7**	**1.11**
Seah_97-24	**U4**	36 - 60	F	1000	**Circular**	**40**	-	-	-	-	2.750	**20**	**8.7**	**1.11**
Seah_97-25	**U5**	36 - 60	F	1000	**Circular**	**40**	-	-	-	-	3.320	**20**	**8.7**	**1.11**
Seah_97-26	**U6**	36 - 60	F	1000	**Circular**	**40**	-	-	-	-	3.890	**20**	**8.7**	**1.11**

Seah, L. H. (1997). "Erosion at Culvert Outlet." *Final Year Project Report*, Nanyang Technological University, Singapore.

Database #	**dse** **mm**	Wse mm	Lse mm	Vse ml	Rh mm	**Fo**	dse/Rh	Wse/Rh	Lse/Rh	Vse/Rh3
Seah_97-01	**59**	320	730	5160	10.00	**5.463**	5.900	32.000	73.000	5160.000
Seah_97-02	**80**	390	868	9250	10.00	**6.769**	8.000	39.000	86.800	9250.000
Seah_97-03	**99**	455	987	15560	10.00	**7.648**	9.900	45.500	98.700	15560.000
Seah_97-04	**106**	579	1064	19665	10.00	**8.581**	10.600	57.900	106.400	19665.000
Seah_97-05	**120**	552	1162	25895	10.00	**9.460**	12.000	55.200	116.200	25895.000
Seah_97-06	**137**	690	1269	34860	10.00	**11.459**	13.700	69.000	126.900	34860.000
Seah_97-07	**25**	177	413	420	10.00	**3.677**	2.500	17.700	41.300	420.000
Seah_97-08	**36**	237	534	1450	10.00	**4.557**	3.600	23.700	53.400	1450.000
Seah_97-09	**57**	415	720	4660	10.00	**5.463**	5.700	41.500	72.000	4660.000
Seah_97-10	**71**	450	858	7930	10.00	**6.262**	7.100	45.000	85.800	7930.000
Seah_97-11	**92**	478	1004	13860	10.00	**7.595**	9.200	47.800	100.400	13860.000
Seah_97-12	**102**	502	1061	20110	10.00	**9.167**	10.200	50.200	106.100	20110.000
Seah_97-13	**118**	597	1171	25450	10.00	**10.659**	11.800	59.700	117.100	25450.000
Seah_97-14	**127**	660	1242	37440	10.00	**11.698**	12.700	66.000	124.200	37440.000
Seah_97-15	**52**	395	679	3690	10.00	**5.489**	5.200	39.500	67.900	3690.000
Seah_97-16	**75**	428	841	9390	10.00	**6.582**	7.500	42.800	84.100	9390.000
Seah_97-17	**82**	458	975	16050	10.00	**7.861**	8.200	45.800	97.500	16050.000
Seah_97-18	**112**	547	1100	22610	10.00	**9.300**	11.200	54.700	110.000	22610.000
Seah_97-19	**126**	601	1211	29530	10.00	**10.499**	12.600	60.100	121.100	29530.000
Seah_97-20	**139**	683	1272	40330	10.00	**11.912**	13.900	68.300	127.200	40330.000
Seah_97-21	**59**	262	388	1690	10.00	**3.597**	5.900	26.200	38.800	1690.000
Seah_97-22	**84**	356	691	6430	10.00	**5.303**	8.400	35.600	69.100	6430.000
Seah_97-23	**90**	424	791	8390	10.00	**5.809**	9.000	42.400	79.100	8390.000
Seah_97-24	**117**	539	963	20060	10.00	**7.328**	11.700	53.900	96.300	20060.000
Seah_97-25	**117**	625	1150	24390	10.00	**8.847**	11.700	62.500	115.000	24390.000
Seah_97-26	**127**	795	1311	35290	10.00	**10.366**	12.700	79.500	131.100	35290.000

Lau (1998). "Culvert Scour in Graded Material." *Final Year Project Report*, Nanyang Technological University, Singapore.

Database #	Original Run #	Duration	F/NF	W	Shape	do	b	slope	ho	Q	Uo	H	d50	sigma_g
		hr		mm		mm	mm		mm	L/s	m/s	mm	mm	
Lau_98-01	**V1**	>18	F	1000	**Circular**	**5**	-	-	-	-	12.610	**150**	**2.68**	**1.33**
Lau_98-02	**V2**	>18	F	1000	**Circular**	**5**	-	-	-	-	9.410	**150**	**2.68**	**1.33**
Lau_98-03	**V3**	>18	F	1000	**Circular**	**5**	-	-	-	-	8.150	**150**	**2.68**	**1.33**
Lau_98-04	**V4**	>18	F	1000	**Circular**	**5**	-	-	-	-	6.080	**150**	**2.68**	**1.33**
Lau_98-05	**V5**	>18	F	1000	**Circular**	**5**	-	-	-	-	6.710	**150**	**2.68**	**1.33**
Lau_98-06	**W1**	>18	F	1000	**Circular**	**5**	-	-	-	-	10.980	**150**	**2.55**	**1.45**
Lau_98-07	**W2**	>18	F	1000	**Circular**	**5**	-	-	-	-	10.420	**150**	**2.55**	**1.45**
Lau_98-08	**W3**	>18	F	1000	**Circular**	**5**	-	-	-	-	10.210	**150**	**2.55**	**1.45**
Lau_98-09	**W4**	>18	F	1000	**Circular**	**5**	-	-	-	-	8.570	**150**	**2.55**	**1.45**
Lau_98-10	**W5**	>18	F	1000	**Circular**	**5**	-	-	-	-	7.360	**150**	**2.55**	**1.45**
Lau_98-11	**W6**	>18	F	1000	**Circular**	**5**	-	-	-	-	6.350	**150**	**2.55**	**1.45**
Lau_98-12	**X1**	>18	F	1000	**Circular**	**5**	-	-	-	-	10.420	**150**	**2.57**	**1.66**
Lau_98-13	**X2**	>18	F	1000	**Circular**	**5**	-	-	-	-	12.420	**150**	**2.57**	**1.66**
Lau_98-14	**X3**	>18	F	1000	**Circular**	**5**	-	-	-	-	7.930	**150**	**2.57**	**1.66**
Lau_98-15	**X4**	>18	F	1000	**Circular**	**5**	-	-	-	-	8.950	**150**	**2.57**	**1.66**
Lau_98-16	**X5**	>18	F	1000	**Circular**	**5**	-	-	-	-	7.570	**150**	**2.57**	**1.66**
Lau_98-17	**Y1**	>18	F	1000	**Circular**	**5**	-	-	-	-	7.450	**150**	**2.37**	**1.77**
Lau_98-18	**Y2**	>18	F	1000	**Circular**	**5**	-	-	-	-	9.890	**150**	**2.37**	**1.77**
Lau_98-19	**Y3**	>18	F	1000	**Circular**	**5**	-	-	-	-	11.820	**150**	**2.37**	**1.77**
Lau_98-20	**Y4**	>18	F	1000	**Circular**	**5**	-	-	-	-	12.490	**150**	**2.37**	**1.77**
Lau_98-21	**Y5**	>18	F	1000	**Circular**	**5**	-	-	-	-	6.850	**150**	**2.37**	**1.77**
Lau_98-22	**Y6**	>18	F	1000	**Circular**	**5**	-	-	-	-	8.870	**150**	**2.37**	**1.77**
Lau_98-23	**Z1**	>18	F	1000	**Circular**	**5**	-	-	-	-	7.680	**150**	**2.35**	**2.16**
Lau_98-24	**Z2**	>18	F	1000	**Circular**	**5**	-	-	-	-	9.380	**150**	**2.35**	**2.16**
Lau_98-25	**Z3**	>18	F	1000	**Circular**	**5**	-	-	-	-	10.720	**150**	**2.35**	**2.16**
Lau_98-26	**Z4**	>18	F	1000	**Circular**	**5**	-	-	-	-	12.580	**150**	**2.35**	**2.16**
Lau_98-27	**Z5**	>18	F	1000	**Circular**	**5**	-	-	-	-	8.580	**150**	**2.35**	**2.16**
Lau_98-28	**Z6**	>18	F	1000	**Circular**	**5**	-	-	-	-	9.780	**150**	**2.35**	**2.16**

Lau (1998). "Culvert Scour in Graded Material." *Final Year Project Report*, Nanyang Technological University, Singapore.

Database #	**dse**	Wse	Lse	Vse	Rh	**Fo**	dse/Rh	Wse/Rh	Lse/Rh	Vse/Rh3
	mm	mm	mm	ml	mm					
Lau_98-01	**60**	329	650	3950	1.25	**60.544**	48.000	263.200	520.000	2022400.000
Lau_98-02	**55**	319	593	2890	1.25	**45.180**	44.000	255.200	474.400	1479680.000
Lau_98-03	**48**	209	476	1615	1.25	**39.130**	38.400	167.200	380.800	826880.000
Lau_98-04	**30**	175	397	715	1.25	**29.192**	24.000	140.000	317.600	366080.000
Lau_98-05	**39**	188	416	1160	1.25	**32.217**	31.200	150.400	332.800	593920.000
Lau_98-06	**64**	312	648	3465	1.25	**54.045**	51.200	249.600	518.400	1774080.000
Lau_98-07	**58**	308	631	2950	1.25	**51.289**	46.400	246.400	504.800	1510400.000
Lau_98-08	**58**	282	582	2760	1.25	**50.255**	46.400	225.600	465.600	1413120.000
Lau_98-09	**42**	253	508	1475	1.25	**42.183**	33.600	202.400	406.400	755200.000
Lau_98-10	**38**	207	448	1050	1.25	**36.227**	30.400	165.600	358.400	537600.000
Lau_98-11	**32**	175	396	630	1.25	**31.256**	25.600	140.000	316.800	322560.000
Lau_98-12	**57**	312	635	3450	1.25	**51.089**	45.600	249.600	508.000	1766400.000
Lau_98-13	**65**	344	702	3900	1.25	**60.895**	52.000	275.200	561.600	1996800.000
Lau_98-14	**41**	212	505	890	1.25	**38.880**	32.800	169.600	404.000	455680.000
Lau_98-15	**53**	265	553	1920	1.25	**43.881**	42.400	212.000	442.400	983040.000
Lau_98-16	**37**	198	465	880	1.25	**37.115**	29.600	158.400	372.000	450560.000
Lau_98-17	**37**	213	432	1205	1.25	**38.037**	29.600	170.400	345.600	616960.000
Lau_98-18	**59**	296	577	2790	1.25	**50.495**	47.200	236.800	461.600	1428480.000
Lau_98-19	**65**	316	616	3820	1.25	**60.349**	52.000	252.800	492.800	1955840.000
Lau_98-20	**66**	318	648	3890	1.25	**63.769**	52.800	254.400	518.400	1991680.000
Lau_98-21	**29**	159	385	460	1.25	**34.974**	23.200	127.200	308.000	235520.000
Lau_98-22	**43**	227	493	1425	1.25	**45.287**	34.400	181.600	394.400	729600.000
Lau_98-23	**43**	221	481	1195	1.25	**39.378**	34.400	176.800	384.800	611840.000
Lau_98-24	**55**	256	572	1910	1.25	**48.094**	44.000	204.800	457.600	977920.000
Lau_98-25	**63**	278	626	2580	1.25	**54.965**	50.400	222.400	500.800	1320960.000
Lau_98-26	**70**	349	673	3970	1.25	**64.502**	56.000	279.200	538.400	2032640.000
Lau_98-27	**55**	241	533	1800	1.25	**43.992**	44.000	192.800	426.400	921600.000
Lau_98-28	**63**	264	610	2320	1.25	**50.145**	50.400	211.200	488.000	1187840.000

Chia, H. H. (2000). "Effects of the Characterization of Sediment Mixtures for Culvert Scour." *Final Year Project Report*, Nanyang Technological University, Singapore.

Database #	**Original Run #**	Duration hr	F/NF	W mm	**Shape**	**do mm**	**b mm**	**slope**	**ho mm**	Q L/s	Uo m/s	**H mm**	**d50 mm**	**sigma_g**
Chia_00-01	**A1**	>24	F	1000	**Circular**	**5.92**	-	-	-	-	12.830	**200**	**3.97**	**4.09**
Chia_00-02	**A2**	>24	F	1000	**Circular**	**5.92**	-	-	-	-	9.870	**200**	**3.97**	**4.09**
Chia_00-03	**A3**	>24	F	1000	**Circular**	**5.92**	-	-	-	-	8.480	**200**	**3.97**	**4.09**
Chia_00-04	**A4**	>24	F	1000	**Circular**	**5.92**	-	-	-	-	6.230	**200**	**3.97**	**4.09**
Chia_00-05	**A5**	>24	F	1000	**Circular**	**5.92**	-	-	-	-	4.370	**200**	**3.97**	**4.09**
Chia_00-06	**B1**	>24	F	1000	**Circular**	**9.71**	-	-	-	-	6.760	**200**	**3.97**	**4.09**
Chia_00-07	**B2**	>24	F	1000	**Circular**	**9.71**	-	-	-	-	6.310	**200**	**3.97**	**4.09**
Chia_00-08	**B3**	>24	F	1000	**Circular**	**9.71**	-	-	-	-	5.570	**200**	**3.97**	**4.09**
Chia_00-09	**B4**	>24	F	1000	**Circular**	**9.71**	-	-	-	-	5.060	**200**	**3.97**	**4.09**
Chia_00-10	**B5**	>24	F	1000	**Circular**	**9.71**	-	-	-	-	4.640	**200**	**3.97**	**4.09**
Chia_00-11	**B6**	>24	F	1000	**Circular**	**9.71**	-	-	-	-	3.930	**200**	**3.97**	**4.09**
Chia_00-12	**B7**	>24	F	1000	**Circular**	**9.71**	-	-	-	-	3.170	**200**	**3.97**	**4.09**
Chia_00-13	**C1**	>24	F	1000	**Circular**	**13.35**	-	-	-	-	3.780	**200**	**3.97**	**4.09**
Chia_00-14	**C2**	>24	F	1000	**Circular**	**13.35**	-	-	-	-	3.660	**200**	**3.97**	**4.09**
Chia_00-15	**C3**	>24	F	1000	**Circular**	**13.35**	-	-	-	-	3.240	**200**	**3.97**	**4.09**
Chia_00-16	**C4**	>24	F	1000	**Circular**	**13.35**	-	-	-	-	2.930	**200**	**3.97**	**4.09**
Chia_00-17	**C5**	>24	F	1000	**Circular**	**13.35**	-	-	-	-	2.430	**200**	**3.97**	**4.09**
Chia_00-18	**C6**	>24	F	1000	**Circular**	**13.35**	-	-	-	-	2.250	**200**	**3.97**	**4.09**
Chia_00-19	**D1**	>24	F	1000	**Circular**	**16.97**	-	-	-	-	4.030	**200**	**3.97**	**4.09**
Chia_00-20	**D2**	>24	F	1000	**Circular**	**16.97**	-	-	-	-	3.440	**200**	**3.97**	**4.09**
Chia_00-21	**D3**	>24	F	1000	**Circular**	**16.97**	-	-	-	-	3.110	**200**	**3.97**	**4.09**
Chia_00-22	**D4**	>24	F	1000	**Circular**	**16.97**	-	-	-	-	2.790	**200**	**3.97**	**4.09**
Chia_00-23	**D5**	>24	F	1000	**Circular**	**16.97**	-	-	-	-	2.530	**200**	**3.97**	**4.09**
Chia_00-24	**D6**	>24	F	1000	**Circular**	**16.97**	-	-	-	-	2.330	**200**	**3.97**	**4.09**
Chia_00-25	**D7**	>24	F	1000	**Circular**	**16.97**	-	-	-	-	2.140	**200**	**3.97**	**4.09**
Chia_00-26	**D8**	>24	F	1000	**Circular**	**16.97**	-	-	-	-	1.910	**200**	**3.97**	**4.09**
Chia_00-27	**D9**	>24	F	1000	**Circular**	**16.97**	-	-	-	-	1.600	**200**	**3.97**	**4.09**

Chia, H. H. (2000). "Effects of the Characterization of Sediment Mixtures for Culvert Scour." *Final Year Project Report*, Nanyang Technological University, Singapore.

Database #	**dse**	Wse	Lse	Vse	Rh	**Fo**	dse/Rh	Wse/Rh	Lse/Rh	Vse/Rh3
	mm	mm	mm	ml	mm					
Chia_00-01	**59**	335	630	3950	1.48	**50.612**	39.865	226.351	425.676	1218461.888
Chia_00-02	**47.5**	290	535	2975	1.48	**38.935**	32.095	195.946	361.486	917702.308
Chia_00-03	**39.5**	230	440	1185	1.48	**33.452**	26.689	155.405	297.297	365538.566
Chia_00-04	**23.5**	175	380	570	1.48	**24.576**	15.878	118.243	256.757	175828.677
Chia_00-05	**11.5**	105	280	110	1.48	**17.239**	7.770	70.946	189.189	33931.850
Chia_00-06	**60.5**	305	645	4655	2.43	**26.667**	24.923	125.644	265.705	325418.298
Chia_00-07	**60**	265	590	3365	2.43	**24.892**	24.717	109.166	243.048	235237.932
Chia_00-08	**46**	255	520	2100	2.43	**21.973**	18.950	105.046	214.212	146805.247
Chia_00-09	**41**	245	510	1930	2.43	**19.961**	16.890	100.927	210.093	134921.013
Chia_00-10	**39**	220	475	1315	2.43	**18.304**	16.066	90.628	195.675	91928.048
Chia_00-11	**26.5**	185	415	835	2.43	**15.503**	10.917	76.210	170.958	58372.563
Chia_00-12	**20**	147	325	405	2.43	**12.505**	8.239	60.556	133.883	28312.441
Chia_00-13	**50**	375	680	3760	3.34	**14.911**	14.981	112.360	203.745	101140.250
Chia_00-14	**50**	285	575	3450	3.34	**14.438**	14.981	85.393	172.285	92801.559
Chia_00-15	**41.5**	235	485	1710	3.34	**12.781**	12.434	70.412	145.318	45997.294
Chia_00-16	**35.5**	210	460	1290	3.34	**11.558**	10.637	62.921	137.828	34699.713
Chia_00-17	**33**	185	420	1020	3.34	**9.586**	9.888	55.431	125.843	27436.983
Chia_00-18	**26.5**	165	375	665	3.34	**8.876**	7.940	49.438	112.360	17887.837
Chia_00-19	**64**	290	685	4700	4.24	**15.898**	15.085	68.356	161.461	61550.602
Chia_00-20	**52**	275	620	3450	4.24	**13.570**	12.257	64.820	146.140	45180.761
Chia_00-21	**45**	255	566	2150	4.24	**12.268**	10.607	60.106	133.412	28156.126
Chia_00-22	**32**	220	490	1430	4.24	**11.006**	7.543	51.856	115.498	18727.098
Chia_00-23	**26.5**	190	460	1050	4.24	**9.980**	6.246	44.785	108.427	13750.666
Chia_00-24	**24**	195	420	825	4.24	**9.191**	5.657	45.963	98.998	10804.095
Chia_00-25	**21**	165	360	615	4.24	**8.442**	4.950	38.892	84.856	8053.962
Chia_00-26	**18**	145	275	355	4.24	**7.535**	4.243	34.178	64.820	4649.035
Chia_00-27	**14.5**	110	235	160	4.24	**6.312**	3.418	25.928	55.392	2095.340

Tan, Y. P. (2003). "Protection Apron Below A Cluvert Outlet." *Final Year Project Report*, Nanyang Technological University, Singapore.

Database #	Original Run #	Duration	F/NF	W	Shape	do	b	slope	ho	Q	Uo	H	d50	sigma_g
		hr		mm		mm	mm		mm	L/s	m/s	mm	mm	
Tan_03-01	**1**	67	F	1000	**Circular**	**25.4**	-	-	-	-	1.160	**250**	**1.6**	**1.13**
Tan_03-02	**2**	72	F	1000	**Circular**	**25.4**	-	-	-	-	1.510	**250**	**1.6**	**1.13**
Tan_03-03	**3**	92	F	1000	**Circular**	**25.4**	-	-	-	-	1.830	**250**	**1.6**	**1.13**
Tan_03-04	**4**	69	F	1000	**Circular**	**25.4**	-	-	-	-	1.910	**250**	**1.6**	**1.13**
Tan_03-05	**5**	93	F	1000	**Circular**	**25.4**	-	-	-	-	2.000	**250**	**1.6**	**1.13**
Tan_03-06	**6**	69	F	1000	**Circular**	**25.4**	-	-	-	-	2.470	**250**	**1.6**	**1.13**

Zaihan, N. S. (2014). "Small scale 3D jet scour." *Final Year Project Report*, Nanyang Technological University, Singapore.

Database #	Original Run #	Duration	F/NF	W	Shape	do	b	slope	ho	Q	Uo	H	d50	sigma_g
		hr		mm		mm	mm		mm	L/s	m/s	mm	mm	
Zaihan_14-01	**Run_2 124**	24	F	300	**Circular**	**4**	-	-	-	-	1.757	**120**	**1.55**	**1.2**
Zaihan_14-02	**Run_3 113**	24	F	300	**Circular**	**4**	-	-	-	-	2.110	**90**	**1.55**	**1.2**
Zaihan_14-03	**Run_4 123**	22	F	300	**Circular**	**4**	-	-	-	-	1.504	**90**	**1.55**	**1.2**
Zaihan_14-04	**Run_8 112**	19	F	300	**Circular**	**4**	-	-	-	-	2.124	**60**	**1.55**	**1.2**
Zaihan_14-05	**Run_5 122**	25	F	300	**Circular**	**4**	-	-	-	-	1.501	**60**	**1.55**	**1.2**
Zaihan_14-06	**Run_7 111**	21	F	300	**Circular**	**4**	-	-	-	-	2.110	**30**	**1.55**	**1.2**
Zaihan_14-07	**Run_6 121**	25	F	300	**Circular**	**4**	-	-	-	-	1.504	**30**	**1.55**	**1.2**
Zaihan_14-08	**Run_9 213**	20	F	300	**Circular**	**4**	-	-	-	-	2.128	**90**	**0.77**	**1.15**
Zaihan_14-09	**Run_14 223**	20	F	300	**Circular**	**4**	-	-	-	-	1.518	**90**	**0.77**	**1.15**
Zaihan_14-10	**Run_11 212**	22	F	300	**Circular**	**4**	-	-	-	-	2.150	**60**	**0.77**	**1.15**
Zaihan_14-11	**Run_13 222**	23	F	300	**Circular**	**4**	-	-	-	-	1.505	**60**	**0.77**	**1.15**
Zaihan_14-12	**Run_10 211**	23	F	300	**Circular**	**4**	-	-	-	-	2.150	**30**	**0.77**	**1.15**
Zaihan_14-13	**Run_12 221**	20	F	300	**Circular**	**4**	-	-	-	-	1.519	**30**	**0.77**	**1.15**

Tan, Y. P. (2003). "Protection Apron Below A Cluvert Outlet." *Final Year Project Report*, Nanyang Technological University, Singapore.

Database #	**dse**	Wse	Lse	Vse	Rh	**Fo**	dse/Rh	Wse/Rh	Lse/Rh	Vse/Rh3
	mm	mm	mm	ml	mm					
Tan_03-01	**62**	236	528	2660	6.35	**7.192**	9.764	37.165	83.150	10388.682
Tan_03-02	**96**	305	665	5920	6.35	**9.367**	15.118	48.031	104.724	23120.676
Tan_03-03	**109**	342	776	9240	6.35	**11.391**	17.165	53.858	122.205	36087.001
Tan_03-04	**110**	380	812	12180	6.35	**11.835**	17.323	59.843	127.874	47569.229
Tan_03-05	**112**	382	847	12780	6.35	**12.437**	17.638	60.157	133.386	49912.541
Tan_03-06	**120**	420	924	15800	6.35	**15.375**	18.898	66.142	145.512	61707.210

Zaihan, N. S. (2014). "Small scale 3D jet scour." *Final Year Project Report*, Nanyang Technological University, Singapore.

Database #	**dse**	Wse	Lse	Vse	Rh	**Fo**	dse/Rh	Wse/Rh	Lse/Rh	Vse/Rh3
	mm	mm	mm	ml	mm					
Zaihan_14-01	**23**	61	172	62	1.00	**11.092**	23.000	61.000	172.000	62000.000
Zaihan_14-02	**24**	81	193	120	1.00	**13.320**	24.000	81.000	193.000	120000.000
Zaihan_14-03	**15**	50.5	127	28.4	1.00	**9.492**	15.000	50.500	127.000	28400.000
Zaihan_14-04	**24.8**	78	186	120	1.00	**13.406**	24.800	78.000	186.000	120000.000
Zaihan_14-05	**17.5**	57.5	150	45	1.00	**9.477**	17.500	57.500	150.000	45000.000
Zaihan_14-06	**26**	86	201	148	1.00	**13.319**	26.000	86.000	201.000	148000.000
Zaihan_14-07	**19**	62	151.5	42.4	1.00	**9.498**	19.000	62.000	151.500	42400.000
Zaihan_14-08	**33**	101	243	300	1.00	**19.061**	33.000	101.000	243.000	300000.000
Zaihan_14-09	**27.4**	85	198	138.2	1.00	**13.597**	27.400	85.000	198.000	138200.000
Zaihan_14-10	**34.9**	109	255	340	1.00	**19.258**	34.900	109.000	255.000	340000.000
Zaihan_14-11	**26.4**	83	203	151.6	1.00	**13.481**	26.400	83.000	203.000	151600.000
Zaihan_14-12	**33.8**	106	244	265	1.00	**19.258**	33.800	106.000	244.000	265000.000
Zaihan_14-13	**27.3**	84	202	150	1.00	**13.606**	27.300	84.000	202.000	150000.000

Pee, J. (2016). "Scale Series Experiments Of Scour On Non-Cohesive Sediment By Deeply Submerged Circular Jet " *Final Year Project Report*, Nanyang Technological University, Singapore.

Database #	**Original Run #**	Duration hr	F/NF	W mm	**Shape**	**do mm**	**b mm**	**slope**	**ho mm**	Q L/s	Uo m/s	**H mm**	**d50 mm**	**sigma_g**
Pee_16-01	**1**	46.83	F	300	**Circular**	**16**	-	-	-	0.123	0.614	**240**	**0.77**	**1.165**
Pee_16-02	**2**	43.83	F	300	**Circular**	**16**	-	-	-	0.160	0.797	**240**	**0.77**	**1.165**
Pee_16-03	**3**	44.5	F	300	**Circular**	**16**	-	-	-	0.123	0.610	**240**	**0.77**	**1.165**
Pee_16-04	**4**	47.25	F	300	**Circular**	**16**	-	-	-	0.202	1.006	**240**	**0.77**	**1.165**
Pee_16-05	**5**	46.5	F	300	**Circular**	**16**	-	-	-	0.220	1.100	**240**	**0.77**	**1.165**
Pee_16-06	**6**	47.17	F	300	**Circular**	**20**	-	-	-	0.188	0.599	**300**	**0.77**	**1.165**
Pee_16-07	**7**	44.83	F	300	**Circular**	**20**	-	-	-	0.250	0.796	**300**	**0.77**	**1.165**
Pee_16-08	**8**	43.92	F	300	**Circular**	**20**	-	-	-	0.310	0.990	**300**	**0.77**	**1.165**
Pee_16-09	**9**	42.67	F	300	**Circular**	**20**	-	-	-	0.158	0.503	**300**	**0.77**	**1.165**
Pee_16-10	**10**	47.5	F	300	**Circular**	**12**	-	-	-	0.068	0.599	**180**	**0.77**	**1.165**
Pee_16-11	**11**	48	F	300	**Circular**	**12**	-	-	-	0.091	0.801	**180**	**0.77**	**1.165**
Pee_16-12	**12**	48	F	300	**Circular**	**12**	-	-	-	0.113	1.002	**180**	**0.77**	**1.165**
Pee_16-13	**13**	45.25	F	300	**Circular**	**12**	-	-	-	0.135	1.196	**180**	**0.77**	**1.165**
Pee_16-14	**14**	46.33	F	300	**Circular**	**12**	-	-	-	0.091	0.801	**180**	**0.77**	**1.165**
Pee_16-15	**15**	45.5	F	300	**Circular**	**12**	-	-	-	0.068	0.600	**180**	**0.77**	**1.165**
Pee_16-16	**16**	47	F	300	**Circular**	**8**	-	-	-	0.105	2.099	**120**	**0.77**	**1.165**
Pee_16-17	**17**	43.83	F	300	**Circular**	**8**	-	-	-	0.075	1.501	**120**	**0.77**	**1.165**
Pee_16-18	**18**	47.5	F	300	**Circular**	**8**	-	-	-	0.060	1.202	**120**	**0.77**	**1.165**
Pee_16-19	**19**	46.67	F	300	**Circular**	**8**	-	-	-	0.050	0.999	**120**	**0.77**	**1.165**

Pee, J. (2016). "Scale Series Experiments Of Scour On Non-Cohesive Sediment By Deeply Submerged Circular Jet " *Final Year Project Report*, Nanyang Technological University, Singapore.

Database #	**dse**	Wse	Lse	Vse	Rh	**Fo**	dse/Rh	Wse/Rh	Lse/Rh	Vse/Rh3
	mm	mm	mm	ml	mm					
Pee_16-01	**27.7**	113	345	380	4.00	**5.500**	6.925	28.250	86.250	5937.500
Pee_16-02	**37.8**	151	407	800	4.00	**7.117**	9.450	37.750	101.750	12500.000
Pee_16-03	**27.5**	111	348	385	4.00	**5.462**	6.875	27.750	87.000	6015.625
Pee_16-04	**45.7**	190	494	1313	4.00	**9.012**	11.425	47.500	123.500	20515.625
Pee_16-05	**51.1**	206	511	1643	4.00	**9.849**	12.775	51.500	127.750	25671.875
Pee_16-06	**27.3**	121	394	456	5.00	**5.360**	5.460	24.200	78.800	3648.000
Pee_16-07	**40.9**	165	467	1143	5.00	**7.128**	8.180	33.000	93.400	9144.000
Pee_16-08	**53.7**	203	518	1925	5.00	**8.836**	10.740	40.600	103.600	15400.000
Pee_16-09	**21.9**	96	327	248	5.00	**4.502**	4.380	19.200	65.400	1984.000
Pee_16-10	**20**	85	254	170	3.00	**5.363**	6.667	28.333	84.667	6296.296
Pee_16-11	**29.1**	108	291	330	3.00	**7.176**	9.700	36.000	97.000	12222.222
Pee_16-12	**40.7**	143	372	724	3.00	**8.976**	13.567	47.667	124.000	26814.815
Pee_16-13	**46.8**	161	386	965	3.00	**10.722**	15.600	53.667	128.667	35740.741
Pee_16-14	**31.9**	109	291	352	3.00	**7.176**	10.633	36.333	97.000	13037.037
Pee_16-15	**23**	80	263	175	3.00	**5.373**	7.667	26.667	87.667	6481.481
Pee_16-16	**54**	200	443	1684	2.00	**18.800**	27.000	100.000	221.500	210500.000
Pee_16-17	**43.7**	167	357	860	2.00	**13.450**	21.850	83.500	178.500	107500.000
Pee_16-18	**39.2**	140	323	597	2.00	**10.740**	19.600	70.000	161.500	74625.000
Pee_16-19	**35.1**	120	291	406	2.00	**8.950**	17.550	60.000	145.500	50750.000

Salam, M. R. A. (2016). "Difference In Effect Of Tailwater Depth On Circular Jet And Culvert Scour." *Final Year Project Report*, Nanyang Technological University, Singapore.

Database #	**Original Run #**	Duration hr	F/NF	W mm	**Shape**	**do mm**	**b mm**	**slope**	**ho mm**	Q L/s	Uo m/s	**H mm**	**d50 mm**	**sigma_g**
Rizal_16-01	**Run 11**	47.5	F	1000	**Circular**	**27.5**	-	-	-	0.443	0.746	**27.5**	**0.5**	**1.45**
Rizal_16-02	**Run 12**	47.5	F	1000	**Circular**	**27.5**	-	-	-	0.434	0.730	**13.75**	**0.5**	**1.45**
Rizal_16-03	**Run 1**	44.5	F	1000	**Circular**	**27.5**	-	-	-	0.489	0.823	**110**	**0.5**	**1.45**
Rizal_16-04	**Run 3**	47.8	F	1000	**Circular**	**27.5**	-	-	-	0.495	0.834	**55**	**0.5**	**1.45**
Rizal_16-05	**Run 4**	44.2	F	1000	**Circular**	**27.5**	-	-	-	0.491	0.826	**27.5**	**0.5**	**1.45**
Rizal_16-06	**Run 5**	47.2	F	1000	**Circular**	**27.5**	-	-	-	0.475	0.800	**13.75**	**0.5**	**1.45**
Rizal_16-07	**Run 14***	47.5	F	1000	**Circular**	**27.5**	-	-	-	0.588	0.991	**110**	**0.5**	**1.45**
Rizal_16-08	**Run 13***	47.5	F	1000	**Circular**	**27.5**	-	-	-	0.610	1.027	**55**	**0.5**	**1.45**
Rizal_16-09	**Run 15***	47.5	F	1000	**Circular**	**27.5**	-	-	-	0.590	0.993	**27.5**	**0.5**	**1.45**
Rizal_16-10	**Run 16***	47.5	F	1000	**Circular**	**27.5**	-	-	-	0.589	0.992	**13.75**	**0.5**	**1.45**
Rizal_16-11	**Run 2**	44.5	F	1000	**Circular**	**27.5**	-	-	-	0.679	1.143	**110**	**0.5**	**1.45**
Rizal_16-12	**Run 6**	47.2	F	1000	**Circular**	**27.5**	-	-	-	0.689	1.160	**55**	**0.5**	**1.45**
Rizal_16-13	**Run 7**	47	F	1000	**Circular**	**27.5**	-	-	-	0.689	1.160	**27.5**	**0.5**	**1.45**
Rizal_16-14	**Run 8**	45	F	1000	**Circular**	**27.5**	-	-	-	0.618	1.041	**13.75**	**0.5**	**1.45**
Rizal_16-15	**Run 9**	45	F	1000	**Circular**	**27.5**	-	-	-	0.747	1.258	**110**	**0.5**	**1.45**
Rizal_16-16	**Run 10**	47.5	F	1000	**Circular**	**27.5**	-	-	-	0.747	1.258	**55**	**0.5**	**1.45**

Salam, M. R. A. (2016). "Difference In Effect Of Tailwater Depth On Circular Jet And Culvert Scour." *Final Year Project Report*, Nanyang Technological University, Singapore.

Database #	**dse**	Wse	Lse	Vse	Rh	**Fo**	dse/Rh	Wse/Rh	Lse/Rh	Vse/Rh3
	mm	mm	mm	ml	mm					
Rizal_16-01	**73.5**	292	600	4155	6.88	**8.289**	10.691	42.473	87.273	12786.536
Rizal_16-02	**49.6**	307	735	3345	6.88	**8.117**	7.215	44.655	106.909	10293.854
Rizal_16-03	**54.3**	247	697	3395	6.88	**9.145**	7.898	35.927	101.382	10447.724
Rizal_16-04	**51.3**	240	799	3630	6.88	**9.266**	7.462	34.909	116.218	11170.909
Rizal_16-05	**78.5**	368	690	6000	6.88	**9.184**	11.418	53.527	100.364	18464.313
Rizal_16-06	**48.7**	329	890	4760	6.88	**8.888**	7.084	47.855	129.455	14648.355
Rizal_16-07	**67.5**	305	735	5280	6.88	**11.013**	9.818	44.364	106.909	16248.595
Rizal_16-08	**82.5**	318	770	6400	6.88	**11.411**	12.000	46.255	112.000	19695.267
Rizal_16-09	**90**	354	845	8750	6.88	**11.043**	13.091	51.491	122.909	26927.122
Rizal_16-10	**65.2**	439	1010	8250	6.88	**11.024**	9.484	63.855	146.909	25388.430
Rizal_16-11	**83.1**	356	840	8170	6.88	**12.708**	12.087	51.782	122.182	25142.239
Rizal_16-12	**94.4**	346	918	8830	6.88	**12.898**	13.731	50.327	133.527	27173.313
Rizal_16-13	**87.4**	514	1000	12370	6.88	**12.892**	12.713	74.764	145.455	38067.258
Rizal_16-14	**68.5**	411	1040	9505	6.88	**11.569**	9.964	59.782	151.273	29250.548
Rizal_16-15	**88**	398	920	9565	6.88	**13.987**	12.800	57.891	133.818	29435.192
Rizal_16-16	**94.3**	421	990	13500	6.88	**13.987**	13.716	61.236	144.000	41544.703

Lim, S. Y. (unpublished)

Database #	Original Run #	Duration	F/NF	W	Shape	do	b	slope	ho	Q	Uo	H	d50	sigma_g
		hr		mm		mm	mm		mm	L/s	m/s	mm	mm	
Un-F-01	**F1**	91.3	F	-	**Circular**	**15**	-	-	-	-	2.870	**35**	**1.65**	**2.5**
Un-F-02	**F2**	75.5	F	-	**Circular**	**15**	-	-	-	-	2.870	**50**	**1.65**	**2.5**
Un-F-03	**F3**	99	F	-	**Circular**	**15**	-	-	-	-	2.870	**100**	**1.65**	**2.5**
Un-F-04	**F4**	68	F	-	**Circular**	**15**	-	-	-	-	2.870	**150**	**1.65**	**2.5**
Un-F-05	**F5**	43	F	-	**Circular**	**15**	-	-	-	-	2.870	**15**	**1.65**	**2.5**
Un-F-06	**F6**	47.5	F	-	**Circular**	**15**	-	-	-	-	2.870	**75**	**1.65**	**2.5**
Un-F-07	**F7**	114	F	-	**Circular**	**15**	-	-	-	-	2.870	**60**	**1.65**	**2.5**
Un-F-08	**F8**	-	F	-	**Circular**	**15**	-	-	-	-	2.870	**6**	**1.65**	**2.5**
Un-F-09	**F9**	-	F	-	**Circular**	**15**	-	-	-	-	2.870	**50**	**1.65**	**2.5**
Un-A-01	**1* A22**	-	F	1000	**Circular**	**25.4**	-	-	-	-	1.508	**25**	**0.25**	**1.44**
Un-A-02	**2 A21**	-	F	1000	**Circular**	**25.4**	-	-	-	-	1.585	**25**	**0.25**	**1.44**
Un-A-03	**3 A23**	-	F	1000	**Circular**	**25.4**	-	-	-	-	1.591	**50**	**0.25**	**1.44**
Un-A-04	**4 A24**	-	F	1000	**Circular**	**25.4**	-	-	-	-	1.603	**100**	**0.25**	**1.44**
Un-A-05	**5* A26**	-	F	1000	**Circular**	**25.4**	-	-	-	-	1.514	**100**	**0.25**	**1.44**
Un-A-06	**6* A25**	-	F	1000	**Circular**	**25.4**	-	-	-	-	1.543	**100**	**0.25**	**1.44**
Un-A-07	**7***	-	F	1000	**Circular**	**25.4**	-	-	-	-	1.524	**150**	**0.25**	**1.44**
Un-A-08	**8 A27**	-	F	1000	**Circular**	**25.4**	-	-	-	-	1.601	**150**	**0.25**	**1.44**
Un-H-01	**H1**	-	F	-	**Circular**	**15**	-	-	-	-	2.870	**33**	**1.65**	**1.25**
Un-H-02	**H2**	-	F	-	**Circular**	**15**	-	-	-	-	2.870	**90**	**1.65**	**1.25**
Un-H-03	**H3**	-	F	-	**Circular**	**15**	-	-	-	-	2.870	**50**	**1.65**	**1.25**
Un-H-04	**H4**	-	F	-	**Circular**	**15**	-	-	-	-	2.870	**75**	**1.65**	**1.25**
Un-H-05	**H5**	-	F	-	**Circular**	**15**	-	-	-	-	2.870	**95**	**1.65**	**1.25**
Un-H-06	**H6**	-	F	-	**Circular**	**15**	-	-	-	-	2.870	**7**	**1.65**	**1.25**

Lim, S. Y. (unpublished)

Database #	**dse**	Wse	Lse	Vse	Rh	**Fo**	dse/Rh	Wse/Rh	Lse/Rh	Vse/Rh3
	mm	mm	mm	ml	mm					
Un-F-01	**62**	260	700	5600	3.75	**17.560**	16.533	69.333	186.667	106192.593
Un-F-02	**72**	335	850	6360	3.75	**17.560**	19.200	89.333	226.667	120604.444
Un-F-03	**52**	275	600	3000	3.75	**17.560**	13.867	73.333	160.000	56888.889
Un-F-04	**55**	263	620	3000	3.75	**17.560**	14.667	70.133	165.333	56888.889
Un-F-05	**61**	285	700	2500	3.75	**17.560**	16.267	76.000	186.667	47407.407
Un-F-06	**57.5**	275	675	3125	3.75	**17.560**	15.333	73.333	180.000	59259.259
Un-F-07	**56**	270	730	3500	3.75	**17.560**	14.933	72.000	194.667	66370.370
Un-F-08	**73**	380	700	3330	3.75	**17.560**	19.467	101.333	186.667	63146.667
Un-F-09	**54**	300	700	3415	3.75	**17.560**	14.400	80.000	186.667	64758.519
Un-A-01	**92**	-	-	-	6.35	**23.706**	14.488	-	-	-
Un-A-02	**95**	-	-	-	6.35	**24.916**	14.961	-	-	-
Un-A-03	**92**	-	-	-	6.35	**25.011**	14.488	-	-	-
Un-A-04	**115**	-	-	-	6.35	**25.199**	18.110	-	-	-
Un-A-05	**100**	-	-	-	6.35	**23.800**	15.748	-	-	-
Un-A-06	**103**	-	-	-	6.35	**24.256**	16.220	-	-	-
Un-A-07	**96**	-	-	-	6.35	**23.957**	15.118	-	-	-
Un-A-08	**130**	-	-	-	6.35	**25.168**	20.472	-	-	-
Un-H-01	**75**	-	-	-	3.75	**17.560**	20.000	-	-	-
Un-H-02	**85**	-	-	-	3.75	**17.560**	22.667	-	-	-
Un-H-03	**98**	-	-	-	3.75	**17.560**	26.133	-	-	-
Un-H-04	**89**	-	-	-	3.75	**17.560**	23.733	-	-	-
Un-H-05	**87**	-	-	-	3.75	**17.560**	23.200	-	-	-
Un-H-06	**73**	-	-	-	3.75	**17.560**	19.467	-	-	-

Lim, S. Y. (unpublished)

Database #	Original Run #	Duration	F/NF	W	Shape	do	b	slope	ho	Q	Uo	H	d50	sigma_g
		hr		mm		mm	mm		mm	L/s	m/s	mm	mm	
Un-G-01	**G1**	66	F	-	**Circular**	**15**	-	-	-	-	2.160	**200**	**1.65**	**3.26**
Un-G-02	**G2**	71	F	-	**Circular**	**15**	-	-	-	-	2.870	**200**	**1.65**	**3.26**
Un-G-03	**G3**	160	F	-	**Circular**	**15**	-	-	-	-	3.480	**200**	**1.65**	**3.26**
Un-G-04	**G4**	89	F	-	**Circular**	**15**	-	-	-	-	4.550	**200**	**1.65**	**3.26**
Un-G-05	**G5**	167	F	-	**Circular**	**15**	-	-	-	-	5.090	**200**	**1.65**	**3.26**
Un-J-01	**J1**	36	F	-	**Circular**	**25.4**	-	-	-	-	3.100	**12.7**	**8.7**	**1.11**
Un-J-02	**J2**	36	F	-	**Circular**	**25.4**	-	-	-	-	3.640	**12.7**	**8.7**	**1.11**
Un-J-03	**J3**	36	F	-	**Circular**	**25.4**	-	-	-	-	1.860	**12.7**	**8.7**	**1.11**
Un-J-04	**J4**	36	F	-	**Circular**	**25.4**	-	-	-	-	2.380	**12.7**	**8.7**	**1.11**
Un-J-05	**J5**	36	F	-	**Circular**	**25.4**	-	-	-	-	1.420	**12.7**	**8.7**	**1.11**
Un-J-06	**J6**	36	F	-	**Circular**	**25.4**	-	-	-	-	2.670	**12.7**	**8.7**	**1.11**
Un-K-01	**K1**	36	F	-	**Circular**	**25.4**	-	-	-	-	3.590	**200**	**8.7**	**1.11**
Un-K-02	**K2**	36	F	-	**Circular**	**25.4**	-	-	-	-	2.740	**200**	**8.7**	**1.11**
Un-K-03	**K3**	36	F	-	**Circular**	**25.4**	-	-	-	-	2.050	**200**	**8.7**	**1.11**
Un-K-04	**K4**	36	F	-	**Circular**	**25.4**	-	-	-	-	2.350	**200**	**8.7**	**1.11**
Un-K-05	**K5**	36	F	-	**Circular**	**25.4**	-	-	-	-	2.570	**200**	**8.7**	**1.11**
Un-K-06	**K6**	36	F	-	**Circular**	**25.4**	-	-	-	-	3.140	**200**	**8.7**	**1.11**
Un-L-01	**L1**	36	F	-	**Circular**	**25.4**	-	-	-	-	2.720	**12.7**	**4.9**	**1.17**
Un-L-02	**L2**	36	F	-	**Circular**	**25.4**	-	-	-	-	1.010	**12.7**	**4.9**	**1.17**
Un-L-03	**L3**	36	F	-	**Circular**	**25.4**	-	-	-	-	1.502	**12.7**	**4.9**	**1.17**
Un-L-04	**L4**	36	F	-	**Circular**	**25.4**	-	-	-	-	3.350	**12.7**	**4.9**	**1.17**
Un-L-05	**L5**	36	F	-	**Circular**	**25.4**	-	-	-	-	1.214	**12.7**	**4.9**	**1.17**
Un-L-06	**L6**	36	F	-	**Circular**	**25.4**	-	-	-	-	2.552	**12.7**	**4.9**	**1.17**

Lim, S. Y. (unpublished)

Database #	**dse**	Wse	Lse	Vse	Rh	**Fo**	dse/Rh	Wse/Rh	Lse/Rh	Vse/Rh3
	mm	mm	mm	ml	mm					
Un-G-01	**26**	230	571	1000	3.75	**13.200**	6.933	61.333	152.267	18962.963
Un-G-02	**43**	320	680	2750	3.75	**17.560**	11.467	85.333	181.333	52148.148
Un-G-03	**56**	390	778	4500	3.75	**21.270**	14.933	104.000	207.467	85333.333
Un-G-04	**73**	390	885	7500	3.75	**27.870**	19.467	104.000	236.000	142222.222
Un-G-05	**101**	550	990	10500	3.75	**31.140**	26.933	146.667	264.000	199111.111
Un-J-01	**73**	380	600	4615	6.35	**8.261**	11.496	59.843	94.488	18023.973
Un-J-02	**84**	440	720	6600	6.35	**9.700**	13.228	69.291	113.386	25776.430
Un-J-03	**59**	230	400	1000	6.35	**4.957**	9.291	36.220	62.992	3905.520
Un-J-04	**60**	280	485	1940	6.35	**6.342**	9.449	44.094	76.378	7576.708
Un-J-05	**41**	200	350	500	6.35	**3.784**	6.457	31.496	55.118	1952.760
Un-J-06	**71**	320	527	3420	6.35	**7.115**	11.181	50.394	82.992	13356.877
Un-K-01	**88**	365	782	8150	6.35	**9.571**	13.858	57.480	123.150	31829.985
Un-K-02	**50**	280	600	2500	6.35	**7.300**	7.874	44.094	94.488	9763.799
Un-K-03	**44**	240	500	1500	6.35	**5.462**	6.929	37.795	78.740	5858.279
Un-K-04	**50**	260	550	2000	6.35	**6.256**	7.874	40.945	86.614	7811.039
Un-K-05	**52**	270	580	2445	6.35	**6.850**	8.189	42.520	91.339	9548.995
Un-K-06	**69**	330	690	5320	6.35	**8.372**	10.866	51.969	108.661	20777.364
Un-L-01	**107**	-	-	-	6.35	**9.658**	16.850	-	-	-
Un-L-02	**43**	-	-	-	6.35	**3.586**	6.772	-	-	-
Un-L-03	**65**	-	-	-	6.35	**5.333**	10.236	-	-	-
Un-L-04	**114**	-	-	-	6.35	**11.895**	17.953	-	-	-
Un-L-05	**57**	-	-	-	6.35	**4.311**	8.976	-	-	-
Un-L-06	**94**	-	-	-	6.35	**9.062**	14.803	-	-	-

Lim, S. Y., and Chin, C. O. (1992). "Scour by circular wall Jets with non-uniform sediments." *Advances in hydro-science and engineering*, S. S. Y. Wang, ed.

Database #	**Original Run #**	Duration hr	F/NF	W mm	**Shape**	**do mm**	**b mm**	**slope**	**ho mm**	Q L/s	Uo m/s	**H mm**	**d50 mm**	**sigma_g**
LimC_93-01	**C1**	80	F	1000	**Circular**	**15**	-	-	-	-	1.540	**200**	**1.65**	**1.25**
LimC_93-02	**C2**	93	F	1000	**Circular**	**15**	-	-	-	-	4.550	**200**	**1.65**	**1.25**
LimC_93-03	**C3**	48	F	1000	**Circular**	**15**	-	-	-	-	2.170	**200**	**1.65**	**1.25**
LimC_93-04	**C4**	65	F	1000	**Circular**	**15**	-	-	-	-	3.510	**200**	**1.65**	**1.25**
LimC_93-05	**C5**	43	F	1000	**Circular**	**15**	-	-	-	-	0.790	**200**	**1.65**	**1.25**
LimC_93-06	**C6**	47	F	1000	**Circular**	**15**	-	-	-	-	2.870	**200**	**1.65**	**1.25**
LimC_93-07	**D1**	74	F	1000	**Circular**	**15**	-	-	-	-	4.340	**200**	**1.65**	**1.78**
LimC_93-08	**D2**	43	F	1000	**Circular**	**15**	-	-	-	-	0.790	**200**	**1.65**	**1.78**
LimC_93-09	**D3**	48	F	1000	**Circular**	**15**	-	-	-	-	2.170	**200**	**1.65**	**1.78**
LimC_93-10	**D4**	70	F	1000	**Circular**	**15**	-	-	-	-	3.510	**200**	**1.65**	**1.78**
LimC_93-11	**D5**	41	F	1000	**Circular**	**15**	-	-	-	-	1.540	**200**	**1.65**	**1.78**
LimC_93-12	**D6**	46	F	1000	**Circular**	**15**	-	-	-	-	2.870	**200**	**1.65**	**1.78**
LimC_93-13	**E1**	96	F	1000	**Circular**	**15**	-	-	-	-	4.550	**200**	**1.65**	**2.5**
LimC_93-14	**E2**	137	F	1000	**Circular**	**15**	-	-	-	-	3.510	**200**	**1.65**	**2.5**
LimC_93-15	**E3**	94	F	1000	**Circular**	**15**	-	-	-	-	2.170	**200**	**1.65**	**2.5**
LimC_93-16	**E5**	45	F	1000	**Circular**	**15**	-	-	-	-	2.870	**200**	**1.65**	**2.5**
LimC_93-17	**E6**	48	F	1000	**Circular**	**15**	-	-	-	-	1.540	**200**	**1.65**	**2.5**

Lim, S. Y., and Chin, C. O. (1992). "Scour by circular wall Jets with non-uniform sediments." *Advances in hydro-science and engineering*, S. S. Y. Wang, ed.

Database #	**dse**	Wse	Lse	Vse	Rh	**Fo**	dse/Rh	Wse/Rh	Lse/Rh	Vse/Rh3
	mm	mm	mm	ml	mm					
LimC_93-01	**45**	173	460	1225	3.75	**9.420**	12.000	46.133	122.667	23229.630
LimC_93-02	**138**	580	1080	32000	3.75	**27.840**	36.800	154.667	288.000	606814.815
LimC_93-03	**66**	229	570	2650	3.75	**13.280**	17.600	61.067	152.000	50251.852
LimC_93-04	**103**	390	850	10000	3.75	**21.480**	27.467	104.000	226.667	189629.630
LimC_93-05	**10**	85	290	140	3.75	**4.830**	2.667	22.667	77.333	2654.815
LimC_93-06	**75**	320	670	5000	3.75	**17.560**	20.000	85.333	178.667	94814.815
LimC_93-07	**94**	470	900	8450	3.75	**26.540**	25.067	125.333	240.000	160237.037
LimC_93-08	**6**	60	230	50	3.75	**4.830**	1.600	16.000	61.333	948.148
LimC_93-09	**44**	170	520	2300	3.75	**13.290**	11.733	45.333	138.667	43614.815
LimC_93-10	**72**	330	700	7400	3.75	**21.490**	19.200	88.000	186.667	140325.926
LimC_93-11	**32**	170	380	830	3.75	**9.430**	8.533	45.333	101.333	15739.259
LimC_93-12	**62**	290	660	4950	3.75	**17.550**	16.533	77.333	176.000	93866.667
LimC_93-13	**77**	440	790	8640	3.75	**27.850**	20.533	117.333	210.667	163840.000
LimC_93-14	**69**	325	700	5000	3.75	**21.490**	18.400	86.667	186.667	94814.815
LimC_93-15	**34**	270	520	1400	3.75	**13.290**	9.067	72.000	138.667	26548.148
LimC_93-16	**49**	315	620	3400	3.75	**17.550**	13.067	84.000	165.333	64474.074
LimC_93-17	**19**	150	420	325	3.75	**9.430**	5.067	40.000	112.000	6162.963

Lim, S. Y. (1995). "Scour Below Unsubmerged Full-Flowing Culvert Outlets." *Proceedings of the ICE - Water Maritime and Energy*, 136-149.

Database #	Original Run #	Duration	F/NF	W	Shape	do	b	slope	ho	Q	Uo	H	d50	sigma_g
		hr		mm		mm	mm		mm	L/s	m/s	mm	mm	
Lim_95-01	**H6**	78	F	1000	**Circular**	**15**	-	-	-	-	2.826	**7.05**	**1.65**	**1.25**
Lim_95-02	**H9**	46	F	1000	**Circular**	**15**	-	-	-	-	4.020	**7.05**	**1.65**	**1.25**
Lim_95-03	**H10**	65.67	F	1000	**Circular**	**15**	-	-	-	-	1.464	**7.05**	**1.65**	**1.25**
Lim_95-04	**H11**	24	F	1000	**Circular**	**15**	-	-	-	-	0.720	**7.05**	**1.65**	**1.25**
Lim_95-05	**H12**	22	F	1000	**Circular**	**15**	-	-	-	-	1.012	**7.05**	**1.65**	**1.25**
Lim_95-06	**H13**	47.25	F	1000	**Circular**	**15**	-	-	-	-	2.065	**7.05**	**1.65**	**1.25**
Lim_95-07	**H14**	24	F	1000	**Circular**	**15**	-	-	-	-	0.450	**7.05**	**1.65**	**1.25**
Lim_95-08	**H15**	46.58	F	1000	**Circular**	**15**	-	-	-	-	2.410	**7.05**	**1.65**	**1.25**
Lim_95-09	**H16**	25.75	F	1000	**Circular**	**15**	-	-	-	-	1.800	**7.05**	**1.65**	**1.25**
Lim_95-10	**J1**	97.25	F	260	**Circular**	**26**	-	-	-	-	0.521	**12.22**	**1.65**	**1.25**
Lim_95-11	**J2**	68.13	F	260	**Circular**	**26**	-	-	-	-	0.680	**12.22**	**1.65**	**1.25**
Lim_95-12	**J3**	70	F	260	**Circular**	**26**	-	-	-	-	0.312	**12.22**	**1.65**	**1.25**
Lim_95-13	**J4**	72.05	F	260	**Circular**	**26**	-	-	-	-	0.425	**12.22**	**1.65**	**1.25**
Lim_95-14	**J5**	94.92	F	260	**Circular**	**26**	-	-	-	-	1.053	**12.22**	**1.65**	**1.25**
Lim_95-15	**J6**	69.67	F	260	**Circular**	**26**	-	-	-	-	1.250	**12.22**	**1.65**	**1.25**
Lim_95-16	**K1**	55.42	F	130	**Circular**	**26**	-	-	-	-	1.250	**12.22**	**1.65**	**1.25**
Lim_95-17	**K2**	66.08	F	130	**Circular**	**26**	-	-	-	-	1.003	**12.22**	**1.65**	**1.25**
Lim_95-18	**K3**	99.83	F	130	**Circular**	**26**	-	-	-	-	0.747	**12.22**	**1.65**	**1.25**
Lim_95-19	**K4**	71.07	F	130	**Circular**	**26**	-	-	-	-	0.531	**12.22**	**1.65**	**1.25**
Lim_95-20	**K5**	95.25	F	130	**Circular**	**26**	-	-	-	-	0.421	**12.22**	**1.65**	**1.25**

Lim, S. Y. (1995). "Scour Below Unsubmerged Full-Flowing Culvert Outlets." *Proceedings of the ICE - Water Maritime and Energy*, 136-149.

Database #	**dse**	Wse	Lse	Vse	Rh	**Fo**	dse/Rh	Wse/Rh	Lse/Rh	Vse/Rh3	H/do
	mm	mm	mm	ml	mm						
Lim_95-01	**73**	460	877	9000	3.75	**17.292**	19.467	122.667	233.867	170666.667	0.47
Lim_95-02	**65**	570	1156	12500	3.75	**24.598**	17.333	152.000	308.267	237037.037	0.47
Lim_95-03	**48**	260	400	1500	3.75	**8.958**	12.800	69.333	106.667	28444.444	0.47
Lim_95-04	**21**	100	100	65	3.75	**4.406**	5.600	26.667	26.667	1232.593	0.47
Lim_95-05	**30**	160	215	375	3.75	**6.192**	8.000	42.667	57.333	7111.111	0.47
Lim_95-06	**61**	280	500	2510	3.75	**12.636**	16.267	74.667	133.333	47597.037	0.47
Lim_95-07	**13**	-	-	-	3.75	**2.754**	3.467	-	-	-	0.47
Lim_95-08	**64**	515	620	3900	3.75	**14.747**	17.067	137.333	165.333	73955.556	0.47
Lim_95-09	**51**	320	430	1500	3.75	**11.014**	13.600	85.333	114.667	28444.444	0.47
Lim_95-10	**37**	170	412	700	6.50	**3.188**	5.692	26.154	63.385	2548.930	0.47
Lim_95-11	**29**	145	330	550	6.50	**4.161**	4.462	22.308	50.769	2002.731	0.47
Lim_95-12	**30**	125	170	300	6.50	**1.909**	4.615	19.231	26.154	1092.399	0.47
Lim_95-13	**30**	110	376	350	6.50	**2.601**	4.615	16.923	57.846	1274.465	0.47
Lim_95-14	**57**	170	480	4500	6.50	**6.443**	8.769	26.154	73.846	16385.981	0.47
Lim_95-15	**65**	190	560	3980	6.50	**7.649**	10.000	29.231	86.154	14492.490	0.47
Lim_95-16	**56**	-	660	2500	6.50	**7.649**	8.615	-	101.538	9103.323	0.47
Lim_95-17	**46**	-	537	1750	6.50	**6.137**	7.077	-	82.615	6372.326	0.47
Lim_95-18	**28**	-	410	860	6.50	**4.571**	4.308	-	63.077	3131.543	0.47
Lim_95-19	**26**	-	365	750	6.50	**3.249**	4.000	-	56.154	2730.997	0.47
Lim_95-20	**21**	-	180	340	6.50	**2.576**	3.231	-	27.692	1238.052	0.47

Chiew, Y., and Lim, S. (1996). "Local Scour by a Deeply Submerged Horizontal Circular Jet." *Journal of Hydraulic Engineering*, 122(9), 529-532.

Database #	**Original Run #**	Duration	F/NF	W	**Shape**	**do**	**b**	**slope**	**ho**	Q	Uo	**H**	**d50**	**sigma_g**
		hr		mm		**mm**	**mm**		**mm**	L/s	m/s	**mm**	**mm**	
ChiewL_98A-01	**A-1**	-	AIR	500	**Circular**	**4**	-	-	-	-	61.61	-	**0.94**	**1.29**
ChiewL_98A-02	**A-2**	-	AIR	500	**Circular**	**4**	-	-	-	-	73.75	-	**0.94**	**1.29**
ChiewL_98A-03	**A-3**	-	AIR	500	**Circular**	**4**	-	-	-	-	124.17	-	**0.94**	**1.29**
ChiewL_98A-04	**A-4**	-	AIR	500	**Circular**	**4**	-	-	-	-	148.13	-	**0.94**	**1.29**
ChiewL_98A-05	**A-5**	-	AIR	500	**Circular**	**4**	-	-	-	-	151.65	-	**0.94**	**1.29**
ChiewL_98A-06	**A-6**	-	AIR	500	**Circular**	**4**	-	-	-	-	47.86	-	**0.94**	**1.29**
ChiewL_98A-07	**A-7**	-	AIR	500	**Circular**	**4**	-	-	-	-	36.63	-	**0.94**	**1.29**
ChiewL_98A-08	**A-8**	-	AIR	500	**Circular**	**4**	-	-	-	-	94.4	-	**0.94**	**1.29**
ChiewL_98-01	**BI-1**	-	F	1000	**Circular**	**25.4**	-	-	-	-	1.49	**200**	**0.25**	**1.44**
ChiewL_98-02	**BI-2**	-	F	1000	**Circular**	**25.4**	-	-	-	-	1.3	**200**	**0.25**	**1.44**
ChiewL_98-03	**BI-3**	-	F	1000	**Circular**	**25.4**	-	-	-	-	0.88	**200**	**0.25**	**1.44**
ChiewL_98-04	**BI-4**	-	F	1000	**Circular**	**25.4**	-	-	-	-	0.53	**200**	**0.25**	**1.44**
ChiewL_98-05	**BI-5**	-	F	1000	**Circular**	**25.4**	-	-	-	-	1.58	**200**	**0.25**	**1.44**
ChiewL_98-06	**BI-6**	-	F	1000	**Circular**	**25.4**	-	-	-	-	1.59	**300**	**0.25**	**1.44**
ChiewL_98-07	**BI-7**	-	F	1000	**Circular**	**25.4**	-	-	-	-	1.64	**400**	**0.25**	**1.44**
ChiewL_98-08	**BI-8**	-	F	1000	**Circular**	**25.4**	-	-	-	-	1.6	**550**	**0.25**	**1.44**
ChiewL_98-09	**BI-9**	-	F	1000	**Circular**	**12.7**	-	-	-	-	5.43	**400**	**0.25**	**1.44**
ChiewL_98-10	**BI-10**	-	F	1000	**Circular**	**12.7**	-	-	-	-	3.03	**400**	**0.25**	**1.44**
ChiewL_98-11	**BI-11**	-	F	1000	**Circular**	**12.7**	-	-	-	-	1.89	**400**	**0.25**	**1.44**
ChiewL_98-12	**BI-12**	-	F	1000	**Circular**	**12.7**	-	-	-	-	0.84	**400**	**0.25**	**1.44**
ChiewL_98-13	**BI-13**	-	F	1000	**Circular**	**12.7**	-	-	-	-	3.67	**400**	**0.25**	**1.44**

Chiew, Y., and Lim, S. (1996). "Local Scour by a Deeply Submerged Horizontal Circular Jet." *Journal of Hydraulic Engineering*, 122(9), 529-532.

Database #	**dse**	Wse	Lse	Vse	Rh	**Fo**	dse/Rh	Wse/Rh	Lse/Rh	Vse/Rh3
	mm	mm	mm	ml	mm					
ChiewL_98A-01	**20**	68	220	-	1.00	**13.190**	20.000	68.000	220.000	-
ChiewL_98A-02	**25**	89	255	-	1.00	**15.790**	25.000	89.000	255.000	-
ChiewL_98A-03	**45**	166	415	-	1.00	**26.580**	45.000	166.000	415.000	-
ChiewL_98A-04	**57**	203	500	-	1.00	**31.710**	57.000	203.000	500.000	-
ChiewL_98A-05	**56**	205	510	-	1.00	**32.460**	56.000	205.000	510.000	-
ChiewL_98A-06	**16**	55	185	-	1.00	**10.250**	16.000	55.000	185.000	-
ChiewL_98A-07	**12**	38	155	-	1.00	**7.840**	12.000	38.000	155.000	-
ChiewL_98A-08	**34**	120	325	-	1.00	**20.210**	34.000	120.000	325.000	-
ChiewL_98-01	**103**	456	953	-	6.35	**23.360**	16.220	71.811	150.079	-
ChiewL_98-02	**90**	392	912	-	6.35	**20.420**	14.173	61.732	143.622	-
ChiewL_98-03	**72**	290	815	-	6.35	**13.900**	11.339	45.669	128.346	-
ChiewL_98-04	**27**	186	490	-	6.35	**8.280**	4.252	29.291	77.165	-
ChiewL_98-05	**103**	460	955	-	6.35	**24.790**	16.220	72.441	150.394	-
ChiewL_98-06	**117**	440	1028	-	6.35	**24.920**	18.425	69.291	161.890	-
ChiewL_98-07	**127**	476	1064	-	6.35	**25.810**	20.000	74.961	167.559	-
ChiewL_98-08	**121**	510	1110	-	6.35	**25.100**	19.055	80.315	174.803	-
ChiewL_98-09	**203**	764	1454	-	3.18	**85.280**	63.937	240.630	457.953	-
ChiewL_98-10	**135**	550	1022	-	3.18	**47.580**	42.520	173.228	321.890	-
ChiewL_98-11	**97**	430	768	-	3.18	**29.050**	30.551	135.433	241.890	-
ChiewL_98-12	**56**	222	490	-	3.18	**13.140**	17.638	69.921	154.331	-
ChiewL_98-13	**162**	536	1190	-	3.18	**57.660**	51.024	168.819	374.803	-

Chiew, Y., and Lim, S. (1996). "Local Scour by a Deeply Submerged Horizontal Circular Jet." *Journal of Hydraulic Engineering*, 122(9), 529-532.

Database #	**Original Run #**	Duration	F/NF	W	**Shape**	**do**	**b**	**slope**	**ho**	Q	Uo	**H**	**d50**	**sigma_g**
		hr		mm		**mm**	**mm**		**mm**	L/s	m/s	**mm**	**mm**	
ChiewL_98-14	**BII-1**	-	F	1000	**Circular**	**15**	**-**	**-**	**-**	-	1.54	**200**	**1.65**	**1.25**
ChiewL_98-15	**BII-2**	-	F	1000	**Circular**	**15**	**-**	**-**	**-**	-	4.55	**200**	**1.65**	**1.25**
ChiewL_98-16	**BII-3**	-	F	1000	**Circular**	**15**	**-**	**-**	**-**	-	2.17	**200**	**1.65**	**1.25**
ChiewL_98-17	**BII-4**	-	F	1000	**Circular**	**15**	**-**	**-**	**-**	-	3.51	**200**	**1.65**	**1.25**
ChiewL_98-18	**BII-5**	-	F	1000	**Circular**	**15**	**-**	**-**	**-**	-	0.79	**200**	**1.65**	**1.25**
ChiewL_98-19	**BII-6**	-	F	1000	**Circular**	**15**	**-**	**-**	**-**	-	2.87	**200**	**1.65**	**1.25**
ChiewL_98-20	**BII-7**	-	F	1000	**Circular**	**15**	**-**	**-**	**-**	-	1.84	**200**	**0.39**	**1.44**
ChiewL_98-21	**BII-8**	-	F	1000	**Circular**	**15**	**-**	**-**	**-**	-	3.22	**200**	**0.39**	**1.44**
ChiewL_98-22	**BII-9**	-	F	1000	**Circular**	**15**	**-**	**-**	**-**	-	5.78	**200**	**0.39**	**1.44**
ChiewL_98-23	**BII-10**	-	F	1000	**Circular**	**15**	**-**	**-**	**-**	-	4.62	**200**	**0.39**	**1.44**
ChiewL_98-24	**BII-11**	-	F	1000	**Circular**	**15**	**-**	**-**	**-**	-	0.6	**200**	**0.39**	**1.44**
ChiewL_98-25	**BII-12**	-	F	1000	**Circular**	**25.4**	**-**	**-**	**-**	-	1.24	**200**	**0.39**	**1.44**
ChiewL_98-26	**BII-13**	-	F	1000	**Circular**	**25.4**	**-**	**-**	**-**	-	0.56	**200**	**0.39**	**1.44**
ChiewL_98-27	**BII-14**	-	F	1000	**Circular**	**25.4**	**-**	**-**	**-**	-	0.91	**200**	**0.39**	**1.44**
ChiewL_98-28	**BII-15**	-	F	1000	**Circular**	**25.4**	**-**	**-**	**-**	-	1.6	**200**	**0.39**	**1.44**
ChiewL_98-29	**BII-16**	-	F	1000	**Circular**	**25.4**	**-**	**-**	**-**	-	2.57	**200**	**0.39**	**1.44**
ChiewL_98-30	**BII-17**	-	F	1000	**Circular**	**25.4**	**-**	**-**	**-**	-	1.95	**200**	**0.39**	**1.44**
ChiewL_98-31	**BII-18**	-	F	1000	**Circular**	**25.4**	**-**	**-**	**-**	-	1.230	**200**	**0.39**	**1.44**
ChiewL_98-32	**BII-19**	-	F	1000	**Circular**	**25.4**	**-**	**-**	**-**	-	0.940	**200**	**0.39**	**1.44**
ChiewL_98-33	**BII-20a**	-	F	1000	**Circular**	**15**	**-**	**-**	**-**	-	3.240	**200**	**1.65**	**1.25**

Chiew, Y., and Lim, S. (1996). "Local Scour by a Deeply Submerged Horizontal Circular Jet." *Journal of Hydraulic Engineering*, 122(9), 529-532.

Database #	**dse**	Wse	Lse	Vse	Rh	**Fo**	dse/Rh	Wse/Rh	Lse/Rh	Vse/Rh3
	mm	mm	mm	ml	mm					
ChiewL_98-14	**45**	173	460	-	3.75	**9.420**	12.000	46.133	122.667	-
ChiewL_98-15	**138**	580	1080	-	3.75	**27.840**	36.800	154.667	288.000	-
ChiewL_98-16	**66**	229	570	-	3.75	**13.280**	17.600	61.067	152.000	-
ChiewL_98-17	**103**	390	850	-	3.75	**21.480**	27.467	104.000	226.667	-
ChiewL_98-18	**10**	85	290	-	3.75	**4.830**	2.667	22.667	77.333	-
ChiewL_98-19	**75**	320	670	-	3.75	**17.560**	20.000	85.333	178.667	-
ChiewL_98-20	**73**	329	850	-	3.75	**23.100**	19.467	87.733	226.667	-
ChiewL_98-21	**126**	470	1100	-	3.75	**40.520**	33.600	125.333	293.333	-
ChiewL_98-22	**170**	-	1265	-	3.75	**72.730**	45.333	-	337.333	-
ChiewL_98-23	**172**	630	1300	-	3.75	**58.110**	45.867	168.000	346.667	-
ChiewL_98-24	**22**	80	400	-	3.75	**7.580**	5.867	21.333	106.667	-
ChiewL_98-25	**100**	-	-	-	6.35	**15.610**	15.748	-	-	-
ChiewL_98-26	**35**	194	490	-	6.35	**7.050**	5.512	30.551	77.165	-
ChiewL_98-27	**56**	244	748	-	6.35	**11.450**	8.819	38.425	117.795	-
ChiewL_98-28	**111**	438	1130	-	6.35	**20.140**	17.480	68.976	177.953	-
ChiewL_98-29	**124**	525	1285	-	6.35	**32.350**	19.528	82.677	202.362	-
ChiewL_98-30	**111**	485	1180	-	6.35	**24.540**	17.480	76.378	185.827	-
ChiewL_98-31	**80**	343	950	-	6.35	**15.480**	12.598	54.016	149.606	-
ChiewL_98-32	**50**	250	800	-	6.35	**11.830**	7.874	39.370	125.984	-
ChiewL_98-33	**88**	-	720	-	3.75	**19.820**	23.467	-	192.000	-

Clarke, F. R. W. (1962). "The Action of Submerged Jets on Moveable Material." M.S. Thesis, London University, London.

Database #	Original Run #	Duration	F/NF	W	Shape	do	b	slope	ho	Q	Uo	H	d50	sigma_g
		hr		mm		mm	mm		mm	L/s	m/s	mm	mm	
Clarke_62-01	**A1**	-	F	-	**Circular**	**4.78**	-	-	-	-	6.500	**279**	**0.82**	**1.38**
Clarke_62-02	**A2**	-	F	-	**Circular**	**4.78**	-	-	-	-	4.280	**279**	**0.82**	**1.38**
Clarke_62-03	**A3**	-	F	-	**Circular**	**4.78**	-	-	-	-	5.520	**279**	**0.82**	**1.38**
Clarke_62-04	**A4**	-	F	-	**Circular**	**4.78**	-	-	-	-	2.560	**279**	**0.82**	**1.38**
Clarke_62-05	**A5**	-	F	-	**Circular**	**4.78**	-	-	-	-	8.200	**279**	**0.82**	**1.38**
Clarke_62-06	**B1**	-	F	-	**Circular**	**4.78**	-	-	-	-	6.500	**279**	**2.02**	**1.22**
Clarke_62-07	**B2**	-	F	-	**Circular**	**4.78**	-	-	-	-	4.280	**279**	**2.02**	**1.22**
Clarke_62-08	**B3**	-	F	-	**Circular**	**4.78**	-	-	-	-	9.560	**279**	**2.02**	**1.22**
Clarke_62-09	**B4**	-	F	-	**Circular**	**4.78**	-	-	-	-	2.560	**279**	**2.02**	**1.22**
Clarke_62-10	**B5**	-	F	-	**Circular**	**4.78**	-	-	-	-	8.200	**279**	**2.02**	**1.22**
Clarke_62-11	**C1**	-	F	-	**Circular**	**2.38**	-	-	-	-	8.390	**159**	**0.82**	**1.38**
Clarke_62-12	**C2**	-	F	-	**Circular**	**2.38**	-	-	-	-	6.730	**159**	**0.82**	**1.38**
Clarke_62-13	**C3**	-	F	-	**Circular**	**2.38**	-	-	-	-	2.940	**159**	**0.82**	**1.38**
Clarke_62-14	**C4**	-	F	-	**Circular**	**2.38**	-	-	-	-	9.770	**159**	**0.82**	**1.38**
Clarke_62-15	**C5**	-	F	-	**Circular**	**2.38**	-	-	-	-	4.540	**159**	**0.82**	**1.38**
Clarke_62-16	**C6**	-	F	-	**Circular**	**2.38**	-	-	-	-	11.020	**159**	**0.82**	**1.38**
Clarke_62-17	**D1**	-	F	-	**Circular**	**2.38**	-	-	-	-	6.570	**279**	**0.82**	**1.38**
Clarke_62-18	**D2**	-	F	-	**Circular**	**2.38**	-	-	-	-	9.660	**279**	**0.82**	**1.38**
Clarke_62-19	**D3**	-	F	-	**Circular**	**2.38**	-	-	-	-	4.300	**279**	**0.82**	**1.38**
Clarke_62-20	**D4**	-	F	-	**Circular**	**2.38**	-	-	-	-	2.540	**279**	**0.82**	**1.38**
Clarke_62-21	**D5**	-	F	-	**Circular**	**2.38**	-	-	-	-	8.240	**279**	**0.82**	**1.38**
Clarke_62-22	**D6**	-	F	-	**Circular**	**2.38**	-	-	-	-	12.000	**279**	**0.82**	**1.38**
Clarke_62-23	**E1**	-	F	-	**Circular**	**14.3**	-	-	-	-	5.770	**279**	**0.82**	**1.38**
Clarke_62-24	**E2**	-	F	-	**Circular**	**14.3**	-	-	-	-	3.060	**279**	**0.82**	**1.38**
Clarke_62-25	**E3**	-	F	-	**Circular**	**14.3**	-	-	-	-	2.100	**279**	**0.82**	**1.38**

Clarke, F. R. W. (1962). "The Action of Submerged Jets on Moveable Material." M.S. Thesis, London University, London.

Database #	**dse**	Wse	Lse	Vse	Rh	**Fo**	dse/Rh	Wse/Rh	Lse/Rh	Vse/Rh3
	mm	mm	mm	ml	mm					
Clarke_62-01	**117**	434	785	-	1.20	**56.420**	97.908	363.180	656.904	-
Clarke_62-02	**80**	315	561	-	1.20	**37.150**	66.946	263.598	469.456	-
Clarke_62-03	**91**	361	655	-	1.20	**47.910**	76.151	302.092	548.117	-
Clarke_62-04	**59**	226	391	-	1.20	**22.220**	49.372	189.121	327.197	-
Clarke_62-05	**134**	521	874	-	1.20	**71.180**	112.134	435.983	731.381	-
Clarke_62-06	**86**	305	559	-	1.20	**35.950**	71.967	255.230	467.782	-
Clarke_62-07	**64**	234	411	-	1.20	**23.670**	53.556	195.816	343.933	-
Clarke_62-08	**114**	422	739	-	1.20	**52.870**	95.397	353.138	618.410	-
Clarke_62-09	**44**	163	264	-	1.20	**14.160**	36.820	136.402	220.921	-
Clarke_62-10	**98**	378	648	-	1.20	**45.350**	82.008	316.318	542.259	-
Clarke_62-11	**69**	274	470	-	0.60	**72.820**	115.966	460.504	789.916	-
Clarke_62-12	**60**	246	419	-	0.60	**58.420**	100.840	413.445	704.202	-
Clarke_62-13	**36**	142	239	-	0.60	**25.520**	60.504	238.655	401.681	-
Clarke_62-14	**84**	330	584	-	0.60	**84.800**	141.176	554.622	981.513	-
Clarke_62-15	**43**	180	292	-	0.60	**39.410**	72.269	302.521	490.756	-
Clarke_62-16	**92**	368	640	-	0.60	**95.650**	154.622	618.487	1075.630	-
Clarke_62-17	**63**	234	419	-	0.60	**57.030**	105.882	393.277	704.202	-
Clarke_62-18	**85**	335	582	-	0.60	**83.850**	142.857	563.025	978.151	-
Clarke_62-19	**47**	175	290	-	0.60	**37.320**	78.992	294.118	487.395	-
Clarke_62-20	**36**	135	213	-	0.60	**22.050**	60.504	226.891	357.983	-
Clarke_62-21	**78**	297	500	-	0.60	**71.520**	131.092	499.160	840.336	-
Clarke_62-22	**105**	386	676	-	0.60	**104.160**	176.471	648.739	1136.134	-
Clarke_62-23	**152**	594	1130	-	3.58	**50.080**	42.517	166.154	316.084	-
Clarke_62-24	**114**	452	785	-	3.58	**26.560**	31.888	126.434	219.580	-
Clarke_62-25	**101**	406	711	-	3.58	**18.230**	28.252	113.566	198.881	-

Opie, T. R. (1967). "Scour at Culvert Outlets." M.Sc. thesis, Colorado State University, Fort Collins.

Database #	Original Run #	Duration	F/NF	W	Shape	do	b	slope	ho	Q	Uo	H	d50	sigma_g
		hr		mm		mm	mm		mm	L/s	m/s	mm	mm	
Opie_67-01	**B10**	-	F	2441.1	**Circular**	**309**	**-**	**-**	**-**	-	3.020	**122**	**91.4**	**1.1**
Opie_67-02	**B12**	-	F	2441.1	**Circular**	**309**	**-**	**-**	**-**	-	2.530	**122**	**91.4**	**1.1**
Opie_67-03	**B18**	-	F	2441.1	**Circular**	**309**	**-**	**-**	**-**	-	3.010	**152**	**91.4**	**1.1**
Opie_67-04	**D26**	-	F	6099.6	**Circular**	**442**	**-**	**-**	**-**	-	3.490	**189**	**99.1**	**1.03**
Opie_67-05	**D27**	-	F	6099.6	**Circular**	**442**	**-**	**-**	**-**	-	2.640	**165**	**99.1**	**1.03**
Opie_67-06	**E38**	-	F	2441.1	**Circular**	**309**	**-**	**-**	**-**	-	2.180	**134**	**25.3**	**1.03**
Opie_67-07	**F42**	-	F	6099.6	**Circular**	**442**	**-**	**-**	**-**	-	3.060	**192**	**204.2**	**0.99**
Opie_67-08	**F43**	-	F	6099.6	**Circular**	**442**	**-**	**-**	**-**	-	4.080	**223**	**204.2**	**0.99**
Opie_67-09	**F44**	-	F	6099.6	**Circular**	**442**	**-**	**-**	**-**	-	4.150	**488**	**204.2**	**0.99**
Opie_67-10	**G55**	-	F	6126.48	**Circular**	**914.4**	**-**	**-**	**-**	-	4.110	**442**	**204.2**	**0.99**
Opie_67-11	**G59**	-	F	6126.48	**Circular**	**914.4**	**-**	**-**	**-**	-	4.210	**411**	**204.2**	**0.99**
Opie_67-12	**K67**	-	F	6126.48	**Circular**	**914.4**	**-**	**-**	**-**	-	4.130	**351**	**92.1**	**1.18**

Opie, T. R. (1967). "Scour at Culvert Outlets." M.Sc. thesis, Colorado State University, Fort Collins.

Database #	**dse**	Wse	Lse	Vse	Rh	**Fo**	dse/Rh	Wse/Rh	Lse/Rh	Vse/Rh3
	mm	mm	mm	ml	mm					
Opie_67-01	**244**	1829	1829	222570	77.25	**2.492**	3.159	23.676	23.676	482.804
Opie_67-02	**219**	1829	1372	148380	77.25	**2.089**	2.835	23.676	17.761	321.870
Opie_67-03	**162**	-	1591	-	77.25	**2.485**	2.097	-	20.595	-
Opie_67-04	**451**	2591	3353	1213941	110.50	**2.698**	4.081	23.448	30.344	899.727
Opie_67-05	**366**	1829	2134	532356	110.50	**2.041**	3.312	16.552	19.312	394.562
Opie_67-06	**375**	1829	2286	670825	77.25	**3.410**	4.854	23.676	29.592	1455.170
Opie_67-07	**213**	305	1524	9061	110.50	**1.690**	1.928	2.760	13.792	6.716
Opie_67-08	**336**	1981	2926	430415	110.50	**2.251**	3.041	17.928	26.480	319.007
Opie_67-09	**152**	1676	4145	189723	110.50	**2.291**	1.376	15.167	37.511	140.615
Opie_67-10	**518**	3200	3962	2234479	228.60	**2.267**	2.266	13.998	17.332	187.046
Opie_67-11	**549**	3749	4572	4036843	228.60	**2.324**	2.402	16.400	20.000	337.919
Opie_67-12	**792**	4877	5486	19814681	228.60	**3.310**	3.465	21.334	23.998	1658.664

Rajaratnam, N., and Berry, B. (1977). "Erosion By Circular Turbulent Wall Jets." *Journal of Hydraulic Research*, 15(3), 277-289.

Database #	**Original Run #**	Duration	F/NF	W	**Shape**	**do**	**b**	**slope**	**ho**	Q	Uo	**H**	**d50**	**sigma_g**
		hr		mm		**mm**	**mm**		**mm**	L/s	m/s	**mm**	**mm**	
RajaB_77A-01	**111**	-	AIR	-	**Circular**	**23.5**	-	-	-	-	10.058	-	**1.4**	**1.26**
RajaB_77A-02	**112**	-	AIR	-	**Circular**	**23.5**	-	-	-	-	14.326	-	**1.4**	**1.26**
RajaB_77A-03	**113**	-	AIR	-	**Circular**	**23.5**	-	-	-	-	19.202	-	**1.4**	**1.26**
RajaB_77A-04	**114**	-	AIR	-	**Circular**	**23.5**	-	-	-	-	22.250	-	**1.4**	**1.26**
RajaB_77A-05	**115**	-	AIR	-	**Circular**	**23.5**	-	-	-	-	27.127	-	**1.4**	**1.26**
RajaB_77A-06	**116**	-	AIR	-	**Circular**	**23.5**	-	-	-	-	30.785	-	**1.4**	**1.26**
RajaB_77A-07	**117**	-	AIR	-	**Circular**	**23.5**	-	-	-	-	34.442	-	**1.4**	**1.26**
RajaB_77A-08	**118**	-	AIR	-	**Circular**	**23.5**	-	-	-	-	41.453	-	**1.4**	**1.26**
RajaB_77A-09	**119**	-	AIR	-	**Circular**	**23.5**	-	-	-	-	45.720	-	**1.4**	**1.26**
RajaB_77A-10	**121**	-	AIR	-	**Circular**	**6.35**	-	-	-	-	24.079	-	**1.4**	**1.26**
RajaB_77A-11	**122**	-	AIR	-	**Circular**	**6.35**	-	-	-	-	29.566	-	**1.4**	**1.26**
RajaB_77A-12	**123**	-	AIR	-	**Circular**	**6.35**	-	-	-	-	34.747	-	**1.4**	**1.26**
RajaB_77A-13	**124**	-	AIR	-	**Circular**	**6.35**	-	-	-	-	41.148	-	**1.4**	**1.26**
RajaB_77A-14	**125**	-	AIR	-	**Circular**	**6.35**	-	-	-	-	45.720	-	**1.4**	**1.26**
RajaB_77A-15	**211**	-	AIR	-	**Circular**	**23.5**	-	-	-	-	14.935	-	**1.4**	**1.5**
RajaB_77A-16	**212**	-	AIR	-	**Circular**	**23.5**	-	-	-	-	20.422	-	**1.4**	**1.5**
RajaB_77A-17	**213**	-	AIR	-	**Circular**	**23.5**	-	-	-	-	26.822	-	**1.4**	**1.5**
RajaB_77A-18	**214**	-	AIR	-	**Circular**	**23.5**	-	-	-	-	31.090	-	**1.4**	**1.5**
RajaB_77A-19	**215**	-	AIR	-	**Circular**	**23.5**	-	-	-	-	35.052	-	**1.4**	**1.5**
RajaB_77A-20	**216**	-	AIR	-	**Circular**	**23.5**	-	-	-	-	40.538	-	**1.4**	**1.5**
RajaB_77A-21	**217**	-	AIR	-	**Circular**	**23.5**	-	-	-	-	46.330	-	**1.4**	**1.5**
RajaB_77A-22	**218**	-	AIR	-	**Circular**	**23.5**	-	-	-	-	52.730	-	**1.4**	**1.5**
RajaB_77A-23	**221**	-	AIR	-	**Circular**	**6.35**	-	-	-	-	20.422	-	**1.4**	**1.5**
RajaB_77A-24	**222**	-	AIR	-	**Circular**	**6.35**	-	-	-	-	32.614	-	**1.4**	**1.5**
RajaB_77A-25	**223**	-	AIR	-	**Circular**	**6.35**	-	-	-	-	47.549	-	**1.4**	**1.5**
RajaB_77A-26	**224**	-	AIR	-	**Circular**	**6.35**	-	-	-	-	54.864	-	**1.4**	**1.5**
RajaB_77-01	**331**	-	F	1092	**Circular**	**25.4**	-	-	-	-	1.280	**610**	**1.4**	**1.5**
RajaB_77-02	**332**	-	F	1092	**Circular**	**25.4**	-	-	-	-	1.570	**610**	**1.4**	**1.5**
RajaB_77-03	**333**	-	F	1092	**Circular**	**25.4**	-	-	-	-	1.680	**610**	**1.4**	**1.5**
RajaB_77-04	**334**	-	F	1092	**Circular**	**25.4**	-	-	-	-	1.810	**610**	**1.4**	**1.5**

Rajaratnam, N., and Berry, B. (1977). "Erosion By Circular Turbulent Wall Jets." *Journal of Hydraulic Research*, 15(3), 277-289.

Database #	**dse**	Wse	Lse	Vse	Rh	**Fo**	dse/Rh	Wse/Rh	Lse/Rh	Vse/Rh3
	mm	mm	mm	ml	mm					
RajaB_77A-01	**6.7**	-	-	-	5.88	**2.930**	1.140	-	-	-
RajaB_77A-02	**18.3**	-	-	-	5.88	**4.170**	3.115	-	-	-
RajaB_77A-03	**29**	-	-	-	5.88	**5.590**	4.936	-	-	-
RajaB_77A-04	**36.6**	-	-	-	5.88	**6.470**	6.230	-	-	-
RajaB_77A-05	**48.2**	-	-	-	5.88	**7.890**	8.204	-	-	-
RajaB_77A-06	**52.4**	-	-	-	5.88	**8.950**	8.919	-	-	-
RajaB_77A-07	**61**	-	-	-	5.88	**10.020**	10.383	-	-	-
RajaB_77A-08	**77.7**	-	-	-	5.88	**12.060**	13.226	-	-	-
RajaB_77A-09	**87.8**	-	-	-	5.88	**13.300**	14.945	-	-	-
RajaB_77A-10	**12.8**	-	-	-	1.59	**7.000**	8.063	-	-	-
RajaB_77A-11	**15.8**	-	-	-	1.59	**8.600**	9.953	-	-	-
RajaB_77A-12	**18.9**	-	-	-	1.59	**10.110**	11.906	-	-	-
RajaB_77A-13	**25.3**	-	-	-	1.59	**11.970**	15.937	-	-	-
RajaB_77A-14	**29.3**	-	-	-	1.59	**13.300**	18.457	-	-	-
RajaB_77A-15	**11.6**	-	-	-	5.88	**2.720**	1.974	-	-	-
RajaB_77A-16	**20.7**	-	-	-	5.88	**3.720**	3.523	-	-	-
RajaB_77A-17	**32**	-	-	-	5.88	**4.890**	5.447	-	-	-
RajaB_77A-18	**38.1**	-	-	-	5.88	**5.670**	6.485	-	-	-
RajaB_77A-19	**46.6**	-	-	-	5.88	**6.390**	7.932	-	-	-
RajaB_77A-20	**54.6**	-	-	-	5.88	**7.390**	9.294	-	-	-
RajaB_77A-21	**65.2**	-	-	-	5.88	**8.440**	11.098	-	-	-
RajaB_77A-22	**76.2**	-	-	-	5.88	**9.610**	12.970	-	-	-
RajaB_77A-23	**2.7**	-	-	-	1.59	**3.720**	1.701	-	-	-
RajaB_77A-24	**11.6**	-	-	-	1.59	**5.940**	7.307	-	-	-
RajaB_77A-25	**18.6**	-	-	-	1.59	**8.670**	11.717	-	-	-
RajaB_77A-26	**22.9**	-	-	-	1.59	**10.000**	14.425	-	-	-
RajaB_77-01	**81**	-	-	-	6.35	**8.570**	12.756	-	-	-
RajaB_77-02	**94**	-	-	-	6.35	**10.100**	14.803	-	-	-
RajaB_77-03	**98**	-	-	-	6.35	**11.220**	15.433	-	-	-
RajaB_77-04	**117**	-	-	-	6.35	**12.140**	18.425	-	-	-

Rajaratnam, N., and Diebel, M. (1981). "Erosion Below Culvert-like Structures." *Fifth Canadian Hydrotechnical Conference*, 469 - 484.

Database #	**Original Run #**	Duration	F/NF	W	**Shape**	**do**	**b**	**slope**	**ho**	Q	Uo	**H**	**d50**	**sigma_g**
		hr		mm		**mm**	**mm**		**mm**	L/s	m/s	**mm**	**mm**	
RajaD_81-01	**A11**	-	F	1091.946	**Circular**	**12.7**	-	-	-	-	1.250	**22.6**	**1.05**	**1.5**
RajaD_81-02	**A12**	-	F	1091.946	**Circular**	**12.7**	-	-	-	-	1.630	**24.1**	**1.05**	**1.5**
RajaD_81-03	**A13**	-	F	1091.946	**Circular**	**12.7**	-	-	-	-	1.800	**43**	**1.05**	**1.5**
RajaD_81-04	**A14**	-	F	1091.946	**Circular**	**12.7**	-	-	-	-	2.320	**42.7**	**1.05**	**1.5**
RajaD_81-05	**A15**	-	F	1091.946	**Circular**	**12.7**	-	-	-	-	0.580	**25.6**	**1.05**	**1.5**
RajaD_81-06	**A16**	-	F	1091.946	**Circular**	**12.7**	-	-	-	-	1.790	**10.2**	**1.05**	**1.5**
RajaD_81-07	**A17**	-	F	1091.946	**Circular**	**12.7**	-	-	-	-	1.480	**10.2**	**1.05**	**1.5**
RajaD_81-08	**A18**	-	F	1091.946	**Circular**	**12.7**	-	-	-	-	1.080	**2.5**	**1.05**	**1.5**
RajaD_81-09	**A19**	-	F	1091.946	**Circular**	**12.7**	-	-	-	-	1.290	**2.5**	**1.05**	**1.5**
RajaD_81-10	**B11**	-	F	38.1	**Circular**	**12.7**	-	-	-	-	2.130	**32**	**1.05**	**1.5**
RajaD_81-11	**B12**	-	F	38.1	**Circular**	**12.7**	-	-	-	-	1.530	**31.7**	**1.05**	**1.5**
RajaD_81-12	**B21**	-	F	88.9	**Circular**	**25.4**	-	-	-	-	0.450	**22.3**	**1.05**	**1.5**
RajaD_81-13	**B22**	-	F	88.9	**Circular**	**25.4**	-	-	-	-	0.530	**23.5**	**1.05**	**1.5**
RajaD_81-14	**B23**	-	F	88.9	**Circular**	**25.4**	-	-	-	-	0.710	**29.3**	**1.05**	**1.5**
RajaD_81-15	**B24**	-	F	88.9	**Circular**	**25.4**	-	-	-	-	0.410	**22.2**	**1.05**	**1.5**
RajaD_81-16	**B25**	-	F	25.4	**Circular**	**25.4**	-	-	-	-	1.410	**16.5**	**1.05**	**1.5**
RajaD_81-17	**B26**	-	F	25.4	**Circular**	**25.4**	-	-	-	-	0.900	**6.7**	**1.05**	**1.5**

Rajaratnam, N., and Diebel, M. (1981). "Erosion Below Culvert-like Structures." *Fifth Canadian Hydrotechnical Conference*, 469 - 484.

Database #	**dse**	Wse	Lse	Vse	Rh	**Fo**	dse/Rh	Wse/Rh	Lse/Rh	Vse/Rh3
	mm	mm	mm	ml	mm					
RajaD_81-01	**36.5**	-	-	-	3.18	**9.650**	11.496	-	-	-
RajaD_81-02	**61.6**	-	-	-	3.18	**12.610**	19.402	-	-	-
RajaD_81-03	**60.1**	-	-	-	3.18	**13.380**	18.929	-	-	-
RajaD_81-04	**82.6**	-	-	-	3.18	**17.930**	26.016	-	-	-
RajaD_81-05	**12.5**	-	-	-	3.18	**4.490**	3.937	-	-	-
RajaD_81-06	**65.4**	-	-	-	3.18	**13.700**	20.598	-	-	-
RajaD_81-07	**54.3**	-	-	-	3.18	**11.400**	17.102	-	-	-
RajaD_81-08	**34.1**	-	-	-	3.18	**8.300**	10.740	-	-	-
RajaD_81-09	**38.4**	-	-	-	3.18	**9.900**	12.094	-	-	-
RajaD_81-10	**76.2**	-	-	-	3.18	**16.450**	24.000	-	-	-
RajaD_81-11	**43.6**	-	-	-	3.18	**11.790**	13.732	-	-	-
RajaD_81-12	**25.3**	-	-	-	6.35	**3.460**	3.984	-	-	-
RajaD_81-13	**25.6**	-	-	-	6.35	**4.120**	4.031	-	-	-
RajaD_81-14	**32**	-	-	-	6.35	**5.460**	5.039	-	-	-
RajaD_81-15	**16.8**	-	-	-	6.35	**3.130**	2.646	-	-	-
RajaD_81-16	**79.3**	-	-	-	6.35	**10.500**	12.488	-	-	-
RajaD_81-17	**51.2**	-	-	-	6.35	**6.520**	8.063	-	-	-

Rajaratnam, N., and Humphries, J. (1983). "Diffusion of Bluff Wall Jets in Finite Depth Tailwater." *Journal of Hydraulic Engineering*, 109(11), 1471-1485.

Database #	Original Run #	Duration	F/NF	W	Shape	do	b	slope	ho	Q	Uo	H	d50	sigma_g
		hr		mm		mm	mm		mm	L/s	m/s	mm	mm	
RajaH_83-01	**S2**	-	(F)	2400	**Rect**	**31**	**50**	-	**34.7**	-	0.232	**31**	**0.11**	**1.5**
RajaH_83-02	**S3**	-	(F)	2400	**Rect**	**31**	**50**	-	**33.8**	-	0.188	**31**	**0.11**	**1.5**
RajaH_83-03	**S4**	-	(F)	2400	**Rect**	**31**	**50**	-	**33.8**	-	0.089	**31**	**0.11**	**1.5**
RajaH_83-04	**S5**	-	(F)	2400	**Rect**	**31**	**50**	-	**35.1**	-	0.332	**31**	**0.11**	**1.5**
RajaH_83-05	**S6**	-	(F)	2400	**Rect**	**31**	**50**	-	**34.1**	-	0.159	**31**	**0.11**	**1.5**
RajaH_83-06	**S7**	-	(F)	2400	**Rect**	**31**	**50**	-	**33.8**	-	0.180	**31**	**0.11**	**1.5**
RajaH_83-07	**S8**	-	(F)	2400	**Rect**	**31**	**50**	-	**35.3**	-	0.287	**31**	**0.11**	**1.5**
RajaH_83-08	**S9**	-	(F)	2400	**Rect**	**31**	**50**	-	**35.9**	-	0.404	**31**	**0.11**	**1.5**

Ade, F., and Rajaratnam, N. (1998). "Generalized study of erosion by circular horizontal turbulent jets." *Journal of Hydraulic Research*, 36(4), 613-636.

Database #	Original Run #	Duration	F/NF	W	Shape	do	b	slope	ho	Q	Uo	H	d50	sigma_g
		hr		mm		mm	mm		mm	L/s	m/s	mm	mm	
Araja_98-01	**1**	94	F	1090	**Circular**	**25.4**	-	-	-	-	5.400	**619.76**	**7.2**	**1.33**
Araja_98-02	**2**	34	F	1090	**Circular**	**25.4**	-	-	-	-	2.700	**619.76**	**7.2**	**1.33**
Araja_98-03	**3**	84	F	1090	**Circular**	**25.4**	-	-	-	-	4.200	**619.76**	**7.2**	**1.33**
Araja_98-04	**4**	73	F	1090	**Circular**	**25.4**	-	-	-	-	3.500	**619.76**	**7.2**	**1.33**
Araja_98-05	**5**	219	F	1090	**Circular**	**25.4**	-	-	-	-	4.700	**619.76**	**7.2**	**1.33**
Araja_98-06	**6**	15	F	1090	**Circular**	**25.4**	-	-	-	-	2.200	**19.05**	**7.2**	**1.33**
Araja_98-07	**7**	12	F	1090	**Circular**	**25.4**	-	-	-	-	4.000	**19.05**	**7.2**	**1.33**
Araja_98-08	**8**	18	F	1090	**Circular**	**25.4**	-	-	-	-	5.400	**19.05**	**7.2**	**1.33**
Araja_98-09	**9**	20	F	1090	**Circular**	**19**	-	-	-	-	5.100	**14.25**	**7.2**	**1.33**
Araja_98-10	**10**	72	F	1090	**Circular**	**5**	-	-	-	-	4.300	**620**	**0.24**	**1.46**
Araja_98-11	**11**	108	F	1090	**Circular**	**5**	-	-	-	-	4.900	**620**	**0.24**	**1.46**
Araja_98-12	**12**	186	F	1090	**Circular**	**5**	-	-	-	-	5.500	**620**	**0.24**	**1.46**
Araja_98A-01	**1**	26	AIR	-	**Circular**	**12.5**	-	-	-	-	52.000	-	**1.47**	**1.12**
Araja_98A-02	**2**	24	AIR	-	**Circular**	**12.5**	-	-	-	-	20.300	-	**1.47**	**1.12**
Araja_98A-03	**3**	19	AIR	-	**Circular**	**12.5**	-	-	-	-	25.500	-	**1.47**	**1.12**
Araja_98A-04	**4**	18	AIR	-	**Circular**	**12.5**	-	-	-	-	37.300	-	**1.47**	**1.12**
Araja_98A-05	**5**	22	AIR	-	**Circular**	**12.5**	-	-	-	-	41.200	-	**1.47**	**1.12**
Araja_98A-06	**6**	17	AIR	-	**Circular**	**12.5**	-	-	-	-	32.800	-	**1.47**	**1.12**
Araja_98A-07	**7**	25	AIR	-	**Circular**	**12.5**	-	-	-	-	80.000	-	**1.47**	**1.12**

Rajaratnam, N., and Humphries, J. (1983). "Diffusion of Bluff Wall Jets in Finite Depth Tailwater." *Journal of Hydraulic Engineering*, 109(11), 1471-1485.

Database #	**dse**	Wse	Lse	Vse	Rh	**Fo**	dse/Rh	Wse/Rh	Lse/Rh	Vse/Rh3
	mm	mm	mm	ml	mm					
RajaH_83-01	**46.5**	-	-	-	-	**5.500**	6.000	-	-	-
RajaH_83-02	**32.55**	-	-	-	-	**4.460**	4.200	-	-	-
RajaH_83-03	**17.05**	-	-	-	-	**2.110**	2.200	-	-	-
RajaH_83-04	**78.43**	-	-	-	-	**7.870**	10.120	-	-	-
RajaH_83-05	**27.9**	-	-	-	-	**3.770**	3.600	-	-	-
RajaH_83-06	**34.1**	-	-	-	-	**4.270**	4.400	-	-	-
RajaH_83-07	**62**	-	-	-	-	**6.800**	8.000	-	-	-
RajaH_83-08	**77.5**	-	-	-	-	**9.570**	10.000	-	-	-

Ade, F., and Rajaratnam, N. (1998). "Generalized study of erosion by circular horizontal turbulent jets." *Journal of Hydraulic Research*, 36(4), 613-636.

Database #	**dse**	Wse	Lse	Vse	Rh	**Fo**	dse/Rh	Wse/Rh	Lse/Rh	Vse/Rh3	H/do
	mm	mm	mm	ml	mm						
Araja_98-01	**130.5**	647	1110	-	6.35	**15.910**	20.551	101.890	174.803	-	24.4
Araja_98-02	**79**	350	735	-	6.35	**8.000**	12.441	55.118	115.748	-	24.4
Araja_98-03	**107.7**	470	945	-	6.35	**12.390**	16.961	74.016	148.819	-	24.4
Araja_98-04	**87.5**	389	770	-	6.35	**10.190**	13.780	61.260	121.260	-	24.4
Araja_98-05	**128.5**	583	1050	-	6.35	**13.830**	20.236	91.811	165.354	-	24.4
Araja_98-06	**59.5**	207	512	-	6.35	**6.290**	9.370	32.598	80.630	-	0.75
Araja_98-07	**87**	486	940	-	6.35	**11.730**	13.701	76.535	148.031	-	0.75
Araja_98-08	**99**	716	1120	-	6.35	**15.790**	15.591	112.756	176.378	-	0.75
Araja_98-09	**64.4**	453	940	-	4.75	**14.820**	13.558	95.368	197.895	-	0.75
Araja_98-10	**72**	286	635	-	1.25	**68.700**	57.600	228.800	508.000	-	124
Araja_98-11	**95.5**	371	790	-	1.25	**77.810**	76.400	296.800	632.000	-	124
Araja_98-12	**95.5**	-	900	-	1.25	**88.200**	76.400	#VALUE!	720.000	-	124
Araja_98A-01	**56.5**	-	633	-	3.13	**14.510**	18.080	#VALUE!	202.560	-	-
Araja_98A-02	**21.8**	68	280	-	3.13	**5.670**	6.976	21.760	89.600	-	-
Araja_98A-03	**30.2**	95	359	-	3.13	**7.100**	9.664	30.400	114.880	-	-
Araja_98A-04	**38.8**	141	499	-	3.13	**10.410**	12.416	45.120	159.680	-	-
Araja_98A-05	**40**	144	493	-	3.13	**11.480**	12.800	46.080	157.760	-	-
Araja_98A-06	**36.5**	94	395	-	3.13	**9.160**	11.680	30.080	126.400	-	-
Araja_98A-07	**77**	305	830	-	3.13	**22.310**	24.640	97.600	265.600	-	-

Ruff, J. F., Abt, S. R., Mendoza, C., Shaikh, A., and Kloberdanz, R. (1982). *Scour at Culvert Outlets in Mixed Bed Materials*, FHWA.

Database #	Original Run #	Duration	F/NF	W	Shape	do	b	slope	ho	Q	Uo	H	d50	sigma_g
		hr		mm		mm	mm		mm	L/s	m/s	mm	mm	
Ruff_82-01	**G1**	1000	NF	1200	**circular**	**102**	-	-	-	4.531	1.268	**45.9**	**1.86**	**1.33**
Ruff_82-02	**G2**	1000	NF	1200	**circular**	**102**	-	-	-	6.796	1.344	**45.9**	**1.86**	**1.33**
Ruff_82-03	**G3**	1000	NF	1200	**circular**	**102**	-	-	-	9.061	1.286	**45.9**	**1.86**	**1.33**
Ruff_82-04	**G4**	1000	F	1200	**circular**	**102**	-	-	-	11.327	1.386	**45.9**	**1.86**	**1.33**
Ruff_82-08	**H1**	1000	NF	1200	**circular**	**102**	-	-	-	4.531	1.268	**45.9**	**1.86**	**1.33**
Ruff_82-09	**H2**	1000	NF	1200	**circular**	**102**	-	-	-	6.796	1.344	**45.9**	**1.86**	**1.33**
Ruff_82-10	**H3**	1000	NF	1200	**circular**	**102**	-	-	-	9.061	1.286	**45.9**	**1.86**	**1.33**
Ruff_82-11	**H4**	1000	F	1200	**circular**	**102**	-	-	-	11.327	1.386	**45.9**	**1.86**	**1.33**
Ruff_82-21	**A1**	316	NF	6100	**circular**	**102**	-	-	-	3.115	1.119	**45.9**	**1.86**	**1.33**
Ruff_82-22	**A2**	316	NF	6100	**circular**	**102**	-	-	-	5.097	1.247	**45.9**	**1.86**	**1.33**
Ruff_82-23	**A3**	316	F	6100	**circular**	**102**	-	-	-	10.194	1.248	**45.9**	**1.86**	**1.33**
Ruff_82-24	**A4**	316	F	6100	**circular**	**102**	-	-	-	15.574	1.906	**45.9**	**1.86**	**1.33**
Ruff_82-25	**A5**	316	F	6100	**circular**	**102**	-	-	-	20.671	2.530	**45.9**	**1.86**	**1.33**
Ruff_82-26	**A6**	316	F	6100	**circular**	**102**	-	-	-	25.768	3.154	**45.9**	**1.86**	**1.33**
Ruff_82-27	**A7**	316	F	6100	**circular**	**102**	-	-	-	32.281	3.951	**45.9**	**1.86**	**1.33**
Ruff_82-28	**B1**	316	NF	6100	**circular**	**254**	-	-	-	32.564	2.338	**0**	**1.86**	**1.33**
Ruff_82-29	**B2**	316	NF	6100	**circular**	**254**	-	-	-	54.085	2.006	**0**	**1.86**	**1.33**
Ruff_82-30	**B3**	316	F	6100	**circular**	**254**	-	-	-	162.538	3.208	**0**	**1.86**	**1.33**
Ruff_82-31	**B4**	316	F	6100	**circular**	**254**	-	-	-	216.624	4.275	**0**	**1.86**	**1.33**
Ruff_82-32	**C1**	316	NF	6100	**circular**	**254**	-	-	-	32.564	2.338	**63.5**	**1.86**	**1.33**
Ruff_82-33	**C2**	316	NF	6100	**circular**	**254**	-	-	-	54.085	2.006	**63.5**	**1.86**	**1.33**
Ruff_82-34	**C3**	316	F	6100	**circular**	**254**	-	-	-	162.538	3.208	**63.5**	**1.86**	**1.33**
Ruff_82-35	**C4**	316	F	6100	**circular**	**254**	-	-	-	216.624	4.275	**63.5**	**1.86**	**1.33**
Ruff_82-36	**D1**	1000	NF	6100	**circular**	**254**	-	-	-	53.519	2.006	**114.3**	**1.86**	**1.33**
Ruff_82-37	**D2**	1000	F	6100	**circular**	**254**	-	-	-	107.038	2.112	**114.3**	**1.86**	**1.33**
Ruff_82-38	**D3**	1000	F	6100	**circular**	**254**	-	-	-	107.038	2.112	**114.3**	**1.86**	**1.33**
Ruff_82-39	**D4**	1000	F	6100	**circular**	**254**	-	-	-	160.556	3.169	**114.3**	**1.86**	**1.33**
Ruff_82-40	**D5**	1000	F	6100	**circular**	**254**	-	-	-	214.075	4.225	**114.3**	**1.86**	**1.33**
Ruff_82-41	**D6**	1000	F	6100	**circular**	**254**	-	-	-	267.594	5.281	**114.3**	**1.86**	**1.33**

Ruff, J. F., Abt, S. R., Mendoza, C., Shaikh, A., and Kloberdanz, R. (1982). *Scour at Culvert Outlets in Mixed Bed Materials*, FHWA.

Database #	**dse**	Wse	Lse	Vse	Rh	**Fo**	dse/Rh	Wse/Rh	Lse/Rh	Vse/Rh3	H/do
	mm	mm	mm	ml	mm						
Ruff_82-01	**152.4**	832.104	1493.52	68243.60029	23.64	**7.308**	6.446	35.196	63.172	5164.168	0.45
Ruff_82-02	**176.784**	835.152	1737.36	89481.23523	28.07	**7.747**	6.297	29.748	61.884	4043.792	0.45
Ruff_82-03	**213.36**	883.92	1706.88	128558.4835	31.01	**7.413**	6.880	28.502	55.039	4310.226	0.45
Ruff_82-04	**240.792**	1103.376	1981.2	207562.4855	25.50	**7.989**	9.443	43.270	77.694	12517.809	0.45
Ruff_82-08	**143.256**	838.2	1524	65411.91563	23.64	**7.308**	6.059	35.454	64.461	4949.888	0.45
Ruff_82-09	**185.928**	1066.8	1645.92	90047.57216	28.07	**7.747**	6.623	37.999	58.627	4069.386	0.45
Ruff_82-10	**207.264**	990.6	1798.32	132522.8421	31.01	**7.413**	6.683	31.942	57.987	4443.141	0.45
Ruff_82-11	**216.408**	1051.56	1889.76	149796.1185	25.50	**7.989**	8.487	41.238	74.108	9033.999	0.45
Ruff_82-21	**109.728**	487.68	1188.72	17839.61335	20.76	**6.447**	5.284	23.486	57.246	1992.463	0.45
Ruff_82-22	**170.688**	786.384	944.88	32847.54205	25.51	**7.185**	6.692	30.831	37.045	1979.512	0.45
Ruff_82-23	**268.224**	1207.008	1188.72	167069.3949	25.50	**7.190**	10.519	47.334	46.616	10075.726	0.45
Ruff_82-24	**338.328**	1536.192	2590.8	348297.2131	25.50	**10.985**	13.268	60.243	101.600	21005.328	0.45
Ruff_82-25	**344.424**	1999.488	3413.76	430416.0682	25.50	**14.580**	13.507	78.411	133.873	25957.803	0.45
Ruff_82-26	**307.848**	1981.2	4876.8	809861.8125	25.50	**18.174**	12.072	77.694	191.247	48841.656	0.45
Ruff_82-27	**341.376**	2785.872	4572	824020.2358	25.50	**22.768**	13.387	109.250	179.294	49695.531	0.45
Ruff_82-28	**335.28**	1563.624	2264.664	401532.8847	45.67	**13.473**	7.342	34.239	49.590	4215.919	0
Ruff_82-29	**454.152**	2865.12	3145.536	1285301.667	65.44	**11.559**	6.940	43.780	48.065	4585.628	0
Ruff_82-30	**667.512**	3227.832	5632.704	4585630.137	63.50	**18.487**	10.512	50.832	88.704	17909.268	0
Ruff_82-31	**777.24**	3514.344	6940.296	7336611.784	63.50	**24.639**	12.240	55.344	109.296	28653.281	0
Ruff_82-32	**335.28**	1563.624	2264.664	401532.8847	45.67	**13.473**	7.342	34.239	49.590	4215.919	0.25
Ruff_82-33	**454.152**	2865.12	3145.536	1285301.667	65.44	**11.559**	6.940	43.780	48.065	4585.628	0.25
Ruff_82-34	**667.512**	3227.832	5632.704	4585630.137	63.50	**18.487**	10.512	50.832	88.704	17909.268	0.25
Ruff_82-35	**777.24**	3514.344	6940.296	7336611.784	63.50	**24.639**	12.240	55.344	109.296	28653.281	0.25
Ruff_82-36	**426.72**	1493.52	5791.2	3179415.535	65.44	**11.559**	6.520	22.821	88.491	11343.342	0.45
Ruff_82-37	**457.2**	1920.24	5791.2	#VALUE!	63.50	**12.174**	7.200	30.240	91.200	#VALUE!	0.45
Ruff_82-38	**429.768**	1676.4	5486.4	2963924.333	63.50	**12.174**	6.768	26.400	86.400	11575.665	0.45
Ruff_82-39	**582.168**	2194.56	7315.2	6403854.857	63.50	**18.262**	9.168	34.560	115.200	25010.381	0.45
Ruff_82-40	**655.32**	2987.04	8534.4	7256191.939	63.50	**24.349**	10.320	47.040	134.400	28339.200	0.45
Ruff_82-41	**734.568**	3535.68	10058.4	15575398.3	63.50	**30.436**	11.568	55.680	158.400	60830.024	0.45

Ruff, J. F., Abt, S. R., Mendoza, C., Shaikh, A., and Kloberdanz, R. (1982). *Scour at Culvert Outlets in Mixed Bed Materials*, FHWA.

Database #	Original Run #	Duration	F/NF	W	Shape	do	b	slope	ho	Q	Uo	H	d50	sigma_g
		hr		mm		mm	mm		mm	L/s	m/s	mm	mm	
Ruff_82-42	**E1**	1000	NF	6100	**circular**	**356**	-	-	-	109.020	2.323	**160.2**	**1.86**	**1.33**
Ruff_82-43	**E2**	1000	F	6100	**circular**	**356**	-	-	-	218.039	2.191	**160.2**	**1.86**	**1.33**
Ruff_82-44	**E3**	1000	F	6100	**circular**	**356**	-	-	-	327.059	3.286	**160.2**	**1.86**	**1.33**
Ruff_82-45	**E4**	1000	F	6100	**circular**	**356**	-	-	-	436.079	4.381	**160.2**	**1.86**	**1.33**
Ruff_82-46	**E5**	1000	F	6100	**circular**	**356**	-	-	-	545.382	5.479	**160.2**	**1.86**	**1.33**
Ruff_82-47	**F1**	1000	NF	6100	**circular**	**457**	-	-	-	206.996	2.673	**205.65**	**1.86**	**1.33**
Ruff_82-48	**F2**	1000	F	6100	**circular**	**457**	-	-	-	413.992	2.524	**205.65**	**1.86**	**1.33**
Ruff_82-49	**F3**	1000	F	6100	**circular**	**457**	-	-	-	620.421	3.782	**205.65**	**1.86**	**1.33**
Ruff_82-50	**F4**	1000	F	6100	**circular**	**457**	-	-	-	827.700	5.046	**205.65**	**1.86**	**1.33**
Ruff_82-54	**K1**	316	NF	1200	**circular**	**102**	-	-	-	3.115	1.119	**45.9**	**2**	**4.38**
Ruff_82-55	**K2**	316	NF	1200	**circular**	**102**	-	-	-	5.097	1.247	**45.9**	**2**	**4.38**
Ruff_82-56	**K3**	316	NF	1200	**circular**	**102**	-	-	-	4.248	1.271	**45.9**	**2**	**4.38**
Ruff_82-57	**K4**	316	F	1200	**circular**	**102**	-	-	-	10.194	1.248	**45.9**	**2**	**4.38**
Ruff_82-60	**M1**	316	NF	6100	**circular**	**254**	-	-	-	54.085	2.006	**63.5**	**7.62**	**1.32**
Ruff_82-61	**M2**	316	F	6100	**circular**	**254**	-	-	-	162.538	3.208	**63.5**	**7.62**	**1.32**
Ruff_82-62	**M3**	316	F	6100	**circular**	**254**	-	-	-	216.624	4.275	**63.5**	**7.62**	**1.32**
Ruff_82-63	**N1**	316	NF	6100	**circular**	**254**	-	-	-	54.085	2.006	**114.3**	**7.62**	**1.32**
Ruff_82-64	**N2**	316	F	6100	**circular**	**254**	-	-	-	108.453	2.140	**114.3**	**7.62**	**1.32**
Ruff_82-65	**N3**	316	F	6100	**circular**	**254**	-	-	-	162.538	3.208	**114.3**	**7.62**	**1.32**
Ruff_82-66	**N4**	316	F	6100	**circular**	**254**	-	-	-	216.624	4.275	**114.3**	**7.62**	**1.32**
Ruff_82-67	**L1**	316	NF	6100	**circular**	**254**	-	-	-	54.085	2.006	**0**	**7.62**	**1.32**
Ruff_82-68	**L2**	316	F	6100	**circular**	**254**	-	-	-	162.538	3.208	**0**	**7.62**	**1.32**
Ruff_82-69	**L3**	316	F	6100	**circular**	**254**	-	-	-	216.624	4.275	**0**	**7.62**	**1.32**
Ruff_82-70	**O1**	316	NF	6100	**circular**	**254**	-	-	-	54.085	2.006	**114.3**	**7.34**	**4.78**
Ruff_82-71	**O2**	316	F	6100	**circular**	**254**	-	-	-	108.453	2.140	**114.3**	**7.34**	**4.78**
Ruff_82-72	**O3**	316	F	6100	**circular**	**254**	-	-	-	162.538	3.208	**114.3**	**7.34**	**4.78**
Ruff_82-73	**O4**	316	F	6100	**circular**	**254**	-	-	-	216.624	4.275	**114.3**	**7.34**	**4.78**

Ruff, J. F., Abt, S. R., Mendoza, C., Shaikh, A., and Kloberdanz, R. (1982). *Scour at Culvert Outlets in Mixed Bed Materials*, FHWA.

Database #	**dse**	Wse	Lse	Vse	Rh	**Fo**	dse/Rh	Wse/Rh	Lse/Rh	Vse/Rh3	H/do
	mm	mm	mm	ml	mm						
Ruff_82-42	**576.072**	2346.96	6705.6	6788963.97	85.92	**13.386**	6.705	27.315	78.042	10702.333	0.45
Ruff_82-43	**633.984**	2255.52	6705.6	4887770.89	89.00	**12.624**	7.123	25.343	75.344	6933.313	0.45
Ruff_82-44	**810.768**	3657.6	8229.6	9720890.267	89.00	**18.937**	9.110	41.097	92.467	13789.103	0.45
Ruff_82-45	**1030.224**	4114.8	9448.8	17995922.35	89.00	**25.249**	11.576	46.234	106.166	25527.253	0.45
Ruff_82-46	**1069.848**	-	10668	20419561.25	89.00	**31.577**	12.021	-	119.865	28965.190	0.45
Ruff_82-47	**551.688**	2130.552	6858	4018443.7	110.72	**15.406**	4.983	19.242	61.938	2960.271	0.45
Ruff_82-48	**853.44**	3538.728	7315.2	7267518.678	114.25	**14.546**	7.470	30.974	64.028	4873.237	0.45
Ruff_82-49	**1191.768**	3745.992	9753.6	20299780.98	114.25	**21.799**	10.431	32.788	85.371	13612.025	0.45
Ruff_82-50	**1240.536**	3934.968	11582.4	27152457.86	114.25	**29.082**	10.858	34.442	101.378	18207.089	0.45
Ruff_82-54	**45.72**	295.656	822.96	2831.684659	20.76	**6.217**	2.202	14.238	39.632	316.264	0.45
Ruff_82-55	**70.104**	429.768	1066.8	8495.053978	25.51	**6.929**	2.748	16.849	41.825	511.943	0.45
Ruff_82-56	**57.912**	691.896	1158.24	7362.380114	22.62	**7.064**	2.560	30.588	51.205	636.160	0.45
Ruff_82-57	**115.824**	905.256	1097.28	26334.66733	25.50	**6.934**	4.542	35.500	43.031	1588.208	0.45
Ruff_82-60	**240.792**	1405.128	2218.944	200766.4423	65.44	**5.711**	3.679	21.471	33.906	716.283	0.25
Ruff_82-61	**563.88**	3721.608	4779.264	2318583.399	63.50	**9.134**	8.880	58.608	75.264	9055.273	0.25
Ruff_82-62	**661.416**	3776.472	5998.464	4391659.738	63.50	**12.173**	10.416	59.472	94.464	17151.713	0.25
Ruff_82-63	**350.52**	1536.192	2770.632	346881.3708	65.44	**5.711**	5.356	23.473	42.336	1237.584	0.45
Ruff_82-64	**454.152**	2420.112	3154.68	1031016.384	63.50	**6.094**	7.152	38.112	49.680	4026.655	0.45
Ruff_82-65	**560.832**	2983.992	5967.984	2438929.997	63.50	**9.134**	8.832	46.992	93.984	9525.289	0.45
Ruff_82-66	**655.32**	3691.128	7205.472	4651891.558	63.50	**12.173**	10.320	58.128	113.472	18168.054	0.45
Ruff_82-67	**320.04**	1691.64	1627.632	276938.7597	65.44	**5.711**	4.890	25.849	24.871	988.047	0
Ruff_82-68	**576.072**	3358.896	4392.168	2387959.673	63.50	**9.134**	9.072	52.896	69.168	9326.223	0
Ruff_82-69	**691.896**	3852.672	5952.744	4728347.044	63.50	**12.173**	10.896	60.672	93.744	18466.652	0
Ruff_82-70	**277.368**	1164.336	2834.64	165370.3841	65.44	**5.819**	4.238	17.791	43.314	589.999	0.45
Ruff_82-71	**377.952**	2319.528	2532.888	626085.4781	63.50	**6.210**	5.952	36.528	39.888	2445.189	0.45
Ruff_82-72	**469.392**	3721.608	4541.52	1841161.365	63.50	**9.306**	7.392	58.608	71.520	7190.692	0.45
Ruff_82-73	**569.976**	3721.608	5660.136	3958128.817	63.50	**12.403**	8.976	58.608	89.136	15458.550	0.45

Abt, S., Ruff, J., Doehring, F., and Donnell, C. (1987). "Influence of Culvert Shape on Outlet Scour." *Journal of Hydraulic Engineering*, 113(3), 393-400.

Database #	Original Run #	Duration	F/NF	W	Shape	do	b	slope	ho	Q	Uo	H	d50	sigma_g
		hr		mm		mm	mm		mm	L/s	m/s	mm	mm	
Abt_87-01	-	-	(F)	6100	**Square**	**100**	-	-	-	-	-	-	**1.86**	**1.33**
Abt_87-02	-	-	(F)	6100	**Square**	**100**	-	-	-	-	-	-	**1.86**	**1.33**
Abt_87-03	-	-	(F)	6100	**Square**	**100**	-	-	-	-	-	-	**1.86**	**1.33**
Abt_87-04	-	-	(F)	6100	**Square**	**100**	-	-	-	-	-	-	**1.86**	**1.33**
Abt_87-05	-	-	(F)	6100	**Rectangular**	**100**	**160**	-	-	-	-	-	**1.86**	**1.33**
Abt_87-06	-	-	(F)	6100	**Rectangular**	**100**	**160**	-	-	-	-	-	**1.86**	**1.33**
Abt_87-07	-	-	(F)	6100	**Rectangular**	**100**	**160**	-	-	-	-	-	**1.86**	**1.33**
Abt_87-08	-	-	(F)	6100	**Rectangular**	**100**	**160**	-	-	-	-	-	**1.86**	**1.33**
Abt_87-09	-	-	(F)	6100	**Rectangular**	**100**	**160**	-	-	-	-	-	**1.86**	**1.33**
Abt_87-10	-	-	(F)	6100	**Rectangular**	**100**	**160**	-	-	-	-	-	**1.86**	**1.33**
Abt_87-11	-	-	(F)	6100	**Rectangular**	**100**	**200**	-	-	-	-	-	**1.86**	**1.33**
Abt_87-12	-	-	(F)	6100	**Rectangular**	**100**	**200**	-	-	-	-	-	**1.86**	**1.33**
Abt_87-13	-	-	(F)	6100	**Rectangular**	**100**	**200**	-	-	-	-	-	**1.86**	**1.33**
Abt_87-14	-	-	(F)	6100	**Rectangular**	**100**	**200**	-	-	-	-	-	**1.86**	**1.33**
Abt_87-15	-	-	(F)	6100	**Arch**	**100**	**150**	-	-	-	-	-	**1.86**	**1.33**
Abt_87-16	-	-	(F)	6100	**Arch**	**100**	**150**	-	-	-	-	-	**1.86**	**1.33**
Abt_87-17	-	-	(F)	6100	**Arch**	**100**	**150**	-	-	-	-	-	**1.86**	**1.33**
Abt_87-18	-	-	(F)	6100	**Arch**	**100**	**150**	-	-	-	-	-	**1.86**	**1.33**
Abt_87-19	-	-	(F)	6100	**Arch**	**100**	**150**	-	-	-	-	-	**1.86**	**1.33**

Ali, K. H. M., and Lim, S. Y. (1986). "Local Scour Caused by Submerged Wall Jets." *ICE Proceedings*, 607-645.

Database #	Original Run #	Duration	F/NF	W	Shape	do	b	slope	ho	Q	Uo	H	d50	sigma_g
		hr		mm		mm	mm		mm	L/s	m/s	mm	mm	
AliL_86-01	**LS1**	-	(F)	-	**Square**	**50.8**	-	-	-	-	0.323	**50.8**	**0.82**	**1.13**
AliL_86-02	**LS2**	-	(F)	-	**Square**	**50.8**	-	-	-	-	0.504	**50.8**	**0.82**	**1.13**
AliL_86-03	**LS3**	-	(F)	-	**Square**	**50.8**	-	-	-	-	0.507	**50.8**	**0.82**	**1.13**
AliL_86-04	**LS4**	-	(F)	-	**Square**	**50.8**	-	-	-	-	0.603	**50.8**	**0.82**	**1.13**
AliL_86-05	**LS5**	-	(F)	-	**Square**	**50.8**	-	-	-	-	0.673	**50.8**	**0.82**	**1.13**
AliL_86-06	**LS6**	-	(F)	-	**Square**	**50.8**	-	-	-	-	0.947	**50.8**	**0.82**	**1.13**
AliL_86-07	**LS7**	-	(F)	-	**Square**	**50.8**	-	-	-	-	0.112	**50.8**	**0.82**	**1.13**

Abt, S., Ruff, J., Doehring, F., and Donnell, C. (1987). "Influence of Culvert Shape on Outlet Scour." *Journal of Hydraulic Engineering*, 113(3), 393-400.

Database #	**dse**	Wse	Lse	Vse	Rh	**Fo**	dse/Rh	Wse/Rh	Lse/Rh	Vse/Rh3
	mm	mm	mm	ml	mm					
Abt_87-01	-	-	-	-	25.00	**7.200**	11.594	-	-	-
Abt_87-02	-	-	-	-	25.00	**8.670**	10.584	-	-	-
Abt_87-03	-	-	-	-	25.00	**11.460**	12.242	-	-	-
Abt_87-04	-	-	-	-	25.00	**17.180**	12.864	-	-	-
Abt_87-05	-	-	-	-	30.00	**7.830**	10.416	-	-	-
Abt_87-06	-	-	-	-	30.00	**9.440**	10.267	-	-	-
Abt_87-07	-	-	-	-	30.00	**12.490**	10.218	-	-	-
Abt_87-08	-	-	-	-	30.00	**15.590**	11.373	-	-	-
Abt_87-09	-	-	-	-	30.00	**17.720**	13.431	-	-	-
Abt_87-10	-	-	-	-	30.00	**21.810**	12.884	-	-	-
Abt_87-11	-	-	-	-	34.00	**8.060**	10.373	-	-	-
Abt_87-12	-	-	-	-	34.00	**9.850**	10.831	-	-	-
Abt_87-13	-	-	-	-	34.00	**11.520**	11.310	-	-	-
Abt_87-14	-	-	-	-	34.00	**12.600**	10.677	-	-	-
Abt_87-15	-	-	-	-	31.00	**7.630**	9.258	-	-	-
Abt_87-16	-	-	-	-	31.00	**9.580**	9.968	-	-	-
Abt_87-17	-	-	-	-	31.00	**11.950**	10.714	-	-	-
Abt_87-18	-	-	-	-	31.00	**15.060**	11.315	-	-	-
Abt_87-19	-	-	-	-	31.00	**17.800**	12.339	-	-	-

Ali, K. H. M., and Lim, S. Y. (1986). "Local Scour Caused by Submerged Wall Jets." *ICE Proceedings*, 607-645.

Database #	**dse**	Wse	Lse	Vse	Rh	**Fo**	dse/Rh	Wse/Rh	Lse/Rh	Vse/Rh3
	mm	mm	mm	ml	mm					
AliL_86-01	-	-	-	-	12.70	**2.795**	1.652	-	-	-
AliL_86-02	-	-	-	-	12.70	**4.359**	3.936	-	-	-
AliL_86-03	-	-	-	-	12.70	**4.386**	4.056	-	-	-
AliL_86-04	-	-	-	-	12.70	**5.219**	5.984	-	-	-
AliL_86-05	-	-	-	-	12.70	**5.827**	6.852	-	-	-
AliL_86-06	-	-	-	-	12.70	**8.196**	7.364	-	-	-
AliL_86-07	-	-	-	-	12.70	**9.672**	7.400	-	-	-

Liriano, S. L. (1999). "The influence of near bed turbulent flow structures on scour hole development at pipe culvert outlets." Thesis (Ph.D.), University of Herfordshire.

Database #	Original Run #	Duration	F/NF	W	Shape	do	b	slope	ho	Q	Uo	H	d50	sigma_g
		hr		mm		mm	mm		mm	L/s	m/s	mm	mm	
Liriano_99-01	1	-	F	96.2	Circular	13	-	-	-	-	-	6.5	0.38	1.4
Liriano_99-02	2	-	F	148	Circular	20	-	-	-	-	-	10	0.59	1.4
Liriano_99-03	3	-	F	309.92	Circular	52	-	-	-	-	-	26	1.4	1.4
Liriano_99-04	4	-	F	1080.4	Circular	146	-	-	-	-	-	73	4.4	1.4
Liriano_99-05	5	-	F	2301.4	Circular	311	-	-	-	-	-	155.5	9	1.4
Liriano_99-06	6	-	F	96.2	Circular	13	-	-	-	-	-	13	0.38	1.4
Liriano_99-07	7	-	F	148	Circular	20	-	-	-	-	-	20	0.59	1.4
Liriano_99-08	8	-	F	1080.4	Circular	146	-	-	-	-	-	146	4.4	1.4
Liriano_99-09	9	-	F	2301.4	Circular	311	-	-	-	-	-	311	9	1.4
Liriano_99-10	10	-	F	96.2	Circular	13	-	-	-	-	-	19.5	0.38	1.4
Liriano_99-11	11	-	F	148	Circular	20	-	-	-	-	-	30	0.59	1.4
Liriano_99-12	12	-	F	309.92	Circular	52	-	-	-	-	-	78	1.4	1.4
Liriano_99-13	13	-	F	1080.4	Circular	146	-	-	-	-	-	219	4.4	1.4
Liriano_99-14	14	-	F	2301.4	Circular	311	-	-	-	-	-	466.5	9	1.4
Liriano_99-15	15	-	F	96.2	Circular	13	-	-	-	-	-	26	0.38	1.4
Liriano_99-16	16	-	F	148	Circular	20	-	-	-	-	-	40	0.59	1.4
Liriano_99-17	17	-	F	1080.4	Circular	146	-	-	-	-	-	292	4.4	1.4
Liriano_99-18	18	-	F	96.2	Circular	13	-	-	-	-	-	6.5	0.38	1.4
Liriano_99-19	19	-	F	148	Circular	20	-	-	-	-	-	10	0.59	1.4
Liriano_99-20	20	-	F	309.92	Circular	52	-	-	-	-	-	26	1.4	1.4
Liriano_99-21	21	-	F	1080.4	Circular	146	-	-	-	-	-	73	4.4	1.4
Liriano_99-22	22	-	F	2301.4	Circular	311	-	-	-	-	-	155.5	9	1.4
Liriano_99-23	23	-	F	96.2	Circular	13	-	-	-	-	-	19.5	0.38	1.4
Liriano_99-24	24	-	F	148	Circular	20	-	-	-	-	-	30	0.59	1.4
Liriano_99-25	25	-	F	309.92	Circular	52	-	-	-	-	-	78	1.4	1.4
Liriano_99-26	26	-	F	1080.4	Circular	146	-	-	-	-	-	219	4.4	1.4
Liriano_99-27	27	-	F	2301.4	Circular	311	-	-	-	-	-	466.5	9	1.4
Liriano_99-28	28	-	F	96.2	Circular	13	-	-	-	-	-	26	0.38	1.4
Liriano_99-29	29	-	F	148	Circular	20	-	-	-	-	-	40	0.59	1.4
Liriano_99-30	30	-	F	1080.4	Circular	146	-	-	-	-	-	292	4.4	1.4

Liriano, S. L. (1999). "The influence of near bed turbulent flow structures on scour hole development at pipe culvert outlets." Thesis (Ph.D.), University of Herfordshire.

Database #	**dse**	Wse	Lse	Vse	Rh	**Fo**	dse/Rh	Wse/Rh	Lse/Rh	Vse/Rh3	H/do
	mm	mm	mm	ml	mm						
Liriano_99-01	**-**	-	-	-	3.25	**3.4**	3	-	34	-	0.5
Liriano_99-02	**-**	-	-	-	5	**3.4**	2.8	-	26	-	0.5
Liriano_99-03	**-**	-	-	-	13	**3.4**	3.8	-	39	-	0.5
Liriano_99-04	**-**	-	-	-	36.5	**3.4**	5	-	45	-	0.5
Liriano_99-05	**-**	-	-	-	77.75	**3.4**	4.4	-	50	-	0.5
Liriano_99-06	**-**	-	-	-	3.25	**3.4**	4	-	34	-	1
Liriano_99-07	**-**	-	-	-	5	**3.4**	3.2	-	36	-	1
Liriano_99-08	**-**	-	-	-	36.5	**3.4**	3.4	-	32	-	1
Liriano_99-09	**-**	-	-	-	77.75	**3.4**	3.2	-	32	-	1
Liriano_99-10	**-**	-	-	-	3.25	**3.4**	2.2	-	30	-	1.5
Liriano_99-11	**-**	-	-	-	5	**3.4**	2.4	-	30	-	1.5
Liriano_99-12	**-**	-	-	-	13	**3.4**	2.6	-	30	-	1.5
Liriano_99-13	**-**	-	-	-	36.5	**3.4**	2.2	-	32	-	1.5
Liriano_99-14	**-**	-	-	-	77.75	**3.4**	2.2	-	30	-	1.5
Liriano_99-15	**-**	-	-	-	3.25	**3.4**	2.4	-	38	-	2
Liriano_99-16	**-**	-	-	-	5	**3.4**	2.4	-	32	-	2
Liriano_99-17	**-**	-	-	-	36.5	**3.4**	2.8	-	36	-	2
Liriano_99-18	**-**	-	-	-	3.25	**4.5**	4.4	-	30	-	0.5
Liriano_99-19	**-**	-	-	-	5	**4.5**	4	-	38	-	0.5
Liriano_99-20	**-**	-	-	-	13	**4.5**	5.6	-	54	-	0.5
Liriano_99-21	**-**	-	-	-	36.5	**4.5**	4.8	-	52	-	0.5
Liriano_99-22	**-**	-	-	-	77.75	**4.5**	4.8	-	50	-	0.5
Liriano_99-23	**-**	-	-	-	3.25	**4.5**	4	-	34	-	1.5
Liriano_99-24	**-**	-	-	-	5	**4.5**	4.4	-	38	-	1.5
Liriano_99-25	**-**	-	-	-	13	**4.5**	4	-	34	-	1.5
Liriano_99-26	**-**	-	-	-	36.5	**4.5**	4.4	-	36	-	1.5
Liriano_99-27	**-**	-	-	-	77.75	**4.5**	4	-	36	-	1.5
Liriano_99-28	**-**	-	-	-	3.25	**4.5**	3	-	38	-	2
Liriano_99-29	**-**	-	-	-	5	**4.5**	4	-	40	-	2
Liriano_99-30	**-**	-	-	-	36.5	**4.5**	3.8	-	38	-	2

Liriano, S. L. (1999). "The influence of near bed turbulent flow structures on scour hole development at pipe culvert outlets." Thesis (Ph.D.), University of Herfordshire.

Database #	Original Run #	Duration	F/NF	W	Shape	do	b	slope	ho	Q	Uo	H	d50	sigma_g
		hr		mm		mm	mm		mm	L/s	m/s	mm	mm	
Liriano_99-31	31	-	F	96.2	Circular	13	-	-	-	-	-	6.5	0.38	1.4
Liriano_99-32	32	-	F	148	Circular	20	-	-	-	-	-	10	0.59	1.4
Liriano_99-33	33	-	F	1080.4	Circular	146	-	-	-	-	-	73	4.4	1.4
Liriano_99-34	34	-	F	2301.4	Circular	311	-	-	-	-	-	155.5	9	1.4
Liriano_99-35	35	-	F	96.2	Circular	13	-	-	-	-	-	13	0.38	1.4
Liriano_99-36	36	-	F	148	Circular	20	-	-	-	-	-	20	0.59	1.4
Liriano_99-37	37	-	F	1080.4	Circular	146	-	-	-	-	-	146	4.4	1.4
Liriano_99-38	38	-	F	96.2	Circular	13	-	-	-	-	-	19.5	0.38	1.4
Liriano_99-39	39	-	F	148	Circular	20	-	-	-	-	-	30	0.59	1.4
Liriano_99-40	40	-	F	1080.4	Circular	146	-	-	-	-	-	219	4.4	1.4
Liriano_99-41	41	-	F	2301.4	Circular	311	-	-	-	-	-	466.5	9	1.4
Liriano_99-42	42	-	F	96.2	Circular	13	-	-	-	-	-	26	0.38	1.4
Liriano_99-43	43	-	F	148	Circular	20	-	-	-	-	-	40	0.59	1.4
Liriano_99-44	44	-	F	1080.4	Circular	146	-	-	-	-	-	292	4.4	1.4
Liriano_99-45	45	-	F	96.2	Circular	13	-	-	-	-	-	13	0.38	1.4
Liriano_99-46	46	-	F	148	Circular	20	-	-	-	-	-	20	0.59	1.4
Liriano_99-47	47	-	F	1080.4	Circular	146	-	-	-	-	-	146	4.4	1.4
Liriano_99-48	48	-	F	148	Circular	20	-	-	-	-	-	30	0.59	1.4
Liriano_99-49	49	-	F	1080.4	Circular	146	-	-	-	-	-	219	4.4	1.4

Liriano, S. L. (1999). "The influence of near bed turbulent flow structures on scour hole development at pipe culvert outlets." Thesis (Ph.D.), University of Herfordshire.

Database #	**dse**	Wse	Lse	Vse	Rh	**Fo**	dse/Rh	Wse/Rh	Lse/Rh	Vse/Rh3	H/do
	mm	mm	mm	ml	mm						
Liriano_99-31	**-**	-	-	-	3.25	**6.8**	4	-	40	-	0.5
Liriano_99-32	**-**	-	-	-	5	**6.8**	5	-	66	-	0.5
Liriano_99-33	**-**	-	-	-	36.5	**6.8**	5.4	-	70	-	0.5
Liriano_99-34	**-**	-	-	-	77.75	**6.8**	6	-	66	-	0.5
Liriano_99-35	**-**	-	-	-	3.25	**6.8**	4.4	-	50	-	1
Liriano_99-36	**-**	-	-	-	5	**6.8**	5.2	-	58	-	1
Liriano_99-37	**-**	-	-	-	36.5	**6.8**	5.6	-	64	-	1
Liriano_99-38	**-**	-	-	-	3.25	**6.8**	4.6	-	42	-	1.5
Liriano_99-39	**-**	-	-	-	5	**6.8**	5.2	-	52	-	1.5
Liriano_99-40	**-**	-	-	-	36.5	**6.8**	4.6	-	52	-	1.5
Liriano_99-41	**-**	-	-	-	77.75	**6.8**	4.4	-	42	-	1.5
Liriano_99-42	**-**	-	-	-	3.25	**6.8**	4.8	-	48	-	2
Liriano_99-43	**-**	-	-	-	5	**6.8**	4.2	-	52	-	2
Liriano_99-44	**-**	-	-	-	36.5	**6.8**	4.6	-	52	-	2
Liriano_99-45	**-**	-	-	-	3.25	**9.0**	5.8	-	68	-	1
Liriano_99-46	**-**	-	-	-	5	**9.0**	7.6	-	72	-	1
Liriano_99-47	**-**	-	-	-	36.5	**9.0**	6.4	-	70	-	1
Liriano_99-48	**-**	-	-	-	5	**9.0**	5.8	-	62	-	1.5
Liriano_99-49	**-**	-	-	-	36.5	**9.0**	5.3	-	62	-	1.5

Faruque, M., Sarathi, P., and Balachandar, R. (2006). "Clear Water Local Scour by Submerged Three-Dimensional Wall Jets: Effect of Tailwater Depth." *Journal of Hydraulic Engineering*, 132(6), 575-580.

Database #	**Original Run #**	Duration hr	F/NF	W mm	**Shape**	**do mm**	**b mm**	**slope**	**ho mm**	Q L/s	Uo m/s	**H mm**	**d50 mm**	**sigma_g**
Faruque_06-01	**A**	72	F	1100	**Square**	-	**76**	-	-	-	1.310	**456**	**2.46**	**1.24**
Faruque_06-02	**B**	72	F	1100	**Square**	-	**76**	-	-	-	1.310	**304**	**2.46**	**1.24**
Faruque_06-03	**D**	24	F	1100	**Square**	-	**26.6**	-	-	-	1.310	**53.2**	**2.46**	**1.24**
Faruque_06-04	**E**	6	F	1100	**Square**	-	**26.6**	-	-	-	0.780	**53.2**	**2.46**	**1.24**
Faruque_06-05	**F**	24	F	1100	**Square**	-	**26.6**	-	-	-	1.310	**106.4**	**2.46**	**1.24**
Faruque_06-06	**G**	6	F	1100	**Square**	-	**26.6**	-	-	-	0.780	**106.4**	**2.46**	**1.24**
Faruque_06-07	**H**	24	F	1100	**Square**	-	**26.6**	-	-	-	1.310	**159.6**	**2.46**	**1.24**
Faruque_06-08	**I**	6	F	1100	**Square**	-	**26.6**	-	-	-	0.780	**159.6**	**2.46**	**1.24**
Faruque_06-09	**J**	3	F	1100	**Square**	-	**76**	-	-	-	0.870	**119.32**	**2.46**	**1.24**

Sarathi, P., Faruque, M. A. A., and Balachandar, R. (2008). "Influence of tailwater depth, sediment size and densimetric Froude number on scour by submerged square wall jets." *Journal of Hydraulic Research*, 46(2), 158-175.

Database #	**Original Run #**	Duration hr	F/NF	W mm	**Shape**	**do mm**	**b mm**	**slope**	**ho mm**	Q L/s	Uo m/s	**H mm**	**d50 mm**	**sigma_g**
Sarathi_08-01	**101**	24	F	1100	**Square**	-	**26.6**	-	-	-	0.780	**26.6**	**2.46**	**1.24**
Sarathi_08-02	**102**	24	F	1100	**Square**	-	**26.6**	-	-	-	0.780	**53.2**	**2.46**	**1.24**
Sarathi_08-03	**103**	24	F	1100	**Square**	-	**26.6**	-	-	-	0.780	**79.8**	**2.46**	**1.24**
Sarathi_08-04	**104**	24	F	1100	**Square**	-	**26.6**	-	-	-	0.780	**106.4**	**2.46**	**1.24**
Sarathi_08-05	**106**	24	F	1100	**Square**	-	**26.6**	-	-	-	0.780	**159.6**	**2.46**	**1.24**
Sarathi_08-06	**112**	24	F	1100	**Square**	-	**26.6**	-	-	-	0.780	**319.2**	**2.46**	**1.24**
Sarathi_08-07	**115**	24	F	1100	**Square**	-	**26.6**	-	-	-	0.780	**399**	**2.46**	**1.24**
Sarathi_08-08	**118**	24	F	1100	**Square**	-	**26.6**	-	-	-	0.780	**478.8**	**2.46**	**1.24**

Faruque, M., Sarathi, P., and Balachandar, R. (2006). "Clear Water Local Scour by Submerged Three-Dimensional Wall Jets: Effect of Tailwater Depth." *Journal of Hydraulic Engineering*, 132(6), 575-580.

Database #	**dse**	Wse	Lse	Vse	Rh	**Fo**	dse/Rh	Wse/Rh	Lse/Rh	Vse/Rh3	H/do
	mm	mm	mm	ml	mm						
Faruque_06-01	**135.77**	680	1325	42000	19.00	**6.600**	7.146	35.789	69.737	6123.342	6
Faruque_06-02	**140.86**	580	1285	43000	19.00	**6.600**	7.414	30.526	67.632	6269.135	4
Faruque_06-03	**68.74**	247	575	-	6.65	**6.600**	10.337	37.143	86.466	-	2
Faruque_06-04	**29.21**	124	288	-	6.65	**3.900**	4.392	18.647	43.308	-	2
Faruque_06-05	**55.85**	250	555	-	6.65	**6.600**	8.398	37.594	83.459	-	4
Faruque_06-06	**32.41**	147	345	-	6.65	**3.900**	4.874	22.105	51.880	-	4
Faruque_06-07	**56.06**	234	535	-	6.65	**6.600**	8.430	35.188	80.451	-	6
Faruque_06-08	**31.77**	137	365	-	6.65	**3.900**	4.777	20.602	54.887	-	6
Faruque_06-09	**82.95**	370	710	-	19.00	**4.400**	4.366	19.474	37.368	-	1.57

Sarathi, P., Faruque, M. A. A., and Balachandar, R. (2008). "Influence of tailwater depth, sediment size and densimetric Froude number on scour by submerged square wall jets." *Journal of Hydraulic Research*, 46(2), 158-175.

Database #	**dse**	Wse	Lse	Vse	Rh	**Fo**	dse/Rh	Wse/Rh	Lse/Rh	Vse/Rh3	H/do
	mm	mm	mm	ml	mm						
Sarathi_08-01	**45.5**	194	385	980	6.65	**3.900**	6.842	29.173	57.895	3332.431	1
Sarathi_08-02	**29.7**	135	288	340	6.65	**3.900**	4.466	20.301	43.308	1156.149	2
Sarathi_08-03	**27.8**	140	330	400	6.65	**3.900**	4.180	21.053	49.624	1360.176	3
Sarathi_08-04	**31.3**	154	355	490	6.65	**3.900**	4.707	23.158	53.383	1666.215	4
Sarathi_08-05	**30.1**	145	370	490	6.65	**3.900**	4.526	21.805	55.639	1666.215	6
Sarathi_08-06	**29.3**	132	370	560	6.65	**3.900**	4.406	19.850	55.639	1904.246	12
Sarathi_08-07	**28.4**	127	376	390	6.65	**3.900**	4.271	19.098	56.541	1326.171	15
Sarathi_08-08	**27.5**	128	371	325	6.65	**3.900**	4.135	19.248	55.789	1105.143	18

Sarathi, P., Faruque, M. A. A., and Balachandar, R. (2008). "Influence of tailwater depth, sediment size and densimetric Froude number on scour by submerged square wall jets." *Journal of Hydraulic Research*, 46(2), 158-175.

Database #	**Original Run #**	Duration hr	F/NF	W mm	**Shape**	**do mm**	**b mm**	**slope**	**ho mm**	Q L/s	Uo m/s	**H mm**	**d50 mm**	**sigma_g**
Sarathi_08-09	**201**	24	F	1100	**Square**	-	**26.6**	-	-	-	1.310	**26.6**	**2.46**	**1.24**
Sarathi_08-10	**202**	24	F	1100	**Square**	-	**26.6**	-	-	-	1.310	**53.2**	**2.46**	**1.24**
Sarathi_08-11	**203**	24	F	1100	**Square**	-	**26.6**	-	-	-	1.310	**79.8**	**2.46**	**1.24**
Sarathi_08-12	**204**	24	F	1100	**Square**	-	**26.6**	-	-	-	1.310	**106.4**	**2.46**	**1.24**
Sarathi_08-13	**206**	24	F	1100	**Square**	-	**26.6**	-	-	-	1.310	**159.6**	**2.46**	**1.24**
Sarathi_08-14	**212**	24	F	1100	**Square**	-	**26.6**	-	-	-	1.310	**319.2**	**2.46**	**1.24**
Sarathi_08-15	**215**	24	F	1100	**Square**	-	**26.6**	-	-	-	1.310	**399**	**2.46**	**1.24**
Sarathi_08-16	**218**	24	F	1100	**Square**	-	**26.6**	-	-	-	1.310	**478.8**	**2.46**	**1.24**
Sarathi_08-17	**301**	24	F	1100	**Square**	-	**26.6**	-	-	-	2.000	**26.6**	**2.46**	**1.24**
Sarathi_08-18	**302**	24	F	1100	**Square**	-	**26.6**	-	-	-	2.000	**53.2**	**2.46**	**1.24**
Sarathi_08-19	**303**	24	F	1100	**Square**	-	**26.6**	-	-	-	2.000	**79.8**	**2.46**	**1.24**
Sarathi_08-20	**304**	24	F	1100	**Square**	-	**26.6**	-	-	-	2.000	**106.4**	**2.46**	**1.24**
Sarathi_08-21	**306**	24	F	1100	**Square**	-	**26.6**	-	-	-	2.000	**159.6**	**2.46**	**1.24**
Sarathi_08-22	**312**	24	F	1100	**Square**	-	**26.6**	-	-	-	2.000	**319.2**	**2.46**	**1.24**
Sarathi_08-23	**315**	24	F	1100	**Square**	-	**26.6**	-	-	-	2.000	**399**	**2.46**	**1.24**
Sarathi_08-24	**318**	24	F	1100	**Square**	-	**26.6**	-	-	-	2.000	**478.8**	**2.46**	**1.24**
Sarathi_08-25	**402**	96	F	1100	**Square**	-	**26.6**	-	-	-	1.080	**53.2**	**0.71**	**1.14**
Sarathi_08-26	**404**	96	F	1100	**Square**	-	**26.6**	-	-	-	1.080	**106.4**	**0.71**	**1.14**
Sarathi_08-27	**406**	96	F	1100	**Square**	-	**26.6**	-	-	-	1.080	**159.6**	**0.71**	**1.14**
Sarathi_08-28	**418**	96	F	1100	**Square**	-	**26.6**	-	-	-	1.080	**478.8**	**0.71**	**1.14**
Sarathi_08-29	**506**	96	F	1100	**Square**	-	**26.6**	-	-	-	0.710	**159.6**	**0.71**	**1.14**
Sarathi_08-30	**518**	96	F	1100	**Square**	-	**26.6**	-	-	-	0.710	**478.8**	**0.71**	**1.14**
Sarathi_08-31	**606**	96	F	1100	**Square**	-	**26.6**	-	-	-	0.420	**159.6**	**0.71**	**1.14**

Sarathi, P., Faruque, M. A. A., and Balachandar, R. (2008). "Influence of tailwater depth, sediment size and densimetric Froude number on scour by submerged square wall jets." *Journal of Hydraulic Research*, 46(2), 158-175.

Database #	**dse**	Wse	Lse	Vse	Rh	**Fo**	dse/Rh	Wse/Rh	Lse/Rh	Vse/Rh3	H/do
	mm	mm	mm	ml	mm						
Sarathi_08-09	**75.4**	340	600	3340	6.65	**6.600**	11.338	51.128	90.226	11357.468	1
Sarathi_08-10	**69.9**	259	585	3010	6.65	**6.600**	10.511	38.947	87.970	10235.323	2
Sarathi_08-11	**61.5**	246	563	2320	6.65	**6.600**	9.248	36.992	84.662	7889.020	3
Sarathi_08-12	**60.1**	228	546	2440	6.65	**6.600**	9.038	34.286	82.105	8297.073	4
Sarathi_08-13	**57.2**	255	525	2320	6.65	**6.600**	8.602	38.346	78.947	7889.020	6
Sarathi_08-14	**61.9**	248	550	2720	6.65	**6.600**	9.308	37.293	82.707	9249.196	12
Sarathi_08-15	**61.7**	240	550	2600	6.65	**6.600**	9.278	36.090	82.707	8841.143	15
Sarathi_08-16	**58.7**	234	539	2285	6.65	**6.600**	8.827	35.188	81.053	7770.004	18
Sarathi_08-17	**106.4**	534	840	13370	6.65	**10.000**	16.000	80.301	126.316	45463.877	1
Sarathi_08-18	**106.1**	420	830	11135	6.65	**10.000**	15.955	63.158	124.812	37863.895	2
Sarathi_08-19	**103.6**	400	820	10500	6.65	**10.000**	15.579	60.150	123.308	35704.616	3
Sarathi_08-20	**95.7**	410	795	9090	6.65	**10.000**	14.391	61.654	119.549	30909.996	4
Sarathi_08-21	**91**	390	783	8950	6.65	**10.000**	13.684	58.647	117.744	30433.934	6
Sarathi_08-22	**93.9**	368	780	8850	6.65	**10.000**	14.120	55.338	117.293	30093.890	12
Sarathi_08-23	**90.2**	355	780	7830	6.65	**10.000**	13.564	53.383	117.293	26625.442	15
Sarathi_08-24	**92.4**	367	790	8740	6.65	**10.000**	13.895	55.188	118.797	29719.842	18
Sarathi_08-25	**94.9**	445	850	10000	6.65	**10.000**	14.271	66.917	127.820	34004.396	2
Sarathi_08-26	**89**	454	810	9920	6.65	**10.000**	13.383	68.271	121.805	33732.361	4
Sarathi_08-27	**92**	403	795	9490	6.65	**10.000**	13.835	60.602	119.549	32270.172	6
Sarathi_08-28	**90.1**	397	783	8520	6.65	**10.000**	13.549	59.699	117.744	28971.745	18
Sarathi_08-29	**57.8**	246	545	2600	6.65	**6.600**	8.692	36.992	81.955	8841.143	6
Sarathi_08-30	**58**	238	570	2610	6.65	**6.600**	8.722	35.789	85.714	8875.147	18
Sarathi_08-31	**29.1**	124	355	495	6.65	**3.900**	4.376	18.647	53.383	1683.218	6

Leow, C. S. (2006). "Erosion below Non-Full Flowing Rectangular Outlet." *Final Year Project Report*, Nanyang Technological University, Singapore.

Database #	**Original Run #**	Duration hr	F/NF	W mm	**Shape**	**do mm**	**b mm**	**slope**	**ho mm**	Q L/s	Uo m/s	**H mm**	**d50 mm**	**sigma_g**
Leow_06-01	**A1****	46	NF	1000	**Rectangular**	-	**78**	-	**29**	1.494	0.660	**17**	**1.76**	**1.13**
Leow_06-02	**A2****	45.5	NF	1000	**Rectangular**	-	**78**	-	**26**	1.194	0.589	**17**	**1.76**	**1.13**
Leow_06-03	**A3****	47.33	NF	1000	**Rectangular**	-	**78**	-	**28**	1.383	0.633	**17**	**1.76**	**1.13**
Leow_06-04	**A4***	44	NF	1000	**Rectangular**	-	**78**	-	**18**	0.641	0.456	**17**	**1.76**	**1.13**
Leow_06-05	**A5***	46	NF	1000	**Rectangular**	-	**78**	-	**19**	0.773	0.522	**17**	**1.76**	**1.13**
Leow_06-06	**A6***	46.5	NF	1000	**Rectangular**	-	**78**	-	**21**	0.887	0.541	**17**	**1.76**	**1.13**
Leow_06-07	**A7****	48.6	NF	1000	**Rectangular**	-	**78**	-	**29**	1.521	0.673	**17**	**1.76**	**1.13**
Leow_06-08	**B1***	47	NF	1000	**Rectangular**	-	**78**	-	**25**	1.394	0.715	**12**	**1.76**	**1.13**
Leow_06-09	**B2****	47	NF	1000	**Rectangular**	-	**78**	-	**24**	1.134	0.606	**12**	**1.76**	**1.13**
Leow_06-10	**B3***	47	NF	1000	**Rectangular**	-	**78**	-	**21**	0.957	0.584	**12**	**1.76**	**1.13**
Leow_06-11	**B4****	48	NF	1000	**Rectangular**	-	**78**	-	**18**	0.798	0.569	**12**	**1.76**	**1.13**
Leow_06-12	**B5****	44	NF	1000	**Rectangular**	-	**78**	-	**24**	1.133	0.605	**12**	**1.76**	**1.13**
Leow_06-13	**B6***	47.25	NF	1000	**Rectangular**	-	**78**	-	**17**	0.703	0.530	**12**	**1.76**	**1.13**
Leow_06-14	**B7****	46.6	NF	1000	**Rectangular**	-	**78**	-	**25**	1.307	0.670	**12**	**1.76**	**1.13**
Leow_06-15	**C1*****	44.6	NF	1000	**Rectangular**	-	**78**	-	**25**	1.393	0.714	**12**	**3.8**	**3.28**
Leow_06-16	**C2*****	46	NF	1000	**Rectangular**	-	**78**	-	**24**	1.268	0.678	**12**	**3.8**	**3.28**
Leow_06-17	**C3*****	45.3	NF	1000	**Rectangular**	-	**78**	-	**19**	0.899	0.607	**12**	**3.8**	**3.28**
Leow_06-18	**C4*****	47	NF	1000	**Rectangular**	-	**78**	-	**21**	1.002	0.612	**12**	**3.8**	**3.28**
Leow_06-19	**C5*****	44	NF	1000	**Rectangular**	-	**78**	-	**23**	1.141	0.636	**12**	**3.8**	**3.28**
Leow_06-20	**C6*****	48	NF	1000	**Rectangular**	-	**78**	-	**24**	1.244	0.665	**12**	**3.8**	**3.28**
Leow_06-21	**C7*****	45	NF	1000	**Rectangular**	-	**78**	-	**24**	1.237	0.661	**12**	**3.8**	**3.28**

Leow, C. S. (2006). "Erosion below Non-Full Flowing Rectangular Outlet." *Final Year Project Report*, Nanyang Technological University, Singapore.

Database #	**dse**	Wse	Lse	Vse	Rh	**Fo**	dse/Rh	Wse/Rh	Lse/Rh	Vse/Rh3
	mm	mm	mm	ml	mm					
Leow_06-01	**89**	300	820	7600	16.63	**3.912**	5.351	18.037	49.302	1651.781
Leow_06-02	**68**	230	770	4950	15.60	**3.487**	4.359	14.744	49.359	1303.861
Leow_06-03	**73**	285	800	6425	16.30	**3.751**	4.479	17.486	49.084	1483.985
Leow_06-04	**27**	160	470	825	12.32	**2.704**	2.192	12.991	38.162	441.639
Leow_06-05	**37**	155	545	950	12.78	**3.092**	2.896	12.132	42.659	455.568
Leow_06-06	**53**	170	620	2050	13.65	**3.207**	3.883	12.454	45.421	806.039
Leow_06-07	**98**	310	850	8200	16.63	**3.985**	5.892	18.638	51.105	1782.185
Leow_06-08	**115**	470	800	11600	15.23	**4.236**	7.549	30.851	52.513	3280.833
Leow_06-09	**89**	380	610	5600	14.86	**3.589**	5.990	25.577	41.058	1707.584
Leow_06-10	**45**	290	380	1900	13.65	**3.461**	3.297	21.245	27.839	747.060
Leow_06-11	**38**	240	310	1150	12.32	**3.369**	3.085	19.487	25.171	615.618
Leow_06-12	**88**	385	660	6200	14.86	**3.586**	5.923	25.913	44.423	1890.540
Leow_06-13	**32**	220	300	1070	11.84	**3.139**	2.703	18.582	25.339	644.774
Leow_06-14	**102**	420	680	7950	15.23	**3.970**	6.695	27.569	44.636	2248.502
Leow_06-15	**43**	240	300	1100	15.23	**2.880**	2.823	15.754	19.692	311.113
Leow_06-16	**39**	210	260	800	14.86	**2.732**	2.625	14.135	17.500	243.941
Leow_06-17	**17**	170	200	225	12.78	**2.446**	1.331	13.306	15.655	107.898
Leow_06-18	**26**	180	240	300	13.65	**2.468**	1.905	13.187	17.582	117.957
Leow_06-19	**27**	190	240	380	14.47	**2.564**	1.866	13.133	16.589	125.482
Leow_06-20	**36**	200	250	550	14.86	**2.680**	2.423	13.462	16.827	167.709
Leow_06-21	**33**	190	250	520	14.86	**2.664**	2.221	12.788	16.827	158.561

Peh, F. W. (2007). "Erosion Below Non-Full Flowing Rectangular Culvert Outlets." *Final Year Project Report*, Nanyang Technological University, Singapore.

Database #	Original Run #	Duration hr	F/NF	W mm	Shape	do mm	b mm	slope	ho mm	Q L/s	Uo m/s	H mm	d50 mm	sigma_g
Peh_07-01	**B-A2**	29	NF	1000	**Rectangular**	-	**160**	-	**33.5**	5.400	1.007	**26**	**3.1**	**3.56**
Peh_07-02	**B-A3**	28	NF	1000	**Rectangular**	-	**160**	-	**35**	5.419	0.968	**28**	**3.1**	**3.56**
Peh_07-03	**B-A4**	28.5	NF	1000	**Rectangular**	-	**160**	-	**36**	5.354	0.930	**31**	**3.1**	**3.56**
Peh_07-04	**B-A6****	29	NF	1000	**Rectangular**	-	**160**	-	**37**	5.402	0.912	**38**	**3.1**	**3.56**
Peh_07-05	**B-B1****	29	NF	1000	**Rectangular**	-	**160**	-	**36.5**	5.346	0.915	**35**	**3.1**	**3.56**
Peh_07-06	**B-B3***	29	NF	1000	**Rectangular**	-	**160**	-	**36**	4.992	0.867	**38**	**3.1**	**3.56**
Peh_07-07	**B-B5***	29.3	NF	1000	**Rectangular**	-	**160**	-	**37**	5.075	0.857	**38**	**3.1**	**3.56**
Peh_07-08	**B-B6***	29	NF	1000	**Rectangular**	-	**160**	-	**36**	4.748	0.824	**38**	**3.1**	**3.56**
Peh_07-09	**B-C1**	29	NF	1000	**Rectangular**	-	**160**	-	**34**	5.325	0.979	**27**	**3.1**	**3.56**
Peh_07-10	**B-C2**	29	NF	1000	**Rectangular**	-	**160**	-	**34**	5.277	0.970	**25**	**3.1**	**3.56**
Peh_07-11	**B-C3**	29	NF	1000	**Rectangular**	-	**160**	-	**34**	5.187	0.953	**27**	**3.1**	**3.56**
Peh_07-12	**B-C4**	29	NF	1000	**Rectangular**	-	**160**	-	**33**	4.787	0.907	**25**	**3.1**	**3.56**
Peh_07-13	**B-C5**	29	NF	1000	**Rectangular**	-	**160**	-	**34**	5.226	0.961	**26**	**3.1**	**3.56**
Peh_07-14	**B-C6**	29	NF	1000	**Rectangular**	-	**160**	-	**28**	3.873	0.865	**23**	**3.1**	**3.56**

Tan, J. J. P. (2009). "Scour Downstream of Unsubmerged Non-full Flowing Trapezoidal Culvert Outlet." *Final Year Project Report*, Nanyang Tecnological University, Singapore

Database #	Original Run #	Duration hr	F/NF	W mm	Shape	do mm	b mm	slope	ho mm	Q L/s	Uo m/s	H mm	d50 mm	sigma_g
Tan_09-01	**Run 9**	91	NF	2000	**Trapezoidal**	-	**120**	**1.732**	**38**	4.700	0.871	**26**	**4.9**	**1.27**
Tan_09-02	**Run 10**	45	NF	2000	**Trapezoidal**	-	**120**	**1.732**	**37.5**	4.200	0.791	**32**	**4.9**	**1.27**
Tan_09-03	**Run 11**	95	NF	2000	**Trapezoidal**	-	**120**	**1.732**	**45**	5.200	0.791	**37**	**4.9**	**1.27**
Tan_09-04	**Run 13**	73	NF	2000	**Trapezoidal**	-	**120**	**1.732**	**40**	5.100	0.891	**33**	**4.9**	**1.27**
Tan_09-05	**Run 14**	71	NF	2000	**Trapezoidal**	-	**120**	**1.732**	**47**	5.900	0.853	**36**	**4.9**	**1.27**
Tan_09-06	**Run 16**	48	NF	2000	**Trapezoidal**	-	**120**	**1.732**	**48**	4.800	0.677	**38**	**4.9**	**1.27**
Tan_09-07	**Run 17**	48	NF	2000	**Trapezoidal**	-	**120**	**1.732**	**39**	5.630	1.013	**39**	**4.9**	**1.27**
Tan_09-08	**Run 3***	48	NF	2000	**Trapezoidal**	-	**120**	**1.732**	**44**	5.700	0.891	**27**	**4.9**	**1.27**
Tan_09-09	**Run 4***	41.83	NF	2000	**Trapezoidal**	-	**120**	**1.732**	**39**	4.500	0.810	**25**	**4.9**	**1.27**
Tan_09-10	**Run 5***	45	NF	2000	**Trapezoidal**	-	**120**	**1.732**	**36**	4.000	0.789	**23**	**4.9**	**1.27**
Tan_09-11	**Run 6***	44	NF	2000	**Trapezoidal**	-	**120**	**1.732**	**39**	4.800	0.864	**23**	**4.9**	**1.27**
Tan_09-12	**Run 7***	48	NF	2000	**Trapezoidal**	-	**120**	**1.732**	**40**	5.000	0.874	**30**	**4.9**	**1.27**
Tan_09-13	**Run 15***	85	NF	2000	**Trapezoidal**	-	**120**	**1.732**	**47**	5.500	0.795	**31**	**4.9**	**1.27**

Peh, F. W. (2007). "Erosion Below Non-Full Flowing Rectangular Culvert Outlets." *Final Year Project Report*, Nanyang Technological University, Singapore.

Database #	**dse**	Wse	Lse	Vse	Rh	**Fo**	dse/Rh	Wse/Rh	Lse/Rh	Vse/Rh3
	mm	mm	mm	ml	mm					
Peh_07-01	**70.6**	395	520	4500	23.61	**4.497**	2.990	16.729	22.022	341.819
Peh_07-02	**69.6**	420	480	4250	24.35	**4.320**	2.858	17.250	19.714	294.448
Peh_07-03	**74.5**	380	500	4000	24.83	**4.150**	3.000	15.306	20.139	261.370
Peh_07-04	**85.6**	330	600	5250	25.30	**4.073**	3.383	13.044	23.716	324.221
Peh_07-05	**81.6**	340	620	5672	25.06	**4.086**	3.256	13.565	24.736	360.218
Peh_07-06	**57.8**	305	700	3500	24.83	**3.869**	2.328	12.285	28.194	228.699
Peh_07-07	**46.1**	280	620	2340	25.30	**3.827**	1.822	11.068	24.507	144.510
Peh_07-08	**46.1**	245	565	1735	24.83	**3.680**	1.857	9.868	22.757	113.369
Peh_07-09	**77.9**	380	490	4040	23.86	**4.370**	3.266	15.926	20.537	297.433
Peh_07-10	**72.6**	380	490	3400	23.86	**4.330**	3.042	15.926	20.537	250.315
Peh_07-11	**76.7**	380	475	4000	23.86	**4.256**	3.214	15.926	19.908	294.488
Peh_07-12	**63.4**	360	450	2900	23.36	**4.047**	2.714	15.409	19.261	227.416
Peh_07-13	**72.6**	380	490	3580	23.86	**4.289**	3.044	15.926	20.537	263.567
Peh_07-14	**48.3**	330	400	1650	20.74	**3.859**	2.329	15.911	19.286	184.932

Tan, J. J. P. (2009). "Scour Downstream of Unsubmerged Non-full Flowing Trapezoidal Culvert Outlet." *Final Year Project Report*, Nanyang Tecnological University, Singapore

Database #	**dse**	Wse	Lse	Vse	Rh	**Fo**	dse/Rh	Wse/Rh	Lse/Rh	Vse/Rh3
	mm	mm	mm	ml	mm					
Tan_09-01	**83**	356	405	4700	25.96	**3.094**	3.197	13.713	15.600	268.601
Tan_09-02	**66**	290	410	2000	25.71	**2.808**	2.567	11.279	15.947	117.676
Tan_09-03	**69**	375	730	8250	29.34	**2.810**	2.352	12.783	24.884	326.758
Tan_09-04	**77**	375	710	6120	26.95	**3.164**	2.857	13.914	26.344	312.625
Tan_09-05	**111**	515	660	13400	30.26	**3.030**	3.668	17.020	21.812	483.678
Tan_09-06	**78**	305	680	5050	30.71	**2.404**	2.540	9.931	22.140	174.305
Tan_09-07	**70**	325	634	5200	26.46	**3.597**	2.646	12.283	23.962	280.727
Tan_09-08	**101**	500	580	9500	28.87	**3.163**	3.499	17.320	20.091	394.849
Tan_09-09	**91**	405	490	5700	26.46	**2.875**	3.439	15.307	18.519	307.720
Tan_09-10	**74**	422	350	4000	24.95	**2.803**	2.966	16.914	14.028	257.551
Tan_09-11	**87**	470	380	6400	26.46	**3.067**	3.288	17.763	14.362	345.510
Tan_09-12	**86**	384	425	5950	26.95	**3.102**	3.191	14.248	15.769	303.941
Tan_09-13	**106**	540	640	11100	30.26	**2.824**	3.503	17.846	21.151	400.659

Ma, Y. (2010). "Bed Protection Below Culvert Outlets." *Final Year Project Report*, Nanyang Technological University, Singapore.

Database #	Original Run #	Duration	F/NF	W	Shape	do	b	slope	ho	Q	Uo	H	d50	sigma_g
		hr		mm		mm	mm		mm	L/s	m/s	mm	mm	
Ma_10-01	**C5***	26	NF	2000	**Trapezoidal**	-	**120**	**1.732**	**33**	4.200	0.915	**32**	**5.2**	**1.26**
Ma_10-02	**C6***	25	NF	2000	**Trapezoidal**	-	**120**	**1.732**	**44**	5.600	0.875	**35**	**5.2**	**1.26**
Ma_10-03	**D7***	24	NF	2000	**Trapezoidal**	-	**120**	**1.732**	**40**	5.100	0.891	**37**	**5.2**	**1.26**
Ma_10-04	**D8***	25	NF	2000	**Trapezoidal**	-	**120**	**1.732**	**41**	4.800	0.815	**38**	**5.2**	**1.26**

Theodosius, S. (2012). "Localized Scour Downstream of Unsubmerged Non-full Flowing Triangular Culvert Outlet." *Final Year Project Report*, Nanyang Technological University, Singapore.

Database #	Original Run #	Duration	F/NF	W	Shape	do	b	slope	ho	Q	Uo	H	d50	sigma_g
		hr		mm		mm	mm		mm	L/s	m/s	mm	mm	
Theodosius_12-01	**C1**	48	NF	1000	**Triangular**	-	-	**1**	**58**	2.187	0.650	**51.4**	**1.63**	**1.19**
Theodosius_12-02	**C2**	48.2	NF	1000	**Triangular**	-	-	**1**	**61**	2.724	0.732	**53.2**	**1.63**	**1.19**
Theodosius_12-03	**C3**	48	NF	1000	**Triangular**	-	-	**1**	**55**	1.811	0.599	**51**	**1.63**	**1.19**
Theodosius_12-04	**C4**	49.5	NF	1000	**Triangular**	-	-	**1**	**58**	2.007	0.597	**52.4**	**1.63**	**1.19**
Theodosius_12-05	**D1**	48.3	NF	1000	**Triangular**	-	-	**1**	**58**	2.201	0.654	**54.4**	**1.63**	**1.19**
Theodosius_12-06	**D2**	50	NF	1000	**Triangular**	-	-	**1**	**62**	2.635	0.685	**55.8**	**1.63**	**1.19**
Theodosius_12-07	**D3**	48	NF	1000	**Triangular**	-	-	**1**	**60**	2.392	0.664	**54.8**	**1.63**	**1.19**
Theodosius_12-08	**D4**	48.8	NF	1000	**Triangular**	-	-	**1**	**63**	3.089	0.778	**55.4**	**1.63**	**1.19**
Theodosius_12-09	**B5**	48	NF	1000	**Triangular**	-	-	**1**	**40**	0.976	0.610	**31.4**	**1.63**	**1.19**
Theodosius_12-10	**B1****	48.2	NF	1000	**Triangular**	-	-	**1**	**53**	2.012	0.716	**40**	**1.63**	**1.19**
Theodosius_12-11	**B4****	48	NF	1000	**Triangular**	-	-	**1**	**45**	1.269	0.626	**33.2**	**1.63**	**1.19**
Theodosius_12-12	**B6****	48	NF	1000	**Triangular**	-	-	**1**	**50**	1.767	0.707	**34**	**1.63**	**1.19**
Theodosius_12-13	**B7****	48.5	NF	1000	**Triangular**	-	-	**1**	**55**	2.176	0.719	**35**	**1.63**	**1.19**
Theodosius_12-14	**A1***	48	NF	1000	**Triangular**	-	-	**1**	**43**	1.357	0.734	**23**	**1.63**	**1.19**
Theodosius_12-15	**A2***	48	NF	1000	**Triangular**	-	-	**1**	**52**	2.038	0.754	**22**	**1.63**	**1.19**
Theodosius_12-16	**A3***	48	NF	1000	**Triangular**	-	-	**1**	**34**	0.696	0.602	**19**	**1.63**	**1.19**
Theodosius_12-17	**A4***	48.5	NF	1000	**Triangular**	-	-	**1**	**45**	1.538	0.759	**20**	**1.63**	**1.19**
Theodosius_12-18	**E1***	48	NF	1000	**Triangular**	-	-	**1**	**33**	0.620	0.570	**18.8**	**1.63**	**1.19**
Theodosius_12-19	**E2***	48.5	NF	1000	**Triangular**	-	-	**1**	**37**	0.745	0.544	**21**	**1.63**	**1.19**
Theodosius_12-20	**E3***	48.2	NF	1000	**Triangular**	-	-	**1**	**45**	1.377	0.680	**22.6**	**1.63**	**1.19**
Theodosius_12-21	**E4***	50	NF	1000	**Triangular**	-	-	**1**	**50**	1.685	0.674	**24.8**	**1.63**	**1.19**

Ma, Y. (2010). "Bed Protection Below Culvert Outlets." *Final Year Project Report*, Nanyang Technological University, Singapore.

Database #	**dse**	Wse	Lse	Vse	Rh	**Fo**	dse/Rh	Wse/Rh	Lse/Rh	Vse/Rh3
	mm	mm	mm	ml	mm					
Ma_10-01	**70**	307	409	-	23.39	**3.155**	2.993	13.127	17.488	-
Ma_10-02	**65**	308	516	-	28.87	**3.017**	2.252	10.669	17.874	-
Ma_10-03	**65**	278	470	-	26.95	**3.071**	2.412	10.315	17.439	-
Ma_10-04	**59**	272	446	-	27.44	**2.809**	2.150	9.913	16.255	-

Theodosius, S. (2012). "Localized Scour Downstream of Unsubmerged Non-full Flowing Triangular Culvert Outlet." *Final Year Project Report*, Nanyang Technological University, Singapore.

Database #	**dse**	Wse	Lse	Vse	Rh	**Fo**	dse/Rh	Wse/Rh	Lse/Rh	Vse/Rh3
	mm	mm	mm	ml	mm					
Theodosius_12-01	**100.6**	343	865	8620	20.51	**4.002**	4.906	16.727	42.183	999.674
Theodosius_12-02	**119.6**	396	1030	14975	21.57	**4.508**	5.546	18.362	47.759	1492.837
Theodosius_12-03	**79.2**	364	905	6645	19.45	**3.686**	4.073	18.719	46.540	903.737
Theodosius_12-04	**96.6**	348	910	7780	20.51	**3.673**	4.711	16.971	44.377	902.258
Theodosius_12-05	**99.6**	365	940	8915	20.51	**4.028**	4.857	17.800	45.840	1033.885
Theodosius_12-06	**121.6**	416	960	9882.5	21.92	**4.220**	5.547	18.978	43.795	938.268
Theodosius_12-07	**104.6**	381	885	9642.5	21.21	**4.090**	4.931	17.961	41.719	1010.115
Theodosius_12-08	**130.2**	433	1110	20000	22.27	**4.791**	5.845	19.440	49.834	1809.853
Theodosius_12-09	**76.8**	230	600	2100	14.14	**3.757**	5.431	16.263	42.426	742.462
Theodosius_12-10	**118.2**	485	555	10390	18.74	**4.409**	6.308	25.883	29.618	1579.148
Theodosius_12-11	**77.5**	313	470	3975	15.91	**3.857**	4.871	19.673	29.541	987.040
Theodosius_12-12	**106.4**	357	505	6495	17.68	**4.351**	6.019	20.195	28.567	1175.721
Theodosius_12-13	**118.8**	385	565	8830	19.45	**4.428**	6.109	19.799	29.056	1200.902
Theodosius_12-14	**102**	420	360	3413	15.20	**4.518**	6.709	27.626	23.680	971.328
Theodosius_12-15	**121**	526	535	10542	18.38	**4.640**	6.582	28.611	29.100	1696.477
Theodosius_12-16	**61.7**	320	280	2273	12.02	**3.708**	5.133	26.620	23.293	1308.572
Theodosius_12-17	**102.2**	414	385	5335	15.91	**4.675**	6.424	26.022	24.199	1324.744
Theodosius_12-18	**58.4**	197	255	865	11.67	**3.506**	5.005	16.885	21.856	544.640
Theodosius_12-19	**65**	261	275	1862.5	13.08	**3.351**	4.969	19.952	21.022	832.005
Theodosius_12-20	**92.4**	343	365	3500	15.91	**4.187**	5.808	21.559	22.942	869.091
Theodosius_12-21	**100.6**	372	405	4520	17.68	**4.149**	5.691	21.043	22.910	818.207

Tan, B. E. (2013). "Scour Below a Non-Full Flowing Rectangular Culvert Outlet." *Final Year Project Report*, Nanyang Technological University, Singapore.

Database #	**Original Run #**	Duration hr	F/NF	W mm	**Shape**	**do mm**	**b mm**	**slope**	**ho mm**	Q L/s	Uo m/s	**H mm**	**d50 mm**	**sigma_g**
Tan_13-01	**A1**	48	NF	1000	**Rectangular**	-	**50**	-	**32**	1.786	1.116	**17**	**1.63**	**1.19**
Tan_13-02	**A2**	48	NF	1000	**Rectangular**	-	**50**	-	**27**	1.053	0.780	**18**	**1.63**	**1.19**
Tan_13-03	**A3**	48	NF	1000	**Rectangular**	-	**50**	-	**30**	1.333	0.889	**17**	**1.63**	**1.19**
Tan_13-04	**A4***	48	NF	1000	**Rectangular**	-	**50**	-	**20**	0.645	0.645	**10**	**1.63**	**1.19**
Tan_13-05	**B1**	48	NF	1000	**Rectangular**	-	**50**	-	**42**	2.041	0.972	**22**	**1.63**	**1.19**
Tan_13-06	**B2***	48	NF	1000	**Rectangular**	-	**50**	-	**37**	1.429	0.772	**21**	**1.63**	**1.19**
Tan_13-07	**B3***	48	NF	1000	**Rectangular**	-	**50**	-	**32**	1.235	0.772	**20**	**1.63**	**1.19**
Tan_13-08	**B4***	48	NF	1000	**Rectangular**	-	**50**	-	**28**	0.847	0.605	**17**	**1.63**	**1.19**
Tan_13-09	**C1**	48	NF	1000	**Rectangular**	-	**50**	-	**42**	1.099	0.523	**30**	**1.63**	**1.19**
Tan_13-10	**C2**	48	NF	1000	**Rectangular**	-	**50**	-	**44**	1.220	0.554	**31**	**1.63**	**1.19**
Tan_13-11	**C3**	48	NF	1000	**Rectangular**	-	**50**	-	**45**	1.471	0.654	**32**	**1.63**	**1.19**
Tan_13-12	**C4**	48	NF	1000	**Rectangular**	-	**50**	-	**47**	1.818	0.774	**32**	**1.63**	**1.19**
Tan_13-13	**D4**	48	NF	1000	**Rectangular**	-	**50**	-	**50**	1.075	0.430	**37**	**1.63**	**1.19**

Akhtar, A. (2014). "Rectangular Culvert Scour with Non-Uniform Sand." *Final Year Project Report*, Nanyang Technological University, Singapore.

Database #	**Original Run #**	Duration hr	F/NF	W mm	**Shape**	**do mm**	**b mm**	**slope**	**ho mm**	Q L/s	Uo m/s	**H mm**	**d50 mm**	**sigma_g**
Akhtar_14-01	**A1**	47	NF	1000	**Rectangular**	-	**50**	-	**23**	0.978	0.851	**6.5**	**1.803**	**2.67**
Akhtar_14-02	**A2**	69	NF	1000	**Rectangular**	-	**50**	-	**24**	0.982	0.818	**8**	**1.803**	**2.67**
Akhtar_14-03	**A3**	45.5	NF	1000	**Rectangular**	-	**50**	-	**22**	0.933	0.849	**10**	**1.803**	**2.67**
Akhtar_14-04	**B1***	47	NF	1000	**Rectangular**	-	**50**	-	**23**	0.928	0.807	**15**	**1.803**	**2.67**
Akhtar_14-05	**B2***	47	NF	1000	**Rectangular**	-	**50**	-	**18**	0.685	0.762	**15**	**1.803**	**2.67**
Akhtar_14-06	**B3***	49	NF	1000	**Rectangular**	-	**50**	-	**28**	1.147	0.819	**16.5**	**1.803**	**2.67**
Akhtar_14-07	**B4**	44.5	NF	1000	**Rectangular**	-	**50**	-	**29**	1.238	0.854	**16.5**	**1.803**	**2.67**
Akhtar_14-08	**B5***	94	NF	1000	**Rectangular**	-	**50**	-	**29**	1.190	0.821	**17.5**	**1.803**	**2.67**
Akhtar_14-09	**B6**	71	NF	1000	**Rectangular**	-	**50**	-	**37**	1.856	1.003	**16.5**	**1.803**	**2.67**
Akhtar_14-10	**C1***	43	NF	1000	**Rectangular**	-	**50**	-	**26**	0.884	0.680	**23**	**1.803**	**2.67**
Akhtar_14-11	**C2**	47.5	NF	1000	**Rectangular**	-	**50**	-	**33**	1.451	0.879	**23.5**	**1.803**	**2.67**
Akhtar_14-12	**C3***	45	NF	1000	**Rectangular**	-	**50**	-	**31**	1.221	0.788	**23**	**1.803**	**2.67**
Akhtar_14-13	**C4**	70	NF	1000	**Rectangular**	-	**50**	-	**38**	1.724	0.907	**26**	**1.803**	**2.67**
Akhtar_14-14	**D1***	45	NF	1000	**Rectangular**	-	**50**	-	**40**	1.541	0.770	**34.5**	**1.803**	**2.67**

Tan, B. E. (2013). "Scour Below a Non-Full Flowing Rectangular Culvert Outlet." *Final Year Project Report*, Nanyang Technological University, Singapore.

Database #	**dse mm**	Wse mm	Lse mm	Vse ml	Rh mm	**Fo**	dse/Rh	Wse/Rh	Lse/Rh	Vse/Rh3
Tan_13-01	**125**	432	1155	15500	14.04	**6.871**	8.906	30.780	82.294	5606.429
Tan_13-02	**90**	250	700	7200	12.98	**4.800**	6.933	19.259	53.926	3291.783
Tan_13-03	**101**	310	1048	9200	13.64	**5.472**	7.407	22.733	76.853	3628.207
Tan_13-04	**56**	178	445	1700	11.11	**3.972**	5.040	16.020	40.050	1239.300
Tan_13-05	**132**	477	1000	16300	15.67	**5.983**	8.423	30.437	63.810	4234.909
Tan_13-06	**102**	355	705	7300	14.92	**4.754**	6.837	23.795	47.254	2198.228
Tan_13-07	**88**	300	631	5200	14.04	**4.750**	6.270	21.375	44.959	1880.866
Tan_13-08	**58**	188	520	2200	13.21	**3.727**	4.391	14.234	39.371	954.896
Tan_13-09	**63**	326	588	3200	15.67	**3.222**	4.020	20.802	37.520	831.393
Tan_13-10	**72**	321	615	3300	15.94	**3.413**	4.516	20.135	38.577	814.485
Tan_13-11	**89**	297	760	5100	16.07	**4.024**	5.538	18.480	47.289	1228.589
Tan_13-12	**105**	394	750	8000	16.32	**4.763**	6.434	24.143	45.957	1840.661
Tan_13-13	**48**	286	550	1900	16.67	**2.648**	2.880	17.160	33.000	410.400

Akhtar, A. (2014). "Rectangular Culvert Scour with Non-Uniform Sand." *Final Year Project Report*, Nanyang Technological University, Singapore.

Database #	**dse mm**	Wse mm	Lse mm	Vse ml	Rh mm	**Fo**	dse/Rh	Wse/Rh	Lse/Rh	Vse/Rh3
Akhtar_14-01	**50**	316	480	1775	11.98	**4.979**	4.174	26.379	40.070	1032.568
Akhtar_14-02	**58**	291	460	2550	12.24	**4.789**	4.737	23.765	37.567	1388.912
Akhtar_14-03	**52**	310	380	1650	11.70	**4.967**	4.444	26.491	32.473	1029.650
Akhtar_14-04	**49**	193	670	1750	11.98	**4.722**	4.090	16.111	55.930	1018.024
Akhtar_14-05	**40**	214	390	800	10.47	**4.458**	3.822	20.449	37.267	698.004
Akhtar_14-06	**56**	252	570	2840	13.21	**4.795**	4.240	19.080	43.157	1232.684
Akhtar_14-07	**65**	334	850	3940	13.43	**4.998**	4.841	24.877	63.310	1628.034
Akhtar_14-08	**63**	265	610	2800	13.43	**4.806**	4.692	19.738	45.434	1156.979
Akhtar_14-09	**82**	458	780	6950	14.92	**5.874**	5.496	30.698	52.281	2092.833
Akhtar_14-10	**50**	198	428	1400	12.75	**3.982**	3.923	15.535	33.582	676.236
Akhtar_14-11	**70**	296	590	3375	14.22	**5.147**	4.921	20.810	41.479	1172.724
Akhtar_14-12	**62**	268	655	3114	13.84	**4.613**	4.480	19.365	47.329	1174.837
Akhtar_14-13	**86**	358	700	1750	15.08	**5.312**	5.703	23.741	46.421	510.374
Akhtar_14-14	**68**	273	650	2275	15.38	**4.510**	4.420	17.745	42.250	624.772

Surya, P. (2014). "Correlation of Scour Below A Non-full Flowing Culvert Outlet." *Final Year Project Report*, Nanyang Technological University, Singapore.

Database #	Original Run #	Duration	F/NF	W	Shape	do	b	slope	ho	Q	Uo	H	d50	sigma_g
		hr		mm		mm	mm		mm	L/s	m/s	mm	mm	
Surya_14-01	**Run 1***	49	NF	1000	**Trapezoidal**	-	**100**	**2.5**	**35.15**	2.035	0.508	**34.3**	**1.622**	**3.71**
Surya_14-02	**Run 2**	45	NF	1000	**Trapezoidal**	-	**100**	**2.5**	**30.6**	2.295	0.668	**23.3**	**1.622**	**3.71**
Surya_14-03	**Run 3**	71	NF	1000	**Trapezoidal**	-	**100**	**2.5**	**33.85**	2.675	0.696	**23.65**	**1.622**	**3.71**
Surya_14-04	**Run 4**	46	NF	1000	**Trapezoidal**	-	**100**	**2.5**	**35.45**	2.970	0.734	**26.35**	**1.622**	**3.71**
Surya_14-05	**Run 5**	45	NF	1000	**Trapezoidal**	-	**100**	**2.5**	**28.5**	2.000	0.630	**20.75**	**1.622**	**3.71**
Surya_14-06	**Run 6***	44	NF	1000	**Trapezoidal**	-	**100**	**2.5**	**26.6**	1.770	0.601	**21.15**	**1.622**	**3.71**
Surya_14-07	**Run 7**	45	NF	1000	**Trapezoidal**	-	**100**	**2.5**	**53.95**	4.705	0.717	**43.35**	**1.622**	**3.71**
Surya_14-08	**Run 8**	45	NF	1000	**Trapezoidal**	-	**100**	**2.5**	**48.5**	4.045	0.699	**45.85**	**1.622**	**3.71**

Miao, W. (2015). "Scour Below Non-full Flowing Trapezoidal Culvert Outlet." *Final Year project Report*, Nanyang Technological University, Singapore.

Database #	Original Run #	Duration	F/NF	W	Shape	do	b	slope	ho	Q	Uo	H	d50	sigma_g
		hr		mm		mm	mm		mm	L/s	m/s	mm	mm	
Miao_15-01	**Run 5**	48.67	NF	1000	**Trapezoidal**	-	**100**	**2.5**	**25.7**	1.660	0.586	**17.5**	**1.686**	**3.83**
Miao_15-02	**Run 6**	48	NF	1000	**Trapezoidal**	-	**100**	**2.5**	**25**	2.000	0.727	**19**	**1.686**	**3.83**
Miao_15-03	**Run 7**	48.75	NF	1000	**Trapezoidal**	-	**100**	**2.5**	**29.1**	2.280	0.702	**24**	**1.686**	**3.83**
Miao_15-04	**Run 8**	71.5	NF	1000	**Trapezoidal**	-	**100**	**2.5**	**30.5**	2.500	0.731	**25.25**	**1.686**	**3.83**
Miao_15-05	**Run 11***	49.5	NF	1000	**Trapezoidal**	-	**100**	**2.5**	**81.5**	3.460	0.320	**81.4**	**1.686**	**3.83**
Miao_15-06	**Run 12***	45.6	NF	1000	**Trapezoidal**	-	**100**	**2.5**	**53.3**	2.330	0.360	**52.95**	**1.686**	**3.83**
Miao_15-07	**Run 13***	50	NF	1000	**Trapezoidal**	-	**100**	**2.5**	**55.5**	3.480	0.513	**54.8**	**1.686**	**3.83**
Miao_15-08	**Run 14***	72	NF	1000	**Trapezoidal**	-	**100**	**2.5**	**56.3**	3.860	0.560	**54.75**	**1.686**	**3.83**

Additional runs after Miao (2015) has completed her project

Database #	Original Run #	Duration	F/NF	W	Shape	do	b	slope	ho	Q	Uo	H	d50	sigma_g
		hr		mm		mm	mm		mm	L/s	m/s	mm	mm	
Trap_15-01	**Run 3**	48	NF	1000	**Trapezoidal**	-	**100**	**2.5**	**36.9**	2.490	0.588	**36.15**	**1.686**	**3.83**
Trap_15-02	**Run 4**	48	NF	1000	**Trapezoidal**	-	**100**	**2.5**	**36.7**	2.260	0.537	**36.3**	**1.686**	**3.83**
Trap_15-03	**Run 5**	46	NF	1000	**Trapezoidal**	-	**100**	**2.5**	**36**	2.300	0.558	**36.1**	**1.686**	**3.83**

Surya, P. (2014). "Correlation of Scour Below A Non-full Flowing Culvert Outlet." *Final Year Project Report*, Nanyang Technological University, Singapore.

Database #	**dse**	Wse	Lse	Vse	Rh	**Fo**	dse/Rh	Wse/Rh	Lse/Rh	Vse/Rh3
	mm	mm	mm	ml	mm					
Surya_14-01	**34.3**	183	531	760	22.82	**3.133**	1.503	8.021	23.273	63.983
Surya_14-02	**60.2**	359	429	2875	20.70	**4.124**	2.908	17.342	20.724	324.103
Surya_14-03	**60.4**	331	514	3275	22.23	**4.296**	2.717	14.892	23.125	298.255
Surya_14-04	**64.8**	352	505	3490	22.95	**4.528**	2.823	15.337	22.003	288.682
Surya_14-05	**52.5**	283	458	1575	19.67	**3.888**	2.669	14.386	23.282	206.884
Surya_14-06	**29.4**	176	460	555	18.71	**3.712**	1.571	9.407	24.586	84.739
Surya_14-07	**102**	419	841	11975	30.34	**4.427**	3.362	13.811	27.722	428.897
Surya_14-08	**97.1**	387	816	9350	28.32	**4.311**	3.429	13.665	28.812	411.601

Miao, W. (2015). "Scour Below Non-full Flowing Trapezoidal Culvert Outlet." *Final Year project Report*, Nanyang Technological University, Singapore.

Database #	**dse**	Wse	Lse	Vse	Rh	**Fo**	dse/Rh	Wse/Rh	Lse/Rh	Vse/Rh3
	mm	mm	mm	ml	mm					
Miao_15-01	**46.2**	286	458	1255	18.24	**3.545**	2.533	15.677	25.106	206.713
Miao_15-02	**53.3**	298	420	1870	17.87	**4.402**	2.982	16.672	23.497	327.454
Miao_15-03	**56**	320	540	2175	19.97	**4.248**	2.804	16.024	27.041	273.118
Miao_15-04	**61.4**	331	479	2475	20.65	**4.422**	2.973	16.027	23.193	280.968
Miao_15-05	**50**	230	415	1065	39.22	**1.938**	1.275	5.865	10.582	17.655
Miao_15-06	**44.4**	221	420	925	30.10	**2.181**	1.475	7.342	13.952	33.911
Miao_15-07	**48.7**	249	435	1400	30.89	**3.106**	1.577	8.061	14.082	47.494
Miao_15-08	**51.3**	279	688	3500	31.17	**3.387**	1.646	8.950	22.070	115.535

Additional runs after Miao (2015) has completed her project

Database #	**dse**	Wse	Lse	Vse	Rh	**Fo**	dse/Rh	Wse/Rh	Lse/Rh	Vse/Rh3
	mm	mm	mm	ml	mm					
Trap_15-01	**61**	318	630	3650	23.59	**3.559**	2.585	13.478	26.702	277.925
Trap_15-02	**61.4**	284	715	2975	23.51	**3.250**	2.612	12.082	30.418	229.076
Trap_15-03	**52**	267	685	2815	23.20	**3.381**	2.242	11.511	29.531	225.542

Das, A. (2015). "Scour Below A Non-full Flowing Trapezoidal Culvert Outlet." *Final Year Project Report*, Nanyang Technological University, Singapore.

Database #	Original Run #	Duration hr	F/NF	W mm	Shape	do mm	b mm	slope	ho mm	Q L/s	Uo m/s	H mm	d50 mm	sigma_g
Das_15-01	**Run 3AD**	69	NF	1000	**Trap**	-	**50**	**1**	**18**	0.609	0.498	**16.5**	**0.49**	**1.47**
Das_15-02	**Run 4AD**	72	NF	1000	**Trap**	-	**50**	**1**	**41.5**	1.370	0.361	**42**	**0.49**	**1.47**
Das_15-03	**Run 5AD**	47	NF	1000	**Trap**	-	**50**	**1**	**41**	1.213	0.325	**41.5**	**0.49**	**1.47**
Das_15-04	**Run 6AD**	51	NF	1000	**Trap**	-	**50**	**1**	**41**	1.328	0.356	**41.5**	**0.49**	**1.47**
Das_15-05	**Run 7AD**	48.5	NF	1000	**Trap**	-	**50**	**1**	**41**	1.259	0.337	**40**	**0.49**	**1.47**
Das_15-06	**Run 8AD**	48	NF	1000	**Trap**	-	**50**	**1**	**20**	0.622	0.444	**20**	**0.49**	**1.47**
Das_15-07	**Run 9AD**	45	NF	1000	**Trap**	-	**50**	**1**	**21**	0.760	0.510	**21**	**0.49**	**1.47**
Das_15-08	**Run 10AD**	45.5	NF	1000	**Trap**	-	**50**	**1**	**20**	0.971	0.694	**12.95**	**0.49**	**1.47**
Das_15-09	**Run 11AD***	19	NF	1000	**Trap**	-	**50**	**1**	**52**	2.332	0.440	**48.75**	**0.49**	**1.47**
Das_15-10	**Run 12AD**	46.5	NF	1000	**Trap**	-	**50**	**1**	**50.4**	1.875	0.371	**49.05**	**0.49**	**1.47**
Das_15-11	**Run 13AD**	43	NF	1000	**Trap**	-	**50**	**1**	**48.5**	1.666	0.349	**48.1**	**0.49**	**1.47**
Das_15-12	**Run 14AD**	45.75	NF	1000	**Trap**	-	**50**	**1**	**17**	0.722	0.634	**10.25**	**0.49**	**1.47**
Das_15-13	**Run 15AD**	46.75	NF	1000	**Trap**	-	**50**	**1**	**18**	0.821	0.671	**10.5**	**0.49**	**1.47**
Das_15-14	**Run 16AD**	47.5	NF	1000	**Trap**	-	**50**	**1**	**22**	0.931	0.588	**21.5**	**0.49**	**1.47**
Das_15-15	**Run 17AD**	47.25	NF	1000	**Trap**	-	**50**	**1**	**41**	1.149	0.308	**41**	**0.49**	**1.47**
Das_15-16	**Run 18AD**	43.5	NF	1000	**Trap**	-	**50**	**1**	**50**	1.505	0.301	**50.25**	**0.49**	**1.47**
Das_15-17	**Run 19AD**	43.5	NF	1000	**Rect**	-	**50**	-	**41.2**	0.768	0.373	**40.85**	**0.49**	**1.47**
Das_15-18	**Run 20AD**	47.83	NF	1000	**Rect**	-	**50**	-	**39.6**	0.668	0.337	**39.65**	**0.49**	**1.47**
Das_15-19	**Run 21AD**	46.66	NF	1000	**Rect**	-	**50**	-	**40.8**	0.701	0.344	**40.7**	**0.49**	**1.47**
Das_15-20	**Run 22AD**	39.75	NF	1000	**Rect**	-	**50**	-	**40**	0.909	0.455	**39.6**	**0.49**	**1.47**

Das, A. (2015). "Scour Below A Non-full Flowing Trapezoidal Culvert Outlet." *Final Year Project Report*, Nanyang Technological University, Singapore.

Database #	**dse**	Wse	Lse	Vse	Rh	**Fo**	dse/Rh	Wse/Rh	Lse/Rh	Vse/Rh3
	mm	mm	mm	ml	mm					
Das_15-01	**51**	375	883	4225	12.13	**5.589**	4.205	30.917	72.798	2367.592
Das_15-02	**63**	265	958	5735	22.69	**4.051**	2.777	11.681	42.228	491.173
Das_15-03	**51**	283	813	3500	22.48	**3.649**	2.269	12.589	36.165	308.067
Das_15-04	**56**	253	983	5120	22.48	**3.997**	2.491	11.254	43.727	450.659
Das_15-05	**63**	248	843	4635	22.48	**3.789**	2.802	11.032	37.499	407.969
Das_15-06	**76**	275	620	3075	13.14	**4.985**	5.785	20.933	47.195	1356.276
Das_15-07	**77**	392	785	4890	13.63	**5.723**	5.650	28.762	57.597	1931.487
Das_15-08	**129.1**	850	670	17805	13.14	**7.789**	9.827	64.702	51.001	7853.169
Das_15-09	**81**	330	1265	10715	26.91	**4.938**	3.010	12.262	47.003	549.664
Das_15-10	**81.3**	300	1050	8000	26.28	**4.161**	3.094	11.416	39.955	440.805
Das_15-11	**67**	262	927	5500	25.52	**3.915**	2.625	10.265	36.321	330.825
Das_15-12	**74**	731	540	4500	11.61	**7.118**	6.372	62.949	46.501	2873.598
Das_15-13	**86**	808	620	7300	12.13	**7.534**	7.090	66.615	51.115	4090.751
Das_15-14	**80**	693	1027	8900	14.11	**6.602**	5.668	49.099	72.762	3165.176
Das_15-15	**48.5**	285	690	2685	22.48	**3.457**	2.157	12.678	30.693	236.332
Das_15-16	**49**	470	825	3010	26.12	**3.379**	1.876	17.994	31.585	168.899
Das_15-17	**63.5**	248	688	3920	15.56	**4.184**	4.081	15.939	44.219	1040.755
Das_15-18	**53.2**	238	630	2720	15.33	**3.786**	3.471	15.530	41.109	755.720
Das_15-19	**57.1**	270	650	3395	15.50	**3.861**	3.684	17.418	41.931	911.417
Das_15-20	**75.2**	298	830	5865	15.38	**5.105**	4.888	19.370	53.950	1610.676

Current study

Database #	Original Run #	Duration hr	F/NF	W mm	Shape	do mm	b mm	slope	ho mm	Q L/s	Uo m/s	H mm	d50 mm	sigma_g
Tan_15-01	**Run11**	47	NF	1000	**Rect**	-	**50**	-	**49.7**	0.999	0.402	**49.8**	**0.5**	**1.45**
Tan_15-02	**Run12**	48	NF	1000	**Rect**	-	**50**	-	**51**	1.232	0.483	**51.5**	**0.5**	**1.45**
Tan_15-03	**Run18**	42	NF	1000	**Rect**	-	**50**	-	**50.7**	0.820	0.324	**50.7**	**0.5**	**1.45**
Tan_15-04	**Run21**	49	NF	1000	**Rect**	-	**50**	-	**51.1**	0.899	0.352	**51.35**	**0.5**	**1.45**
Tan_15-05	**Run26**	41	NF	1000	**Rect**	-	**50**	-	**50.6**	0.761	0.301	**50.6**	**0.5**	**1.45**
Tan_15-06	**Run27**	44	NF	1000	**Rect**	-	**50**	-	**50.5**	1.330	0.527	**50.5**	**0.5**	**1.45**
Tan_15-07	**Run5**	48	NF	1000	**Rect**	-	**50**	-	**40.1**	0.977	0.487	**39.5**	**0.5**	**1.45**
Tan_15-08	**Run22**	44	NF	1000	**Rect**	-	**50**	-	**41.8**	1.175	0.562	**41.85**	**0.5**	**1.45**
Tan_15-09	**Run23**	47	NF	1000	**Rect**	-	**50**	-	**40.9**	0.685	0.335	**40.85**	**0.5**	**1.45**
Tan_15-10	**Run24**	43	NF	1000	**Rect**	-	**50**	-	**41**	0.769	0.375	**41.05**	**0.5**	**1.45**
Tan_15-11	**Run6**	48	NF	1000	**Rect**	-	**50**	-	**32.2**	0.981	0.610	**31.25**	**0.5**	**1.45**
Tan_15-12	**Run7**	47	NF	1000	**Rect**	-	**50**	-	**31.3**	0.794	0.507	**31.2**	**0.5**	**1.45**
Tan_15-13	**Run8**	47	NF	1000	**Rect**	-	**50**	-	**30.6**	0.581	0.380	**31**	**0.5**	**1.45**
Tan_15-14	**Run9**	51	NF	1000	**Rect**	-	**50**	-	**31.7**	0.714	0.450	**31.9**	**0.5**	**1.45**
Tan_15-15	**Run10**	50	NF	1000	**Rect**	-	**50**	-	**21.5**	0.629	0.586	**21**	**0.5**	**1.45**
Tan_15-16	**Run13**	48	NF	1000	**Rect**	-	**50**	-	**20.4**	0.500	0.490	**20.65**	**0.5**	**1.45**
Tan_15-17	**Run14**	46	NF	1000	**Rect**	-	**50**	-	**21.7**	0.555	0.512	**21.95**	**0.5**	**1.45**
Tan_15-18	**Run15**	41	NF	1000	**Rect**	-	**50**	-	**23.9**	0.711	0.595	**22**	**0.5**	**1.45**
Tan_15-19	**Run16**	46.5	NF	1000	**Rect**	-	**50**	-	**25.2**	0.787	0.625	**23**	**0.5**	**1.45**
Tan_15-20	**Run25**	44.5	NF	1000	**Rect**	-	**50**	-	**26.8**	0.910	0.679	**22.8**	**0.5**	**1.45**
Tan_15-21	**Run17**	44	NF	1000	**Rect**	-	**50**	-	**17.7**	0.624	0.705	**5.9**	**0.5**	**1.45**
Tan_15-22	**Run19**	44	NF	1000	**Rect**	-	**50**	-	**19.8**	0.716	0.723	**7**	**0.5**	**1.45**
Tan_15-23	**Run20**	48	NF	1000	**Rect**	-	**50**	-	**15.7**	0.524	0.668	**6.65**	**0.5**	**1.45**

Current study

Database #	**dse**	Wse	Lse	Vse	Rh	**Fo**	dse/Rh	Wse/Rh	Lse/Rh	Vse/Rh3
	mm	mm	mm	ml	mm					
Tan_15-01	**65**	295	805	5635	16.63	**4.467**	3.908	17.736	48.397	1224.522
Tan_15-02	**91.5**	349	860	8820	16.78	**5.368**	5.454	20.803	51.263	1868.008
Tan_15-03	**55**	279	615	3395	16.74	**3.596**	3.285	16.663	36.730	723.242
Tan_15-04	**59.3**	288	690	4200	16.79	**3.911**	3.532	17.156	41.103	887.811
Tan_15-05	**48.7**	265	520	2375	16.73	**3.344**	2.910	15.837	31.077	506.941
Tan_15-06	**96**	390	900	9810	16.72	**5.857**	5.741	23.323	53.822	2098.049
Tan_15-07	**74**	296	890	6425	15.40	**5.416**	4.805	19.222	57.795	1759.393
Tan_15-08	**94.5**	376	960	9360	15.64	**6.250**	6.041	24.035	61.367	2444.873
Tan_15-09	**60**	238	525	2490	15.52	**3.726**	3.867	15.339	33.836	666.601
Tan_15-10	**67**	258	610	3500	15.53	**4.172**	4.314	16.613	39.278	934.390
Tan_15-11	**95.5**	444	900	9040	14.07	**6.775**	6.786	31.549	63.950	3243.164
Tan_15-12	**75**	295	825	6240	13.90	**5.640**	5.396	21.225	59.358	2324.110
Tan_15-13	**55.3**	200	550	2085	13.76	**4.221**	4.019	14.536	39.974	800.472
Tan_15-14	**72.4**	263	640	3955	13.98	**5.007**	5.180	18.817	45.789	1448.431
Tan_15-15	**73**	275	740	5080	11.56	**6.509**	6.315	23.791	64.019	3289.176
Tan_15-16	**63**	233	560	2410	11.23	**5.443**	5.608	20.742	49.851	1700.098
Tan_15-17	**57.1**	247	690	3690	11.62	**5.690**	4.915	21.262	59.397	2353.845
Tan_15-18	**81.4**	429	730	7690	12.22	**6.616**	6.662	35.110	59.744	4215.404
Tan_15-19	**80**	313	885	7345	12.55	**6.946**	6.375	24.941	70.519	3716.048
Tan_15-20	**100.5**	496	1040	11395	12.93	**7.548**	7.770	38.347	80.406	5265.980
Tan_15-21	**90.4**	770	-	9060	10.36	**7.839**	8.723	74.303	-	8140.892
Tan_15-22	**105.8**	-	-	13060	11.05	**8.037**	9.575	-	-	9681.923
Tan_15-23	**81.5**	565	-	6265	9.64	**7.427**	8.451	58.587	-	6985.304

Current study

Database #	Original Run #	Duration hr	F/NF	W mm	Shape	do mm	b mm	slope	ho mm	Q L/s	Uo m/s	H mm	d50 mm	sigma_g
Tan_15-24	**Run_H1***	120	NF	1000	**Rect**	-	**50**	-	**101**	1.472	0.291	**101.4**	**0.5**	**1.45**
Tan_15-25	**Run_H2***	94	NF	1000	**Rect**	-	**50**	-	**101.7**	2.473	0.486	**101.5**	**0.5**	**1.45**
Tan_15-26	**Run_H3***	87	NF	1000	**Rect**	-	**50**	-	**100.7**	1.984	0.394	**100.8**	**0.5**	**1.45**
Tan_15-27	**Run_H4***	89.5	NF	1000	**Rect**	-	**50**	-	**100**	1.657	0.331	**100.25**	**0.5**	**1.45**
Tan_15-28	**Run_H5***	92	NF	1000	**Rect**	-	**50**	-	**80.2**	1.251	0.312	**80.25**	**0.5**	**1.45**
Tan_15-29	**Run_H6***	71	NF	1000	**Rect**	-	**50**	-	**80.8**	1.401	0.347	**80.85**	**0.5**	**1.45**
Tan_15-30	**Run_H7***	70	NF	1000	**Rect**	-	**50**	-	**80.3**	1.649	0.411	**80.5**	**0.5**	**1.45**
Tan_15-31	**Run_H8***	64	NF	1000	**Rect**	-	**50**	-	**80.5**	1.817	0.451	**80.65**	**0.5**	**1.45**
Tan_15-32	**RunA**	41	NF	1000	**Rect**	-	**50**	-	**53**	1.260	0.475	**53**	**0.5**	**1.45**

Current study

Database #	**dse**	Wse	Lse	Vse	Rh	**Fo**	dse/Rh	Wse/Rh	Lse/Rh	Vse/Rh3
	mm	mm	mm	ml	mm					
Tan_15-24	**71**	296	510	4000	20.04	**3.240**	3.543	14.771	25.450	497.036
Tan_15-25	**111**	472	950	16280	20.07	**5.405**	5.531	23.521	47.341	2014.658
Tan_15-26	**83.5**	365	870	10000	20.03	**4.380**	4.169	18.225	43.440	1244.794
Tan_15-27	**80.3**	313	625	5745	20.00	**3.685**	4.015	15.650	31.250	718.125
Tan_15-28	**62.3**	350	640	5345	19.06	**3.468**	3.269	18.364	33.580	772.061
Tan_15-29	**64.5**	315	750	6080	19.09	**3.854**	3.378	16.499	39.282	873.588
Tan_15-30	**78**	329	880	8560	19.06	**4.566**	4.091	17.257	46.159	1235.356
Tan_15-31	**88.5**	346	910	10130	19.08	**5.018**	4.639	18.138	47.704	1459.349
Tan_15-32	**79**	289	880	7315	16.99	**5.285**	4.651	17.013	51.804	1492.281